Size, shape, scope and strength of skeletons, *Evechinus chloroticus*, New Zealand

A thesis submitted in partial fulfilment of the degree of MSc in marine science

Shannon Louise Goodwin

1606092

9 July 2020

Table of Contents

List of Figures

List of Tables

Abstract

Ocean acidification will affect calcifying organisms as calcium carbonate saturation levels decrease due to climate change. Echinoids are important components of the coastal ecosystem and use magnesium in their skeletal calcification. Magnesium-calcite is highly susceptible to dissolution and the effects of lowered pH on the skeletal system of echinoids could be severe. This thesis examines the differences in allometry (shape and size), biomineral composition and flexural strength of *Evechinus chloroticus* skeletal components from six separate populations around New Zealand, including Whakaari White Island as a proxy for future ocean acidification conditions.

I measured 20 parameters for 64 individuals from six different locations. Individual skeletal elements within individuals and populations exhibited little variation in size and shape, particularly in those elements comprising the Aristotle's lantern. Using a standardised measurement to compensate for size of the individual, there was no obvious trend noted amongst locations except for weight of Aristotle lantern components, demonstrating a linear trend of increasing weight with increasing latitude.

Evechinus produces skeletons formed of magnesium-calcite (range=3.2–11.9, average=8.6 wt % $MgCO_3$ in calcite $\pm$ 2.01 SD, N=90); here I compared magnesium content in skeletal elements, which showed little variation within and between individuals of the same population. Variation among populations was also minimal. Magnesium content in test plates and Aristotle's lantern components was 9.5 wt % $MgCO_3$ ($\pm$ 0.4 SD, N=54), whereas spines were in general lower in magnesium (4.9, $\pm$ 0.23 SD, N=18).

Flexural strength of primary spines, measured by a two-point bending test was (average=112.0, $\pm$ 37.0 SD, N=640). The data exhibited a broad latitudinal trend with strength increasing with latitude, presumably linked to temperature. Spines from Fiordland, however, were weaker than expected; and those from White Island were stronger, likely due to the influence of seawater chemistry and/or growth rate.

Skeletal elemnts of *Evechinus chloroticus* around New Zealand exhibit minimal variations in response to different abiotic conditions. Tight morphological constraints on parameters, for example the Aristotle's lantern minimise variations exhibited by individuals and populations, while other parameters like spine morphology are thought to result from biotic pressures. Individual variation in biominerals are minimal and differences observed in magnesium content are expected to arise from different chemical pathways being utilised to offset conditions each calcium structure is exposed to. Strength is the ultimate result from differences in morphology

and biominerlisation, affecting the locomotion and defence mechanisms of *Evechinus chloroticus*. Latitude, and subsequent temperature is linked to spine strength; however, using White Island specimens as a proxy for individuals in future climate change scenarios, there was not an expected decrease in strength below what is anticipated from temperature differences. It is accepted that individuals and populations of *Evechinus chloroticus* around New Zealand have adapted to maintain skeletal conditions.

Keywords: *Evechinus chloroticus* ▪ Ocean acidification ▪ Skeletal allometry ▪ Spine strength ▪ Carbonate mineralogy ▪ Echinoid

Acknowledgments

Firstly, I would like to emphatically thank and acknowledge the amount of time Abby Smith spent encouraging, motivating, and kicking me into gear to accomplish this thesis. The scientific world would be lost without her dedication to her students and the joyous personality she shares with all her team. I would like to acknowledge my husband, Phillip Garland and his patience through this, and the many times he just nodded when I said it would only be a few more months. To my dearest friend, who I meet on the path to this career, Stephanie De Hamel, for the unwavering support while we broke down together. To my mum, Janine Corrigan for sharing her belief that I was intelligent enough to pursue a master's degree and the space for me to fail in my own way. I want to thank my dad, Andrew Goodwin for sharing his love of the water with me, I would not have entered this career without sharing your passion and your unconditional love. My darling step-mum, for being a pillar of strength through this all, and your infectious smiles. To Miles Lamare for taking me on as his student and believing I had what it took to be a post-grad student. To Em St Baker for the study dates that involved motivational wine. To my siblings Mackenzie, Mitchell, Joshua, Luke, Hayden and Riley, for believing I was the smart one and teasing me about it as well. And to every single person that helped me through these trying times, who scraped me off the floor, put a band aid on the bruises and told me to keep at it.

1 Introduction

1.1 Climate Change

Climate change is one of the most important perturbations facing the natural world, gaining momentum in scientific research and public awareness in recent years. Acceleration of climate change by human activities since the Industrial Revolution is prompting extensive investigation and inter-disciplinary research in science, history, policy, and even art (Vink et al. 2013). Climate change affects the world's oceans as a result of increased atmospheric carbon dioxide emissions, global warming and changes in ocean circulation (Harley et al. 2006; Przeslawski et al. 2008; Byrne 2012), all of which contribute to changes in an exhaustive list of abiotic and biotic factors.

Marine life is thought to be especially vulnerable to climate change because many marine environmental parameters may vary beyond current norms (Byrne et al. 2009). Mass mortalities, coral bleaching, species invasion, ecosystem shifts, physiological limitations and deviations to food web structures in a range of habitats over the 20th century have all been attributed to climate change (O'Connor et al. 2007; O'Connor 2009; Wernberg et al. 2011; Pörtner 2010; Byrne 2012; Hoegh-Guldberg & Bruno 2010; Crowley 2000). Coastal regions are likely to be one of the first areas to exhibit responses to ocean acidification, with episodic upwelling events pushing physiological limits of organisms near their limits, especially for calcifying marine organisms (Hauri et al. 2009; Hoffman et al. 2010). Fossil-fuel combustion, agriculture run-off, freshwater inputs, coastal developments and sediment disturbance can all impact the marine system, pushing the environment towards a "stressed" state (Doney et al. 2007; Salisbury et al. 2008; Gattuso et al. 1998; Hoffman et al. 2010).

Preliminary research has focused on single stressors beyond expected levels under future current climate change models, typically presented by International Panel of Climate Change (IPCC) (Byrne et al. 2009), but due to the multi-dimensional, multi-stressor state of the ocean, manipulated multi-factor experiments are becoming more common. Riebesell & Gattuso (2015) postulated a conceptual model (Figure 1.1), suggesting that by comprehending and studying small changes in a species under a single stressor, we can extrapolate to ecosystems acclimation and climate change adaptation under multiple stressors as our understanding of the small scale and fine detail of the environment expands.

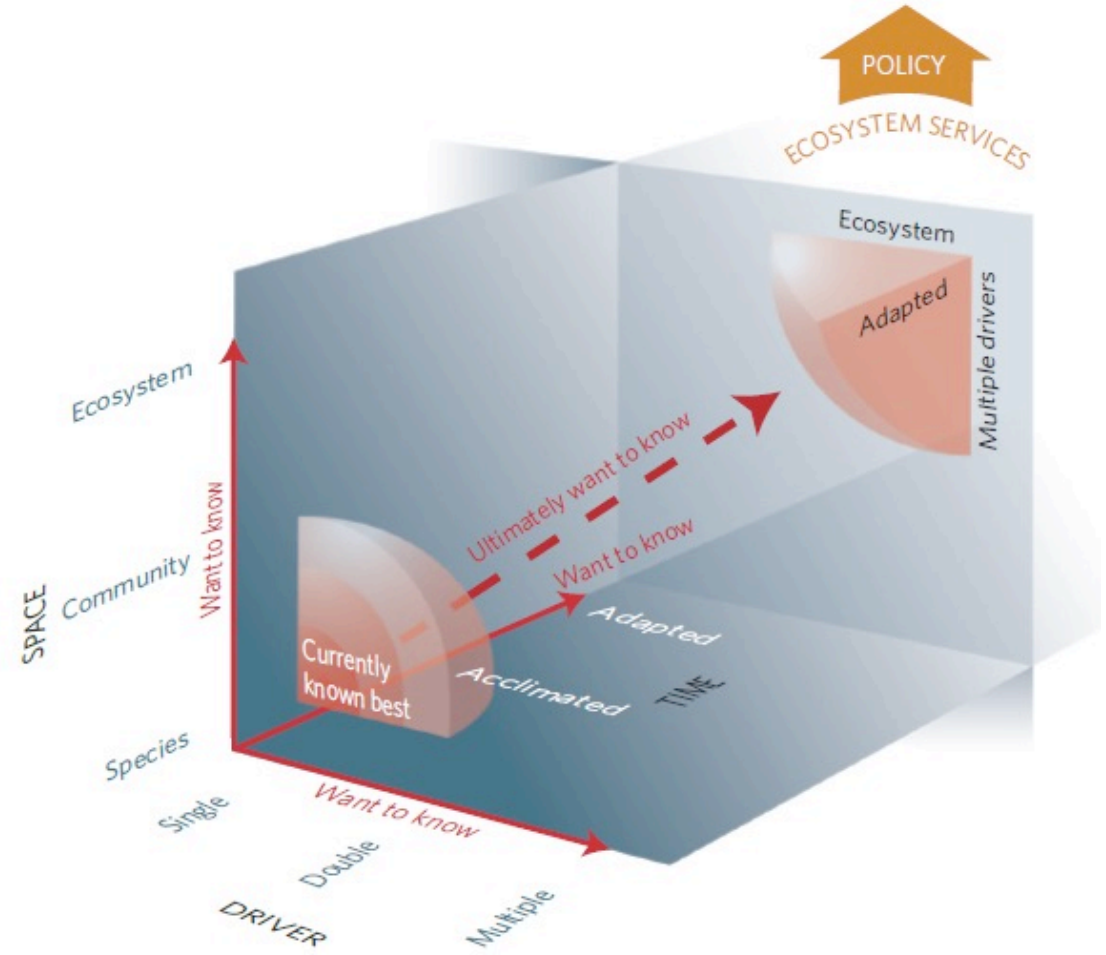

Figure 1.1 Schematic diagram of the current research and the direction we need to head for evidence-based policy making. Red arrow depicts areas needing expansion. Lower left corner is the current research on a single species under one stressor and the upper right corner is adapted responses to multiple stressors on a whole ecosystem. Figure originally presented in Riebesell & Gattuso (2015)

Small changes to one abiotic factor may, and typically do, have consequential effects on other physical conditions (temperature, ocean currents etc.), or abiotic connections (predation, competition etc.). Single-factor scientific experiments can be overly simple, unrealistic, short-term, or heavily controlled, unlike those conditions likely to be experienced by marine organisms. Frequently there is little consideration of the acclimation of individuals, or adaptation over generations to the oceanic conditions that are expected to occur. Compounding this small-scale rationale there can often be little consideration to the rate of climate change that may occur in a local area, with known hotspots already demonstrating faster warming than other comparable locations. Investigating ecologically-relevant and regional climate variation and subsequent effects under realistic near-future conditions would be more representative and may prove vital to understanding key questions such as:

biogeographical distributions, phenotypic plasticity, morphological variability, population connectivity, survival and extinction, larval dispersal, behaviour, and skeletal mineralogy.

1.2 Ocean Acidification

Since the start of the Industrial Revolution, rapidly increasing volumes of carbon dioxide are being produced by large factories, technological advancement and increasing urbanisation; all increasing CO_2 levels that are ultimately taken up by the ocean, one of the world's biggest carbon sinks (Caldeira & Wickett, 2005; Menon et al. 2007; Feely et al. 2004; Sabine et al. 2004, Doney et al. 2020). Atmospheric carbon dioxide (CO_2) is continuously absorbed into the world's oceans where it combines with seawater, changing the ocean chemistry. Increased levels of CO_2 mixed with seawater result in a higher concentration of free hydrogen ions (IPCC 2007; Harley et al. 2006, Terhaar et al. 2020). The increase in hydrogen ions decreases ocean pH, a phenomenon commonly called 'ocean acidification'. As pH decreases, carbonate ion availability also decreases, decreasing the saturation state of calcium carbonate, and ultimately, increasing the amount of calcium carbonate that is dissolved (Hofmann et al. 2010). In Ω values greater than one, when seawater is supersaturated, marine biocalcification is promoted, whereas Ω values less than one indicates undersaturated seawater, and biocalcification may be slowed or inhibited. The pH of the world's oceans is varied, depending on latitude, distance from shore, habitat type, and depth, ranging in pH from 7.8 – 8.2 (IPCC 2001; 2007; 2013; 2020). Future ocean conditions are predicted to decrease in pH a further 0.3 – 0.4 by 2100 (Caldeira & Wickett 2005; IPCC 2020) (Figure 1.2), forcing marine organisms to cope with a changing environment at an unprecedented rate. pH is not expected to change uniformly around the world; there is a strong need for research on specific regions and their corresponding biota.

Ocean acidification affects individuals, populations and species differently based on the ability to cope with reduced pH and increased CO_2 (hypercapnia) (Guinotte & Fabry 2008). The effects of ocean acidification on marine organisms and ecosystems are measurable under changes already exhibited in the present day, and likely to be exacerbated as CO_2 emissions continue to rise (Gattuso et al. 2015). Lowered production of calcium carbonate, difficulty in maintenance of calcified structures, and depressed metabolic activity in marine organisms that calcify (at any point during their life cycle) could lead to metabolic stress and potentially death (Kurihara 2008). For example, the blue mussel, *Mytilus edulis* exhibited significantly reduced growth of planktonic stages in pH expected to occur before the turn of the century (Gazeau et al. 2010). Decreased pH negatively impact fertilisation, cleavage, and settlement in invertebrate species such as the echinoids *Hemicentrotus pulcherrimus*, *Echinonerta mathaei*

and *Anthocidaris crassipina,* in bivalves *Crassostrea gigas* and *Mytilus galloprovincialis,* and in the copepod *Acartia erythraea* (Kurihara 2008), or increase mortality due to an inability to calcify in the bivalve *Chamelea gallina* (Bressan et al. 2014). Depressed calcification has been observed in corals, coccolithophores, foraminiferans and bivalves when CO_2 is increased (Gattuso et al. 1998, Riebesell et al. 2000; Bijma et al. 2002; Kleypas et al. 2006; Gazeau et al. 2007; Kurihara 2008). As pH is expected to continue decreasing, even under best-case scenarios for the near future, the effects of increased CO_2 on marine organisms will accumulate on top of effects already being displayed.

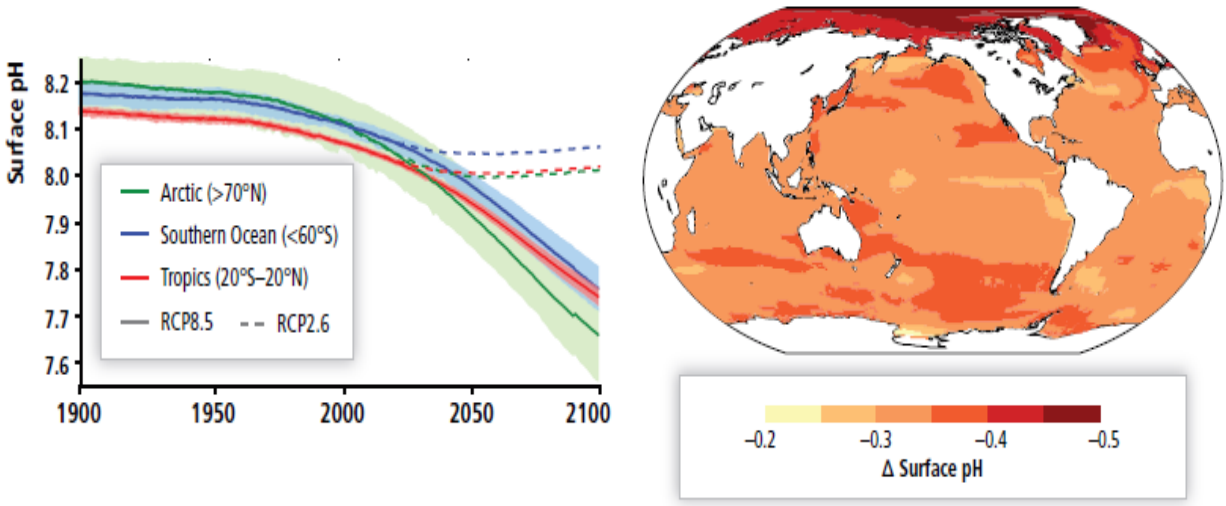

Figure 1.2 (Left graph) IPCC projected ocean acidification from models under representative concentration pathway (RCP) 8.5 (solid line) and mean model results from (RCP) 2.6 (dashed lines). RCP 2.6 models with peak CO_2 emissions in 2020, while RCP 8.5 models continuous CO_2 emissions. Time series of surface pH shown as the mean (solid line) and range of models (shaded area), given as area-weighted averages over the Arctic Ocean (green), the tropical oceans (red), and the Southern Ocean (blue). (Right graph) Map of the median model's change in surface pH from 1990s. Over most of the Ocean, gridded data products of carbonate system variables are used to correct each model for its present-day bias by subtracting the model-data difference at each grid cell following (Orr et al. 2005). Figure originally presented in IPCC 2013 WGI (Figure 6.28).

1.3 Echinoid Responses to pH

Echinoderms are often important keystone species, with global representatives found in almost every marine habitat. They are sub-divided into five classes: crinoids (sea lilies), asteroids (starfish), ophiuroids (brittle stars), echinoids (sea urchins and sand dollars), and holothuroids (sea cucumbers). Echinoids, in particular, are important throughout coastal marine systems as they are commonly classified as habitat engineers, determining the structure of surrounding flora. Equally urchins can overgraze macroalgal communities on reef systems, causing a habitat shift from dense macroalgal beds to sparse barren zones. An urchin-induced phase-

shift (from macroalgae to barren areas) is hard to reverse to the original state and requires extensive reductions in urchin densities which can be difficult, or simply unrealistic, to achieve. Even though their main food source of macroalgae is missing when barren zones are formed in the system, urchins can continue to feed on microalgae, coralline species, and floating algae (Johnson & Mann 1982). After the establishment of these barrens, habitat complexity, biodiversity and productivity suffer rapid reductions (Ling & Johnson 2009; Ling & Johnson 2012, Ling et al. 2015) as structural complexity in the environment is minimised (Aroldi et al. 2008).

Changes in the function of echinoids as a consequence of pH varies, depending on exposure time, pH levels and species (Dupont et al. 2010). Echinoids are robust to ocean acidification, in both larval and adult life stages but noted that impacts are species-, or even population-specific. Free-spawning populations, such as echinoderms, may already be demonstrating natural selection to current fluctuations in pH through gametic and early life stages. Schlegel et al. (2012) reported that acidification decreased the density of motile sperm yet had no effect on sperm speed in *Heliocidaris erythrogramma*. Schelegel et al. (2012) commented that the survival of individuals was resilient to ocean acidification, and those traits (if they were heritable), would lead to adaptive effects, affecting direct offspring and subsequent generations. Martin et al. (2011) suggested that gene expression levels were plastic after observing that *Paracentrotus lividus* larvae development was slowed, but normal in lowered pH. The genes involved in development and biomineralization were upregulated by a factor of up to 26 times, suggesting that the urchin's molecular composition could compensate for the changes in ocean acidification. Most work on the effects of climate change has focused on three species: *Stongylocentrotus purpuratus, Arbacia punctulata* and *Dendraster excentricus*, yet there are approximately 7,000 extant echinoid species globally.

Echinoids have become of increasing interest with respect to ocean acidification as their skeletal components are formed of magnesium calcite, a calcium carbonate mineral that is more vulnerable to dissolution as pH decreases (Shirayama & Thornton, 2005; Byrne et al. 2014). Most marine invertebrate calcifers use calcium carbonate ($CaCO_3$) either in the form of calcite or aragonite; some, such as echinoderms, use magnesium (Mg^{2+}) as a substitute for some of the calcium (Ca^{2+}) creating crystals of $MgCO_3$ within the calcite lattice. Magnesium content has previously been related to Ca^{2+}/Mg^{2+} ratio present in seawater, carbonate mineral saturation states and temperature (e.g., Byrne et al. 2014). Magnesium content in echinoids as a group ranges from 1.5 to 16.4 wt % $MgCO_3$ (average = 7.5 ± 3.23, N=643) (Smith et al. 2016). The addition of $MgCO_3$ makes magnesium-calcite stronger but more soluble than plain calcite (Stephenson et al. 2011), which may be biomechanically important, especially to organisms living in the active coastal zone.

1.4 *Evechinus chloroticus* (Study Organism)

Evechinus chloroticus (Valenciennes 1846) is a New Zealand endemic echinometrid echinoid, commonly found around shallow rocky reefs (Dix 1970). *E. chloroticus* is found throughout New Zealand in both intertidal and subtidal localities, from Three Kings Island in the north to the Snares in the south, ranging from the Chatham Islands in the east, and South Island fiords in the west. Adult *E. chloroticus* can dominate the subtidal landscape, with populations as dense as 50 per m2, but are rarely found below 15m (Barker 2001; 2013). Andrew (1988) boldly stated that *E. chloroticus* is the main species determining the characteristics of rocky reefs where they are found due to their intense herbivory rates, high recruitment and the ability to sustain a large diversity of organisms that predate upon the urchins. Juvenile *E. chloroticus* have predators among the benthic fish and invertebrates, including the commercially important blue cod (*Parapercis colias*) and crayfish (*Jasus edwardsii*). *E. chloroticus* graze primarily on large brown algae species, indirectly affecting invertebrate and fish diversity, abundance, and distribution (Andrew 1988). How this species responds to predicted climate conditions will be important in their respective population success and overall species continuity.

1.5 Aims and Scope of this Thesis

With ocean acidification predicted to increase there is growing concern for calcifying marine organisms, particularly those that are susceptible; how will they adapt and what will be the consequences of those adaptations? *Evechinus chloroticus* in New Zealand has all the characteristics we need to investigate the effects of environment, including ocean acidification, on calcification. This species is widespread throughout New Zealand, covering a range of water temperature and pH, and its skeleton consists of different elements with different roles (e.g., teeth, spines, test). The metabolic response of *E. chloroticus* larvae, juveniles and adults to ocean acidification is well known (Stumpp et al. 2011).

This project investigates how individual urchins calcify in different environments. *Evechinus chloroticus* was collected from six different locations in New Zealand (including the CO_2-rich waters around Whakaari White Island), and abiotic factors at each location were discerned and described (Chapter 2). *E. chloroticus* skeletons were investigated in three ways: allometric relationships within and among skeletal elements (Chapter 3), carbonate mineralogy of skeletal elements (Chapter 4), and consequent variations in strength of spines (Chapter 5). This thesis aims to develop along a natural progression as indicated by Figure 1.3 and Figure 1.4. Each chapter tries to compare within an individual, amongst individuals in a population and amongst populations (Figure 1.5) This combination of approaches allows discussion of

the whole picture of environmental effects on calcification in an important New Zealand ecosystem engineer (Chapter 6).

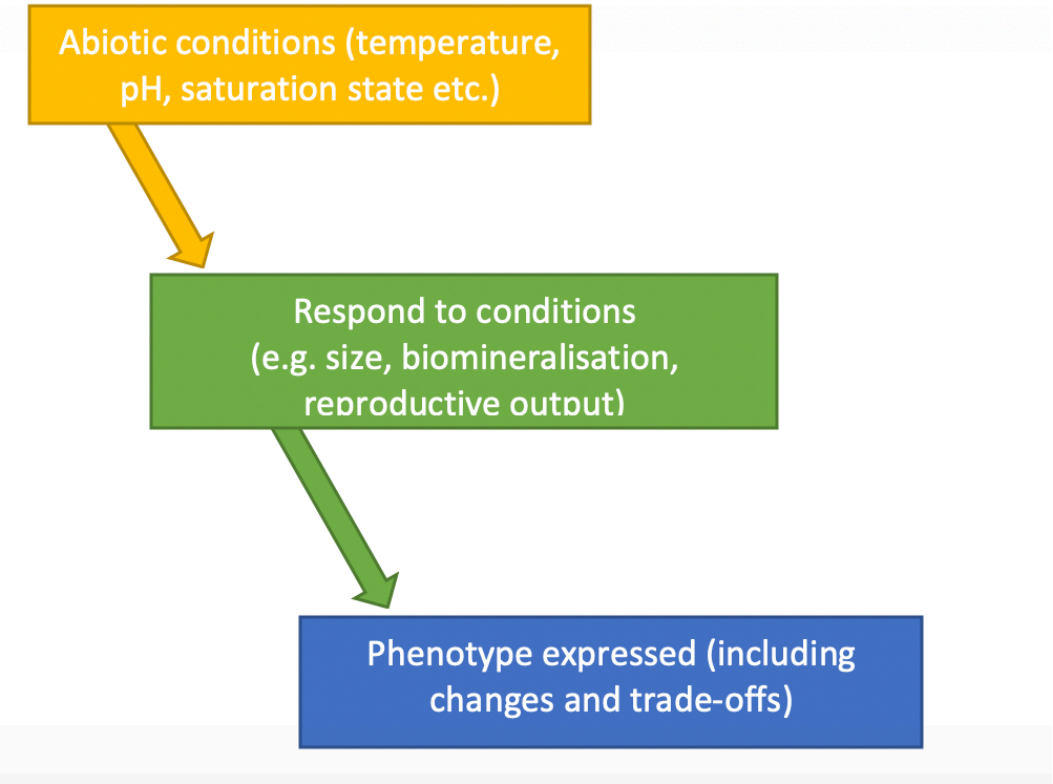

Figure 1.3 Schematic think-scape of thesis and the progression of factors that influence an urchin's phenotype.

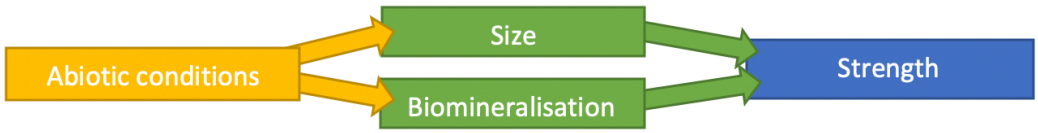

Figure 1.4 Schematic flow of abiotic conditions impacting the size and biomineralisation of spines which will affect the strength of spines.

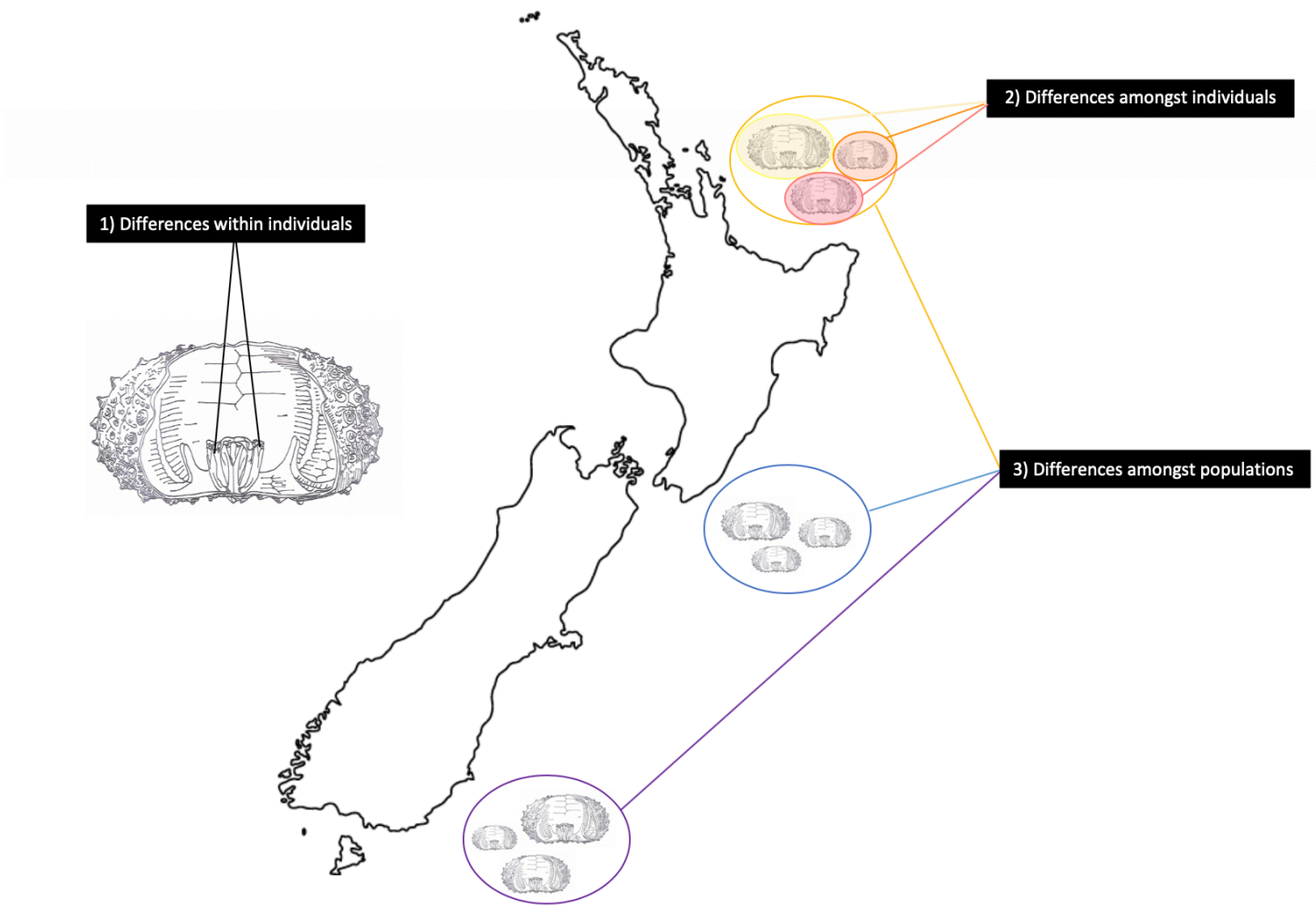

Figure 1.5 Schematic diagram highlighting the different sections investigated for each chapter. Where possible each chapter tries to compare differences within an individual, amongst individuals of the same population and then amongst populations around New Zealand.

2 Location and Collection Methods

2.1 Specimen Collection Locations

New Zealand is a temperate country that sits in the southwest of the Pacific Ocean. Its coastal and marine environment are extensive being the 4th largest exclusive economic zone (EEZ) in the world. New Zealand's coastal habitat are varied and made from three main islands: North Island, South Island and Stewart Island, although there are a considerable number of smaller offshore islands (Blezard 1980). Coastal waters exhibit wider variations in salinities, pH, temperature, contaminants, dissolved organic carbonates, Ω calcite and Ω aragonites both within locations and between locations when compared to more stable oceanic waters. This is primarily due of latitudinal differences, currents, climates, anthropogenic inputs, and oceanographic differences.

For this study, six locations were chosen ranging the length of coastal New Zealand (from 46.56 to -35.23 ° South). These locations sampled covered a wide variety of coastal habitats with consideration to locations monitored by New Zealand Ocean Acidification Observing Network (NZOA-ON) monitoring stations were, as they are currently collecting regular measurements of abiotic factors (Vance et al. 2019). Figure 2.1 shows the position of the study areas around New Zealand and the NZOA-ON monitoring sites that provided environmental data.

Locations for sample collection were: Army Bay, Auckland; White Island, Bay of Plenty; Scorching Bay, Wellington Harbour; Whenuanui Bay, Picton; Doubtful Sound, Fiordland; and Port Pegasus, Stewart Island. More details including the closest NZOA-ON monitoring sites are provided in Table 2.1 and detailed description of sites are below.

Table 2.1 Location, latitude, longitude, depth of collection and number of samples collected, and the NZOA-ON locations used as proxies for long-term monitoring of abiotic conditions.

Location	Latitude	Longitude	NZOA-ON location	Water depth	Number of specimens
Auckland	36.84°S	174.76°E	Auckland	2-3	10
White Island	37.52°S	177.19°E	Bay of Plenty	3-5	10
Wellington	41.28°S	174.77°E	Wellington	4-6	14
Picton	41.29°S	174.00°E	Marlborough Sounds	6-7	10
Fiordland	45.32°S	166.99°E	Jackson Bay, West Coast	4-5	10
Stewart Island	46.93°S	167.83°E	Stewart Island	2-3	10

Table 2.2 Location, latitude, longitude, depth of collection and number of samples collected, and the NZOA-ON locations used as proxies for long-term monitoring of abiotic conditions.

Location	Latitude	Longitude	NZOA-ON location	Water depth	Number of specimens
Auckland	36.84°S	174.76°E	Auckland	2-3	10
White Island	37.52°S	177.19°E	Bay of Plenty	3-5	10
Wellington	41.28°S	174.77°E	Wellington	4-6	14
Picton	41.29°S	174.00°E	Marlborough Sounds	6-7	10
Fiordland	45.32°S	166.99°E	Jackson Bay, West Coast	4-5	10
Stewart Island	46.93°S	167.83°E	Stewart Island	2-3	10

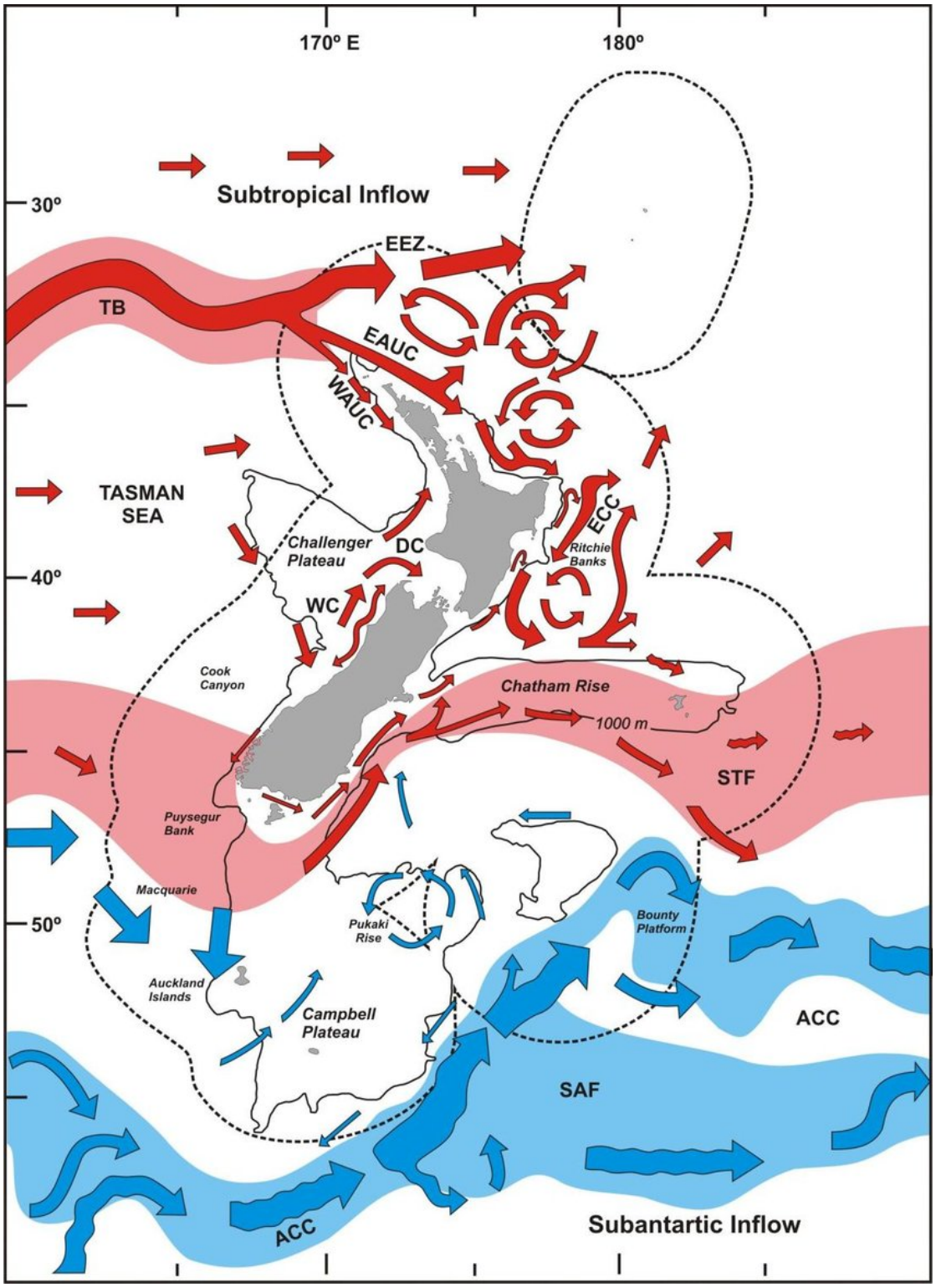

Figure 2.1 Schematic map showing surface circulation around New Zealand. Colours reflect the temperature of the flows with red as warm, and blue as cold. Ocean currents are East Auckland Current (EAUC), West Auckland Current (WAUC) East Australia Current extension (EAC), D'urville Current (DC), Westland Current (WC), Subantarctic front (SAF), Subtropical front (STF), East Cape Current (ECC) and Antarctic Circumpolar Current (ACC). Figure originally presented in Thomas 2012.

2.1.1 Auckland

Auckland is the biggest city in New Zealand with over 32% of the New Zealand population living in its boundary. Annual rainfall is 1280mm in the city and its surrounding districts (New Zealand, 2019). There is a six to eight-week delay between the low temperatures of land and sea. Average water temperature is 17°C, with lows of 11°C and highs of 24.1°C (climate-data.org, 2019). The East Australian current considered one of the most globally energetic western boundary currents (Ridgway & Hill, 2012) makes its way across the Tasman sea where it significantly contributes to the East Auckland current. The East Auckland current (EAUC) flows South-East along the North-East coast, moving at speeds up to 50cm per second (Stevens & Chiswell, 2019) until it hits 34° South, becoming the East Cape current (ECC). Due to the tropical water origins and the high latitudes, some tropical fish and invertebrates are found in this area and its surrounding offshore islands. The urchins collected from this area were sourced from Army Bay, Auckland. The area compromises of hard bed rock in intertidal and subtidal zones with large brown algae dominating the area, although notably absent from *E. chloroticus* associated patches. Low numbers of *E. chloroticus* are present in large intertidal pools from the same area, although these individuals were not included for this study.

2.1.2 White Island (Whakaari)

White Island (Whakaari) is a submarine stratovolcano (Tait & Tait, 2001) and is New Zealand's most active volcano, getting its namesake for the continuous expulsion of white smoke. It is a small island, with an area of approximately 288km^2, about 50km off the coast of North Island. Both the East Auckland and East Cape currents, both subtropical in their origin run past the Island, fostering seawater temperatures approximately 0.5 to 1.3°C warmer than mainland coastal waters. White Island/ Whakaari has underwater volcanic vents, reducing the pH and further increasing the temperatures found adjacent to those vents. Previous studies have found that as proximity to vents increase, pH can be as low as 7.49 (Brinkman 2014); a pH more acidic than those values predicted for 2100 (Caldeira & Wickett 2005). The results collected from multiple investigations into vents has identified these unique systems as naturally occurring scenarios of impacts that may arise from ocean acidification and are crucial for predicting outcomes to marine specimens, populations, and species. Grace (1975) noted 55 fish taxa, many invertebrate and algae species although brown algae was absent and this may be a result of grazing from the native urchin, *Evechinus chloroticus*.

2.1.3 Wellington

Wellington is at the southernmost tip of the North Island and is exposed to a raft of currents. The East Cape Current flows south-east along the east coast until it hits the Chatham Rise where it heads East however some of that water current is expected to add to the currents around Wellington. Westland current from the South Island flows northwards and splits at the top of the South Island, one part continuing northwards and the second part turning eastwards where it is renamed the D'urville current. Th D'urville current flows South-East and through Cook Strait where it heads out to the Chatham Rise. The Southland current flowing northwards from the South Island also contributes to the water body around Wellington. Urchins collected for this study were collected from the harbour of Wellington, specifically Scorching Bay.

2.1.4 Picton

Marlborough Sounds has an average water temperature of 15°C, with a range of 11.6°-20.3°C. Picton has an annual average rainfall of 1435 mm. Between March and September, average air temperatures are lower than average sea surface temperatures. However, in the warmer months, average air temperatures are higher than average sea surface temperatures. The Southland Current, coming along the East coast of the South Island is a main contributor to the water body around Picton as well as the D'urville current coming through the Cook Strait. Whenuanui Bay is to the north west of Picton and receives the same currents and rainfalls as Picton due to the proximity, approximately 5km between Whenuanui Bay and Picton.

2.1.5 Fiordland

New Zealand fiords are typical of global fiords, narrow and steep-sided ranging along the Western side of the lower South Island, from Milford sound to Preservation Inlet (Stanton & Prickard 1980). Westerly winds in combination with the mountainous geography of the land, result in heavy rainfall (5300-6300 mm/year (Villouta et al. 2001)), and strong freshwater inputs, so much so that power dams have been built to utilise the waters energy coming into the system. They have strong gradients in their physical properties, such as salinity, temperature, light quality, and wave action (Wing & Jack 2010). Saltwater wedge, typical of estuaries exist in this area. A permanent low salinity layer (~30ppt) is present throughout the fiords and increases in depth when heavy rainfall occurs (Villouta et al. 2001). High tannin in the freshwater layer reduces intensity of light, in conjunction with the spectral quality available to the marine environment below. Doubtful sound is about 40km long with three primary arms, and ranges in depth up to 421m at the deepest point. Samples were collected at the innermost area of Doubtful Sound at Deep Cove.

2.1.6 Stewart Island

Stewart Island is the southernmost main island in New Zealand. Pristine forests grow down to the sea edge, stopped only by the marine environment at high tides. Water temperatures vary around the year from 10°C in winter months to 16°C in January and February (MacKenzie 1991). The Southland current is the primary current in the area, made from subtropical water; flowing down the westerly side of the South Island from the Tasman front, and sub Antarctic Australasian water; coming up from the south. The Tasman front hits the west coast of the South Island and part of it heads south, wrapping around the southern side of Stewart Island, and cutting through Foveaux Strait and back up the east side of the South Island. The sub Antarctic water makes up 90% of the southland current, working its way up the east side of Stewart Island and South Island, eventually heading out to the Chatham rise (Chiswell 1996; Sutton 2003) Paterson Inlet is the primary bay, situated on the north-east of the Island, with a total area of 65km^2 (Willan 1981). Three islands, Ulva island, Native island, and Bradshaw island as well as the direction of the inlet protect the area from heavy seas. Port Pegasus is at the south-eastern end of Stewart Island and specimens were collected from this area.

2.2 NZOA-ON Monitoring and Data

Long term monitoring of oceanic chemistry is vitally important to understand natural fluctuations and patterns as well as use for future predictions and models. The National Institute of Water and Atmospheric Research (NIWA) has been actively monitoring ocean carbon chemistry since 1998 around Otago, however a more in-depth understanding around New Zealand was required. NIWA joined the Global Ocean Acidification Observing Network (GOA-ON) programme to provide spatially and temporally biogeochemical data from two locations: Dunedin and Firth of Thames sites. The same methodology has been set up for a further 12 different locations to create the New Zealand Ocean Acidification Observing Network (NZOA-ON). Water samples are taken fortnightly for analysis and data is available on a free open-access website (Vance et al. 2020).

Locations sampled for *Evechinus chloroticus* were chosen for their relative proximity to NZOA-ON sites. Table 2.2 provides information on latitude, longitude, the closest NZOA-ON site, water depth and number of urchins collected from each location included in this survey. Figure 2.2 and Figure 2.3 shows data from some of the NZOA-ON sites (https://marinedata.niwa.co.nz/nzoa-on/).

Water temperature typically decreases with increasing latitude as the climate turns from tropical-temperate to temperate down the length of New Zealand. As observed in Figure 2.2, when temperature is lower, pH is generally reduced. The pH reduction associated with warmer

temperatures is attributed to the quantity of active hydrogen bonds. Further to this, present-day average ocean surface pH is 8.1, a decrease of 0.1 pH units lower than pre-industrial values (Doney et al. 2009; Orr, 2011). It is expected that pH will be noted in warmer tropical waters prior to colder regions.

Salinity (ppt) was relatively constant at all NZOA-ON locations except for West Coast, a commonly accepted phenomena in the area resulting from heavy rainfall. The southern west coast of New Zealand is the wettest region because of westerly airflow over the country in conjunction with the orographic effects of the Southern alps; frequently seeing more than 10,000 mm of rainfall annual. Due to saline and freshwater chemical properties, freshwater often remains on top of marine water creating a freshwater wedge or intrusion. As the NZOA-ON samples are collected from the water surface, it is natural that the salinity is heavily reduced at the west coast site.

Carbonate is an important compound for marine organisms. A decrease in carbonate ion availability results in increased metabolic cost to from calcium carbonate structures while also increasing the rate of dissolution of these structures. All sites showed a degree of variability with the largest range at the West Coast. As pH is lowered to a more acidic state, carbonate ions become less abundant although this correlation is not displayed in the data due to the high variability.

Dissolved inorganic carbon (DIC) is the total amount of carbon dioxide (CO_2), bicarbonate (HCO_3^-) and carbonate (CO_3^{2-}) in seawater, and as it increases in the ocean, it drives a decrease in oceanic pH to more acidic conditions as chemical equilibrium is sustained. Dissolved inorganic carbon is relatively stable at all locations, except for West Coast which shows a large range.

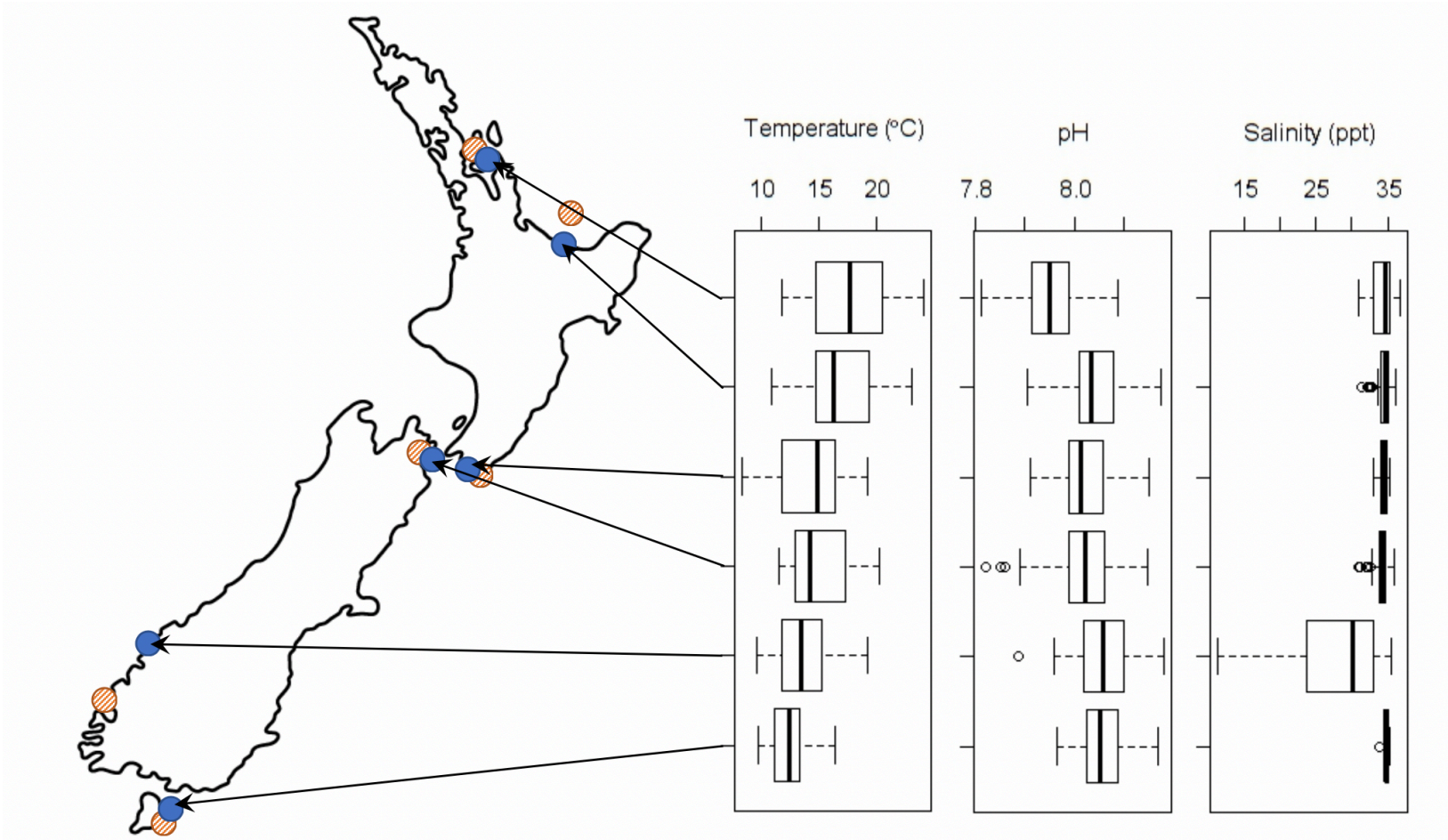

Figure 2.2 Locations of long term NZOA-ON monitoring sites (blue circles) and location sample specimens were collected (orange circles). Data analysed from NZOA-ON presented in graphs. (**Left graph**) Temperature (ºC) per NZOA-ON site (Auckland, Bay of Plenty, Wellington, West Coast, Stewart Island). (**Middle graph**) pH per NZOA-ON site (Auckland, Bay of Plenty, Wellington, West Coast, Stewart Island). (**Right graph**) Salinity (ppt) per NZOA-ON site (Auckland, Bay of Plenty, Wellington, West Coast, Stewart Island)

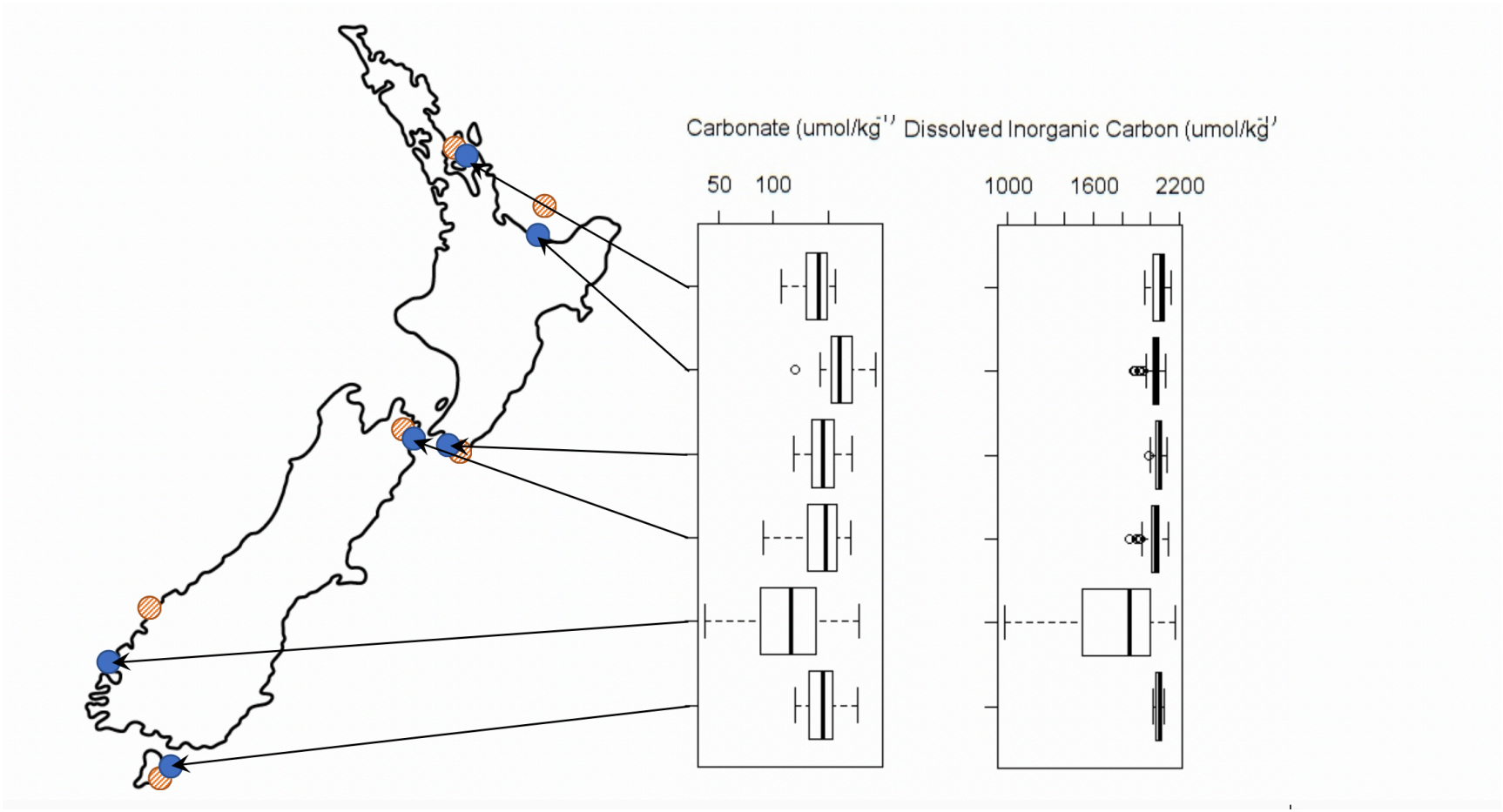

Figure 2.3 Locations of long term NZOA-ON monitoring sites (blue circles) and location sample specimens were collected (orange circles). Data analysed from NZOA-ON presented in graphs. (**Left graph**) Carbonate (µmol/kg-1) per NZOA-ON site (Auckland, Bay of Plenty, Wellington, West Coast, Stewart Island). (**Right graph**) Dissolved inorganic carbon (µmol/kg-1) per NZOA-ON site (Auckland, Bay of Plenty, Wellington, West Coast, Stewart Island).

2.3 Collection Methods

Ten or more adult *Evechinus chloroticus* were collected from subtidal regions by SCUBA or free divers at each location site (see Table 2.1). Urchins were given a unique identifying number, always starting with “Evchl” for the species names (*Evechinus chloroticus*), the next three letters were for their location e.g., “Pic” for Picton, followed by a number relating to the order of collection, for example “Evchl-Pic-6”. All specimens were shipped alive, packed in saltwater-dampened newspaper and ice packs, by overnight courier to the Portobello Marine Laboratory, University of Otago. If specimens required storage in the laboratory before dissection, they were held in filtered saltwater circulating aquariums without food.

Specimens were killed and dissected for analysis in the following chapters on allometry (Chapter 3), mineralogy (Chapter 4), and strength (Chapter 5).

3 Allometry

3.1 Introduction

Allometry is the study of size and its relationship with other biological traits such as morphology, physiology, and behaviour. Allometry can be separated into three different types; during growth (ontogenetic allometry), among individuals of similar developmental levels (static allometry), or among populations or species (evolutionary allometry) (Pelabon et al. 2014). Size relationships have been of interest to biological scientists since first outlined by Otto Snell (1892), particularly focusing on the allocation of resources and consequent effects on function, ecology and ultimately, evolution. Peters (1983) noted that predictions of morphology based on models can be imprecise due to small data sets and without consideration of outliers or shifts under selective pressures. Allometry now encompasses research into any relationship between body parts of an individual, normally described as a monotonic relationship. In echinoderms, for example, a relationship between Aristotle's lantern components and body mass in relation to feeding properties has been documented in five different *Strongylocentrotus* species (Lawrence et al. 1995), though the cause is unclear. It is theorised that allometric relationships constrain phenotypes, forcing evolution along a fixed path with low evolvability chances (Pelabon et al. 2014). The flipside to this theory is that allometry in individuals, populations and species may exhibit patterns of natural selection and functional optimisation to the environment, following abiotic and biotic pressures. Considering climate change, understanding the responses from biological organisms to ocean acidification, warming and ecosystem function has renewed (Riebesell & Gattuso 2014; Howes et al. 2015; Cramer et al. 2018).

The number of experimental studies providing evidence for adaptive differentiation in a wide selection of marine invertebrates has increased recently, particularly those with a focus on strong gradients and interactive conditions. Many these marine invertebrates demonstrating local adaptation have planktonic dispersal that can range in spatial scales, from meters to many kilometres (Sanford & Kelly, 2011), indicating the flow of genes and selection pressure trade-offs.

Marine invertebrates require energy to perform essential processes such as digestion, metabolism and respiration and for those marine invertebrates possessing a hard calcium carbonate skeleton or structure, calcification. Energy is divided to each essential process, ensuring an organism's survival. When energy is abundant, organisms allocate some of that energy to reproduction, ensuring the continuation of their genes and future population survival. If individuals are exerting tremendous amounts of energy to maintain essential processes,

such as calcification, reproduction efforts tend to be reduced (Llodra 2002). As we face climate change and predict future scenarios likely to occur within the next 100 years, it is reasonable to predict resource allocation towards reproduction, calcification and growth to change as a result of shifts in the ocean environment. Decreasing oceanic pH may result in organisms investing into processes to prevent dissolution or maintain skeletal structure for example, that might reduce the resources available for growth or reproduction. Conversely, if increasing temperatures increase metabolic rate, how will that affect growth and calcification? Understanding variation in morphometry and allometry in species undergoing changing oceanic and coastal conditions will be crucial to predicting the fate of species, their overall ecology and evolution over the next century or so.

What is needed here is a systematic approach, investigating a single important species in detail, looking at the size variation in skeletal elements in relation to overall growth of the individual in several different environments. The 'natural laboratory' provided by volcanic vents (Brinkman & Smith 2015; Zitoun et al. 2020), provides a useful proxy for morphometry and allometry under predicted climate change models. Here I investigate the size of skeletal elements of the common subtidal echinoid *Evechinus chloroticus* from six different locations around New Zealand, including an active CO_2 vent.

3.2 Methods

Ten to fourteen *Evechinus chloroticus* urchins were collected from six locations around New Zealand (see Chapter 2). Urchins were collected from the subtidal environment using SCUBA, packed in chilly bins upside down with cooler pads and shipped overnight to Portobello Marine Laboratory, Dunedin

For each urchin, test diameter was measured along two perpendicular lines, using digital calipers with a precision of 0.1 mm, ensuring caliper edges were placed between spines. Average test diameter was calculated as $\frac{Diameter\ 1 + Diameter\ 2}{2}$. Test height was measured from oral to aboral surface as close to the centre (greatest height) using digital calipers. The approximate volume (V) of each urchin was calculated assuming an oblate spheroid, using the formula $V = \frac{4}{3} pi\ (\frac{Diameter\ 1}{2})(\frac{Diameter\ 2}{2})(\frac{Height}{2})$ in mm^3. Each whole urchin was blotted dry with paper towels to remove excess surface water and wet weight was recorded to the nearest 0.1 g. Each urchin was killed and dissected. Aristotle's lanterns were removed; they and tests were scraped clean of excess tissue and wet weighed to the nearest 0.1 g. Individual tests and associated Aristotle's lanterns were placed in 7% sodium hypochlorite (bleach) for three days, rinsed with freshwater twice, dried at 60 °C for three days in a drying oven before being cooled to room temperature (approx. 16 °C) for three days.

3.2.1 Allometric Methods

Cleaned and dried tests and Aristotle's lantern for each urchin were weighed to the nearest 0.1 g to give total dry skeletal weight. Ten test plates were randomly selected, and the thickness was measured using digital calipers to the nearest 0.1 mm. The ten largest primary spines as determined by sight were selected from each individual, and measured for length, distal radius and proximal radius to calculate volume, assuming a truncated cone, given the formula $v = \frac{1}{3}\pi h(R^2 + r^2 + Rr)$ where *R* = proximal radius and *r* is distal radius. Spines were weighed to the nearest 0.01 g and spine density (g/cm^3) was calculated as weight (g) / volume (cm^3).

Cleaned and dried Aristotle's lanterns were weighed, then disassembled. All intact demi-pyramids and rotulas and were measured to the nearest 0.1 mm and weighed to the nearest 0.01 g. Demi-pyramid length was measured from oral tip to the epiphysis junction (Kirby et al. 2006), width was measured at the widest point near the epiphysis junction and weighed. Rotulas were measured for length at the longest axis, width perpendicular to length at the narrowest section near the centre and weighed. Epiphysis were not measured but were weighed. In total, 23 measurement types were taken from each of the 64 urchins.

3.2.2 Statistical Analysis

Analysis was completed using R-studio software to perform one-way ANOVA and data graphing. For each parameter, average, maximum, minimum and standard deviation were calculated.

Variation of an individual's elements was calculated as standard deviation while correlation within an element's measurements and amongst the elemental measurements were analysed using a one-way ANOVA to determine statistical significance of means. The coefficient of determination (r^2) were calculated and used for interpretation of linear correlations. Variations of elements amongst locations was analysed using a one-way ANOVA and a Tukeys test was utilised for post-hoc analysis to determine locations statistically different from each other.

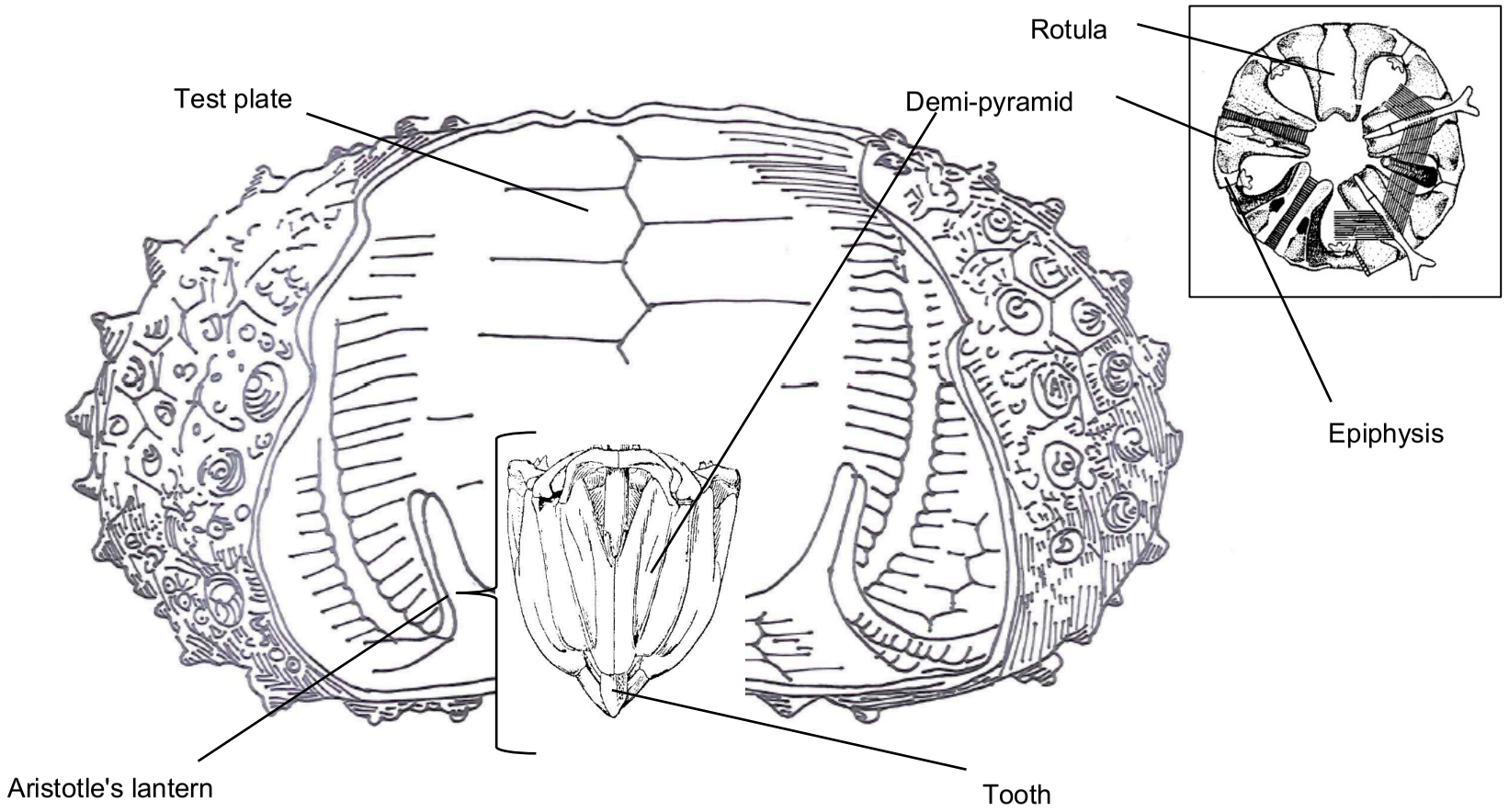

Figure 3.1 Schematic diagram of *Evechinus chloroticus* depicting key structural components measured for allometry, including test plate, and components of the Aristotle's lantern: demi-pyramid, rotula, epiphysis and tooth. Note teeth were not included in this study. Figure adapted from istockphoto (ID 489524854), British Geological Survey & Wilkie et al. (2015). Insert is top down schematic diagram of the Aristotle's lantern originally presented in Wilkie et al. (2015)

3.3 Results

Twenty three parameters were measured for each urchin, giving a total of 9,785 measurements; some measurements could not be made due to broken skeletal structures. Measurements made from the whole organisms (*diameter 1, diameter 2*, average diameter, height, test volume, total wet weight, scraped test weight, scrapped Aristotle's weight, cleaned test weight and cleaned Aristotle's lantern weight) are provided in Appendix A. Measurements compiled from the five different skeletal elements (test, primary spine, demi-pyramid, rotula and epiphysis) are provided in Appendix B. A summary of descriptive statistics from all urchins taken all together, without consideration of location are given in Table 3.1. These measurements have provided a very large and cumbersome dataset. I will approach subsequent analysis by first examining variance associated with each skeletal element – natural variations that occurs within individuals. Then I will examine relationships within and among skeletal elements – do they co-vary in animals of different sizes? In order to make sensible comparisons among measurements from individuals of varying size, a new standardised measurement was calculated as $\frac{measurment\ x}{average\ diameter}$ where measurment *x* is any of the parameters to be investigated.

Table 3.1 Average, standard deviation and number of samples for each parameter measured from 64 *Evechinus chloroticus* specimens collected around New Zealand.

Component	Measurement	Average	Standard deviation	N
Whole Test	Height (mm)	42.28	9.01	64
	Diameter One (mm)	79.03	16.27	64
	Diameter Two (mm)	77.72	16.06	64
	Average Diameter (mm)	78.37	16.14	64
	Total wet weight (g)	194.22	119.6	64
Test	Thickness (mm)	0.37	0.70	640
Primary Spine	Length (mm)	21.91	4.95	640
	Proximal diameter (mm)	1.58	0.21	640
	Distal diameter (mm)	0.72	0.12	640
	Weight (g)	0.04	0.01	640
	Volume (cm^3)	0.02	0.01	640
	Density (g/cm^3)	1.65	0.25	640
Demi-pyramid	Length (mm)	14.61	2.36	602
	Width (mm)	7.15	1.19	602
	Weight (g)	0.17	0.07	602
Rotula	Length (mm)	7.36	1.14	317
	Width (mm)	2.76	0.42	317
	Weight (g)	0.05	0.02	317
Epiphysis	Weight (g)	0.03	0.01	608

3.3.1 Variations in Elements Within an Individual

Size range of skeletal elements within individuals was investigated to quantify the variance within-individual variability. The average for each skeletal parameter measured within an individual was plotted against the test average diameter, with standard deviation plotted as error bars, graphing the variation seen in each measurement. It should be noted that primary

spines, demi-pyramids, and epiphysis were calculated from ten measurements per individual, while rotulae were calculated from five measurements per individual.

3.3.1.1 Test thickness

Measurements of test thickness had small variations with the 64 individuals measured (Figure 3.2, Appendix B). Standard deviation for test thickness ranged from 0.002 to 0.011 mm with an average standard deviation of 0.004 mm (N=64).

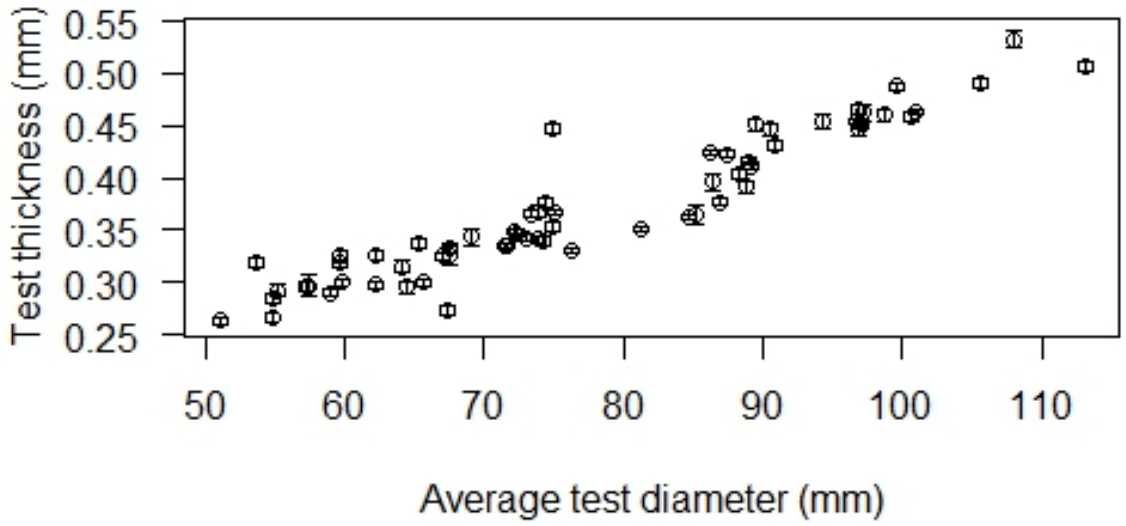

Figure 3.2 Test thickness variation from 64 *Evechinus chloroticus* specimens collected from six locations around New Zealand (N=64).

3.3.1.2 Primary Spine

Measurements of primary spines presented differing degrees of variation with individuals (Figure 3.3, Appendix B). Standard deviation for primary spine length ranged from 0.18 to 0.71 mm with an average standard deviation of 0.36 mm (N=64); a figure of $\pm$ 0.3 SD is a reasonable estimate of "variance" for this variable. Standard deviation for proximal radius and distal radius of the spine were much larger in comparison when plotted, but due to the small values of proximal and distal radius, they both present an average standard deviation of 0.01. Spine weight deviation ranged from 0.0004 to 0.004 g with an average of 0.001g. The error associated with volume calculated for a truncated cone ranged in deviation from 0.0002 to 0.004 cm^3 with an average of 0.001 cm^3. Spine density, calculated from volume and weight, incorporates both their associated deviation and thus the standard deviation ranged from 0.018 to 0.106 g/cm^3 with an average deviation of 0.046 g/cm^3. Graphical presentation of standard deviation relative to the measurement is a much better representation of associated deviation.

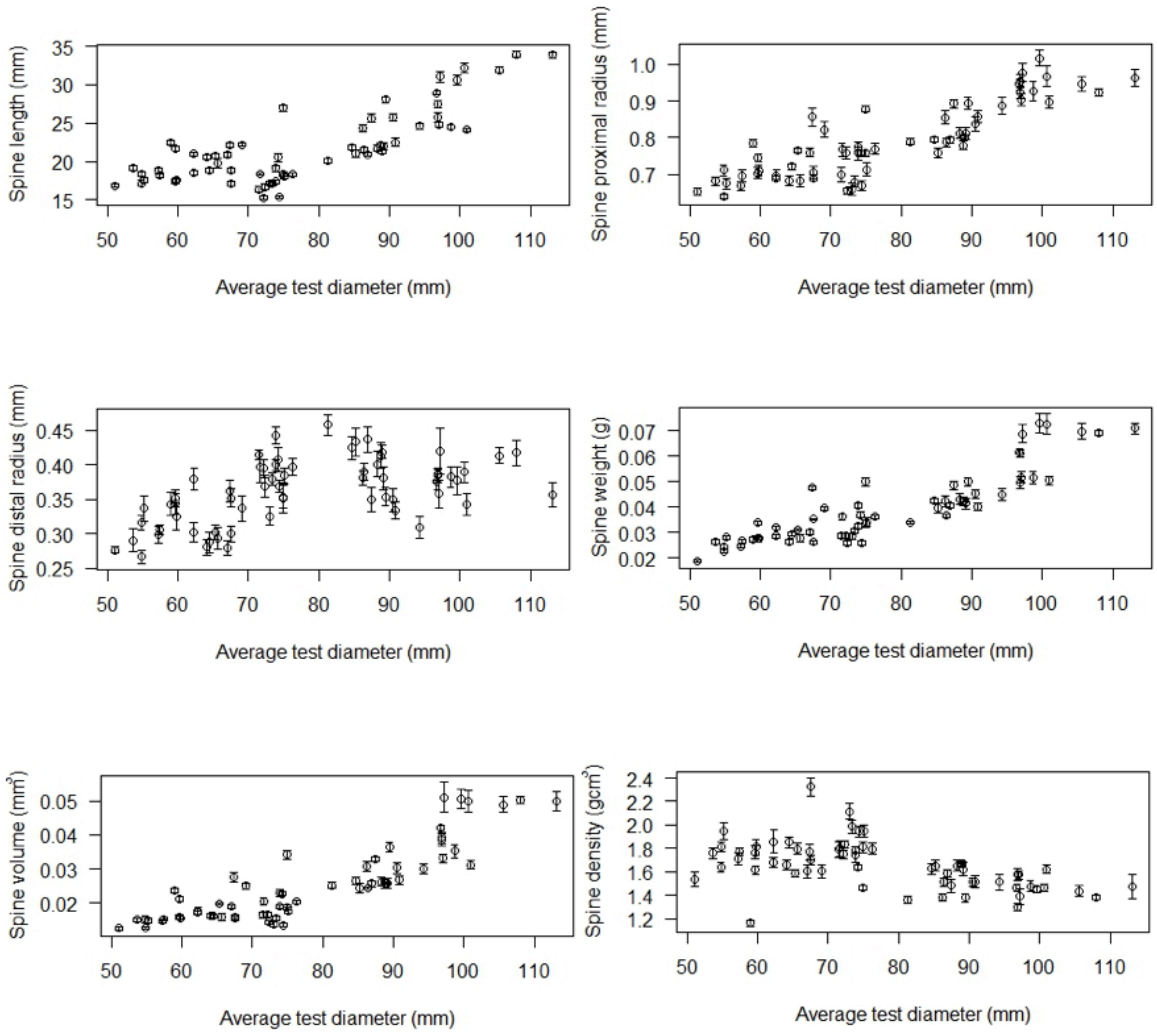

Figure 3.3 Variation of primary spine measurements in 64 *Evechinus chloroticus* individuals compared against average test diameter for the corresponding individual, error bars are standard deviation. Specimens were collected from six locations around New Zealand, each graph N=64. Top left: Spine length; Top right: Spine proximal radius; Middle left: Spine distal radius; Middle right: Spine weight; Bottom left: Spine volume; Bottom right: Spine density.

3.3.1.3 Demi-pyramid

Demi-pyramid measurements showed little variation with individuals (Figure 3.4, Appendix B). Demi-pyramid length had an average standard deviation of 0.04 mm and ranged from 0.02 to 0.12 mm; a low amount of natural variance for this element is expected. Similarly, demi-pyramid width standard deviation ranged from 0.008 to 0.09 mm; with an average demi-pyramid width standard deviation of 0.03 mm. Standard deviation of weight was very small in value but was similar to length and width when compared to the respective averages.

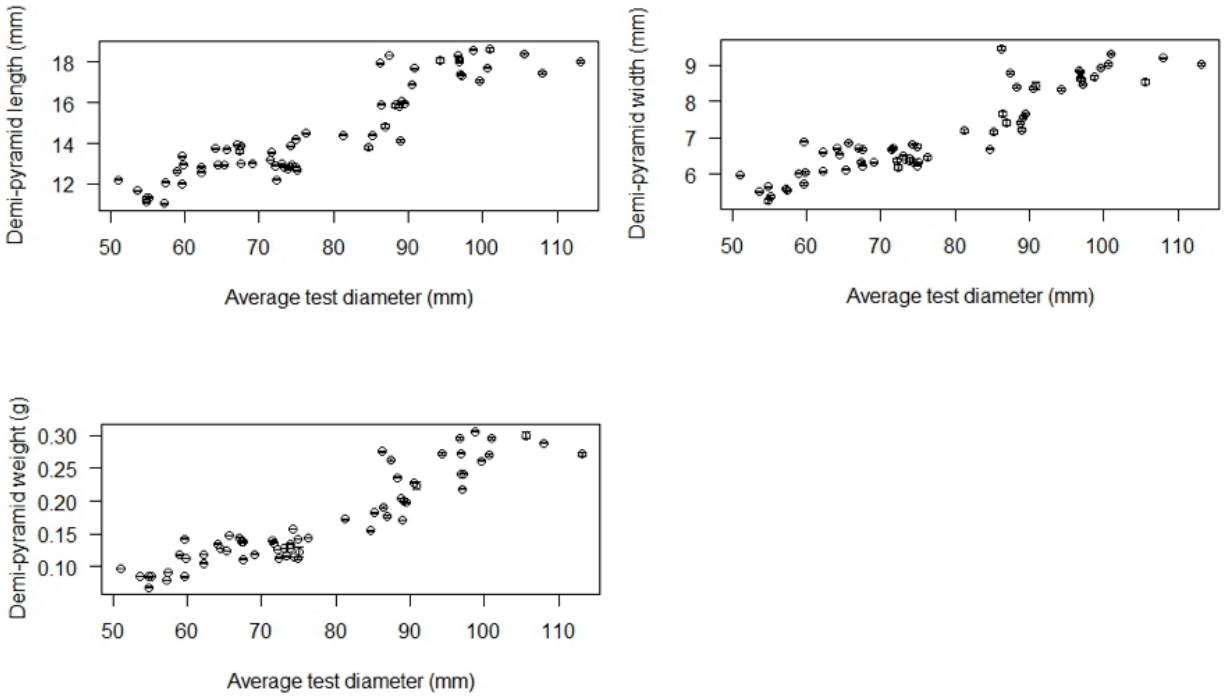

Figure 3.4 Variation of demi-pyramid measurements in 64 *Evechinus chloroticus* individuals compared against average test diameter for the corresponding individual, error bars are standard deviation. Specimens were collected from six locations around New Zealand, each graph N=64. Top left: Demi-pyramid length; Top right: Demi-pyramid width; Bottom left: Demi-pyramid weight.

3.3.1.4 Rotula and Epiphysis

Rotula and epiphysis variations within individuals was extremely small for all measurements presented in this study (Figure 3.5, Appendix B). Rotula length ranged for the urchins presented in this study with an average standard deviation of 0.042 mm. Similarly, rotula width standard deviation ranged from 0.003 to 0.095 mm; with an average standard deviation of 0.02 mm. Rotula weight ranged in deviation from 5.95×10^{-5} to 0.005 g with an average deviation of 0.0006 g per individual. Epiphysis weight standard deviation for individuals, was slightly lower than any rotula measurement, with an average of 0.0003 g. Standard deviation for all these variables is very low, indicating a small amount of variation occurring within individuals.

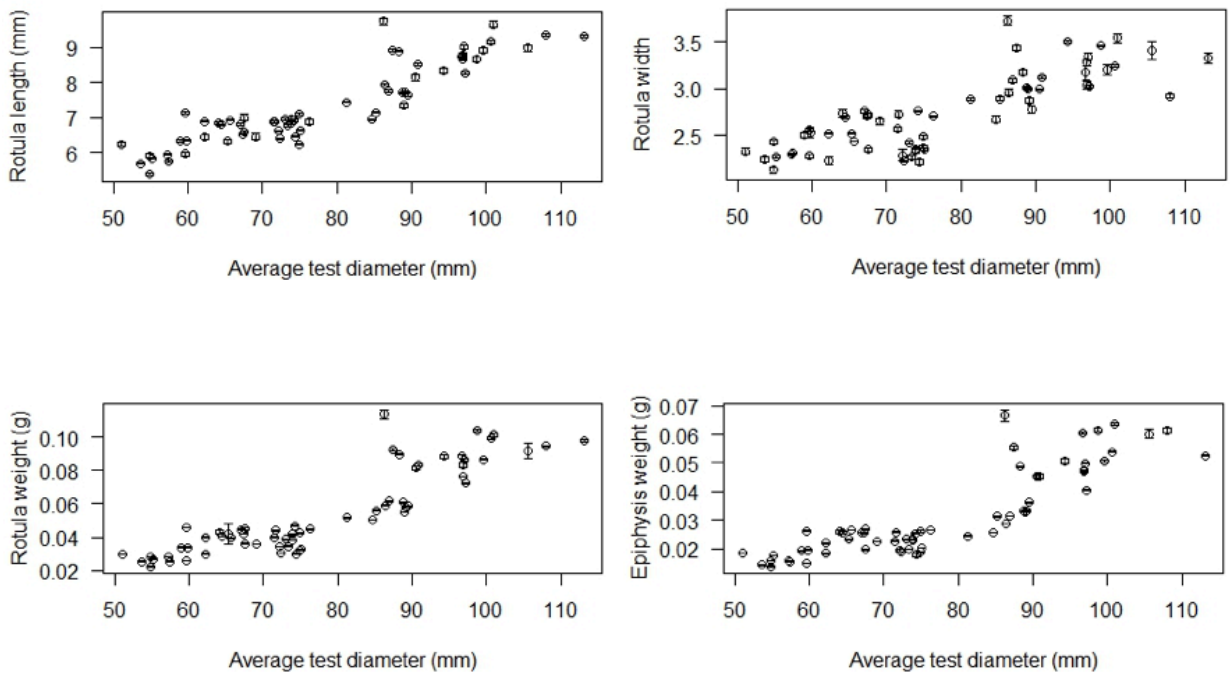

Figure 3.5 Variation of rotula and epiphysis measurements in 64 *Evechinus chloroticus* individuals compared against average test diameter for the corresponding individual, error bars are standard deviation. Specimens were collected from six locations around New Zealand, each graph N=64. Top left: Rotula length; Top right: rotula width; Bottom left: Rotula weight; Bottom right: Epiphysis weight.

Variation among skeletal elements within individuals is generally small, with low standard deviation for first measurements. As expected, standard deviation increases when calculations combine measurements. Average standard deviation was very low relative to the corresponding measurement for all but proximal radius and distal radius of the spines.

3.3.2 Correlations Within Elements

It is likely that various parts of the skeleton are strongly correlated, growing as the animal does. I would expect the parts of the Aristotle's lantern to develop in tandem. Here I examined all the possible cross-correlations among elements, irrespective of individual and location.

3.3.2.1 Whole Test Measurements

Two diameter measurements were taken per individual to further calculate the volume for an oblate spheroid so an assessment of the circular nature of the urchins is important to validate the assumption. The two perpendicular diameter measurements are compared for each individual (Figure 3.6) showing little difference between two measurements on the same individual. Data presented in this study indicates that there is a strong linear relationship between each diameter measured, indicating a circular shape, with at least bilateral symmetry,

however it is likely that the shape is moving towards an infinite number of symmetries, as is such with circles. The average test diameter was calculated for each urchin and is used for further comparisons for the whole test.

Test thickness was replicated ten times per individual and are presented against the corresponding individual's average diameter (Figure 3.7). The r^2 of the test thickness against average test diameter was 0.86 with a linear equation defined as: $y=0.054 + 0.004X + \varepsilon^i$ where $\varepsilon \sim N(0, 0.026^2)$. Test thickness was relatively consistent between individuals with the largest and smallest difference observed within an individual as 0.13 mm and 0.02 mm respectively. Due to the natural variance that can occur, there is some messiness in Figure 3.7 and the average test thickness for each individual was subsequently calculated and plotted against the average diameter and presented in Figure 3.8. When compared with the r^2 of all test thickness measured, the r^2 for average test thickness is higher (0.90), although the equation is very similar ($y=0.054 + 0.004X + \varepsilon^i$ where $\varepsilon \sim N(0, 0.022^2)$).

All test measurements (average diameter, height, weight, and volume) had strong positive correlations with each other as defined by r^2 values above 0.80 (Figures 3.9 – 3.14). Height had consistently lower r^2 values when compared to all other correlations presented in Table 3.2 (Height + measurement $r^2 = < 0.90$, not-height-measurement + not-height-measurement $r^2 = > 0.90$). It should be noted that this is a rather arbitrary cut off, as height vs. volume had a r^2 value of 0.89. The higher r^2 of height + volume is likely because of height when calculating volume. As height was not as strongly correlated compared to other measurements, it provides evidence for differing flatness and roundness of an oblate spheroid. For all test measurements (diameter, height, weight, and volume), as one measurement increases in size, the others increase as well, with a strong linear relationship as determined by the high r^2 values.

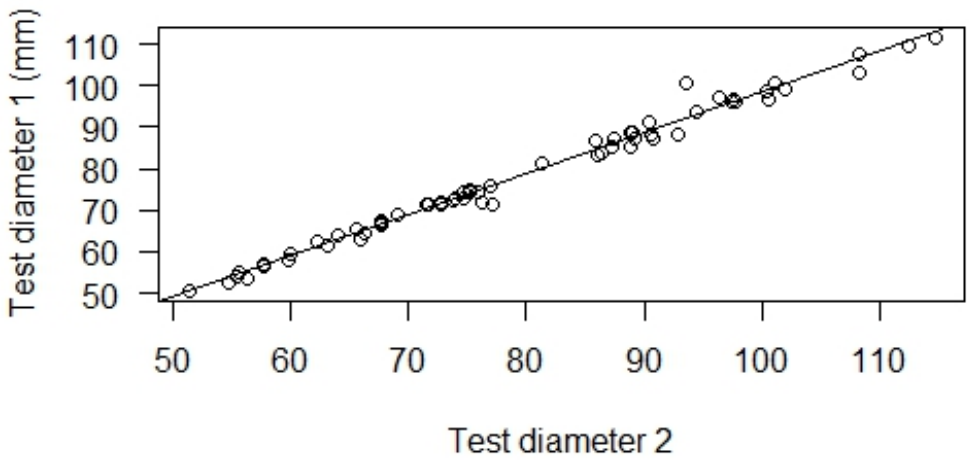

Figure 3.6 Correlation of test diameter 1 and test diameter 2 (perpendicular to test diameter 1) for 64 *Evechinus chloroticus* collected around New Zealand (N=64, r2=0.98).

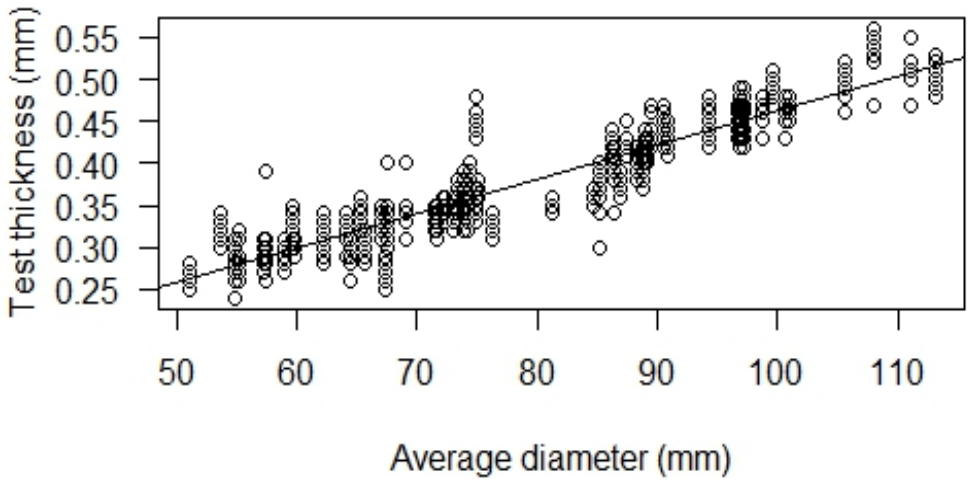

Figure 3.7 Correlation of 10 test thickness for average diameter of 64 *Evechinus chloroticus* species collected around New Zealand from six locations (N=640).

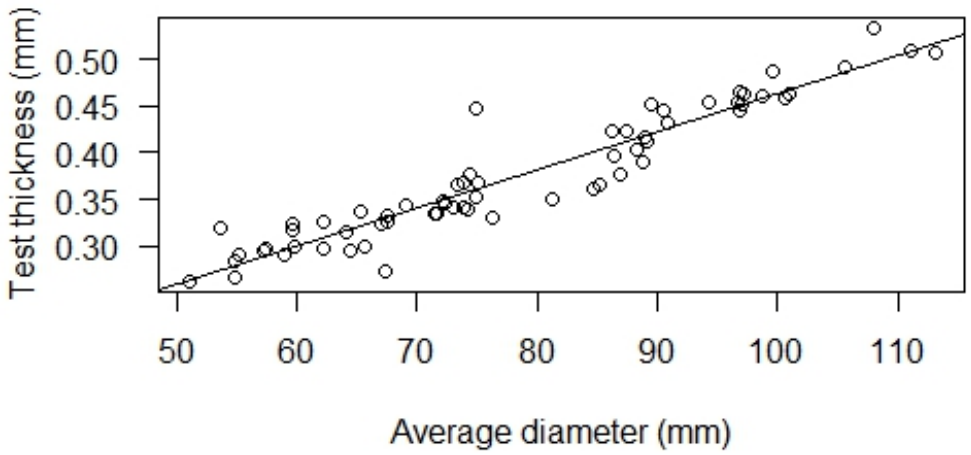

Figure 3.8 Correlation of average test thickness for each individual against the individuals average diameter for 64 *Evechinus chloroticus* collected around New Zealand from six locations (N=64).

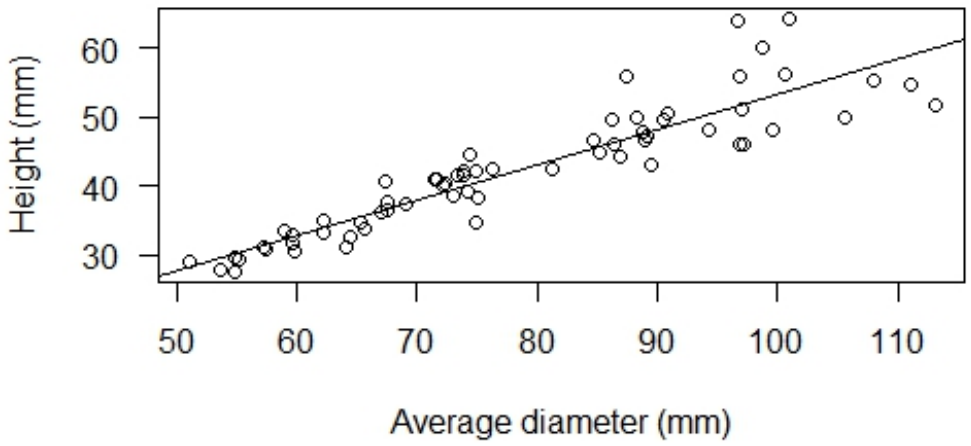

Figure 3.9 Urchin height for each individual against the individuals average diameter for 64 *Evechinus chloroticus* collected around New Zealand from six locations (N=64). Linear regression is added and presented as a solid line (ŷi=9.26218 + 1.63420 xi + ɛ̂i where ε ~ Ɲ (0,6.5432)

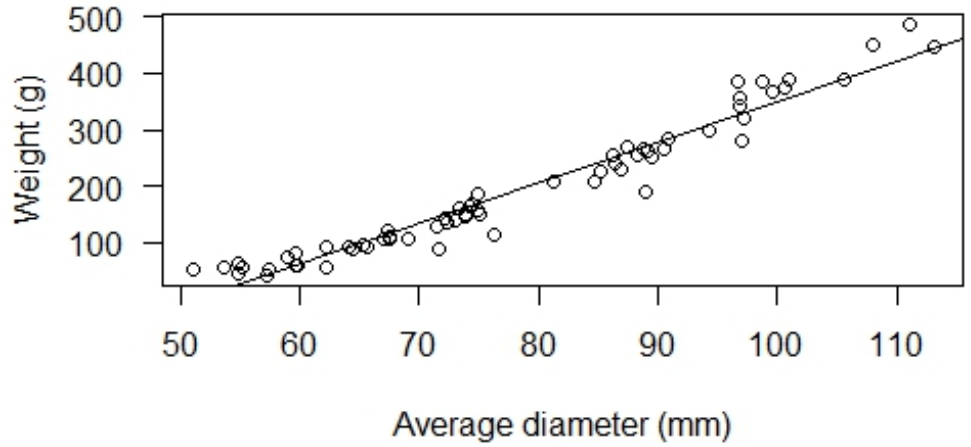

Figure 3.10 Urchin weight for each individual against the individuals average diameter for 64 *Evechinus chloroticus* collected around New Zealand from six locations (N=64). Linear regression is added and presented as a solid line ($\hat{y}i=9.26218 + 1.63420\ xi + \acute{\varepsilon}i$ where $\varepsilon \sim N(0, 6.5432)$).

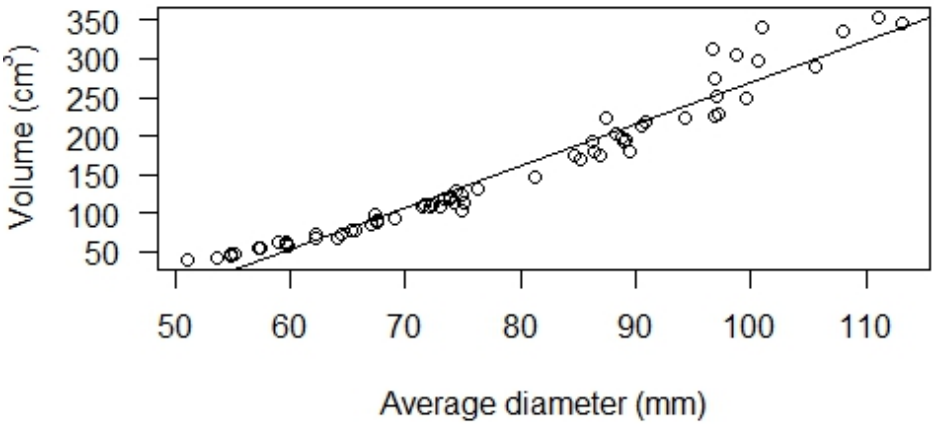

Figure 3.11 Test volume (cm^3) for each individual against the individual's average diameter for 64 *Evechinus chloroticus* collected around New Zealand from six locations (N=64). Linear regression is added and presented as a solid line ($\hat{y}i=51.5682 + 0.1758\ xi + \acute{\varepsilon}i$ where $\varepsilon \sim N(0,3.5952)$).

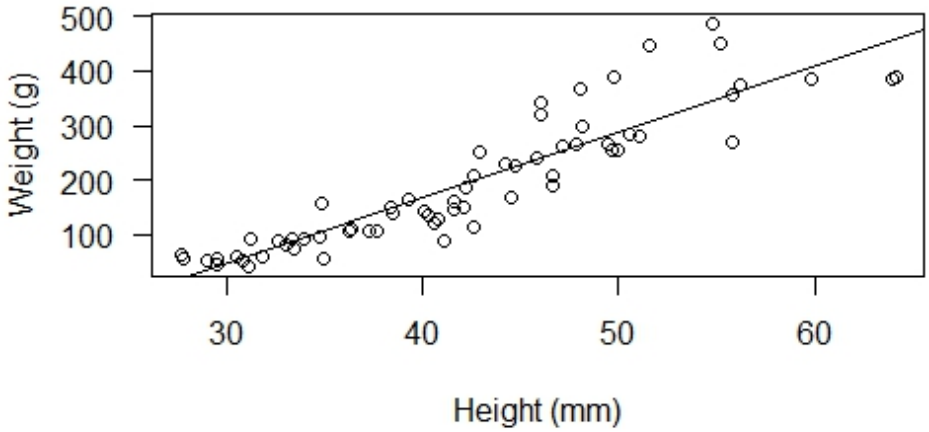

Figure 3.12 Weight for each individual urchin against the individual's height for 64 *Evechinus chloroticus* collected around New Zealand from six locations (N=64). Linear regressions presented as a solid line (ŷi=28.99396 + 0.06846 xi + ɛ́i where ε ~ Ɲ (0,0.82372)).

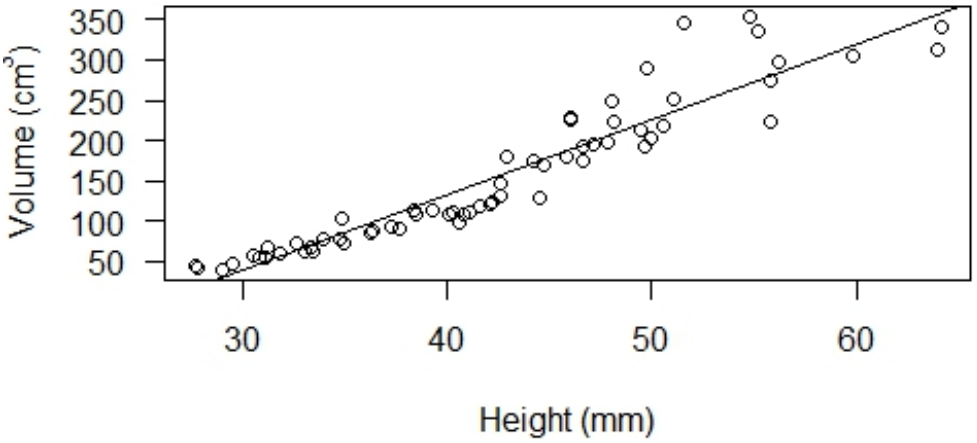

Figure 3.13 Test volume (cm^3) for each individual against the individual's height for 64 *Evechinus chloroticus* collected around New Zealand from six locations (N=64). Linear regressions presented as a solid line (ŷi=27.786876 + 0.095079 xi + ɛ́i where ε ~ Ɲ (0,2.9572)).

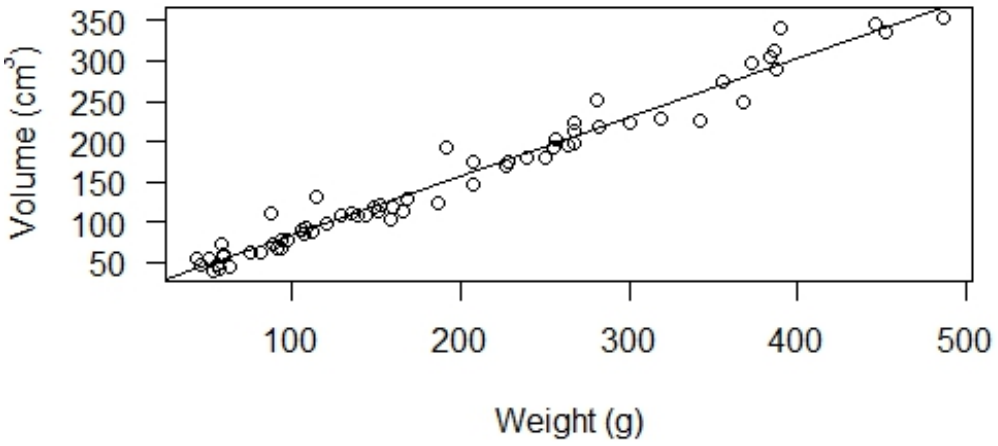

Figure 3.14 Test volume (cm^3) for each individual against the individual's wet weight for 64 *Evechinus chloroticus* collected around New Zealand from six locations (N=64). Linear regression is added and presented as a solid line (ŷi=−6.418953 + 1.315569 xi + ɛ̂i where ε ~ Ɲ (0,20.792)).

Table 3.2 Test measurements (average diameter, height, weight, volume) compared against each other. r^2 value for each comparison is presented in the bottom left section and figure reference is provided in top right of the table; r^2 greater than 0.80 are highlighted in yellow.

	Average diameter	Height	Weight	Volume
Average diameter		*Figure 3.9*	*Figure 3.10*	*Figure 3.11*
Height	r^2= 0.83		*Figure 3.12*	*Figure 3.13*
Weight	r^2=0.95	r^2=0.82		*Figure 3.14*
Volume	r^2=0.84	r^2=0.89	r^2=0.96	

3.3.2.2 Primary Spine

Primary spines were measured from 64 *Evechinus chloroticus* collected around New Zealand. The length, proximal diameter, distal diameter, and weight of ten primary spines per individual

were measured and the volume and density were subsequently calculated. The relationship between each primary spine measurement was investigated and presented in Table 3.3 and Figure 3.15 – Figure 3.29. Length was positively correlated with weight and volume with r^2 values above 0.80 (0.84 and 0.85 respectively). Proximal diameter of primary spines was also positively correlated, although not as strongly (r^2= 0.67) and distal diameter showed no obvious relationship with primary spine length (r^2= 0.02). Primary spine density was negatively correlated with length, although this did not exhibit a strong relationship (r^2= 0.29). Distal diameter of primary spines was not correlated with primary spine proximal diameter. As primary spine proximal diameter increases, primary spine weight also increases as shown in Figure 3.21 and has a r^2 value of 0.76. Proximal diameter was also strongly positively correlated with primary spine weight (r^2=0.85). Primary spine density and primary spine proximal diameter was negatively correlated with a moderately relationship (r^2= 0.41), although this is the strongest correlation of any primary spine measurement to density. Distal diameter had a very low relationship (r^2 < 0.20) for weight, volume, and density (0.16, 0.17 and 0.07 respectively). Weight had a strong correlation with volume, giving the highest r^2 value of any primary spine component correlation (r^2 = 0.91). Volume and distal diameter were only marginally correlated on a linear relationship with a r^2 value of 0.38.

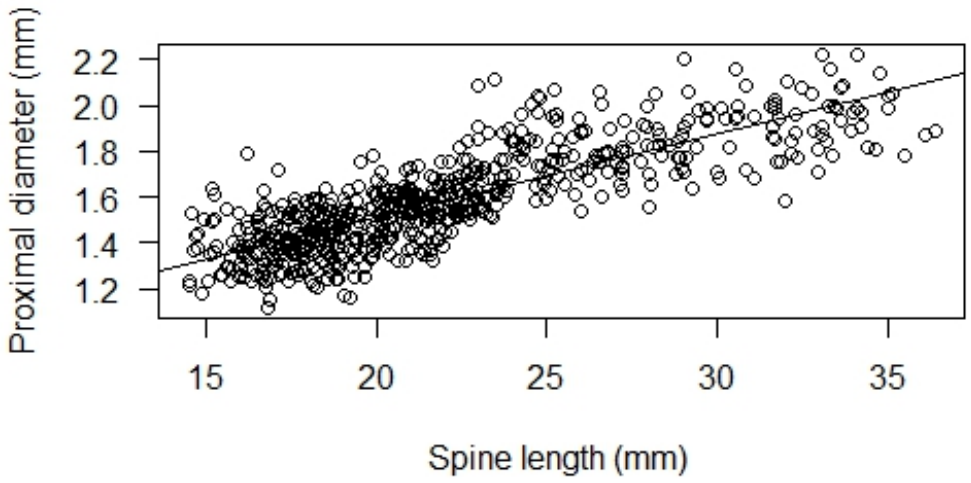

Figure 3.15 Spine length compared vs. proximal diameter for ten spines from each individual of 64 *Evechinus chloroticus* specimens collected around New Zealand (N=640).). Linear regressions presented as a solid line ($\hat{y}_i$=−7.2391 + 18.4131 x_i + $\acute{\varepsilon}_i$ where $\varepsilon \sim N(0, 2.8272)$).

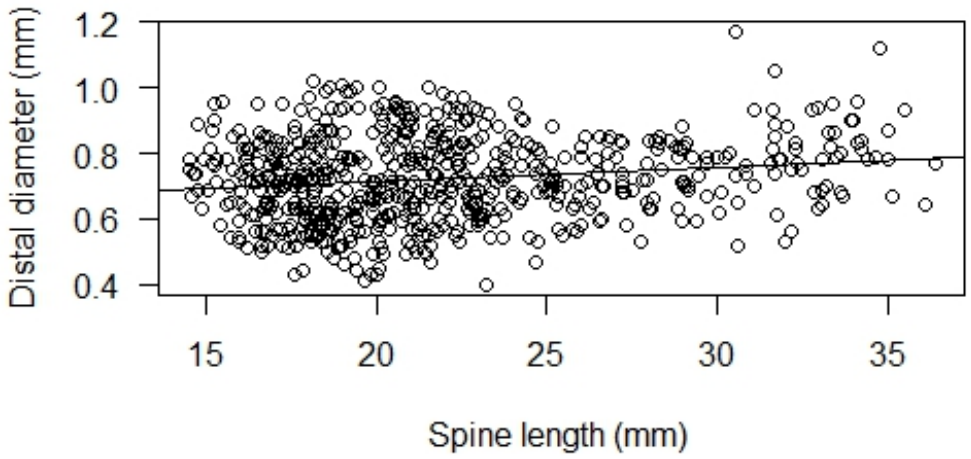

Figure 3.16 Spine length vs. distal diameter for ten spines from each individual of 64 *Evechinus chloroticus* specimens collected around New Zealand (N=640). Linear regressions presented as a solid line ($\hat{y}_i$=17.453 + 6.192 x_i + $\acute{\varepsilon}_i$ where $\varepsilon \sim N(0, 4.8562)$).

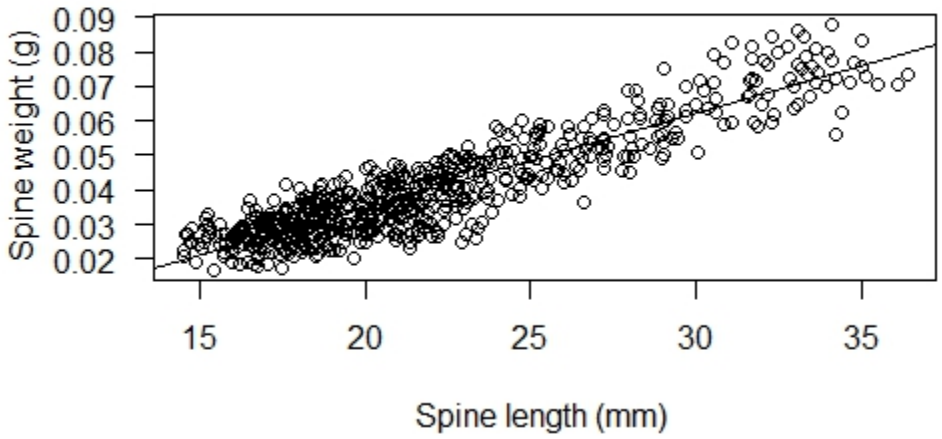

Figure 3.17 Spine length compared vs. spine weight for ten spines from each individual of 64 *Evechinus chloroticus* specimens collected around New Zealand (N=640). Linear regressions presented as a solid line ($\hat{y}_i$=9.8126+ 302.26153 x_i + $\acute{\varepsilon}_i$ where $\varepsilon \sim N(0,2.0642)$).

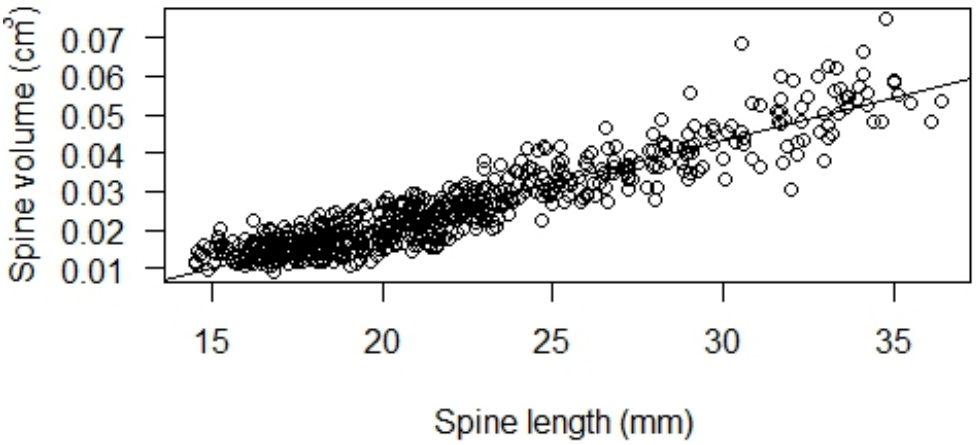

Figure 3.18 Spine length vs. spine volume for ten spines from each individual of 64 *Evechinus chloroticus* specimens collected around New Zealand (N=640). Linear regressions presented as a solid line ($\hat{y}_i = 12.1106 + 386.4249\, x_i + \acute{\varepsilon}_i$ where $\varepsilon \sim N(0,1.8622)$).

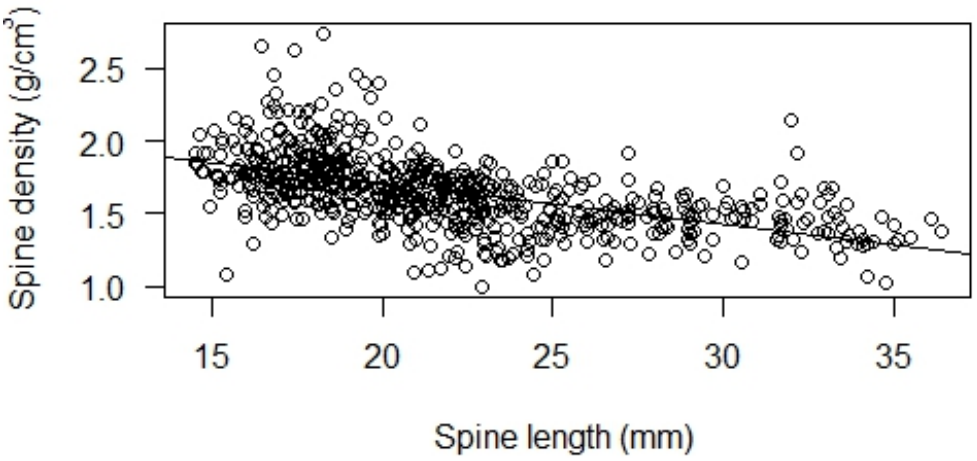

Figure 3.19 Spine length vs. spine density for ten spines from each individual of 64 *Evechinus chloroticus* specimens collected around New Zealand (N=640). Linear regressions presented as a solid line ($\hat{y}i = 39.7761 - 10.8171\, xi + \acute{\varepsilon}i$ where $\varepsilon \sim N(0,4.1132)$).

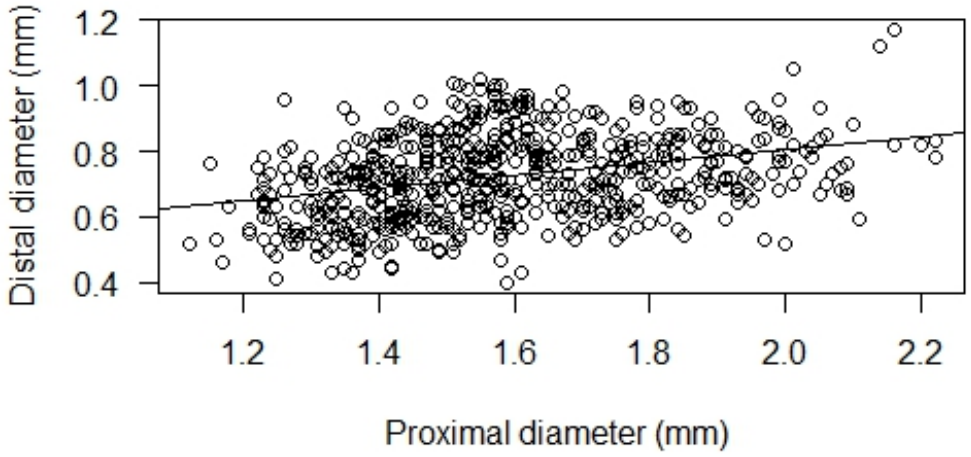

Figure 3.20 Proximal diameter vs. distal diameter for ten spines from each individual of 64 *Evechinus chloroticus* specimens collected around New Zealand (N=640). Linear regressions presented as a solid line (ŷi= 1.19073 + 0.54432 xi + ɛ́ where ε ~ Ɲ (0, 0.20712)).

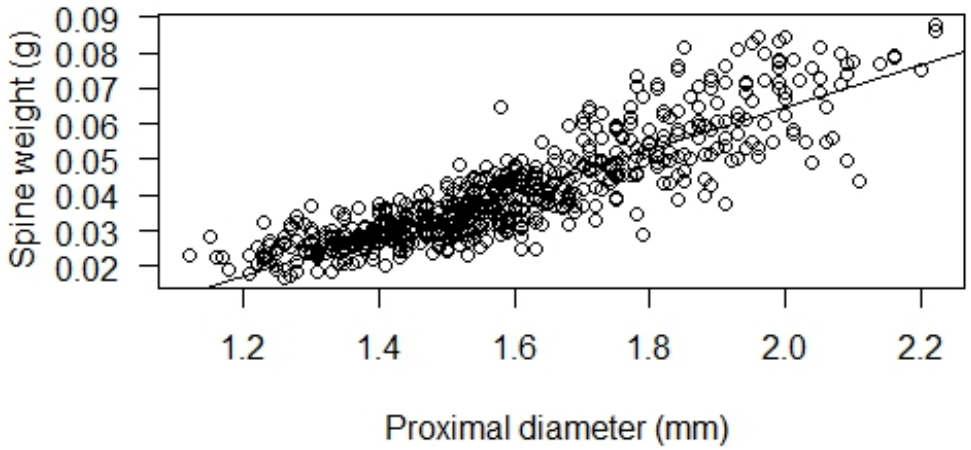

Figure 3.21 Proximal diameter vs. spine weight for ten spines from each individual of 64 *Evechinus chloroticus* specimens collected around New Zealand (N=640). Linear regressions presented as a solid line (ŷi= 1.067008 + 12.89712 xi + ɛ́i where ε ~ Ɲ (0,0.10732)).

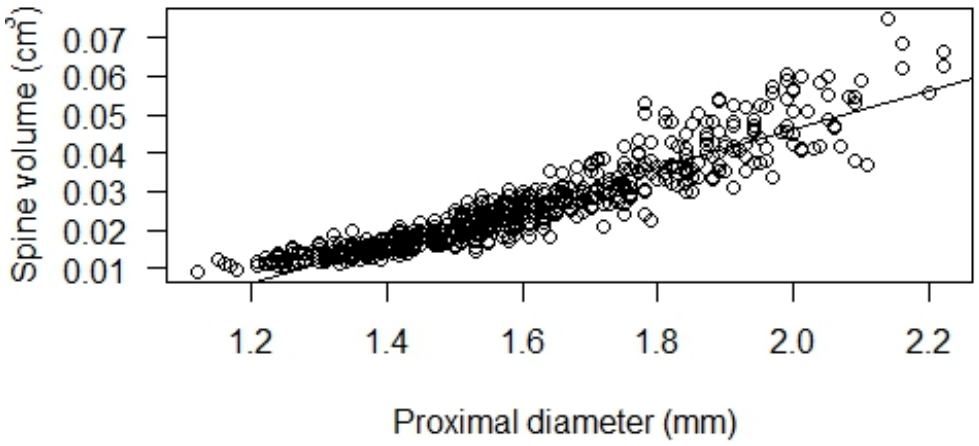

Figure 3.22 Proximal diameter vs. spine volume for ten spines from each individual of 64 *Evechinus chloroticus* specimens collected around New Zealand (N=640). Linear regressions presented as a solid line (ŷi= 1.146549 + 17.219943 xi + έ where ε ~ Ɲ (0,0.081552)).

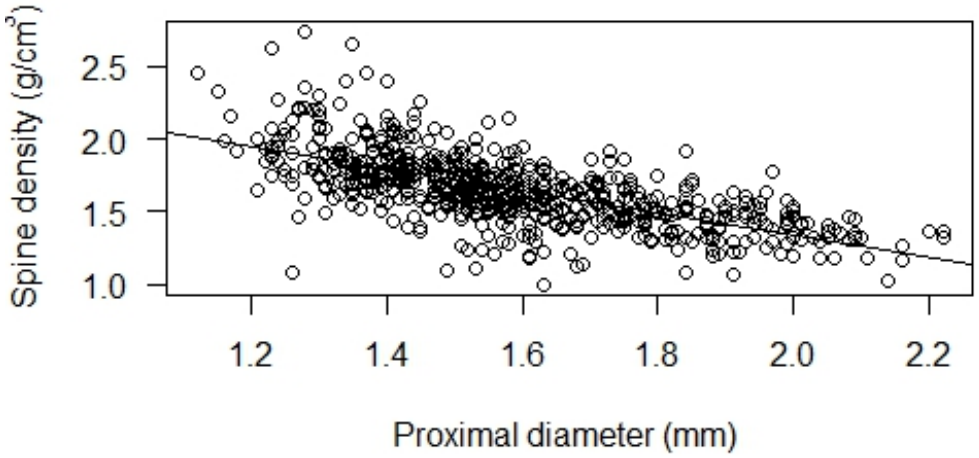

Figure 3.23 Proximal diameter vs. spine density for ten spines from each individual of 64 *Evechinus chloroticus* specimens collected around New Zealand (N=640). Linear regressions presented as a solid line (ŷi= 2.56321 - 0.59344 xi + έi where ε ~ Ɲ (0,0.16082)).

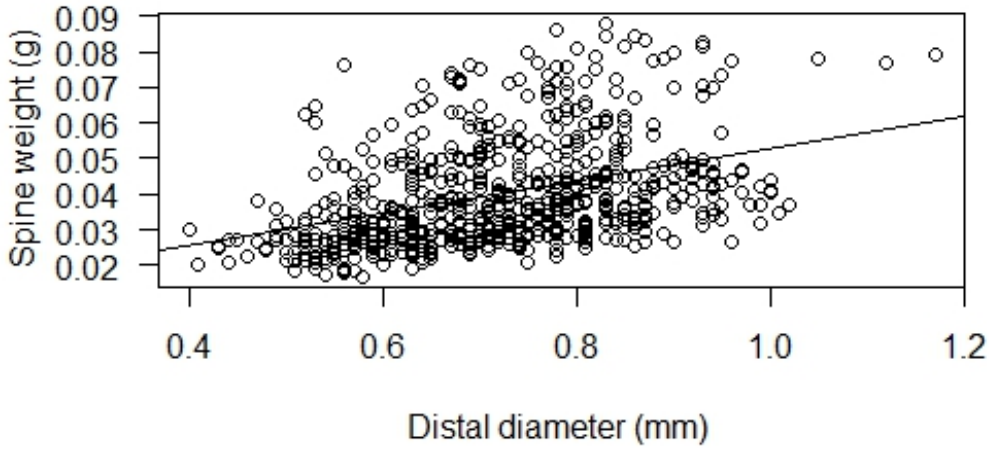

Figure 3.24 Distal diameter vs. spine weight for ten spines from each individual of 64 *Evechinus chloroticus* specimens collected around New Zealand (N=640). Linear regressions presented as a solid line (ŷi=0.58405 + 3.45512 xi + ɛ̂i where ε ~ Ɲ (0,0.11882)).

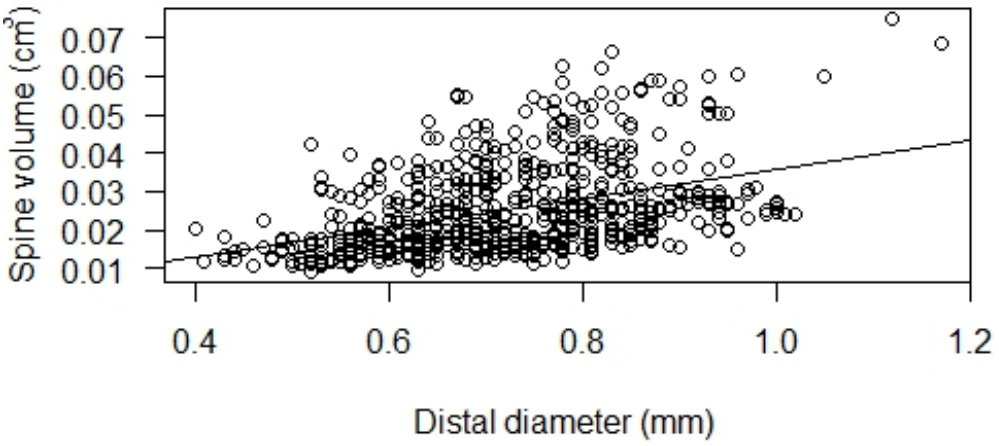

Figure 3.25 Distal diameter vs. spine volume for ten spines from each individual of 64 *Evechinus chloroticus* specimens collected around New Zealand (N=640). Linear regressions presented as a solid line (ŷi=0.60675 + 4.55766 xi + ɛ̂i where ε ~ Ɲ (0,0.11762)).

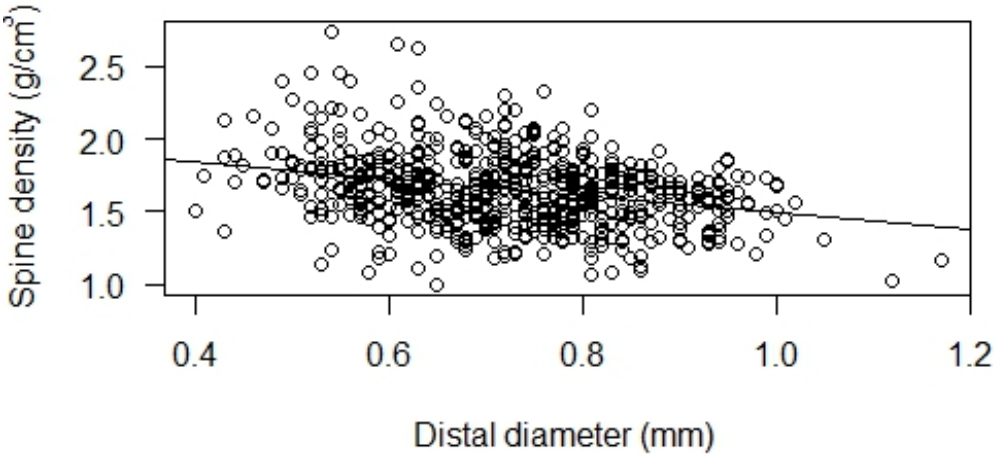

Figure 3.26 Distal diameter vs. spine densitty for ten spines from each individual 64 *Evechinus chloroticus* specimens collected around New Zealand (N=640). Linear regressions presented as a solid line (ŷi= 0.97859 - 0.15519 xi + ɛ́i where ε ~ Ɲ (0,0.12342)).

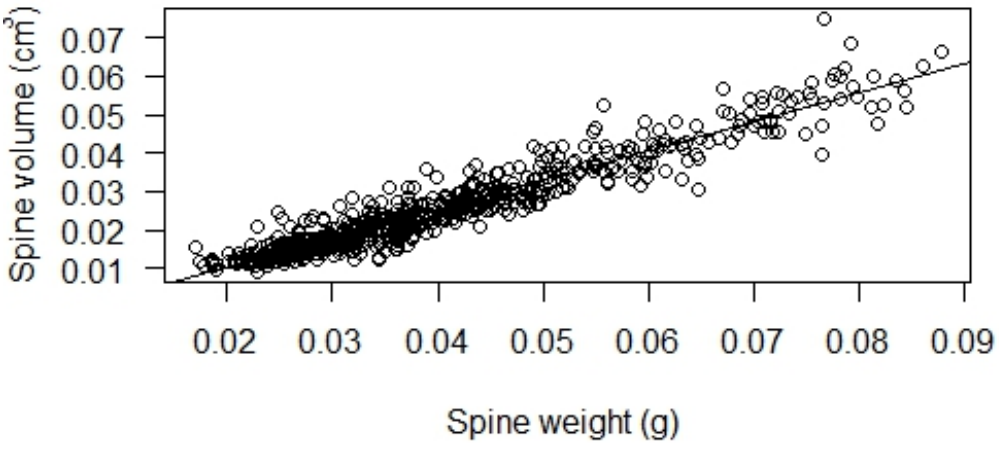

Figure 3.27 Spine weight vs. spine volume for ten spines from each individual of 64 *Evechinus chloroticus* specimens collected around New Zealand (N=640). Linear regressions presented as a solid line (ŷi= 0.0097107 + 1.1954705 xi + ɛ́i where ε ~ Ɲ (0,0.0044582)).

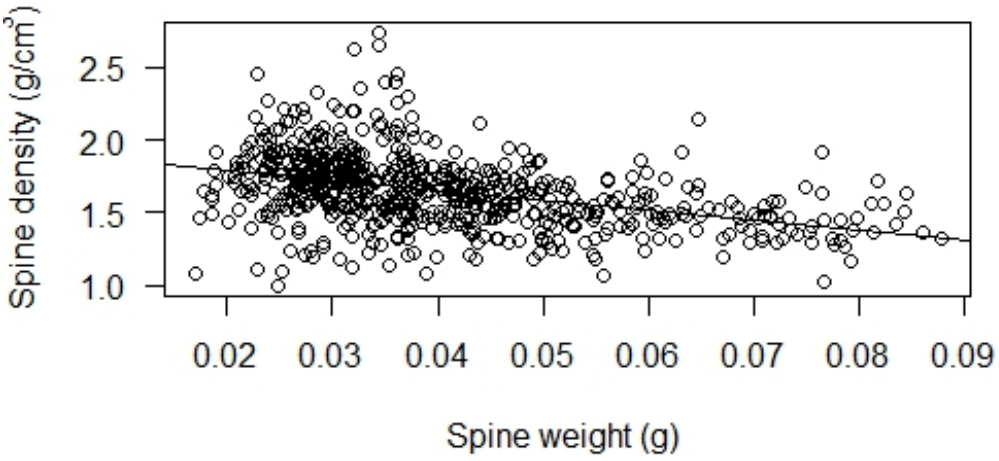

Figure 3.28 Spine weight vs. spine density for ten spines from each individual of 64 *Evechinus chloroticus* specimens collected around New Zealand (N=640). Linear regressions presented as a solid line (ŷi= 0.079517 - 0.023900 xi + ɛ̂i where ε ~ Ɲ (0,0.013522)).

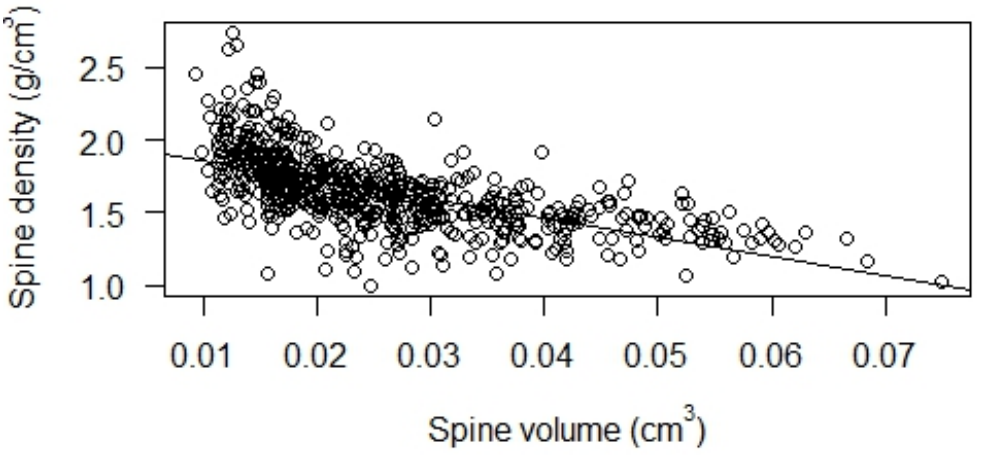

Figure 3.29 Spine volume vs. spine density for ten spines from each individual of 64 *Evechinus chloroticus* specimens collected around New Zealand (N=640). Linear regressions presented as a solid line (ŷi=0.074095 - 0.029509 xi + ɛ̂i where ε ~ Ɲ (0,0.0091992)).

Table 3.3 Primary spine measurements (length, proximal diameter, distal diameter, weight, volume and density) for 64 *Evechinus chloroticus* from six locations around New Zealand. r^2 values for each linear model are presented in the bottom left section; figure reference is provided in top right of the table. r^2 greater than 0.80 are highlighted in yellow.

	Length	Proximal diameter	Distal diameter	Weight	Volume	Density
Length		*Figure 3.15*	*Figure 3.16*	*Figure 3.17*	*Figure 3.18*	*Figure 3.19*
Proximal diameter	r^2=0.67		*Figure 3.20*	*Figure 3.21*	*Figure 3.22*	*Figure 3.23*
Distal diameter	r^2=0.02	r^2=0.10		*Figure 3.24*	*Figure 3.25*	*Figure 3.26*
Weight	r^2=0.82	r^2=0.75	r^2=0.15		*Figure 3.27*	*Figure 3.28*
Volume	r^2=0.85	r^2=0.86	r^2=0.17	r^2=0.90		*Figure 3.29*
Density	r^2=0.30	r^2=0.45	r^2=0.08	r^2=0.16	r^2=0.39	

3.3.2.3 Aristotles Lantern

Three components of the Aristotle's lantern were measured from each of the 64 *Evechinus chloroticus* collected around New Zealand. These were demi-pyramids, rotula and epiphyses. Only complete components were measured so there are differences in the number sampled in this data set.

3.3.2.4 Demi-pyramid

Ten demi-pyramids were measured from each of the 64 *Evechinus chloroticus* collected around New Zealand. The length, width and weight of demi-pyramids were measured for all that were complete; 602 actual measurements from the possible 640. The relationship between each demi-pyramid measurement was investigated and presented in Table 3.4; Figure 3.30 – Figure 3.32. The correlation between length, width and weight were all strongly positively with r^2 values above 0.90 amongst the components measured for all individuals in this study. Length and weight had the strongest correlation, with a r^2 value of 0.95. The correlation between weight and width was only slightly less in terms of r^2 values (0.94) and only marginally higher than the correlation between length and width (0.93). Variation in measurements increased with increasing sizes for all measurements as seen by the wider spread of data points.

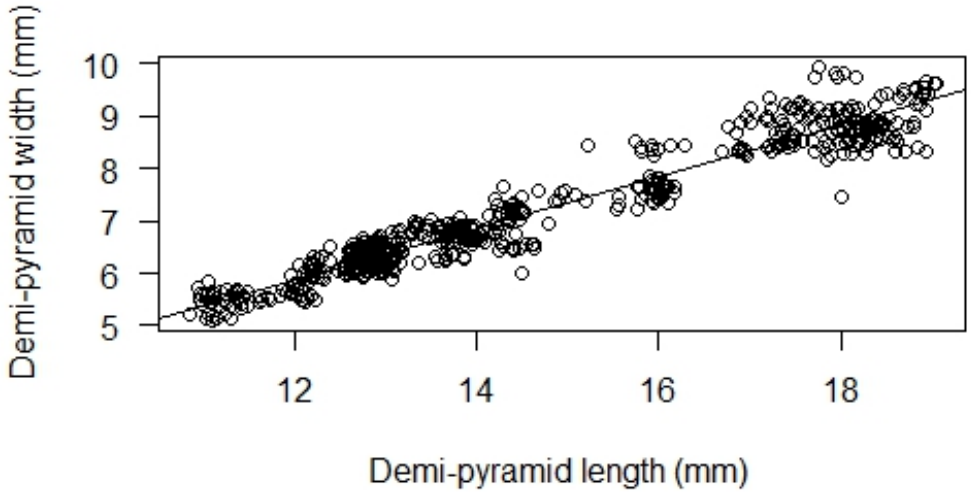

Figure 3.30 Demi-pyramid length vs. demi-pyramid width from each individual of 64 *Evechinus chloroticus* specimens collected around New Zealand (N=601). Linear regressions presented as a solid line (ŷi= 0.99328 + 1.90329 xi + ɛ́i where ε ~ Ɲ (0,0.61082)).

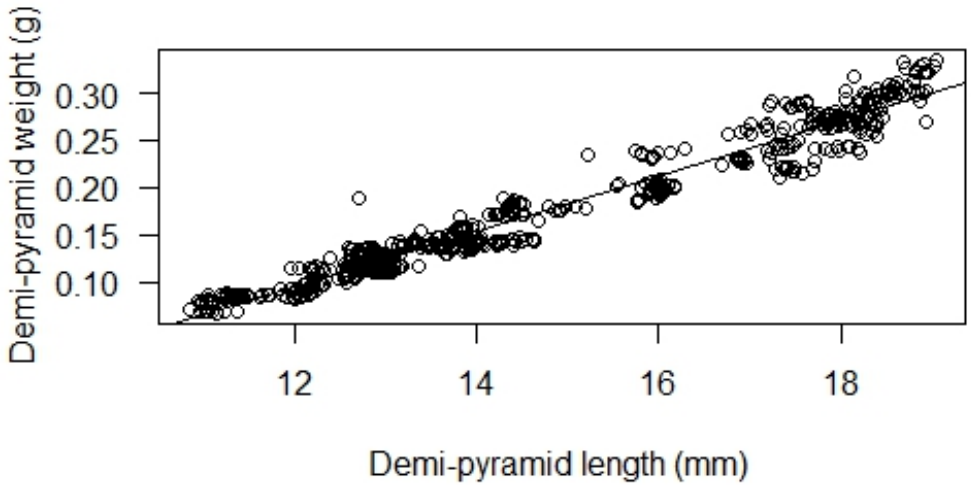

Figure 3.31 Demi-pyramid length vs. demi-pyramid weight from each individual of 64 *Evechinus chloroticus* specimens collected around New Zealand (N=601). Linear regressions presented as a solid line (ŷi= 9.01522 + 32.59098 xi + ɛ́i where ε ~ Ɲ (0,0.4942)).

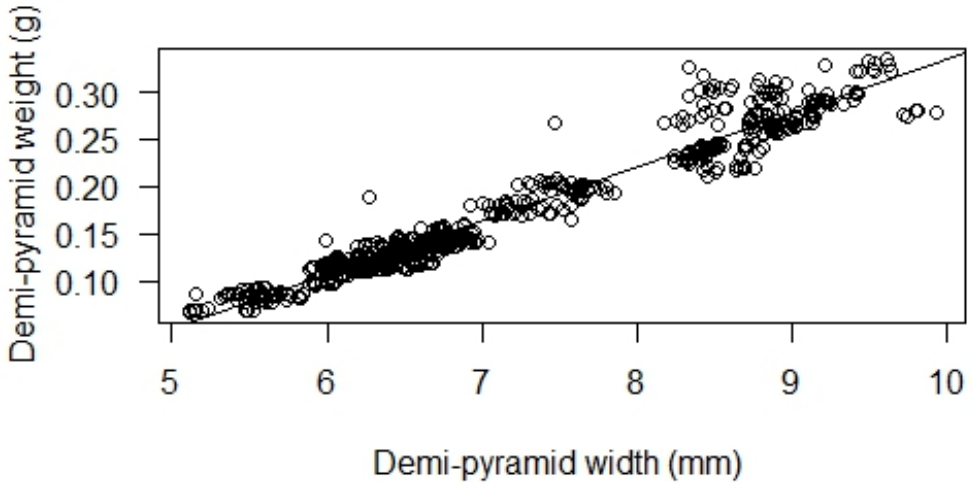

Figure 3.32 Demi-pyramid length vs. demi-pyramid weight from each individual of 64 *Evechinus chloroticus* specimens collected around New Zealand (N=601). Linear regressions presented as a solid line (ŷi= 4.33295 - 16.43324 xi + ɛ́i where ε ~ Ɲ (0,0.28732)).

Table 3.4 Demi-pyramid measurements (length, width, and weight) for 64 *Evechinus chloroticus* collected from six locations around New Zealand. r^2 values for each linear model are presented in the bottom left section and figure references is provided in the top left. r^2 greater than 0.80 are highlighted in yellow.

	Length	Width	Weight
Length		*Figure 3.30*	*Figure 3.31*
Width	r^2=0.93		*Figure 3.32*
Weight	r^2=0.95	r^2=0.94	

3.3.2.5 Rotula

Five rotulas were measured from each of the 64 *Evechinus chloroticus* collected around New Zealand. The length, width, and weight of rotulas were measured for all that were complete; 317 actual measurements from the theoretically possible 320. The relationship between each rotula measurement was investigated and presented in Table 3.5 and Figure 3.33 – Figure 3.35. Rotula length had a higher correlation to weight than width (0.94 and 0.82 respectively). Rotula width also had a stronger association to rotula weight (r^2=0.87).

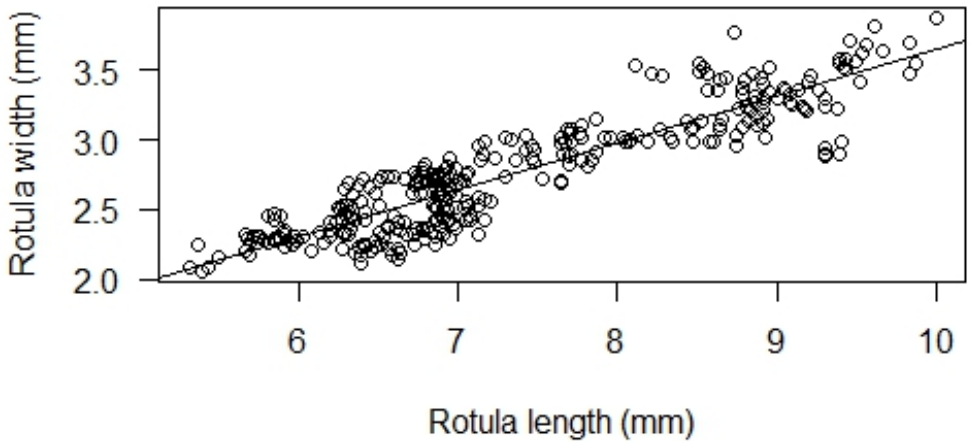

Figure 3.33 Rotula length vs. rotula width from each individual of 64 *Evechinus chloroticus* specimens collected around New Zealand (N=317). Linear regressions presented as a solid line (ŷi= 0.56396 + 2.46218 xi + ɛ̂i where ε ~ Ɲ (0,0.48282)).

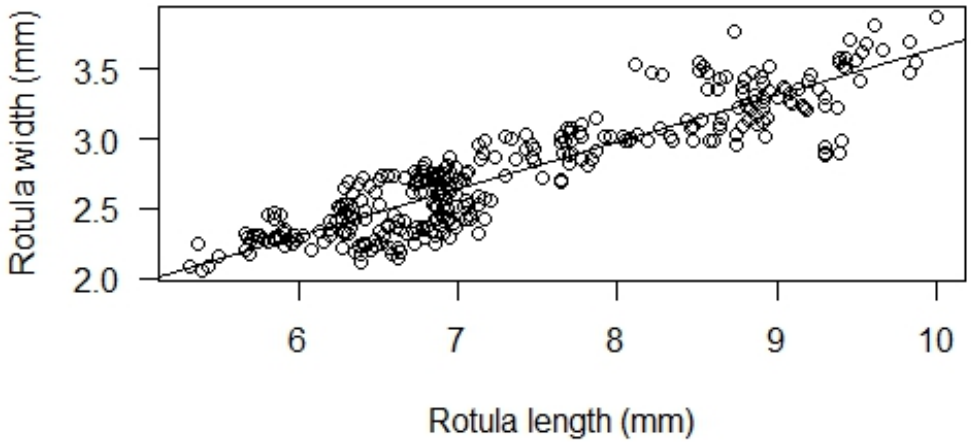

Figure 3.34 Rotula length vs. rotula weight from each individual of 64 *Evechinus chloroticus* specimens collected around New Zealand (N=317). Linear regressions presented as a solid line (ŷi= 4.97660 + 43.23080 xi + ɛ̂i where ε ~ Ɲ (0,0.26642)).

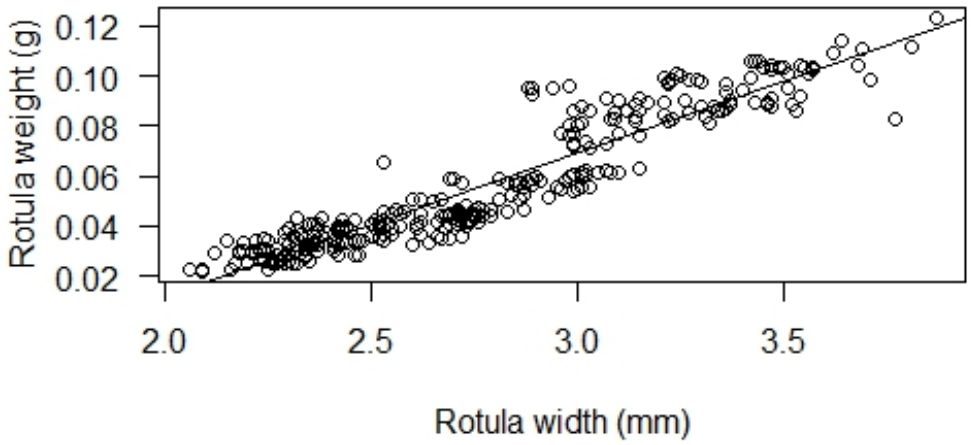

Figure 3.35 Rotula width vs. rotula weight from each individual of 64 *Evechinus chloroticus* specimens collected around New Zealand (N=317). Linear regressions presented as a solid line (ŷi= 1.91545 + 15.33091 xi + ɛ́i where ε ~ Ɲ (0,0.14892)).

Table 3.5 Rotula measurements (length, width, and weight) for 64 *Evechinus chloroticus* collected from six locations around New Zealand. Graphs and linear models are presented in the bottom left section, linear model equations and r^2 values for each, N=317; r^2 greater than 0.80 are highlighted in yellow.

	Length	Width	Weight
Length		*Figure 3.33*	*Figure 3.34*
Width	r^2=0.82		*Figure 3.35*
Weight	r^2=0.94	r^2=0.87	

3.3.2.6 Epiphysis

Ten epiphyses were weighed from each of the 64 *Evechinus chloroticus* collected around New Zealand. There were no other measurements made on epiphysis so correlation within epiphysis could not be undertaken.

In summary, primary spine measurements varied in their correlation with the measurements presented here, with r^2 values from 0.02 (length + distal diameter) to 0.90 (weight + volume). Spine length, weight and volume were all positively correlated with r^2 values > 0.82. As expected, related measurements within elements in the Aristotle's lantern are strongly correlated, with r^2 values greater than 0.80 for all correlations within a single structure. Demi-

pyramid measurements were strongly positively correlated with all correlations above 0.93. Rotula length, width and weight were positively correlated with r^2 values above 0.82.

3.3.3 Correlation Amongst Elements

The relationship of skeletal component measurements against non-related skeletal component measurements was investigated. This was used to explore if skeletal elements measurements were dependent on each other regardless of the differences in element. The coefficient of determination (r^2) values for all comparisons analysed are presented in Table 3.6.

Primary spine measurements did not correlate with demi-pyramid, rotula or epiphysis measurements in this study, all with low r^2 values (r^2 <0.70). Primary spine density consistently had a lower correlation to any other skeletal element measurement, with the largest r^2 value given as 0.22 for rotula weight. When primary spine length, weight and volume was compared with the demi-pyramid measurements, the r^2 values were the largest observed but were still considerably low.

Demi-pyramid, rotula and epiphysis measurements, when compared with each other produced very high r^2 values, with 11 of the 15 possible interactions ≥0.90, and the remaining 4 interactions >0.80. The lowest r^2 value was given for Aristotle's lantern comparative element measurements with demi-pyramid width and rotula width (r^2=0.82), while the largest value was between rotula weight and epiphysis weight (r^2=0.95).

Table 3.6 Coefficient of determination values for each skeletal component measured against each skeletal component of 64 *Evechinus chloroticus* collected from six locations around New Zealand. Dark grey squares indicate correlations within an element, white and yellow squares indicate correlations amongst elements, yellow squares indicate correlations amongst elements with a r^2 value greater than 0.80.

		Primary Spine				Demi-pyramid			Rotulae		
		Length (mm)	Weight (g)	Volume (cm^3)	Density (g/cm^3)	Length (mm)	Width (mm)	Weight (g)	Length (mm)	Width (mm)	Weight (g)
Primary Spine	Length (mm)	-									
	Weight (g)	0.82									
	Volume (cm^3)	0.85	0.90								
	Density (g/cm^3)	0.3	0.16	0.39							
Demi-pyramid	Length (mm)	0.62	0.63	0.62	0.21						
	Width (mm)	0.64	0.63	0.62	0.2	0.93					
	Weight (g)	0.62	0.65	0.64	0.21	0.95	0.94				
Rotulae	Length (mm)	0.56	0.58	0.56	0.19	0.91*	0.96*	0.92*			
	Width (mm)	0.59	0.49	0.47	0.21	0.84*	0.82*	0.83*	0.82		
	Weight (g)	0.49	0.58	0.57	0.22	0.91*	0.94*	0.94*	0.94	0.87	
Epiphysis	Weight (g)	0.61	0.61	0.59	0.18	0.90*	0.92*	0.94*	0.91*	0.83*	0.95*

3.3.4 Elements Amongst Locations

Urchins were collected from six different locations around New Zealand: Auckland, White Island, Wellington, Picton, Fiordland and Stewart Island. The average, standard deviation and number for each specimen from each location is presented in the Table 3.7. Fiordland specimens typically had the largest spines (average=30.59 mm, SD=3.09), proximal diameter (average=1.89 mm, SD=0.14) and weight (average=0.06 g, SD=0.01). Samples from Picton had the largest distal diameter (average=0.83 mm, SD=0.11), however the White Island specimens had the largest spine density compared to other locations in this study (average=1.89 g/cm^3, SD=0.24). Samples from Stewart Island had the largest average for all internal components: demi-pyramids (length, width, and weight), rotula (length, width, and weight) and epiphysis (weight). When investigating the smaller averages for skeletal components measured in this study, the results were less consistent. North Island specimens tended to have the smallest averages; however, it was spread between the three locations:' Auckland, White Island and Wellington. There were two component measurements that had the same average for all three locations: primary spine weight and epiphysis weight. Auckland specimens had the smallest average for primary spine proximal diameter (average =1.42 mm, SD=0.02), demi-pyramid length (average =12.40 mm, SD=1.09), demi-pyramid weight (average=0.10 g, SD=0.02), rotula height (average=6.20 mm, SD=0.49) and rotula weight (average=0.03 g, SD=0.01). White Island specimens had the smallest average primary spine length (average=16.96 mm, SD=1.83), primary spine weight (average=0.03 g, SD=0.01), and rotula width (average=2.35 mm, SD=0.12). Samples from Wellington had the smallest primary spine distal diameter (average=0.61 mm, SD=0.10) and demi-pyramid weight (average=6.38 g, SD=0.41). Fiordland had the smallest primary spine density with an average of 1.43 g/cm^3 (SD=0.16). I investigated the differences between locations for the median, upper quartile, lower quartile, and range excluding outliers from different locations for each skeletal element measurement as depicted by the boxplots in Figure 3.36.

Average body diameter demonstrated variability between individuals within a location as can be seen in Figure 3.36. White Island samples had the smallest variability of average body diameter within the individuals sampled (range 71.43 –75.05 mm), whereas Fiordland had the largest variability (range 74.86 –113.07 mm) as well as the largest specimen (maximum diameter 113.07 mm). Specimens collected from the South Island (Stewart Island, Fiordland and Picton) were larger than the specimens from the North Island (Wellington, White Island and Auckland). Picton and Fiordland had one outlier each, although these specimens were not outside of the observed specimens when compared on a national scale.

Primary spine length was largest in Fiordland in both average (30.58 mm) and individual length of one spine (36.36 mm), although it had a large range. White Island specimens had a smaller difference between its 25% and 75% quantile, yet Auckland organisms had the smallest variability in primary spine length as determined by standard deviation of 0.11 mm, while Stewart Island specimens had a large variability (2.12 SD) and second largest average primary spine length (25.23 mm). When observing the median value (indicated by the thick black line) as latitude increases, primary spine length increases, however White Island has a small dip relative to Auckland, and Fiordland is an obvious exception to this trend.

Primary spine weight was relatively consistent between the North Island sites (Auckland-0.02 g; White Island-0.03 g; Wellington-0.03 g) and were observably smaller than the South Island sites (Picton-0.04 g; Fiordland-0.06 g; Stewart Island-0.04 g). Primary spine weight demonstrates a similar pattern in the South Island sites as the primary spine length; Picton has the smallest average primary spine weight in the South Island, followed by Stewart Island with the heaviest individual specimen obtained from Fiordland (0.08 g).

Primary spine volume was largest at Fiordland with an average volume of 0.045 cm^3, while White Island and Auckland samples had the smallest averages, both with 0.016 cm^3. Spine volume for Auckland, White Island, Wellington and Picton all presented a small difference between 25 and 75% quantile, While Fiordland had the largest distribution of data.

Average spine density for locations were very similar, with only 0.45 g/cm^3 difference between the largest (White Island-1.87 g/cm^3) and smallest (Fiordland-1.42 g/cm^3) average for spine density. Median primary spine density appears to decrease from Northern sites to Southern sites except for Fiordland which is only slightly larger than Stewart Island specimens. The figure for primary spine density has many outliers for all locations, except for Picton and ranges overlap for all locations. There was no significant difference amongst locations when a post-hoc analysis was performed.

Median demi-pyramid length steadily increased from the most northern site (Auckland) to the most southern site (Stewart Island). Demi-pyramid length had the largest variability within the Fiordland samples, primarily because of the outliers included in the data while samples from Stewart Island had the smallest variability in length (range = 16.69 – 18.94 mm). Samples from White Island had several outliers; however, these were all close to the 25 and 75% quantiles.

The same trend of increasing size from North to South was observed in the demi-pyramid width, however the Stewart Island specimens had a smaller median width than the Fiordland median width, even though Fiordland is at a lower latitude. Demi-pyramid width had more outliers than the demi-pyramid length, with the largest difference from the median to the

outliers occurring in the Fiordland samples. Samples from White Island had the smallest variability in demi-pyramid width (range = 5.88 – 6.96 mm).

The median weight for demi-pyramids again increased with increasing latitude, however White Island and Wellington samples were very similar, with Fiordland marginally heavier than Stewart Island. Stewart Island had a large range that was not present when comparing the length and width of the demi-pyramids. Samples from Fiordland again had a large range due to the outliers and samples from White Island had one outlier in the figure. Samples from Wellington had the smallest variability (range=0.15 – 0.08 mm), with a similar range occurring at both Auckland and Picton (0.14 – 0.06 mm and 0.24 – 0.15 mm respectively).

Rotula length did not present any obvious trend in the parameters presented in the graphs. Samples from White Island had the smallest variability, while samples from Fiordland had large outliers, increasing the variability for that location. Samples from Picton and Stewart Island had outliers, although the difference was not as noticeable as that of outliers for samples from Fiordland.

Rotula width showed a clear trend of increasing median as latitude increases, although there is a small dip for the White Island samples. Variability was relatively similar across the locations, except for Fiordland.

Rotula weight was less variable for North Island specimens relative to South Island specimens and were also lighter in weight compared to the North Island samples. Stewart Island was significantly different for median and quantiles (25 and 75%) from all other locations except for Fiordland which overlap.

Epiphysis weight was one of the few components presented in this study that did not show a large separation between North and South Island populations. Picton specimens had a smaller median than the lower latitude Wellington specimens. Samples from Fiordland had a very large range between 25 and 75% quantiles, and Stewart Island had a large range as well. There were many outliers for Picton, while there was only one outlier for both White Island and Stewart Island.

Table 3.7 Average, standard deviation and number of samples for each measurement of a skeletal element per location.

Component	Measurement	Calculation	LOCATION					
			Auckland	White Island	Wellington	Picton	Fiordland	Stewart Island
Primary Spine	Length (mm)	Average	17.88	16.96	20.21	21.28	30.59	25.24
		Standard deviation	1.11	1.83	1.89	1.32	3.09	2.13
		Number	100	100	140	100	100	100
	Prox Diameter (mm)	Average	1.42	1.43	1.46	1.58	1.89	1.78
		Standard deviation	0.11	0.12	0.15	0.08	0.14	0.12
		Number	100	100	140	100	100	100
	Distal Diameter (mm)	Average	0.69	0.77	0.61	0.83	0.77	0.71
		Standard deviation	0.11	0.1	0.1	0.11	0.12	0.1
		Number	100	100	140	100	100	100
	Weight (g)	Average	0.03	0.03	0.03	0.04	0.06	0.05
		Standard deviation	0.00	0.01	0.01	0.01	0.01	0.01
		Number	100	100	140	100	100	100
	Volume (cm3)	Average	0.016	0.016	0.018	0.025	0.04	0.033
		Standard deviation	0.003	0.003	0.005	0.003	0.010	0.006
		Number	100	100	140	100	100	100
	Density (g/cm3)	Average	1.78	1.89	1.70	1.60	1.43	1.51
		Standard deviation	0.20	0.24	0.28	0.15	0.16	0.15
		Number	100	100	140	100	100	100
Demi-pyramid	Length (mm)	Average	12.4	12.94	13.03	15.02	17.19	17.62
		Standard deviation	1.09	0.51	0.77	0.88	1.67	2.73
		Number	96	98	135	87	99	90
	Width (mm)	Average	6.52	6.44	6.38	7.39	8.53	8.55
		Standard deviation	0.46	0.20	0.41	0.48	0.92	1.36
		Number	96	96	135	87	99	90
	Weight (g)	Average	0.10	0.13	0.12	0.19	0.25	0.26
		Standard deviation	0.02	0.02	0.02	0.02	0.06	0.04
		Number	96	98	135	87	100	96

Component	Measurement	Calculation	LOCATION					
			Auckland	White Island	Wellington	Picton	Fiordland	Stewart Island
Rotula	Height (mm)	Average	6.2	6.75	6.56	7.58	8.60	8.83
		Standard deviation	0.49	0.23	0.42	0.55	0.97	0.51
		Number	49	49	70	50	49	50
	Width (mm)	Average	2.39	2.35	2.56	2.93	3.11	3.33
		Standard deviation	0.20	0.12	0.16	0.15	0.35	0.25
		Number	49	49	70	50	49	50
	Weight (g)	Average	0.03	0.04	0.04	0.06	0.08	0.09
		Standard deviation	0.01	0.00	0.01	0.01	0.02	0.01
		Number	49	49	70	50	49	50
Epiphysis	Weight (g)	Average	0.02	0.02	0.02	0.03	0.05	0.05
		Standard deviation	0.01	0.02	0.00	0.01	0.01	0.01
		Number	98	96	127	98	100	95

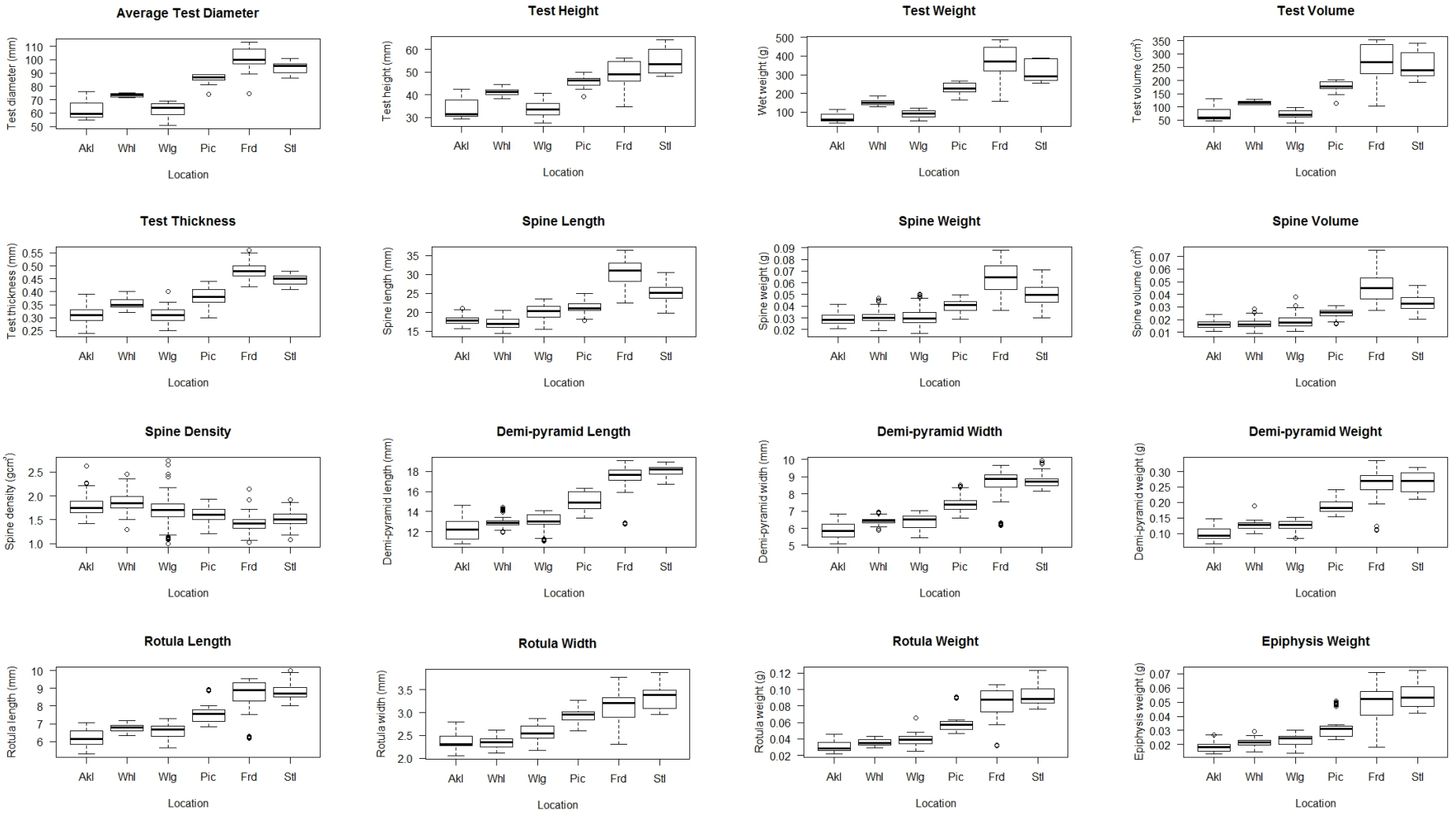

Figure 3.36 Skeletal components of 64 *Evechinus chloroticus* plotted as determined by location from 6 different locations around New Zealand. Akl: Auckland; Whl: White Island; Wlg: Wellington; Pic: Picton; Frd: Fiordland; Stl: Stewart Island.

I calculated a new measurement to account for the differences in urchin size within and amongst locations and term this the “standardised” measurement. I investigated the differences between locations for the median, upper quartile, lower quartile, and range excluding outliers from different locations for each skeletal element measurement as depicted by the boxplots in Figure 3.37. When reassessed using standardised height, there appears to be no obvious latitudinal trend. When a post hoc analysis was used, all locations apart from Fiordland presented a similar average, however Fiordland’s low average separates it from the other locations. Analysing the standardised wet weight of specimens, there are some differences notable, with White Island having a larger weight than either of the two surrounding locations (Auckland and Wellington). Standardised test volume showed huge variation amongst locations. White Island again, had a larger volume than what would be expected following the locations nearest it (Auckland and Wellington) and showed very small variation within the test volume. Sampled from Fiordland and Stewart Island had very similar test volume median, although samples from Fiordland had a much larger lower minimum and samples from Stewart Island had a slightly higher maximum, with very similar 25 and 75% quantiles between the two locations. Test thickness when standardised showed little difference among locations and when post-hoc analysis was undertaken, showed no significant difference amongst locations. Standardised spine length showed a no obvious trend with latitude, with similarity occurring amongst samples from Auckland, Wellington, and Fiordland; while White Island, Picton and Stewart Island showed a similar grouping to each other. Spine length showed a large variance at all locations as indicated by the large box and whiskers. Interestingly, there appeared to be a more similar median amongst all locations except Fiordland. A similar pattern is clear when standardised spine volume is plotted for the locations in this study, with a grouping of Auckland, White Island, Wellington, Picton and Stewart Island. There does appear to be some indication of latitudinal trend emerging, however a post hoc analysis indicated no significant difference between the locations aforementioned. Standardised spine density showed the inverse relationship, with decreasing density occurring at Fiordland and Stewart Island, with the largest density at Auckland and Wellington. White Island showed a much smaller 25 and 75% quantiles than the locations nearest to it, Auckland, and Wellington.

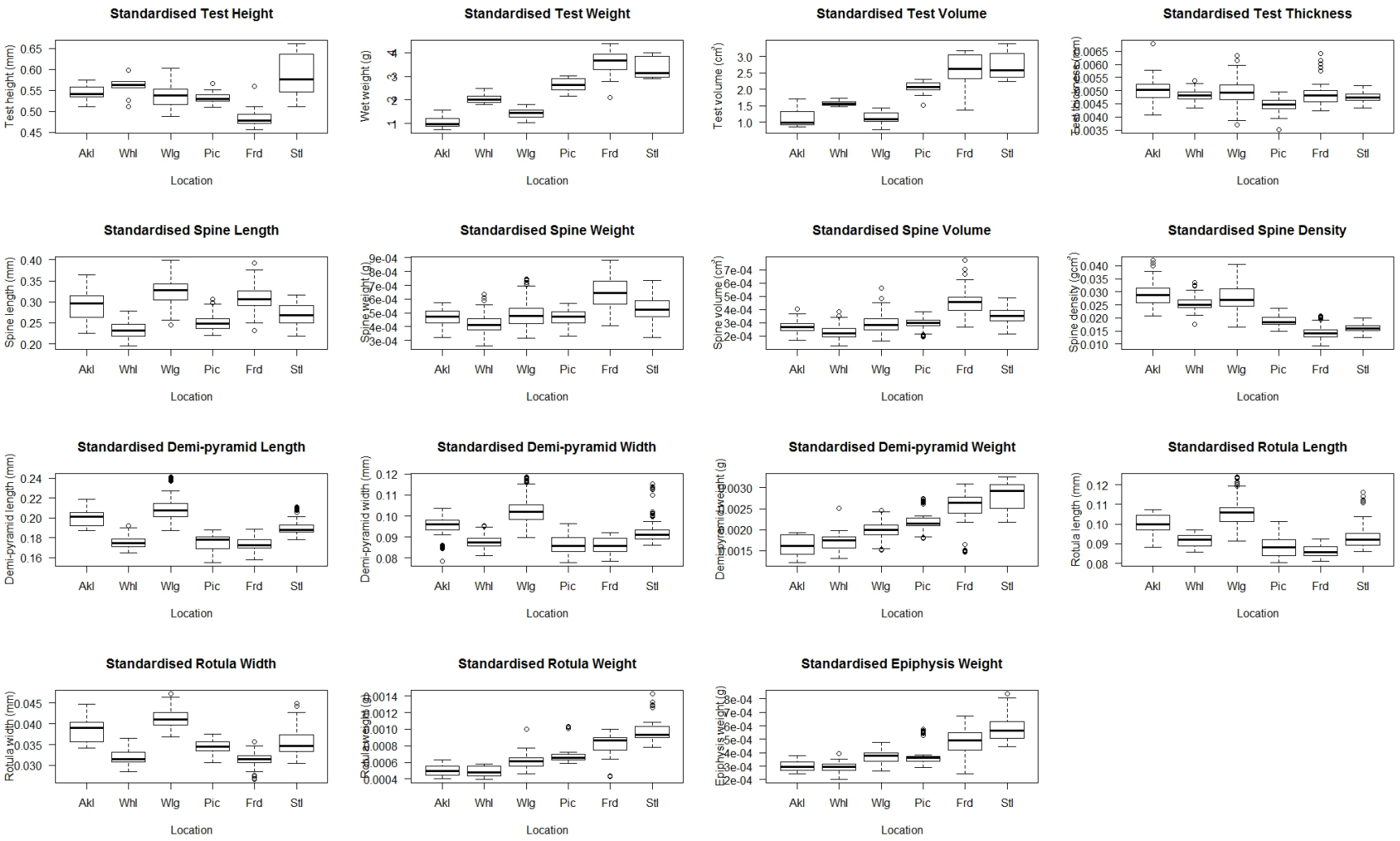

Figure 3.37 Standardised skeletal components of 64 *Evechinus chloroticus* plotted as determined by location from 6 different locations around New Zealand. Akl: Auckland; Whl: White Island; Wlg: Wellington; Pic: Picton; Frd: Fiordland; Stl: Stewart Island

3.4 Allometry Discussion

3.4.1 Variations Within Elements

This is the largest and most comprehensive study on *Evechinus chloroticus* to consider the effects of location on urchin morphometry and allometry. It allowed a detailed examination of variations in skeletal structures within and amongst individuals, as well as within and amongst populations from different locations, with focus to those in areas of identified unusual seawater chemistry.

As oceanic regions will face changes in ocean chemistry because of climate change at different degrees, velocities, and paces; understanding how regional and local populations will react is crucial to developing an understanding of long-term effects of climate change. Important structural parts of an organism must be maintained and repaired for survival, with changes in oceanic chemistry likely to impact on an organism's ability to build, maintain and repair structures. Energy allocation to undertake the essential processes of life is also likely to change because of changes in oceanic chemistry and less-essential processes such as reproduction and continuous growth may be foregone.

My results are one of the first and most comprehensive to provide detailed information about variability within an urchin's individual elements and from our results I have demonstrated different levels of consistency within a single element. Primary spine measurements (length, weight, volume, and density) showed a large degree of variability for a single individual than those of the Aristotle's lantern components.

The larger range of variability within a primary spine measurement is likely a result of the overall large number of spines available to measure. In this study, the ten largest spines were selected as judged by the naked eye and subsequently measured, however there were more than 200 spines available to measure for each individual. It is possible for an error to occur when selecting the 'largest' spines and this must be taken into consideration when giving thought to overall consistency in the individual. Primary spines are biological important for locomotion, sensing and protection from predators and can be limited by the energy state of the surrounding environment. Spines are frequently broken in a high energy environment where wave exposure or currents are particularly strong, or when collected by divers from the environment. The adaptive nature of spines, designed to absorb energy and prevent failure to the test by either breaking along the shaft or tissue connecting the spine to the test is torn or stretched (Strathmann 1981). Further to this, the nature of the break, and the state of regeneration if started will contribute to the variability observed in this study. It is most likely spines are correlated to the abiotic and biotic factors directly impacting on an individual, as

well as the state of repair or growth currently experienced by each individual spine. In this instance, spines demonstrate large variability in all measurements presented in this study and are poor indicators of morphometric growth.

There was very low variability in measurements of the Aristotle's lantern components regardless of location. The demi-pyramid, rotula and epiphysis demonstrated minimal differences within an individual and standard deviation was considerably lower than would be expected for random or uneven growth. Aristotle's lantern displays strict radial symmetry, an obvious requirement for function essential to overall individual survival. Deviations from the model will create irregularities to a complex system that could lead to issues with skeletal ossicles, muscles and ligaments with the addition of the teeth wearing unevenly. Repeat measurements of each demi-pyramid, rotula and epiphysis are unnecessary within a single individual due to the very low standard deviations displayed and it would be sufficient to measure only one of the components mentioned above.

This is the first study to investigate in detail the consistency of elements within an individual urchin with few studies have focusing on urchin allometry. The available data already published have typically focused on the demi-pyramids, while rotulas and epiphysis have remained largely absent from the literature. In this study, I have demonstrated that there are minimal differences between replicate sampling within an individual.

3.4.2 Correlations Within Wlements

When comparing different measurements from an element, there are consistent results for almost all elements regardless of individual or location. As an element gets larger, either in length or width, weight increases in almost a linear fashion with minimal deviations from the model. As different measurements were taken for different elements, discussions are detailed below.

3.4.2.1 Test and Test Plate

As test diameter increases in one direction, the perpendicular diameter also increases, with little variation. It has long been assumed that the urchin, *Evechinus chloroticus* presents itself as an oblate spheroid, with dihedral symmetry of the organs. When compared to the average diameter ($\frac{diameter\ 1+diameter\ 2}{2}$) height also increases with a linear model, although there is more variation to this model than when compared to the diameter comparisons. Ebert 1988 found that during *E. chloroticus* growth, changes in height were relative to the diameter until individuals converged towards $diameter = height \times 2$. Some of the variation exhibited in this model might be a result of the urchins sampled converging towards the model predicted by Ebert (1988). Habitat complexity has also been demonstrated to influence the described shape

and relative changes in urchins. Elliot et al. (2012) found that the purple sea urchin (*Strongylocentrotus purpuratus*) exhibited different shapes (height: diameter) dependent on the substrate that individuals were inhabiting. *S. purpuratus* that were living in pits had a larger height: diameter ration than those that were dwelling on flat surfaces. Two urchin species (*Echinus esculentus* and *Tripneustes ventricosus*) have also demonstrated variation in height: diameter ratio with variations attributed to wave action (Moore 1935 and McPherson 1965 respectively); rounder tests were apparent in calmer waters and flatter tests in more turbulent waters. Habitat complexity data was omitted from this study, but it should be noted that *E. chloroticus* inhabit a wide range of environments around New Zealand (see Section 1.4 for further detail).

Test thickness of *Evechinus chloroticus* increased with average diameter. It is encouraging that our detailed and well-supported data confirm conclusions reached in other studies, primarily Dix (1970). When describing the morphometry of the urchin *Echinus esculentus*, Moore (1935) found that the cube root of volume was sufficient for describing the relationship with test thickness, noting that older organisms typically had thinner shells and locality impacted the observed trends. Dix (1970) also found the same effect of locality on the study species *Evechinus chloroticus*, between 3 areas in Kaikoura and one area in Nelson. An increase of test thickness disproportionate to the expected increase as a result of test diameter has previously been correlated to increased nutrient availability and favourable environmental conditions (Dix 1970; Moore 1935). Growth rate has also been demonstrated to affect test thickness relative to test diameter in the urchin *Strongylocentrotus droebachiensis* (Lang & Mann 1976). Lang and Mann (1976), found those urchins that grew at a slower rate had a thinner test compared to faster growing individuals of the same age. Growth was heavily reliant on the abundance of food, and those individuals in kelp barrens grew slower. The function of food on growth rates and subsequently, on test thickness was not consistent between studies on different urchins. Test thickness of *Paracentrotus lividus* was found to be strongly correlated with test diameter; supporting the results discussed above for *E. chloroticus*; however, diet was not correlated with test thickness (Asnaghi et al. 2014). Tegner & Levin (1983) found that test thickness also varied dependent on the size class of test diameters in the urchin, *S. franciscanus*, supporting the evidence provided by Moore (1935). Urchins that were in the size class of 50-70 mm for test diameter had a slower rate of growth in test thickness, then increased in test thickness when urchins were above 70 mm diameter. This would indicate that the correlation of test thickness to diameter maybe not linear and could be logistic growth, dependent on age and overall size of the organism (Tegner & Levin 1983).

3.4.2.2 Primary Spine

This is the first study to quantify the relationship among measurements of the primary spine. Of the primary spines measured in this study, length, proximal diameter, distal diameter, weight, volume, and density had different correlations and strength of relationships amongst the measurements. Length of primary spines increased with average diameter, however there was a large variability within the data compared to the model. Previously, Dix (1980) found that spines differed with locality, from short, thick and blunt spines in organisms found at Wakatu Point, Nelson compared to long, thin and sharp spines from organisms at Kaiteriteri, with a range between these two shapes found in different locations (Seal Reef, Kaikoura and St Kilda Rocks, Kaikoura). Distal diameter showed a poor relationship to other measurements of a single spine and it is hypothesised to be a result of differences in the state of the spine (broken or whole). High energy environments, predators, and human disturbances can all impact the state of the spine when sampled. This is due to the adaptive nature of the spine by absorbing energy and breaking under pressure, protecting the important test and innards, and ultimately, the survival of the organism. It has been suggested, spine breakage leads to a difference in allocation of resources as calcite is directed to spine repair, cascading onto a slower rate of overall growth (Ebert 1968). Weight and volume had the largest r^2 value for any primary spine relationship presented in this study (r^2=0.90); although this is not particularly expected due to the low correlation between some of the measurements, most notably the distal diameter, but as the overall spine shape is described using length, proximal diameter and distal diameter, maybe it is not such an unexpected result that weight would be closely correlated. Volume was also highly correlated with primary spine length and proximal diameter, a likely effect that length and proximal diameter appeared consistent within an individual.

3.4.2.3 Aristotles Lantern

3.4.2.4 Demi-pyramid

Length, width, and weight of demi-pyramids all demonstrated strong correlations in those organisms measured in this study as all r^2 values were greater than 0.94. There has been little investigation into the relationship and shape of demi-pyramids in any urchin species. Some attention has been given to the relationship of pyramid length and test diameter and deemed to be isometric, or close to (Pomory & Lares 2011). It is believed that as the demi-pyramid is the largest component of the Aristotle's lantern, and this structure takes up a vast amount of space in the internal cavity, that the jaw scales proportionally. From the linear model presented in this study, the length of demi-pyramid scales to the demi-pyramid width with a 2:1 ratio, and it may be possible to hypothesis that the demi-pyramid scales proportionally, as suggested by Pomory & Lares (2011). There is very little variation in this model, and it is more likely that the

variation seen is attributed to human deviation in measurement. The ratio of either the length or the width to the demi-pyramid weight does not follow the same predictable model, based on the data provided in this study. It is possible that the difference from the expected ratio may be dependent on location and the direct effects of the environment (see Chapter 2). Thickness of the demi-pyramid was not measured and may contribute to the differences observed in weight. Density of the structure resulting from the oceanic chemistry, may also directly affect the weight observed and further investigation into this relationship is required.

3.4.2.5 Rotula and Epiphysis

Rotula measurements had strong r^2 values for the data provided in this study. Rotula length and width typically had a linear relationship consisting of a 2.5: 1 ratio, with small variations. As the rotula is an integral part of the Aristotle's lantern, it is expected that the rotula exhibits minimal variation and stable scaling within the Aristotle lantern. The rotulae are located between jaws (two demi-pyramids and tooth) on the aboral side, perpendicular to the jaw and acting as joint hinges for the rotular joint (Trogu 2015). This joint enables the mouth to open and close by using lateroradial rotations of the jaws (Carnevali et al. 1992). Because this is an integral part comprising of the Aristotle's lantern function there is seldom room for variations. Within this study, there were variations from the calculated linear model, which is beyond what I expected. Currently, there is limited published literature on shape and allometry of rotulae in echinoderm species, or rather any echinoid species at all. Epherra et al. (2014) has described changes in rotulae shape for *Arbacia dufresnii*; specifically, as dimeter increased, the length of the rotulae increased disproportionally to the width. The data presented in this study does not support those findings by Epherra et al. (2004) but this could be due to a range of factors. One of these could be the order of species differ between this study and in Epherra et al. (2004) (Echinoida and Arbacioida respectively).

Each rotulae, rest on two epiphyses, each originating from either side of the rotula and are attached to the epiphysis by rotular muscles. The epiphyses act as attachment points for muscles, specifically the lantern protractors. As the epiphyses and rotulae are heavily interlinked, it is expected that the relationship between rotulae measurements and epiphysis weight demonstrates a strong correlation. When r^2 values are given, rotula length, width and weight strongly correlate with epiphysis weight (r^2 = 0.91, 0.83 and 0.95 respectively). Further studies wishing to omit epiphysis measurements would be justified in doing so as there is little additional data that can be gleaned from epiphysis weight that would not be adequately inferred from rotula measurements. Epiphysis weight to rotula measurements appear to be strongly allometric in their relationship to each other.

3.4.3 Correlations Amongst Elements

When comparing measurements from different elements, there are some expected correlations and there are also some interesting results. As a result of growth, as an organism increases in overall size its body components also increase and this is termed isometric growth. This isometric growth is demonstrated in this study, as skeletal components increase in length, width, and weight when diameter increases. Ebert (1988), stated that during growth, the sea urchins test, lantern, and gut take up smaller fractions of the total weight whereas the gonads and coelomic fluid increase in their percentage of total weight. The data presented contain some deviations from the linear model offered and is likely a result of individual variation, genetic predisposition and potential, an impact of the immediate local environment. The allometric parameters may be adaptive and reflect an optimization of allocation to maximize fitness. However, they also might be exptations (Gould & Vrba 1982), epigenetic, or associated with general plasticity and hence reflect features that promote current fitness but not the result of direct selection.

The relationship of function and variations in the Aristotle's lantern components has generally rarely discussed. Published literature has considered feeding habits and nutrient availability to the overall size of the Aristotle's lantern, and some components, with focus on the jaw / demi-pyramid size. This is the first comprehensive study to consider three parts of the Aristotle's lantern and has provided a scope for further studies. The data indicates that classic measurements (length, width and weight) for the feeding apparatus are strongly correlated within components and within the Aristotle's lantern and is likely a result of capacity availability and structural constraints to ensure functionality within an individual.

3.4.4 Elements Amongst Locations

This study investigated the effects of location by sampling from six different areas along the length of New Zealand, from Stewart Island in the South to Auckland in the North. When element measurements were presented as a factor of their location, I saw interesting results.

Average body diameter demonstrated variability amongst individuals, as I would expect within a population. Natural genetic diversity, age, health of organism, reproductive state and small-scale environmental influences are likely to contribute to those expected patterns of variability of a crucial phenotypic trait such as size. Interestingly, samples from White Island had the smallest variability in average body diameter. This is noteworthy, as White Island is an active volcano with hydrothermal vents, changing the water chemistry and temperature in the immediate vicinity, likely affecting organisms in the area, and those in this study collected from

that location. Since organisms collected from White Island have been exposed for the duration of their lives, it is possible that the conditions resulting from volcanic activity may influence urchin size. A reduction in pH produces a decline in carbonate ion concentrations and calcium carbonate saturation, increasing energy expenditure for calcium carbonate synthesising organisms, such as this study organism *E. chloroticus.* When acidification occurs as a result of anthropogenic effort, or by natural occurrence such as that exhibited at White Island due to the volcanic activity, the saturation sate of the environment is altered, making calcium carbonate and its other forms (magnesium carbonate, aragonite carbonate) more difficult to extract from the water itself, and dissolving skeletal structures of carbonates as well. When carbonate sub-saturation occurs and more energy is required to synthesise carbonate and magnesium structures, less energy is available to the organism in terms of growth and reproduction as energy is directed maintaining and repairing existing skeletal structures to ensure organism survivability. Not only would I expect a smaller variability as organisms conform to the challenging conditions, I may have also expected a smaller test diameter as well. Many species exhibiting smaller body size correlated with climate change, and as conditions are exacerbated by continuous and potentially increasing anthropogenic effects, other species may demonstrate size reduction due to the current understanding of metabolic laws (Sheridan & Pickford 2011). In this study, I did not see smaller organisms occurring at White Island as I would expect based on the hypothesis by Sheridan & Pickford (2011). Instead, both Auckland and Wellington have smaller median test diameter even though the variability is larger than White Island. Smaller test diameter at both sites may be a result of younger organisms or environmental conditions such as food availability, intra- and interspecific competition, predation, or wave action. I did not age the organisms in this study however there are some studies that have related age to average diameter (e.g., Lamare & Mladenov 2000; Ebert et al. 1999). Habitat complexity, abiotic and biotic factors were not recorded for this study so inferences and trends should be considered with caution. Linse et al. (2006) found variation in test size of the Antarctic echinoid, *Sterechinus neumayeri* was correlated with food and competition, rather than latitude, as I have assumed here.

Based on the data collected in this study, it appears that test thickness generally increases with latitude (movement towards the poles) however there are two slight deviations from this model from the six locations presented in this study; White Island and Fiordland. Samples from White Island had thicker test plates than organisms from the two other North Island locations, Auckland, and Wellington. White Island with its volcanic properties, has demonstrated both warmer waters and lowered pH. It has long been expected that carbonate sub-saturation because of increased pH, would weaken shells, skeletal components, and carbonate structures through dissolution. Slightly elevated temperatures have shown to increase growth

and development in urchin's species. This study provides some evidence that the interactive effects of temperature and pH are not simple and the urchins in this study, benefit greater from the warmer waters than the decreased pH. This provides evidence like Byrne et al. (2014); the urchin *Tripneustes gratilla* demonstrated increasing temperatures increased shell thickness while decreased pH reduced shell thickness.

Primary spine length, weight and volume increased with increasing latitude, with minor points of interest. Spine length showed no significant difference between the three North Island locations, including White Island, suggesting that conditions may be similar. Spines are used primarily in defence and locomotion, with wave action impacting the morphology of the spines presented in the wild. If abiotic and biotic conditions impacting spine length are similar, I would expect spine length for the organisms to be similar. Conversely, the combination and pressure of conditions affecting the spine length may be such that it elicits the same response in length. Fiordland and Stewart Island organisms demonstrated much larger spine length than those for the other locations, with Fiordland spines greater than Stewart Island spines. This is unusual if I was expecting that latitude alone effected the spine length. Picton, White Island, Fiordland and Stewart Island were collected from relatively sheltered areas with minimal wave turbulence. Both Fiordland and Stewart Island contain the two main predators of *Evechinus chloroticus*; *Jasus edwardsii* (crayfish) and *Parapercis colias* (blue cod). If I were to hypothesis that larger spines in Fiordland specimens was in defence against predators, I may expect to see a larger abundance of predators in the Fiordland region. A 2008 summary of Rock Lobster (NRLMG 2008) indicates Stewart Island and Fiordland have similar estimates of crayfish populations and is therefore an unlikely cause for the difference observed.

All Aristotle lantern measurements produced the same trend for each location, with increasing size correlated with increasing latitude. Previously published data has indicated that Aristotle's lantern demonstrates morphological plasticity and scaling is governed by food type and availability (Ebert 1988). Smaller demi-pyramids indicate high food abundance, whereas larger demi-pyramids, are correlated with low food, urchin barren zones and an increased allocation of resources to the Aristotle's Lantern (Ebert 1980b; Black et al. 1984; Levitan 1991). Levitan (1991) went further and provided evidence for *D. antillarum*, increasing demi-pyramid size compared to the test diameter due to uneven growth in the two structures, showing rather than a relative decrease in test size as was previously hypothesised, demi-pyramid growth decreases on an absolute scale. This indicates the ratio of energy allocation is higher towards Aristotle's lantern growth as energy availability becomes limited while test size remains stable.

Black et al. (1984) also demonstrated the morphological plasticity of the Aristotle's lantern in the species *Echinometra mathaei*, relating an increase of jaw size to a decrease in gonad and spine weight, providing further evidence of the trade-off that organisms may utilise under limited nutrient availability. A decrease in reproductive effort could negatively impact the quality and quantity of eggs and sperm, resulting in a negative feedback loop for population prevalence and species dynamics of *E. chloroticus*. Ebert et al. (2014) hypothesised that differences in jaw allometry arising from differences to resource allocation, is relatively energetically inexpensive than the other option to an organism, consisting of reabsorbing calcium structures to conserve and obtain energy. Resorption has been described in sea urchin ossicles within the endoskeleton but has not been presented in literature to occur within the test plates, or demi-pyramids of the Aristotle's lantern (Ebert et al. 2014). As described earlier, due to the high level of regularity and tight geometry occurring in the Aristotle's lantern, I hypothesis that resorption is unlikely to occur in the epiphysis and rotulae as well.

Based on the data presented in this study, I can determine that variations within an individual's components are minimal, especially in those of the Aristotle's lantern. Correlations within measurements of a single structure were very high, with the lowest correlations observed between spine measurements and the highest within all structures of the Aristotle's lantern. When comparing measurements of structures amongst each other, again, I see a high correlation between Aristotle's lantern components, with no correlation to any spine measurement. I can safely verify that minimal measurements are needed for Aristotle's lantern components and inferences based on the relationships can be made safely. Variations amongst populations were most notable in the Aristotle's lantern with a latitudinal trend clearly visible in the graphs provided. White Island and Fiordland showed deviations to the models predicted and is likely a result of the latitude, from temperature, carbonate sub-saturation levels, or a combination of these three things. A more in-depth study factoring biotic and abiotic factors in these two locations may be required to thoroughly understand the likely impacts climate change will have on populations currently inhabiting these areas.

4 Biomineralisation

4.1 Introduction

Echinoderms have a hard endoskeleton, comprising the test and spines, and a complex feeding apparatus called the Aristotle's lantern (see Figure 3.1), all made from calcite ($CaCO_3$), which is produced and maintained by the mesoderm. Urchins generally substitute some magnesium for calcium during calcification and create a magnesium-calcite skeleton. This becomes problematic in the face of climate change as adding magnesium to calcite increases solubility. The rate of dissolution increases with magnesium content, those with a high magnesium content being more susceptible to dissolution. In some organisms, overall calcification rates decrease as carbonate becomes limited due to ocean acidification (Gattuso et al. 1999; Wood et al. 2008).

The level of magnesium incorporated into the skeletal components is dependent on the amount of magnesium present in the surrounding water, carbonate mineral saturation states, genetics, and latitude, as well as physiological and biochemical limitations. The magnesium: calcite ratio in skeletal components can be used as a proxy (with caution) for seawater chemistry, correlated with abiotic factors that ultimately affect the skeletal concentrations, at least in some organisms. For example, echinoderm skeletons in lower latitudes have demonstrated a higher magnesium content than those of species from the temperate and polar regions (Byrne et al 2014; Smith et al. 2016).

4.2 Methods

Three specimens from six locations (Auckland, White Island, Wellington, Picton, Stewart Island and Fiordland) were randomly selected. Each specimen had three replicates from five different skeletal elements (primary spines, test plate, rotula, epiphysis and demi-pyramids) analysed in the Phillips X-Ray diffractometer (XRD). Each whole skeletal component was analysed separately, and equipment was washed with water and 95% ethanol between samples to prevent contamination. Following previous studies (e.g. Smith et al. 2016), approximately 0.5 g of each sample and about 0.02 g of analytical- grade halite (NaCl) was ground to a fine uniform powder. A 95% ethanol solution was added to the sample + NaCl mix to form a slurry before it was smeared evenly on a clean sterilised glass slide and left to air dry. Each prepared sample was scanned by a Phillips X-Ray diffractometer (XRD) in the spectrum between 26° and 32° 2θ. The count time was 1s with 1 count per degree and the internal standard halite peak was used to correct the calcite peak location after the scan was completed. A machine-specific

calibration for determining magnesium content from relative peak position was applied: y=30*x* – 882, where y= wt % $MgCO_3$ in calcite and x= calcite peak position in °2θ (after Gray & Smith 2004).

Statistical analysis was completed using R-studio software to perform one-way ANOVA and data graphing.

4.3 Results

In total, there was 270 measurements of *Evechinus chloroticus* mineralogy from six locations around New Zealand and from five different skeletal elements (Appendix B). Taken as a collective without consideration for different skeletal elements or location, the average carbonate mineralogy for *Evechinus chloroticus* was 8.6 wt% $MgCO_3$ in calcite (± 2.0 SD, range=3.2–11.9, N=270) for those samples analysed. Weight percentage of magnesium carbonate varied between skeletal components and locations and the relationship between the variations is described below. The average wt % $MgCO_3$ in calcite, standard deviations, and number of samples for each skeletal component and location are given in Table 4.1. Magnesium content was largest in the demi-pyramid element, both in a single specimen and as a skeletal component group (Individual= 11.8, group= 9.9). This was closely followed by the epiphysis, test plate and rotula respectively in decreasing wt % $MgCO_3$ but there was very little apparent difference in mineralogy between the internal structures. Spines had significantly less magnesium content, and the average weight percentage of magnesium carbonate in the spines was at least 40% less compared to the other skeletal components and could be as much as 54% less.

Primary spines had the lowest quantity of magnesium for all locations with an average of 4.9 wt % $MgCO_3$, while rotula, epiphysis, demi-pyramid, and plate had an average of 9.1, 9.8, 9.9 and 9.4 wt % $MgCO_3$, respectively. However, under a pairwise comparison however, only the spines and demi-pyramids, and rotula and demi-pyramids were significantly different; $p<0.05$, (Table 4.2). Variation of wt % $MgCO_3$ within individuals in a single skeletal component from the location can be high for the relative quantity of $MgCO_3$ found. Spines from both Wellington and Auckland samples had the largest range and standard deviation (Wellington range 3.2 and standard deviation 1.0; Auckland range 2.9 and standard deviation 1.1 (Table 4.1)).

Magnesium content of three replicate samples of a skeletal elements within an individual is relatively stable. In all the individuals measured, the range of magnesium content in calcite within each set of three replicates per skeletal element varied from 0.2 to 3.2 wt % $MgCO_3$ (SD

0.11-1.62 wt % $MgCO_3$). Variation within an individual were smaller than variations between individuals of the same location; range 1.2–3.2 wt % $MgCO_3$ (SD 0.38-1.10 wt % $MgCO_3$). Variations between skeletal elements (4.5–10.3) were also larger than variations within the same skeletal element (e.g. 3.2–6.9 for spines). A pairwise comparison was performed on the skeletal elements irrespective of location and P values are given in Table 4.2. Furthermore, a pairwise comparison for location on each skeletal element was completed and P-values are presented in Table 4.3.

Table 4.1 Number of samples, standard deviation, and average weight percentage of magnesium carbonate in skeletal elements at each location measured. For each measurement, N=9.

Component	Calculation	LOCATION					
		Auckland	White Island	Wellington	Picton	Fiordland	Stewart Island
Test plate	Average	9.8	9.4	9.1	9.3	9.5	8.8
	Standard deviation	0.81	0.63	0.38	0.68	0.73	0.43
Primary Spine	Average	4.5	5.1	4.9	5.1	4.9	4.8
	Standard deviation	1.1	0.86	0.99	0.42	0.92	0.67
Demi-pyramid	Average	9.7	10.3	9.8	9.5	10.1	10.1
	Standard deviation	0.65	0.86	0.94	0.49	0.63	0.67
Rotula	Average	8.9	9.6	9.1	8.8	9	9.3
	Standard deviation	0.84	0.76	0.46	0.46	0.79	0.4
Epiphysis	Average	9.7	9.7	9.9	10.1	9.5	9.8
	Standard deviation	0.55	0.92	0.47	0.44	0.48	0.82

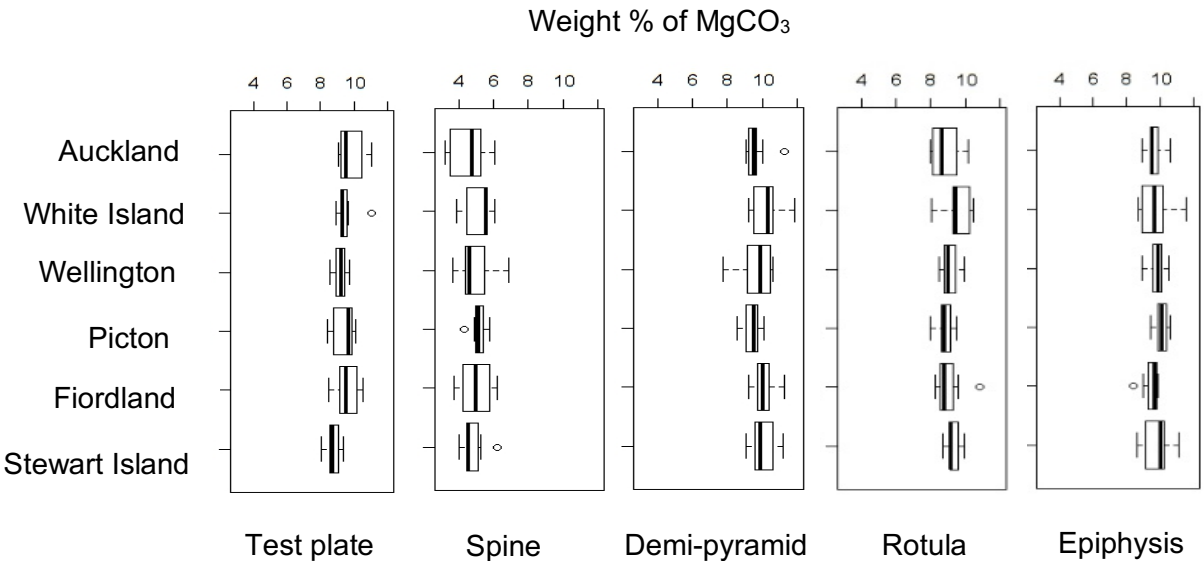

Figure 4.1 Weight percentage of MgCO3 in the skeletal elements of *Evechinus chloroticus* from six different locations; Auckland, White Island, Wellington, Picton, Fiordland, Stewart Island, New Zealand (N=21 for each graph).

Table 4.2 P values for pairwise comparison amongst skeletal elements regardless of location. Significant values (P<.05) are highlighted in yellow.

	Spine	Rotula	Epiphysis	Demi-pyramid	Test plate
Spine					
Rotula	0.84				
Epiphysis	0.53	0.73			
Demi-pyramid	0.04**	0.04**	0.51		
Test plate	0.06	0.54	0.64	0.98	

Table 4.3 P-values for pairwise comparisons amongst location for test plates. Significant values (P<0.05) are highlighted in yellow.

Test plate	Auckland	White Island	Wellington	Picton	Fiordland	Stewart Island
Auckland						
White Island	0.20					
Wellington	0.02**	0.28				
Picton	0.06	0.57	0.61			
Fiordland	0.22	0.94	0.25	0.52		
Stewart Island	0.00**	0.02**	0.22	0.08	0.02**	

Table 4.4 P-values for pairwise comparisons amongst locations for primary spines. Significant values (P<0.05) are highlighted in yellow.

Primary Spine	Auckland	White Island	Wellington	Picton	Fiordland	Stewart Island
Auckland						
White Island	0.14					
Wellington	0.35	0.57				
Picton	0.12	0.94	0.52			
Fiordland	0.29	0.66	0.90	0.60		
Stewart Island	0.52	0.39	0.77	0.35	0.68	

Table 4.5 P-values for pairwise comparisons amongst locations for demi-pyramids. Significant values (P<0.05) are highlighted in orange.

Demi-pyramid	Auckland	White Island	Wellington	Picton	Fiordland	Stewart Island
Auckland						
White Island	0.08					
Wellington	0.86	0.12				
Picton	0.51	0.02**	0.41			
Fiordland	0.18	0.68	0.24	0.05		
Stewart Island	0.27	0.52	0.35	0.08	0.08	

Table 4.6 P-values for pairwise comparisons amongst locations for rotulae. Significant values (P<0.05) are highlighted in orange.

Rotulae	Auckland	White Island	Wellington	Picton	Fiordland	Stewart Island
Auckland						
White Island	0.02**					
Wellington	0.49	0.11				
Picton	0.85	0.01**	0.39			
Fiordland	0.62	0.07	0.85	0.50		
Stewart Island	0.20	0.31	0.54	0.11	0.42	

Table 4.7 P-values for pairwise comparisons amongst locations for epiphysis. Significant values (P<0.05) are highlighted in orange.

Epiphysis	Auckland	White Island	Wellington	Picton	Fiordland	Stewart Island
Auckland						
White Island	0.82					
Wellington	0.52	0.67				
Picton	0.16	0.23	0.44			
Fiordland	0.51	0.38	0.19	0.04**		
Stewart Island	0.69	0.85	0.80	0.31	0.29	

4.4 Discussion

In this study I collected data from five skeletal elements in 18 different specimens of *Evechinus chloroticus* from six different locations around New Zealand, providing a detailed and comprehensive picture of the mineralogical variation that occurs in this species (Appendix C). Overall average magnesium content in *Evechinus chloroticus* was 8.6 wt% MgCO3, with a range from 3.2 to 11.9 wt% $MgCO_3$. This is similar to data reported elsewhere; Smith et al. (2016) found that *Evechinus chloroticus* ranged from 3.4 to 11.7 wt% $MgCO_3$ with an average of 7.1 wt% $MgCO_3$ from three different components (test plate, mouth parts and spines).

4.4.1 Magnesium Content Amongst Elements

Differences in skeletal components within a single individual are the most noticeable regardless of location. Spines contain at least 40% less magnesium than the test plate and mouthparts. LaVigne et al. (2013) noted that *Strongylocentrotus purpuratus*, a sea urchin in the South Pacific near Mexico and Canada exhibited magnesium content approximately 43% more in test components compared to the spine. Localised differences within a single spine have been demonstrated despite the single-crystal structure of the spines. Moureaux et al. (2010) surmised the spine is made up of two different morphological parts; the base and the shaft and these present different magnesium concentrations in the species *Paracentrotus*

*lividu*s, although this was not statistically recognized (Magdans & Gies, 2004). The shaft contains a central core of meshwork stereo and a longitudinal plain septum, each differing in their magnesium content relative to the other part of the shaft. The outer septum is lower in magnesium content than the inner septa. This is hypothesised to be a result of early spine development, the inner septa contain a cyclic pattern of magnesium which may result in observed differences in stiffness and hardness of the septa. Magnesium content within spine tips is also correlated to regeneration in *S. purpuratus*, with the highest magnesium concentration occurring at maturity of the tip (Davies et al. 1972). The magnesium content in the spines of *S. purpuratus* was in the low magnesium-calcite range (<4% $MgCO_3$), while test components had high magnesium-calcite (>4% $MgCO_3$) (LaVigne et al. 2013). This is one of the few species studied to span both categories of magnesium-calcite. The results presented here suggest that *Evechinus chloroticus* can occasionally contain both high and low magnesium-calcite classification within a single individual, for example in the Fiordland specimen #7, magnesium content was 3.82 wt% $MgCO_3$, while the plate had magnesium levels of 10.52 wt% $MgCO_3$. This suggests that at least these two species, *S. purpuratus* and *E. chloroticus* utilises distinct calcification pathways for precipitation dependent on the endoskeleton structure made and maintained (Ebert 2007).

All components of the Aristotle's lantern have a very similar average wt % of $MgCO_3$ which is sensible, as a weaker component could weaken the whole Aristotle's lantern and jeopardise the functionality and reliability of a crucial structure. This similarity in wt % of $MgCO_3$ in all Aristotle's lantern components has also been demonstrated in Smith et al. (2016). Teeth were not included in this mineralogy study however Smith et al. (2016) obtained an average magnesium content in of 4.5 wt% $MgCO_3$ (SD 0.7), which leads further evidence that those skeletal constituents that extend into the water column may resist dissolution due to the lower magnesium content. Those skeletal elements that are crucial for feeding, such as those comprising the Aristotle's lantern could incorporate a higher percentage of magnesium to strengthen the element and are protected from dissolution due to the enclosed area within the animal. This is further supported by Ma et al. (2009) and Killian et al. (2011) reporting higher magnesium in the tip of the tooth where damage is likely to occur due to the grinding of the tooth against a hard substrate. To date, there has been no research to investigate localised differences in magnesium content of the epiphysis, demi-pyramid and rotula. There has been some research into differences along the length of test plates and spines, however this has not extended to include specimens of *E. chloroticus*, and I cannot confirm if this occurs in every species or is unique to those studied in Moureaux et al. (2010).

There has been limited research into localised differences of magnesium content in plates and requires exploration for most species throughout the marine environment. Sumich & McCauley

(1972) published reports of heterogeneity in magnesium content of *Allocentrotus fragilis* plates; the highest magnesium content found in plates near the peristome and decrease in content as proximity to the periproct increases. It should be noted that the plates near the peristome are also the oldest, and slowest growing plates compared to the others.

Due to differences of magnesium content exhibited within skeletal elements of a single individual, it is likely that the amount of magnesium incorporated into the body is not the result of passive assimilation from the environment, suggesting active physiological modification of magnesium integration.

The solubility of a biomineral increases substantially when magnesium is substituted instead of calcium in the calcite structure, as well, as crystal size, surface area and surrounding seawater chemistry (Morse et al. 2007; LaVigne et al. 2013). Although being more impervious to dissolution, low magnesium elements, such as spines are theorised to have a reduced strength relative to other components and are comparatively easier to break under stress (Nickel et al. 2018). Published literature such as Moureaux et al. (2010) support this theory due to the meshwork base, containing less magnesium, has a lower stiffness and hardness than the septa, and the differences related to cyclic patterns of magnesium in the septa results in differences between the transverse and longitudinal sections. Increasing magnesium content, to increase hardness and stiffness, produces complications of its own. This could be an important trade-off for *E.s chloroticus,* yet the magnesium content in the protruding and exposed elements may have to reduce further to prevent dissolution which could jeopardise the functional strength of the important carbonate structures. Differences observed in magnesium concentrations between spines, test plates and Aristotle's lantern elements may have evolved as a function of the exposure to the ambient seawater and better reflects the trade-offs for strength and precipitation.

4.4.2 Magnesium Content Amongst Locations

Magnesium content varies in the same skeletal element between species. *Heterocentrotus trigonarius*, an urchin found in the tropical regions of the Indo-pacific, which has an average of 14.6 wt % $MgCO_3$ in calcite (Chave 1954; Ebert 2007), compared to *Echinarachnius parma*, a sand dollar from North America, British Columbia, Alaska, Siberia and Japan with a 5.6 wt % $MgCO_3$ in calcite (Smith et al. 2016). Differences observed between species has generally been associated with differences in latitude, depth, and coastal proximity.

The most measured skeletal element, the spine, vaires from ~2 to 13 wt % $MgCO_3$ and is correlated with water temperature (Nickel et al. 2018). Increasing latitude is strongly correlated

with decreasing temperature and can often be used in published literature as a proxy for temperature. There exists a linear correlation between magnesium content and water temperature, although Chave (1954) noted the regression analysis was not as high when compared to relationships of magnesium content and water temperature for foraminifera, corals, and sea pens. In contrast, Reis (2004), published results of echinoids demonstrating direct non-linear relationships of magnesium content and seawater in artificial conditions. Ebert (2007) stated that magnesium content is correlated with the Brody–Bertalanffy growth constant, resulting in more magnesium being deposited in the test of slow growing species compared with fast growing species (Ebert 2007). Slower growth rates, and therefore less magnesium, is thought to arise from decreasing sea-water carbonate saturation states as latitude increases (Andersson et al. 2008). Ossicles are embedded in the dermis body wall that form part of the endoskeleton and have been shown to increase in magnesium content as temperature increases (Chave 1954; Weber 1969; Davies et al. 1972; Ebert 2007). As noted above, ossicles also exhibit interspecies differences at a single location (Raup 1966; Weber 1969; Ebert, 2007).

As latitude increases, not only is temperature reduced, affecting the amount of magnesium present due to growth rates, but the saturation levels of calcite also decrease as acidity increases. A lower saturation state of seawater carbonate has been shown to slow growth rates, which as mentioned above, also correlates with reduced magnesium. Reduced growth rates will have ecological consequences, as predation and competition pressures are thought to increase (e.g., Kletpas et al. 1999, 2006; Andersson et al. 2008; Kuffner et al. 2008).

McClintock et al. (2011) demonstrated that the levels of magnesium content were similar between individuals, which are similar to those presented in this study. Research presented in Andersson et al. (2008) and Weber (1973), exhibit data that suggest not only those organisms that have high magnesium-calcite skeletons, but those populations at high latitudes and colder waters are also more susceptible to shifts in seawater carbonate saturation states. There is some preliminary research in the ability for echinoids typically producing high magnesium elements, to switch to low magnesium endoskeletons. This was described in Reis (2004) when the Echinoid *Eucidaris tribuloides*; a typically high magnesium organism was grown for 160 days in artificial seawater of 1 mol Mg/Ca. The mineralogy of spines and test plates changed to a low magnesium state (less than 4%). The ability of *Eucidaris tribuloides* to change its biomineralogy ratio under in magnesium deficient systems, may mean that some echinoids could persist in an oceanic environment with low saturation states such as those in the cretaceous period (145.5-66 mya). It is likely that those species and populations with high magnesium content, occupying areas in the higher latitudes and colder waters will begin to exhibit markedly lower magnesium content if they are able to adapt as the results from Reis

(2004) suggest. Those organisms that continue to inhabit areas that are undersaturated in regards to magnesium and calcite due to ocean acidification are likely to become smaller as calcification rates are hypothesised to become noticeably slower, impacting predation, and intraspecific competition from those non-calcifying organisms inhabiting the same space (e.g. Kleypas et al. 1999; 2005; Andersson et al. 2008; Kuffner et al. 2008; De Villiers 2004). The physiological cost of maintaining and building an endoskeleton under future conditions, is yet, still unknown (Pörter, 2010). It is also possible, that those organisms with external fertilisation could spread towards the equator as conditions in the higher latitudes become unfavourable (Andersson et al. 2008). Predictions about when these possible changes from high magnesium calcifers to low magnesium is unknown due to the relatively unknown kinetic behaviour and solubility of the active skeleton in the natural environment when additional variables like temperature are considered.

Coastal regions are also likely to exhibit responses to ocean acidification episodic upwelling events, pushing calcifying marine organisms near their physiological limits (Hofmann et al. 2010). Fossil-fuel combustion, agriculture run-off, freshwater inputs, coastal developments, and sediment disturbance can all impact the carbonate system, pushing the environment towards an undersaturated condition (Hofmann et al. 2010).

LaVigne et al. (2013) compared the carbonate composition of *Strongylocentrotus purpuratus*, from four diverse regions (Oregon, Northern California, Central California, and Southern California) and determined that there were no statistically significant differences of individuals between the locations studied. The results presented in this study for *E. chloroticus* conforms with those in LaVigne et al. (2013) although there are some differences between locations such as Stewart Island-Auckland and Stewart Island-Fiordland for test plates.

Sanford & Kelly (2011) summarised that organisms may already display local adaptation to environmental conditions that are beyond the “normal” and are likely to occur under future climate change scenarios presented by the IPCC. It is theorised that organisms will present differences in morphology, physiology, or behaviour to provide an advantage under those specific local conditions. These may include areas that are of differing latitudes, such as Stewart Island compared with Auckland, differences in pH, such as White Island, and differences in proximity to major industrial developments, such as Wellingtons larger population compared with the isolation of Fiordland. How populations respond will likely be dependent on the genetic variation with populations and the rate of mutation with individuals.

Oceanic volcanic vents have been viewed as a natural long-term experiment on the effects of ocean acidification arising from climate change on the community diversity, density and on individuals. However oceanic vents are not perfect indicators as climate change will impact

temperature, global currents, and sea level, they do provide a good indicator on the preliminary responses to pH. Hall-Spencer et al. (2008) demonstrated that urchin abundance, specifically *Paracentrotus lividus* and *Arbacia lixula*, reduces along a pH gradient from normal (8.1-8.2) to lowered pH (7.8-7.9) as a result of volcanic carbon dioxide vent. The results presented within this study do not appear to differ regarding magnesium concentration in skeletal elements of individuals collected at White Island; a volcanic Island with a lowered pH when compared to other locations. Data presented in Brinkman & Smith (2015) demonstrate the same results for *Evechinus chloroticus* when comparing the magnesium concentration of elements from individuals close to volcanic vents to those individuals removed from the impacts of vents. Due to the lack of statistically significant results, it is hypothesised that the pH content does not affect the minerology in those individuals sampled. As the endoskeleton is protected by a layer of epidermis, this may add to the ability of *E. chloroticus* to regulate and cope with the pH differences from those under "normal" conditions (Gibson et al. 2011; Dupont et al. 2010; Miles et al. 2007). Miles et al. (2007) exhibited results that sea urchin physiological processes were affected when pH was lowered, such as inability of the coelom pH to regulate when ambient water was decreased by more than 0.5 units. As *Evechinus chloroticus* can persist in the waters surrounding the volcanic vents near White Island and do not demonstrate differences in magnesium content, there exists evidence that *Evechinus chloroticus* may be resilient to the future conditions predicted by IPCC.

4.4.3 Magnesium Content in Future Scenarios

Smith et al. (2016) collated data from published research and found that those elements from echinoids containing 12 wt % $MgCO_3$ or greater were more susceptible to dissolution. This means that in our current climate, due to direct contact with seawater, spines are required to have less than 12 wt % $MgCO_3$. However, as business as usual models predict, the changes in seawater chemistry as a result of increased anthropogenic CO_2 will likely reduce the average magnesium composition throughout the whole organism as precipitation of magnesium calcite becomes increasingly difficult. As climate change continues, there are multiple variables that will be affected. IPCC predicts in conjunction with ocean acidification, sea surface temperatures will also increase around the globe. Saturation state has been correlated with increases in temperature. It has been noted however, that although the warmer oceanic temperatures may increase the possibility of carbonate minerals, the saturation state is likely to remain insufficient due to the amount of anthropogenic carbon dioxide emissions and the uptake by the ocean (Andersson et al. 2008). Although there remains uncertainties around the solubility of magnesium calcite in the natural environment, many scientists believe that high magnesium calcite secreting organisms, that inhabit high latitude, deep, sulpher and nitrogen

enriched, coastal waters may exist, or are soon to exist close to the metastable equilibrium with the surrounding seawater medium in terms of carbonate minerology. When the seawater in an environment becomes deficient in calcite mineral phases, unprecedented changes are probable, impacting structure, integrity, function and distribution of organisms that produce magnesium carbonate, and subsequently, other carbonate states such as aragonite or pure calcite. Unless local adaptation, genetic variation or mutation play a sustainable role, it is likely that the diversity and density of calcifers will decrease (Andersson et al. 2008). Species with calcite, aragonite and low magnesium calcite are proposed to dominate the oceans if high magnesium calcite organisms are unable to modify the physiological and biomineral pathways. Some urchins such as the purple sea urchin *S. purpuratus*, currently make use of a range of biominerals and biomineralization pathways and do not fall into a single mineralogical category (Ebert, 2007; Andersson et al. 2008. LaVigne et al. 2013). It is likely that organisms have altered their physiological capacity to compensate for localised changes due to repeat exposure by increasing or decreasing gene expression related to biomineralization, cellular stress response and metabolism (Todgham & Hofmann 2009). This may already be occurring, as positive responses to acidification have previously been reported, (e.g. Gooding et al. 2009; Todgham & Hofmann 2009; Hofmann et al. 2010).

Understanding trends within species, within populations, within individuals and particularly between generations will be crucial to understanding and predicting the impacts of ocean acidification on the endemic sea urchin, *Evechinus chloroticus*. Population responses as a function of locality and geography will become more important as ocean acidification affects regions differently and due to the nature of New Zealand crossing multiple latitude lines, development of cities, protection of isolated regions, offshore islands, and coastal marine sectors all compound or alleviate the effects of ocean acidification differently. As it has been shown that some urchins can biomineralise through different pathways to make elements of different magnesium content, it is hypothesised that the calcification may demonstrate plasticity to prevent total dissolution in the water (Ebert 2007; Andersson et al. 2008; LaVigne et al. 2013). The cost of shifting current calcification pathways to minimise solubility in future oceans is not known and may come at a price for other life-sustaining activities (Wood 2008; McCintock 2011).

There is an abundance of research still to be completed to understand the variations of magnesium content in calcite within a single species, populations, individuals, and skeletal components. Most of the literature focuses on short-term, isolated environment, manipulated experiments, and frequently uses extreme future case scenarios without regard to adaptation,

evolution, and plasticity. Often, experiments are not comparable due to the range of conditions selected differing between experiments. Inferences about how individuals, populations and species will develop and react to ocean acidification in their local environment is hypothesised rather than firm conclusions derived (Hofmann et al. 2010). As *Evechinus chloroticus* is a long-lived organism; reaching approximately 15 years (Dix 1972) it is important that the changes are put into the relative context and rate of change that these organisms are likely to experience. For example, altering the amount of magnesium incorporated into the skeleton may shift the solubility limits, or an organism may increase the production of calcite to maintain the skeleton but neither has been proven as the way forward for *E. chloroticus* facing ocean acidification. The results presented in this study further illustrates the complexities involved in predicting the responses likely to occur for an important endemic marine calcifier because of anthropogenic ocean acidification. (LaVigne et al. 2013.)

5 Biominerlisation

5.1 Introduction

Echinoids have a skeleton of fused plates (the test) containing essential internal organs, with a large number of spines covering the outside of the test acting as the first defence against predators. There are two types of spines: the obvious larger primary spines, and smaller secondary spines. Primary spines are not only for defence but are used for locomotion and sensing of physical surroundings as well (Tsafnat et al. 2012). Spines and the associated attaching tissues protect the test from impact by absorbing energy, spreading the load over a broader area (Strathmann 1981). Spines are connected to the skeleton at the base using a "ball and socket" arrangement and muscles (Su et al. 2000). When a spine is impacted at the distal tip, whether by a predator, hard substrate, moving objects, or rough, abrupt wave action, the spine normally breaks by brittle fracture occurs via bending (Tsafnat et al. 2012). No matter the direction of impact on the spine, the spine receives the energy from impact and protects the test from force that could otherwise be detrimental to the individual. Even though spines of some echinoderm species can be centimetres long, under X-rays or polarised light they behave as single crystals of magnesium-rich calcite (Su et al. 2000).

Urchin spines are remarkably strong despite being single crystals with high levels of porosity (Tsafnat et al. 2012). The strength of skeletal carbonate has long been suggested to correlate with biomineralization strategies including mineral polymorphs present, incorporation of organic material, and magnesium concentration (Currey 1975), but as regards urchin spines, there is little or no evidence to support these theories. Magnesium ion incorporation into the calcite structure has been reasoned to increase hardness, though it is also the mineral polymorph most vulnerable to dissolution (for example in future anthropogenically-induced ocean acidification). The consequences of dissolution on the mechanical properties of the skeletal system could increase successful predation, increase the likelihood of abiotic damage from wave force, limit mobility if spines break during locomotion and decrease growth if energy allocation is directed to maintenance and repair of spines.

Using laboratory equipment to test the bending and fracture characteristics of brittle material such as spines can help with understanding the factors that influence strength. Bending tests describe flexural stress under impact. Comparing the strength of spines from an individual, amongst individuals in the same location and amongst locations allows an understanding of the natural variation that may occur in *Evechinus chloroticus* around New Zealand. Investigating spine strength from a wide range of environments, including naturally occurring lower-pH environments, may help scientists predict potential effects resulting from ocean

acidification. Current research on spine strength in urchins and the changes that may occur under climate change models have focused on laboratory-based experiments and fail to account for acclimation, adaptation and even the possibility of evolution in lower-pH environments. One might reasonably hypothesise that spines from naturally-occurring lower-pH conditions due to volcanic activity, such as at Whakaari White Island, could be less robust and thus break at a lower stress than those spines that are from more 'normal' pH conditions.

5.2 Methods

Ten spines from each of 64 *Evechinus chloroticus* specimen collected (refer to Chapter 2 for details) were used to perform 2-point-bending tests to measure flexural stress. Whole organisms, and subsequently, spines used in this experiment were soaked in 7% sodium hypochlorite (bleach) for three days, rinsed twice in freshwater and dried in a drying oven at 60 ºC for 72 hours before cooling to room temperature. The ten largest spines as determined by sight, (Chapter 3.2) were individually bagged and labelled to describe the species, location, individual number, body part and replicate letter. Each spine was placed on supports (span of 3.5mm) in an Instron 3369 machine where a tip (radius 0.25 mm) would press down at a 50 N load cell, speed of 1 mm/min, until the spine broke. The length of the spine was measured, and ½ the length was marked on the spine using marker pen to indicate where the loading tip would be positioned. The displacement and force were recorded at a frequency of 10 Hz until breaking, after which, the diameter at the fracture point was measured using digital callipers (to the nearest 0.5 mm). Using a concentrated tip load, the formula is calculated as follows:

$$f_{max} = \frac{PL}{S_A} * \frac{1}{r^3} \; for \; r < 1.5$$

Where $S_A = \frac{\pi}{32} \; {d_A}^3$ and $r = \frac{d_B}{d_A}$

f_{max}= maximum bending strength P= load

L= length S_A= Section modulus

D_A= tip diameter D_B= butt diameter

r= ratio of butt diameter to tip diameter

Analysis was completed using R-studio software to perform one-way ANOVA and data graphing. Errors are presented as standard deviations for individual variation and populations, while standard deviation was used for comparing within and amongst populations.

5.3 Results

5.3.1 Spine Strength of *Evechinus chloroticus*

In total, there were 640 measurements of *Evechinus chloroticus* spine flexural strength from 64 individuals from six locations around New Zealand (Appendix D). Taken all together, without consideration of location, the average spine strength for *Evechinus chloroticus* is 111.98 MPa (±1.95, N=640). The flexural strength of all spines measured was plotted against the reciprocal spine length (Figure 5.1). As seen in Chapter 3, an urchin's spines exhibit variation in length, diameters, density, weight and volume so an average spine length and flexural strength was calculated for each urchin and plotted (Figure 5.2). Overall, shorter spines had greater flexural strength compared to longer spines.

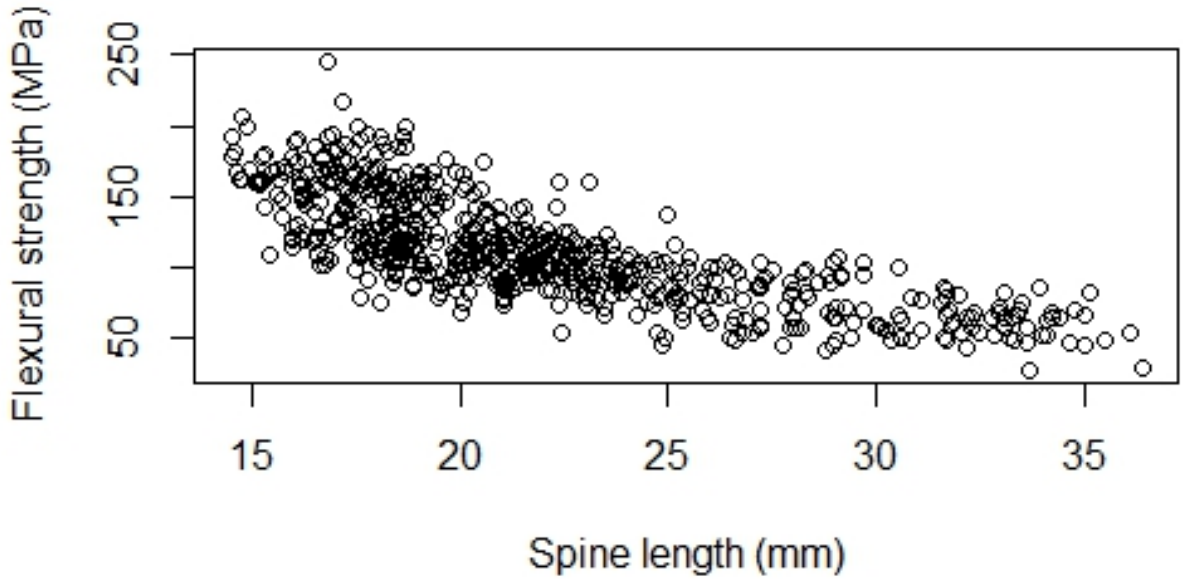

Figure 5.1 Flexural strength of *Evechinus chloroticus* primary spines compared to primary spine length from specimens collected around New Zealand, (N=640)

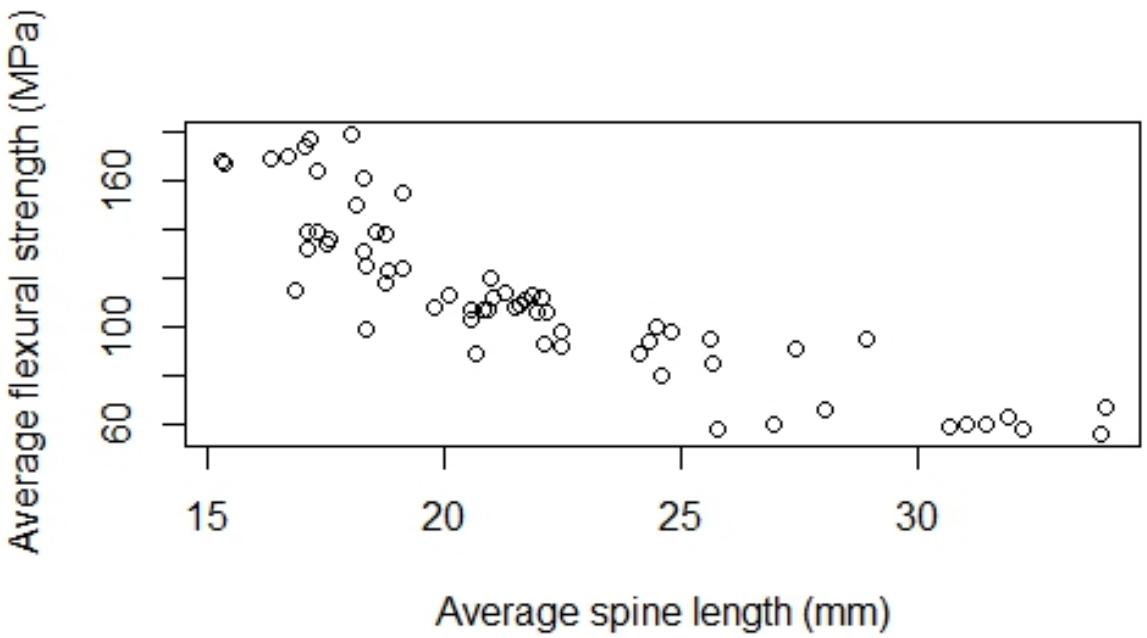

Figure 5.2 Average flexural strength of 10 primary spines compared to the relevant average primary spine length from 64 individual *Evechinus chloroticus* collected around New Zealand, (N=64).

To make sensible comparisons among spines that were of variable length, a new measure of strength-for-length was calculated: MPa/mm. This should take account of test size, (see Chapter 2 where test size and spine size are shown to be correlated).

5.3.2 Variation in Spine Strength Within an Individual

Firstly, it is important to define variation of spine flexural stress within an individual. The average strength compared to spine length with error bars as standard deviations for each urchin is presented in Figure 5.3. Most noticeable of the variation within individuals was the larger standard deviations in Auckland and White Island, with minimal variations within individuals typically occurring in Stewart Island and Fiordland specimens. The largest variation within a specimen was for Auckland, individual #1 with an average flexural stress of 149.88 MPa and standard deviation of 33.07. The smallest variation of flexural stress in a single specimen, was within Fiordland, individual #5, presenting an average stress of 59.83 MPa and standard deviation of 6.89. This creates a 79% difference between the largest and smallest variation of flexural stress between individuals.

Using our new measure of strength-for-length, the average and standard deviation for each individual urchin was calculated and is presented in Figure 5.3. The relative variation within individuals is smaller than Figure 5.4, with reduced error bars for individuals. As strength-for-length is dependent on flexural stress and spine length, the same phenomena is evident, with larger variation in Auckland and White Island specimens, and smaller variation within Fiordland and Stewart Island individuals. The largest variation is for Auckland, Individual #1, with an average of 8.317 mPA / mm and standard deviation of 2.04. The smallest variation was for individual Fiordland, #5 having an average of 1.93 MPa / mm and standard deviation of 0.22. It should be noted that the difference in variation between these two individuals is larger than for flexural stress alone, with a 89% difference in strength-for-length compared to 79% for flexural stress alone. The average strength for length of an individuals is 5.60 with a standard deviation 0.83.

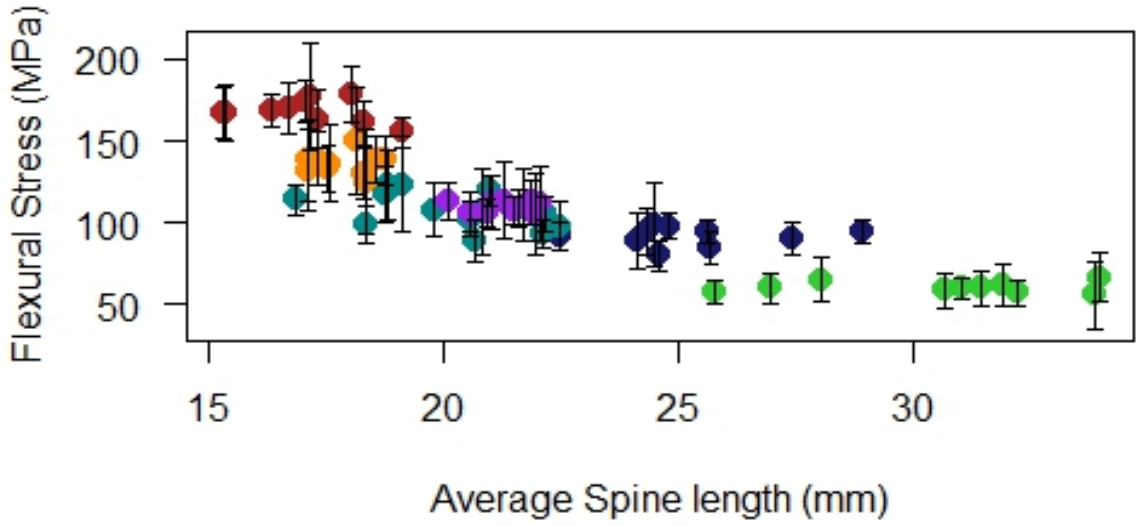

Figure 5.3 Average flexural strength of 10 primary spines for 64 *Evechinus chloroticus* compared to the relevant average primary spine length, with error bars as ± one standard deviation. Colours indicate populations; Auckland=yellow, Whakaari White Island=red, Wellington=cyan, Picton=purple, Stewart Island=navy, Fiordland=green (N=64).

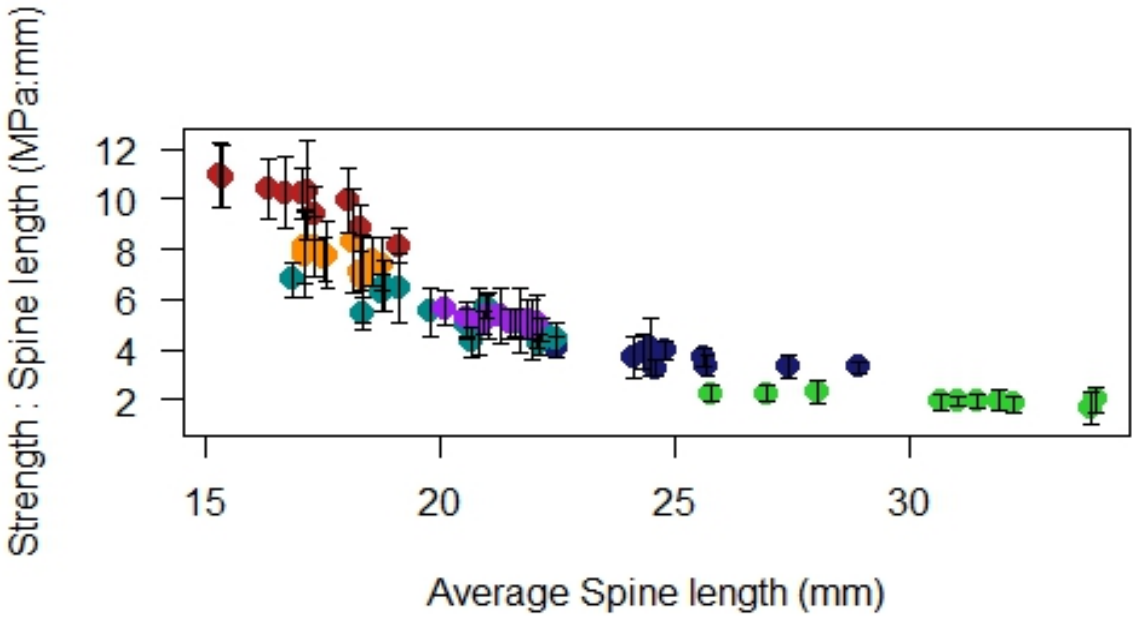

Figure 5.4 Average strength for length of 10 primary spines for 64 *Evechinus chloroticus* compared to the relevant average primary spine length, with error bars as ± one standard deviation. Colours indicate populations; Auckland=yellow, Whakaari White Island=red, Wellington=cyan, Picton=purple, Stewart Island=navy, Fiordland=green (N=64).

5.3.3 Variations Within and Amongst Locations

Flexural strength of primary spines varied within and among locations; a summary of average flexural strength, standard deviation, minimum, maximum, and number of samples is given in Table 5.1. Samples from Fiordland had the lowest average flexural strength (60.37 MPa ± 1.07 SD), while samples from Whakaari White Island had the largest, almost 3 times larger than samples from Fiordland at 168.12 MPa ± 1.22 SD. The largest standard deviation for flexural stress within a population occurred at Auckland (22.24), while the smallest standard deviation was from Fiordland samples, a similar trend to that seen within an individual. Samples from Wellington, White Island and Picton had very similar standard deviations although only the samples from Wellington and Picton had similar maximum and minimums (166.47 – 67.7 and 167.56 – 73.60 respectively). The smallest range was presented from samples collected at Fiordland, while Whakaari White Island's samples range was the largest and almost double of the Fiordland range. All sites were statistically different from each other except for samples from Wellington and Picton when a post-hoc Tukeys test was performed. When presented as a graph, there is some indication of a latitudinal trend, however Whakaari White Island and Fiordland exhibit a variance to the latitudinal trend that is expected (Figure 5.5).

Table 5.1 Average flexural stress (MPa) , minimum, maximum, standard deviation and number of samples for each location on primary spines (n=640).

Calculation	Auckland	White Island	Wellington	Picton	Fiordland	Stewart Island
Average	136.06	168.12	107.66	109.88	60.37	91.53
Standard deviation	22.24	18.00	18.60	17.00	11.90	13.64
Max	199.85	245.20	166.47	167.56	89.15	160.23
Min	81.00	121.01	67.07	73.60	27.03	63.72
Number	100	100	140	100	100	100

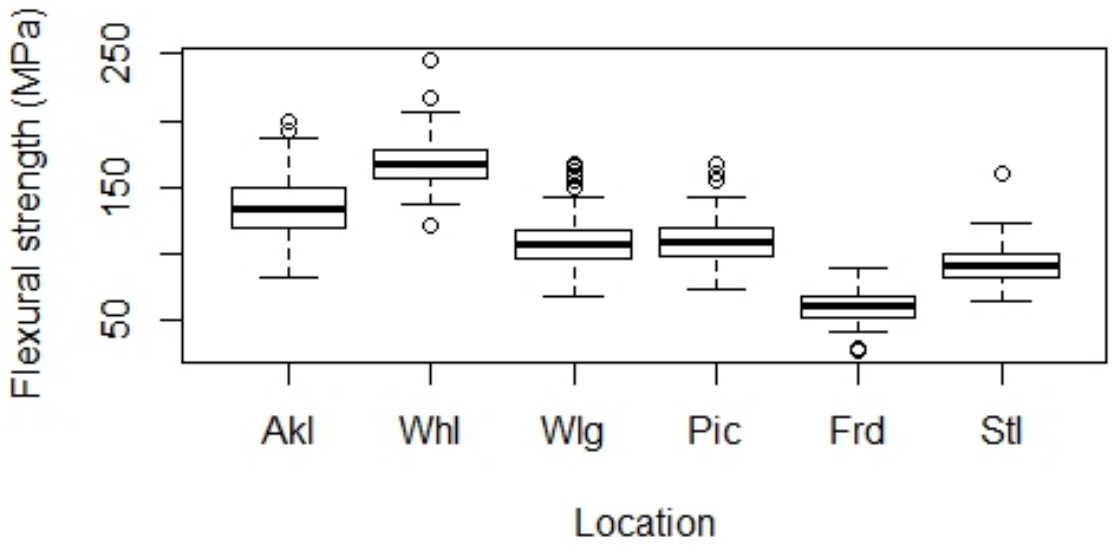

Figure 5.5 Flexural strength of *Evechinus chloroticus* primary spines from six locations around New Zealand. Akl=Auckland, Whl=White Island, Wlg=Wellington, Pic=Picton, Frd=Fiordland, Stl=Stewart Island, (N=100 at each location except Wlg where N=140).

A summary of our new measurement, strength for length is presented in Table 5.2 for average, standard deviation, minimum, maximum, and number of samples for each location. Samples from Fiordland had a very low average flexural strength (1.99 Mpa:mm ± 1.19 SE), while samples from Whakaari White Island had the largest, almost five times larger than Fiordland at 9.94 Mpa:mm ± 1.8 SE. The largest standard deviation for strength for length occurred at Whakaari White Island (1.47 SD), a difference from the flexural stress results. The smallest standard deviation was again, at Fiordland, while the average standard deviation for all specimens was 0.83 with an average strength for length of 5.62 Mpa:mm. Samples from Wellington and Picton had very similar maximums and minimums (8.4-3.19 and 8.66-3.49 respectively). This measurement of strength for length was plotted for each location and results are presented in Figure 5.6. The results presented are similar to that presented in Figure 5.5, with some indication of a latitudinal trend with the exception of White Island and Fiordland. All sites were statistically different from each other except for Wellington and Picton when a post-hoc Tukeys test was performed.

Table 5.2 Average strength for length (Mpa:mm) , minimum, maximum, standard deviation and number of samples for each location on primary spines (n=640).

Calculation	Auckland	White Island	Wellington	Picton	Fiordland	Stewart Island
Average	7.65	9.94	5.39	5.19	1.99	3.65
Standard deviation	1.38	1.47	1.13	0.90	0.43	0.65
Max	10.80	14.57	8.43	8.66	3.12	6.93
Min	4.14	6.81	3.19	3.49	0.75	2.46
Number	100	100	140	100	100	100

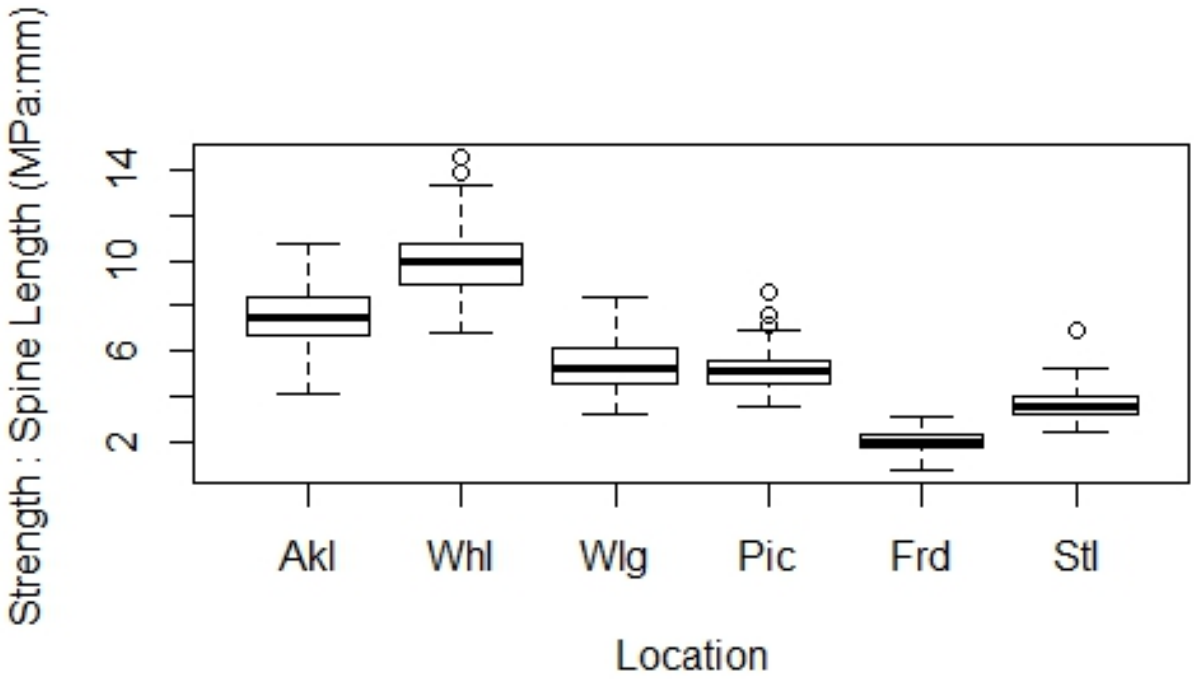

Figure 5.6 Flexural strength : spine length ratio for *Evechinus chloroticus* primary spines from six locations around New Zealand. Akl=Auckland, Whl=White Island, Wlg=Wellington, Pic=Picton, Frd=Fiordland, Stl=Stewart Island, (N=100 at each location except Wlg where N=140).

5.4 Discussion

This is the largest and most comprehensive study ever to consider the effects of seawater chemistry (using location as a proxy) on urchin spine strength. It allows us to look in detail at the variations in spine strength at different scales, with relevance to changing seawater chemistry.

As inshore and offshore oceans undergo changes in ocean chemistry at different rates and amplitudes, understanding how localised populations will react is crucial to developing an understanding of long-term effects of climate change and specifically, ocean acidification. Important structures of an organism must be maintained for survival, and in the face of climate change the energy required to build, maintain and repair the structures will ultimately dictate the amount of available energy for less-essential resources such as reproductive organs. Spines, used for locomotion, defence and tactile reception will be of importance for an urchin's survival. If organisms are unable to compensate for chemistry changes in the marine environment by substituting or altering their calcified structures, then weakness may occur through dissolution. The common blue mussel (*Mytilus edulis*), for example, has demonstrated the formation and maintenance of the shell coating can reduce the energy available to the

organism for other uses (Dery et al. 2017). Echinoderms have been identified as being especially susceptible to ocean acidification due to low metabolism, restricted regulation abilities, and high-magnesium calcite skeletal structures that are particularly soluble (Dery et al. 2017).

The magnesium calcite structure of echinoderms is not uniform throughout the echinoid's skeletal structure, with higher amounts of magnesium found in the test relative to the spines (Smith et al. 2016). This means that spines are, in theory, less susceptible to dissolution from acidification due to the lower magnesium concentration. Yet, the thinner epidermal layer on the spines compared to the test, and abrasion creating lesions in the epidermal layer, can increase the direct exposure of spine calcite to seawater (Dery et al. 2017). Previous research has found that when some echinoid species are exposed to reduced pH seawater, they are able to compensate for the change in oceanic chemistry by changing the chemistry of their internal fluid (coelomic fluid); specifically increasing the bicarbonate concentration (Holtman et al. 2013; Moulin et al. 2014). The buffered coelomic fluid is, however, contained within the test, and does not benefit the spines. It seems likely that climate change will affect spines first, causing changes such as reduced size or density (refer to Chapter 3), different composition (refer to Chapter 4) or brittleness and reduced strength.

Calcium carbonate in marine calcifers is composed of mineral polymorphs including aragonite, calcite (<4 wt % $MgCO_3$) and/or magnesium-calcite (>4 wt % $MgCO_3$). It has been well documented that as the amount of magnesium in calcite increases, solubility increases, and calcified structures thus become less resistant to dissolution in low pH conditions (Andersson et al. 2008). Magnesium in calcite in biogenic carbonate ranges from 0 to 28 wt % $MgCO_3$ (Andersson et al. 2008; Chave 1954). Strength of calcified structures appears to change in inverse proportion to the solubility of polymorphs, with increasing solubility associated with higher strength, but there remains a large gap in the scientific evidence for this phenomenon. Previous published literature states calcified structures are strengthened by the substitution of calcium for magnesium (e.g., Tsafnat et al. 2012), yet to date, there has been no extensive or robust research to investigate this matter. Some research has investigated the effects of strength as a result of anthropogenic climate change such as Hoegh-Guldberg (2007) on coral skeletons, and Gaylord et al. (2011) on the bivalve, *M. californianus*, yet there remains no literature directly comparing strength in biominerals of different polymorphs.

Strength of skeletal biominerals has been tested using nanoindentation, crushing tests, Vickers hardness, elastic modulus, macroindentation, fracture toughness, snap test, two-point bending, three-point bending and penetrometry; there is no currently accepted standard method and comparing results is thus extremely difficult. Even testing within a single method,

such as nanoindentation, can vary greatly for example due to the machine used, embedding techniques such as in resin (Fitzer et al. 2015) vs. no resin (Dell'Acqua et al. 2019), load force used (e.g. 500-7000 μN in San Chan et al. 2012 vs. 1000 μN in Dell'Acqua et al. 2019), nanoindentation tip used (Berkovich tip vs. conical tip) and analysis software. With the lack of comparable research, I am only able to theorise that, if magnesium conveys strength as well as solubility, high magnesium calcifers would be using the strongest polymorph. As indicated in Chapter 4, spines are not as high in magnesium as in test plates or mouthparts, but due to the lack of coelomic-fluid balancing oceanic chemistry and the thinner layer of epidermis covering the spines compared to the test, I may reasonably predict that spines are likely to be influenced by climate change first (Holtman et al. 2013, Moulin et al. 2014), and that variations in their composition, and thus solubility and strength, will have significant implications for the urchins who depend on them.

Strength data on ten spines from each of 64 specimens of *Evechinus chloroticus* from six different locations around New Zealand (Appendix D) provide the largest study of strength in an echinoid species. Spines of *Evechinus chloroticus* demonstrated a high flexural stress, which means that they are very strong for their size. It is not uncommon for biominerals to be especially strong when compared with abiotic materials (see abalone literature for example). Often it is postulated that a combination of protein layers and crystal ultrastructure delivers this extra resilience. Most urchins, however, form the spine of a single crystal of magnesium calcite (Donnay & Pawson 1969; Berman et al. 1990). In more detail, echinoid spines are systematically structured mesocrystals comprising sub-micrometer domains (Presser et al. 2009). Lauer et al. (2018) suggested that the internal structures and porosity of spines may be important in providing strength.

Longer spines in *E. chloroticus* have lower flexural stress point than shorter ones, so it appears that larger spines are weaker, breaking under a lower load. As shown in Chapter 3, *E. chloroticus* specimens with a larger diameter have proportionately larger spines, indicating that larger and older individuals in general have lower spine strength than smaller and younger ones. This result is consistent with the Weibull theory for brittle materials: as size increases (for example, spine length) average experimental strength decreases (Dery et al. 2017). While our results follow the Weibull trend, it does not appear to be the case for all echinoid species. Lauer et al. (2018) demonstrated that the spines of *Heterocentrotus mamillatus* and *H. trigonarius* had spine stress that was not correlated with the specimen size, though they used three-point bending, and their results are not directly comparable to our two-point bending tests.

Lauer et al. (2018) suggested that the internal porous structure of spines is important in determining spine failure and elastic properties. They described struts of similar size in both large and small spines of *H. mamillatus* and *H. trigonarius*, which could mean that the potential for failure increases as size increases because the struts offer less support for a larger spine due to scaling incompatibility. Presser et al. (2009) described differences in pore size, arrangement and distribution between species and individuals, but even between spines of a single individual. This could explain the variation seen in the results of this study, not only within those of the same location but within the same individuals sampled. It would be useful to examine variations in porosity, pore size, pore arrangement and pore distribution in *E. chloroticus* spines. Magdans & Geis, (2004), demonstrated magnesium content differences along the length of a primary spine for five different echinoid species (*Sterechinus antarcticus*, *Echinus esculentus*, *Paracentrotus lividus*, *Lytechinus variegatus* and *Heterocentrotus mammilatus*), decreasing in magnesium towards the tip. As larger spines are likely to have a larger area where this magnesium content is reduced, it is also probable that the larger spines will break under lower loads as demonstrated by the spines in our study. It may be that spine strength is less necessary in larger urchins, so that further investment is energetically unwise. Spines used in defence impale a predator and break off, regenerating quickly. It is possible that as urchins grow, the number of possible predators decreases so energy to maintain spine strength is sacrificed.

In general, urchin strength relative to length was found to increase with water temperature. The strongest spines were found in the North Island, weakening further south. The strongest spines were from White Island and the weakest from Fiordland. There are several possible explanations for this trend: magnesium content, growth rate, and seawater chemistry.

It is widely documented that, in many marine invertebrate taxa, the amount of magnesium in biomineral calcite decreases with decreasing temperature (Chave 1954; Stanley et al. 2006), which may be affecting the strength of the spines. As explained in Chapter 4, magnesium substitution into the calcite structure increases strength, decreases brittleness, and increases solubility. Smith et al. (2016) undertook a comprehensive review of sea urchin skeletal mineralogy from 72°N to 77°S, assessing latitudinal effects on magnesium content from 73 different echinoid species; describing a strong relationship of latitude (using SST proxy) and magnesium content. It is encouraging that our results presented in this study contribute to the trend described in Smith et al. (2016) although our latitudinal differences are much smaller across locations (46-35°S).

Differences of magnesium content in echinoid skeletal structures has been credited to differences in temperature, but also growth rates as a result of temperature (McClintock et al. 2011; Weber 1973). The role of growth influencing skeletal composition may be the underlying principal behind the correlation observed, rather than a dependence of temperature for magnesium incorporation (Weber 1973). Physiological processes such as respiration, digestion and calcification all increase in rate with increasing environmental temperatures. Byrne et al. (2014) clearly demonstrated the role of temperature on magnesium content for the echinoid urchin, *Tripneustes gratilla* in the absence of confounding variables, providing some of the simplest evidence for a direct relationship of calcification rates on magnesium incorporation. However increasing growth rate is not always correlated with warming temperature, as shown by Hermans et al. (2010) for the echinoid *Paracentrotus lividus*; with no significant effect of increased temperature on growth, but a significant effect on Mg/Ca ratio for individuals. Further species-specific experiments are required to understand the effect of temperature on calcification rates, growth rates and magnesium content.

Notably weak spines in the Fiordland population may be exhibiting a strength trade-off associated with sea-water composition. Salinity dissolved inorganic carbon, saturation states of aragonite and calcite, total alkalinity and carbonate concentration are all significantly lower in Fiordland waters than in the other locations included in this study (refer to Chapter 2). Fiordland has a large intrusion of freshwater from heavy localised rainfall and large sills, retaining large freshwater quantities, components that alter the seawater chemistry within a small area. Ferguson et al. (2008) reported a strong salinity - Mg/Ca ratio correlation in Mediterranean foraminiferal skeletons and Malone & Dodd (1967) found that calcification rates increased with increasing salinity for *Mytilus edilus* over 20-37 ‰ at a constant temperature of 18.5°C. For echinoderms, Richter & Bruckschen (1998) analysed the tests of *Echinocyamus pusillus* from a wide salinity and temperature range in 15 locations, and stated that changes in salinity did not correlate with changes in magnesium content; while Borremans et al. (2009) discovered that salinity had a strong correlation with Mg/Ca ratios, to the same extent of temperature effects on Mg/Ca ratios in the starfish, *Asterias rubens*.

The carbonate saturation state of seawater is important for marine calcifers. In Ω values greater than one, when seawater is supersaturated, marine biocalcification is promoted, whereas Ω values less than one indicates undersaturated seawater, and biocalcification may be slowed or inhibited. Although Ω of both calcite and aragonite are greater than one near Fiordland, it is substantially lower than those for the other five locations and could therefore have an impact on the ability for a marine calcifier to form calcium carbonate and its polymorphs. Associated sea-water values (total alkalinity, DIC, pH, carbonate concentration) are also unusually low in Fiordland, presumably increasing the dissolution pressure on

calcification. Fiordland urchins might have lower strength in their spines because they are unable to calcify robustly in their seawater conditions, or because they do so but subsequent dissolution weakens the spines over time.

Urchin spines grown at Whakaari, White Island are exceptionally strong, having a larger average strength-for-length than expected and indeed, presents the largest single value of strength-for-length. The oceanic environment immediately surrounding White Island is different than what a latitudinal trend of temperature would indicate due to the extensive undersea volcanism in the area. CO_2 vents around White Island not only reduce the pH of the immediate water from 8.1 to 7.9, but also increase the temperature, with seawater warming analogous to future climate change scenarios (Grace 1975). The stronger spines found here could be a result of the warmer temperatures increasing magnesium availability. Alternatively, the lowered pH seawater could stimulate urchins to invest in their protective spines, resulting in more robust spines.

It is well known that echinoids can compensate for changing sea-water conditions. Collard et al. (2016), for example, combined laboratory-manipulated experiments with naturally-occurring ranges for temperature and pH in areas inhabited by the urchin, *Paracentrotus lividus*. *P. lividus* was found to have no significant differences in fracture force, Young's modulus, second moment of area, material nanohardness, and specific Young's modulus of sea urchin test plates due to low pH and/or increased temperature.

In crushing tests of the urchin, *Tripneustes gratilla*, Byrne et al. (2014) determined that those individuals reared for 146 days in low pH conditions (pH 7.8 and 7.6) crushed under a lesser force than those in normal seawater (8.1) but more force was required to crush those reared in warmer waters (25°C and 28°C); likely a result of increased urchin size from warmer waters. Hazan et al. (2014) also found no differences in skeletal dissolution, widened stereom pores or non-smoothed structures when *Echinometra* sp. were incubated for 11 months under two different pH conditions, 7.7 and the control of 8.1. Dery et al. (2017) found that a cidaroid echinoderm, *Eucidaris tribuloides* showed no difference in spine mechanical properties when live specimens were placed in pH conditions of 7.4, 7.7, and 8.1 for five weeks; whereas an euechinoid species, *Tripneustes ventricosus* showed a reduction in fracture force of 16% when specimens were incubated at pH 7.7 and reduced by 35% when incubated at pH 7.4 for five weeks compared to the control of pH 8.1.

If urchins can up-regulate calcification under lowered-pH conditions, it must come at some cost. Resource allocation to calcification by the individual could reduce investment in somatic and reproductive growth. Haag et al. (2016) has already demonstrated reduced gonad indices in the urchin *Strongylocentrotus purpuratus* when spines are damaged and regenerated. The

energetic effect of growing robust spines in lowered pH seawater could be the subject of future research: a detailed, long-term culture experiment under different sea-water conditions examining somatic, reproductive and skeletal growth parameters would assist our understanding of how anthropogenic climate change might affect these important marine invertebrates.

Our findings demonstrate variation amongst spines of the same individual, within populations and amongst populations along the coast of New Zealand. The results presented in this study clearly establish a relationship of size on the flexural stress of *Evechinus chloroticus* spines, with larger spines breaking at a lower load than smaller spines, a trend observed in other studies and confirming the Weibull theory of brittle materials. Together with the well-described latitude trends of magnesium content in echinoids, I provide some understanding and future implications of sensitivity to breaking loads of this species important calcite structure, primary spines, to global climate change predicted for the coming decades.

6 Summary and Conclusion

6.1 Introduction

This study examined the effects of environment on resource allocation in an important marine calcifier. By taking a holistic approach, the results allow us to look at both size and composition of skeletal elements, and the consequent variations in strength (in spines). As pH decreases, so too does carbonate availability. Authors have found that in acidic conditions, metabolic activity is lowered, reducing growth, and affecting allometry (e.g. Michaelidis et al. 2005). Other authors have also documented ocean acidification reducing calcification and increasing shell dissolution. (e.g. Gattuso et al. 1999, Feeky et al. 2004). The interaction between these two responses, either synergistically or antagonistically may impact other functions and may influence the effectiveness of an organism's response.

6.2 Allometry

Allometry from adult *Evechinus chloroticus* demonstrated minimal variation within elements, particularly those of the Aristotle's lantern. Measurements within elements are strongly proportional, particularly so in the Aristotle's lantern. Due to the spine's purposes for defence and locomotion, it is likely that the lower correlations of spine measurements noted in the data presented are due to spines breaking and regenerating over the duration of the urchin's life. I suggest that spines are a poor indicator measurement for the individual's size, population phenotypes and other morphometric inferences. Tight regularity, rigid geometry and the strict interconnections of the Aristotle's lantern components resulted in a high correlation of measurements of all components that comprise the feeding structure.

Latitude appears to affect the morphometry of the Aristotle's lantern and test components, but not spine parameters. Test thickness increased with latitude, as too did demi-pyramid, rotulae and epiphysis measurements. Most notably, White Island and Fiordland were exceptions to the predicted model; both locations had larger averages and medians than would be predicted based on latitude/temperature. One of the most interesting observations occurred when data was standardised to control for size differences of individuals, the only measurement to demonstrate the same latitudinal trend was the weight of the Aristotle's lantern components (demi-pyramids, rotulae, and epiphysis).

6.3 Biomineralogy

Biomineralogy of the skeletal elements in *Evechinus* varies in the amount of magnesium incorporated into calcium carbonate structures. *E. chloroticus* can produce calcite ranging from 3.2 to 11.9 wt % Mg, with an average of 8.6 (SD=2.01), suggesting that calcite formation is not the result of passive assimilation from the environment, but is actively synthesised and managed. Magnesium incorporation into skeletal components varies within an individual's different components, with 40% less magnesium incorporated in the spines compared to the test plates or Aristotle's lantern. Magnesium content in the Aristotle's lantern components were fairly consistent, and is likely a result of the highly organised, interconnected nature of the feeding apparatus. Ensuring there is no "weak link" by incorporating components of a similar magnesium content, and therefore strength in the Aristotle's lantern is crucial to ensure continuous functionality. Spine magnesium has been shown to vary from ~2 to 13 wt % $MgCO_3$, correlated with water temperature (Nickel et al. 2018), but in *E. chloroticus*, spine calcite contained from 3.2 to 6.9 wt % $MgCO_3$, without a latitudinal trend.

6.4 Strength

Strength of spines exhibited variation amongst spines of the same individual, amongst individuals of the same location, and amongst individuals of different locations. Larger spines demonstrated a lower flexural stress point than spines of a shorter length. White Island specimens were the strongest, with the highest flexural load level, while Fiordland samples were the weakest. It is possible that seawater conditions affect these spines: in White Island the lower pH may cause increased investment in mineralisation, whereas in Fiordland the high amounts of freshwater could compromise calcification.

6.5 Calcification (Allometry + Biomineralogy)

It has been proposed that more magnesium is deposited into calcium carbonate structures in slow-growing organisms and species. Ebert (2007) summarised correlation between the number of magnesium producing ossicles with temperature, and the rate of growth with temperature as determined by the Brody–Bertalanffy growth constant. Faster growth rates and increased magnesium content are present in species with warmer habitats, likely a result of increased metabolic activity. Andersson et al. (2008) proposed slower growth rates and less magnesium as carbonate saturation states are lowered with latitude patterns currently observed. These changes, related to latitude, are also likely to occur as ocean acidification and climate change alters seawater chemistry throughout the world's oceans. Under proposed conditions as set by the IPCC it is probable that organisms will exhibit

smaller size, slower metabolic rates and reduced calcification, all expected to cascade to changes in predation and intraspecific competition, especially those organisms that do not calcify. Calcifying organisms will have difficulty both forming and creating calcified structures as carbonates become limited, but also in repairing and maintaining structures as dissolution becomes favoured. Due to recent increases in carbon dioxide since the Industrial Revolution, it may be feasible that populations and species have already adapted to local changes under a relatively short time frame and are demonstrating a possibility for them to further adapt in the face of exacerbated conditions.

6.6 Spines (Allometry + Biomineralogy + Strength)

The spines of the urchin *Evechinus chloroticus* are crucial to ensuring the survival of the individual, protecting the valuable innards contained within the easily broken test. Primary spines are the ultimate defence mechanism for the slow-moving organism, reducing the probability of becoming prey from species such as NZ rock lobster (*Jasus edwardsii*) and blue cod (*Parapercis colias*). From the results presented in this study, I can confidently conclude longer spines have a lower flexural stress point than shorter ones; and I was able to determine larger individuals of *E. chloroticus* had larger spines. From this connection, I can confidently say that larger organisms had comparatively weaker spines than spines from smaller individuals. It is possible that the purpose of the spine in larger organisms is to act as deterrent to predators, with increasing spine length increasing the risk of impaling a predator; while smaller organisms may require stronger spines to increase the damage as a predator attempts to crush the individual. Low magnesium calcite structures (<4 wt % Mg) are more chemically stable than elements with higher magnesium content (>4 wt % Mg); so that low-magnesium components are more resistant to dissolution than components containing high magnesium (Andersson et al. 2008). Spines have a lower magnesium content than the feeding apparatus, decreasing the solubility of the structure to the surrounding marine environment, since spines don't have the coelom buffering Aristotle's lantern components (demi-pyramids, rotulae and epiphysis). The teeth, which are formed and mostly encased within the Aristotle's lantern demonstrate an intermediate level of magnesium content, providing further evidence that the coelom offers a buffer against the seawater exposure. Magnesium content in structures has been used as a proxy for strength. Substitution of magnesium for calcium in the carbonate structure increases strength and decreases brittleness, all while increasing the solubility of the structure. I was unable to make this association between strength and magnesium content, due in part to the small sample size, and since both tests are destructive. I did not see variations in magnesium content between locations that clearly demonstrated differences in strength.

The difference observed in magnesium concentrations between spines and other skeletal components may have evolved as a function of preventing dissolution to ambient seawater, reflecting the trade-offs for strength and calcification. Due to the exposed nature of the spine, in conjunction with a thinner epidermal layer on the spines relative to the epidermal layer on the test, it is likely that the spines will demonstrate changes as a result of ocean acidification first. Abrasions on the spine during locomotion or defence, and spine breakage from defence, all unavoidable activities will additionally expose the spines to risk from climate change before any other calcium carbonate structure.

As magnesium content within a single individual ranges from low magnesium to high magnesium incorporation in different structures, it is thought that magnesium substitution into the calcite structure is actively managed through multiple pathways. It may be possible for magnesium content in spines to reduce further, however, magnesium reduction in spines could cause cascading effects to other components of the urchin's life. Reducing magnesium incorporation into the spine would decrease the strength, increasing brittleness and increasing predation risk, however reducing the length of the spine at the same time could compensate for the loss of strength as smaller spines are stronger. This would create a feedback loop of reducing magnesium as calcification is hindered and dissolution is favoured, to a smaller spine length, compensating for strength. I have no doubt that there would be a point where spine length could not be reduced further as the risk of predation becomes too great.

Another option to compensate for reduced magnesium incorporation into calcification is reduced to growth for an individual. Ebert et al. (2007) asserted slower growing organisms had a higher quantity of magnesium in their structures compared to faster growing urchins. A point to mention is that climate change, will not only increase the acidification of the world's oceans, but also increase oceanic temperatures, a trend already observed into today's scientific literature. Increased temperature increases the metabolic activity, increasing growth rates and size of organisms until thermal and acidification limits are reached, whereas metabolic activity is strained. Uthicke et al. (2014) has demonstrated that under strained metabolic activity, gonad development and investment suffer, reducing investment to offspring and further generations, ultimately impacting population maintenance.

6.7 Conclusion

This study provides the first investigation into positive and negative feedbacks on *Evechinus chloroticus* allometry, biomineralogy and strength. These three components contribute to the skeletal effectiveness and resilience, and differences amongst populations

will contribute to their success in changing sea water. A cascade of changes, both predicted and unknown, may arise as we stare into the face of climate change, with conditions predicted to worsen. Using populations inhabiting atypical locations, such as Fiordland and White Island, I have demonstrated some fine scale changes compared to other locations and can use inferences about the changes that may occur in the light of climate change, using these locations and the individuals there as proxies.

Evechinus chloroticus, an important ecosystem engineer appears to have adapted to a range of conditions throughout New Zealand, constrained in their Aristotle's lantern morphology, with differences in their biomineralogy obvious in their skeletal structures, ultimately combining to result in individual and population variation.

7 References

Airoldi, L., Balata, D., & Beck, M. W. (2008). The gray zone: relationships between habitat loss and marine diversity and their applications in conservation. *Journal of Experimental Marine Biology and Ecology*, 366(1-2), 8-15.

Andersson, A. J., Mackenzie, F. T., & Bates, N. R. (2008). Life on the margin: implications of ocean acidification on Mg-calcite, high latitude and cold-water marine calcifiers. *Marine Ecology Progress Series*, 373, 265-273.

Andrew, N. L. (1988). Ecological aspects of the common sea urchin, *Evechinus chloroticus*, in northern New Zealand: a review. *New Zealand Journal of Marine and Freshwater research*, 22(3), 415-426.

Asnaghi, V., Mangialajo, L., Gattuso, J.P., Francour, P., Privitera, D. and Chiantore, M., (2014). Effects of ocean acidification and diet on thickness and carbonate elemental composition of the test of juvenile sea urchins. *Marine Environmental Research*, 93, pp.78-84.

Barker, M. F. (2001). The ecology of *Evechinus chloroticus*. *Developments in Aquaculture and Fisheries Science*, 32, 245-260.

Barker, M. F. (2013). *Evechinus chloroticus*. *Developments in Aquaculture and Fisheries Science* (Vol. 38, pp. 355-368). Elsevier.

Berge, J. A., Bjerkeng, B., Pettersen, O., Schaanning, M. T., & Øxnevad, S. (2006). Effects of increased sea water concentrations of CO_2 on growth of the bivalve Mytilus edulis L. *Chemosphere*, 62(4), 681-687.

Berman, A., Addadi, L., Kvick, A., Leiserowitz, L., Nelson, M., Weiner, S. (1990). Intercalation of Sea Urchin Proteins in Calcite: Study of a Crystalline Composite Material. *Science* 250, 664–667.

Black, R., Codd, C., Hebbert, D., Vink, S., & Burt, J. (1984). The functional significance of the relative size of Aristotle's lantern in the sea urchin Echinometramathaei (de Blainville). *Journal of Experimental Marine Biology and Ecology*, 77(1-2), 81-97.

Black, R., Johnson, M. S., & Trendall, J. T. (1982). Relative size of Aristotle's lantern in Echinometra mathaei occuring at different densities. *Marine Biology*, 71(1), 101-106.

Blezard, R. H. (1980). Calculated sea area of the New Zealand 200 nautical mile Exclusive Economic Zone. *New Zealand Journal of Marine and Freshwater research*, 14(2), 137-138.

Borremans, C., Hermans, J., Baillon, S., André, L., & Dubois, P. (2009). Salinity effects on the Mg/Ca and Sr/Ca in starfish skeletons and the echinoderm relevance for paleoenvironmental reconstructions. *Geology*, 37(4), 351-354. Chicago.

Bressan, M., Chinellato, A., Munari, M., Matozzo, V., Manci, A., Marčeta, T., ... & Marin, M. G. (2014). Does seawater acidification affect survival, growth and shell integrity in bivalve juveniles?. *Marine Environmental Research*, 99, 136-148.

Brinkman, T. J., & Smith, A. M. (2015). Effect of climate change on crustose coralline algae at a temperate vent site, White Island, New Zealand. *Marine and Freshwater Research*, 66(4), 360-370.

Broecker, W. S., & Clark, E. (2002). Carbonate ion concentration in glacial-age deep waters of the Caribbean Sea*. Geochemistry, Geophysics, Geosystems*, 3(3), 1-14.

Byrne, M. (2012). Global change ecotoxicology: identification of early life history bottlenecks in marine invertebrates, variable species responses and variable experimental approaches. *Marine Environmental Research*, 76, 3-15.

Byrne, M., Ho, M., Selvakumaraswamy, P., Nguyen, H. D., Dworjanyn, S. A., & Davis, A. R. (2009). Temperature, but not pH, compromises sea urchin fertilization and early development under near-future climate change scenarios. *Proceedings of the Royal Society B: Biological Sciences*, 276(1663), 1883-1888.

Byrne, M., Smith, A. M., West, S., Collard, M., Dubois, P., Graba-Landry, A., & Dworjanyn, S. A. (2014). Warming influences Mg^{2+} content, while warming and acidification influence calcification and test strength of a sea urchin. *Environmental Science & Technology*, 48(21), 12620-12627.

Caldeira, K., & Wickett, M. E. (2005). Ocean model predictions of chemistry changes from carbon dioxide emissions to the atmosphere and ocean. *Journal of Geophysical Research: Oceans*, 110(C9).

Carey, N., & Sigwart, J. D. (2014). Size matters: plasticity in metabolic scaling shows body-size may modulate responses to climate change. *Biology letters*, 10(8), 20140408.

Carey, N., Harianto, J., & Byrne, M. (2016). Sea urchins in a high-CO_2 world: partitioned effects of body size, ocean warming and acidification on metabolic rate. *Journal of Experimental Biology,* 219(8), 1178-1186.

Chakra, M. A., & Stone, J. R. (2011). Classifying echinoid skeleton models: testing ideas about growth and form. *Paleobiology*, 37(4), 686-695.

Chave, K. E. (1954). Aspects of the biogeochemistry of magnesium 2. Calcareous sediments and rocks. *The Journal of Geology*, 62(6), 587-599.

Chiswell, S. M. (1996). Variability in the southland current, New Zealand. *New Zealand Journal of Marine andFfreshwater Research,* 30(1), 1-17.

Chiswell, S. M., Bostock, H. C., Sutton, P. J., & Williams, M. J. (2015). Physical oceanography of the deep seas around New Zealand: a review. *New Zealand Journal of Marine and Freshwater Research*, 49(2), 286-317.

Collard, M., Rastrick, S. P., Calosi, P., Demolder, Y., Dille, J., Findlay, H. S., ... & Dehairs, F. (2016). The impact of ocean acidification and warming on the skeletal mechanical properties of the sea urchin Paracentrotus lividus from laboratory and field observations. *ICES Journal of Marine Science*, 73(3), 727-738.

Cramer, W., Guiot, J., Fader, M., Garrabou, J., Gattuso, J. P., Iglesias, A., ... & Penuelas, J. (2018). Climate change and interconnected risks to sustainable development in the Mediterranean. *Nature Climate Change*, 8(11), 972-980.

Crowley, T. J. (2000). Causes of climate change over the past 1000 years. *Science*, 289(5477), 270-277.

Currey, J. D. (1975). A comparison of the strength of echinoderm spines and mollusc shells. *Journal of the Marine Biological Association of the United Kingdom*, 55(2), 419-424.

Dafni, J. (1980). Abnormal growth patterns in the sea urchin Tripneustes cf. gratilla (L.) under pollution (Echinodermata, Echinoidea). *Journal of Experimental Marine Biology and Ecology*, 47(3), 259-279.

Davies, T. T., Crenshaw, M. A., & Heatfield, B. M. (1972). The effect of temperature on the chemistry and structure of echinoid spine regeneration. *Journal of Paleontology*, 874-883.

De Villiers, S. (2004). Optimum growth conditions as opposed to calcite saturation as a control on the calcification rate and shell-weight of marine foraminifera. *Marine Biology*, 144(1), 45-49.

Dell'Acqua, O., Trębala, M., Chiantore, M., & Hannula, S. P. (2019). Robustness of Adamussium colbecki shell to ocean acidification in a short-term exposure. *Marine Environmental Research*, 149, 90-99.

Dery, A., Collard, M., & Dubois, P. (2017). Ocean acidification reduces spine mechanical strength in Euechinoid but not in Cidaroid sea urchins. *Environmental Science & Technology*, 51(7), 3640-3648.

Dix, T. G. (1970). Biology of *Evechinus chloroticus* (Echinoidea: Echinometridae) from different localities: 1. General. *New Zealand Journal of Marine and Freshwater Research*, 4(2), 91-116.

Dix, T. G. (1972). Biology of *Evechinus chloroticus* (Echinoidia: Echinometridae) from different localities: 4. Age, growth, and size. *New Zealand Journal of Marine and Freshwater Research*, 6(1-2), 48-68.

Doney, S. C., Fabry, V. J., Feely, R. A., & Kleypas, J. A. (2009). Ocean acidification: the other CO_2 problem. *Annual Review of Marine Science*, 1, 169-192.

Doney, S. C., Busch, D. S., Cooley, S. R., & Kroeker, K. J. (2020). The impacts of ocean acidification on marine ecosystems and reliant human communities. Annual Review of Environment and Resources, 45.

Donnay, G., Pawson, D.L. (1969). X-ray diffraction studies of echinoderm plates. *Science* 166, 1147–1150.

Dupont, S., Ortega-Martinez, O., & Thorndyke, M. (2010). Impact of near-future ocean acidification on echinoderms. *Ecotoxicology*, 19(3), 449-462.

Ebert, T. A. (1968). Growth rates of the sea urchin *Strongylocentrotus purpuratus* related to food availability and spine abrasion. *Ecology*, 49(6), 1075-1091.

Ebert, T. A. (1980). Relative growth of sea urchin jaws: an example of plastic resource allocation. *Bulletin of Marine Science*, 30(2), 467-474.

Ebert, T. A. (1988). Calibration of natural growth lines in ossicles of two sea urchins, *Strongylocentrotus purpuratus* and *Echinometra mathaei*, using tetracycline. In 6th International Echinoderm Conference'.(Eds RD, Burke, PV Mladenov, P. Lambert, and RL Parsley.) pp. 435-443.

Ebert, T. A. (2007). Growth and survival of postsettlement sea urchins. *Developments in Aquaculture and Fisheries Science* (Vol. 37, pp. 95-134). Elsevier.

Ebert, T. A., Dixon, J. D., Schroeter, S. C., Kalvass, P. E., Richmond, N. T., Bradbury, W. A., & Woodby, D. A. (1999). Growth and mortality of red sea urchins *Strongylocentrotus franciscanus* across a latitudinal gradient. *Marine Ecology Progress Series*, 190, 189-209.

Ebert, T. A., Hernández, J. C., & Clemente, S. (2014). Annual reversible plasticity of feeding structures: cyclical changes of jaw allometry in a sea urchin. *Proceedings of the Royal Society B: Biological Sciences*, 281(1779), 20132284.

Elliott, L. F., Russell, M. P., & Hernández, J. C. (2012). Estimating echinoid test volume from height and diameter measurements. In Echinoderms in a Changing World: Proceedings of the 13th International Echinoderm Conference, January 5-9 2009, University of Tasmania, Hobart Tasmania, Australia (p. 105). CRC Press.

Emerson, C.E., Reinardy, H.C., Bates, N.R. and Bodnar, A.G., (2017). Ocean acidification impacts spine integrity but not regenerative capacity of spines and tube feet in adult sea urchins. *Royal Society open science*, 4(5), p.170140.

Epherra, L., Crespi-Abril, A., Meretta, P.E., Cledón, M., Morsan, E.M. and Rubilar, T. (2015). Morphological plasticity in the Aristotle's lantern of Arbacia dufresnii (Phymosomatoida: Arbaciidae) off the Patagonian coast. *Revista de Biología Tropical*, 63, pp.339-351.

Feely, R. A., Doney, S. C., & Cooley, S. R. (2009). Ocean acidification: Present conditions and future changes in a high-CO_2 world. *Oceanography*, 22(4), 36-47.

Ferguson, J. E., Henderson, G. M., Kucera, M., & Rickaby, R. E. M. (2008). Systematic change of foraminiferal Mg/Ca ratios across a strong salinity gradient. *Earth and Planetary Science Letters*, 265(1-2), 153-166.

Fitzer, S. C., Zhu, W., Tanner, K. E., Phoenix, V. R., Kamenos, N. A., & Cusack, M. (2015). Ocean acidification alters the material properties of Mytilus edulis shells. *Journal of the Royal Society Interface*, 12(103), 20141227.

Gattuso, J. P., Allemand, D., & Frankignoulle, M. (1999). Photosynthesis and calcification at cellular, organismal and community levels in coral reefs: a review on interactions and control by carbonate chemistry. *American Zoologist*, 39(1), 160-183.

Gattuso, J. P., Frankignoulle, M., Bourge, I., Romaine, S., & Buddemeier, R. W. (1998). Effect of calcium carbonate saturation of seawater on coral calcification. *Global and Planetary Change*, 18(1-2), 37-46.

Gattuso, J. P., Gao, K., Lee, K., Rost, B., Schulz, K. G., Riebesell, U., ... & Hansson, L. (2010). Guide to best practices for ocean acidification research and data reporting. *Marine Chemistry*, 171, 36-43.

Gaylord, B., Hill, T. M., Sanford, E., Lenz, E. A., Jacobs, L. A., Sato, K. N., ... & Hettinger, A. (2011). Functional impacts of ocean acidification in an ecologically critical foundation species. *Journal of Experimental Biology*, 214(15), 2586-2594.

Gazeau, F., Quiblier, C., Jansen, J. M., Gattuso, J. P., Middelburg, J. J., & Heip, C. H. (2007). Impact of elevated CO_2 on shellfish calcification. *Geophysical research letters*, 34(7).

Gibson, R., Atkinson, R., Gordon, J., Smith, I., & Hughes, D. (2011). Impact of ocean warming and ocean acidification on marine invertebrate life history stages: vulnerabilities and potential for persistence in a changing ocean. *Oceanography of Marine Biology Annual Review*, 49, 1-42.

Gooding, R. A., Harley, C. D., & Tang, E. (2009). Elevated water temperature and carbon dioxide concentration increase the growth of a keystone echinoderm. *Proceedings of the National Academy of Sciences*, 106(23), 9316-9321.

Grace, R. V. (1975). White Island notes. Tane, 21, 91-100.

Gray, B. E., & Smith, A. M. (2004). Mineralogical variation in shells of the blackfoot abalone, *Haliotis iris* (Mollusca: Gastropoda: Haliotidae), in southern New Zealand. *Pacific Science*, 58(1), 47-64.

Guillou, M., Lumingas, L. J., & Michel, C. (2000). The effect of feeding or starvation on resource allocation to body components during the reproductive cycle of the sea urchin Sphaerechinus granularis (Lamarck). *Journal of Experimental Marine Biology and Ecology*, 245(2), 183-196.

Guinotte, J. M., & Fabry, V. J. (2008). Ocean acidification and its potential effects on marine ecosystems. *Annals of the New York Academy of Sciences*, 1134(1), 320-342.

Haag, N., Russell, M. P., & Hernandez, J. C. (2016). Effects of spine damage and microhabitat on resource allocation of the purple sea urchin Strongylocentrotus purpuratus (Stimpson 1857). *Journal of Experimental Marine Biology and Ecology, 482*, 106-117.

Hall-Spencer, J. M., Rodolfo-Metalpa, R., Martin, S., Ransome, E., Fine, M., Turner, S. M., ... & Buia, M. C. (2008). Volcanic carbon dioxide vents show ecosystem effects of ocean acidification. *Nature*, 454(7200), 96-99.

Harley, C. D., Randall Hughes, A., Hultgren, K. M., Miner, B. G., Sorte, C. J., Thornber, C. S., ... & Williams, S. L. (2006). The impacts of climate change in coastal marine systems. *Ecology letters*, 9(2), 228-241.

Hazan, Y., Wangensteen, O. S., & Fine, M. (2014). Tough as a rock-boring urchin: adult Echinometra sp. EE from the Red Sea show high resistance to ocean acidification over long-term exposures. *Marine Biology*, 161(11), 2531-2545.

Hermans, J., Borremans, C., Willenz, P., André, L., & Dubois, P. (2010). Temperature, salinity and growth rate dependences of Mg/Ca and Sr/Ca ratios of the skeleton of the sea urchin Paracentrotus lividus (Lamarck): an experimental approach. *Marine Biology*, 157(6), 1293-1300.

Hernández, J. C., & Russell, M. P. (2010). Substratum cavities affect growth-plasticity, allometry, movement and feeding rates in the sea urchin Strongylocentrotus purpuratus. *Journal of Experimental Biology*, 213(3), 520-525.

Hoegh-Guldberg, O., & Bruno, J. F. (2010). The impact of climate change on the world's marine ecosystems. *Science*, 328(5985), 1523-1528.

Hoegh-Guldberg, O., Mumby, P. J., Hooten, A. J., Steneck, R. S., Greenfield, P., Gomez, E., ... & Knowlton, N. (2007). Coral reefs under rapid climate change and ocean acidification. *Science*, 318(5857), 1737-1742.

Hofmann, G. E., Barry, J. P., Edmunds, P. J., Gates, R. D., Hutchins, D. A., Klinger, T., & Sewell, M. A. (2010). The effect of ocean acidification on calcifying organisms in marine ecosystems: an organism-to-ecosystem perspective. *Annual Review of Ecology, Evolution, and Systematics*, 41, 127-147.

Holtmann, W. C., Stumpp, M., Gutowska, M. A., Syré, S., Himmerkus, N., Melzner, F., & Bleich, M. (2013). Maintenance of coelomic fluid pH in sea urchins exposed to elevated CO 2: the role of body cavity epithelia and stereom dissolution. *Marine Biology*, 160(10), 2631-2645.

Howes, E. L., Joos, F., Eakin, M., & Gattuso, J. P. (2015). An updated synthesis of the observed and projected impacts of climate change on the chemical, physical and biological processes in the oceans. *Frontiers in Marine Science*, 2, 36.

Ipcc, C. C. (2001). The scientific basis. IPCC Third Assessment Report of Working Group I.

IPCC, C. C. (2007). The physical science basis.

IPCC, W. (2013). Working Group 1 Contribution to the IPCC Fifth Assessment Report: Climate Change 2013: The Physical Science Basis, Summary for Policymakers. IPCC, UN.

Johnson, C. R., & Mann, K. H. (1982). Adaptations of Strongylocentrotus droebachiensis for survival on barren grounds in Nova Scotia. In Echinoderms: *Proceedings of the International Conference* (pp. 277-283).

Killian, C. E., Metzler, R. A., Gong, Y. U. T., Olson, I. C., Aizenberg, J., Politi, Y., ... & Kunz, M. (2009). Mechanism of calcite co-orientation in the sea urchin tooth. *Journal of the American Chemical Society*, 131(51), 18404-18409.

Kleypas, J. A., Buddemeier, R. W., Archer, D., Gattuso, J. P., Langdon, C., & Opdyke, B. N. (1999). Geochemical consequences of increased atmospheric carbon dioxide on coral reefs. *Science*, 284(5411), 118-120.

Kleypas, J. A., Feely, R. A., Fabry, V. J., Langdon, C., Sabine, C. L., & Robbins, L. L. (2005). Impacts of ocean acidification on coral reefs and other marine calcifiers: a guide for future research. *In Report of a workshop held* (Vol. 18, No. 2005, p. 20).

Kuffner, I. B., Andersson, A. J., Jokiel, P. L., Ku'ulei, S. R., & Mackenzie, F. T. (2008). Decreased abundance of crustose coralline algae due to ocean acidification. *Nature Geoscience*, 1(2), 114-117.

Kurihara, H. (2008). Effects of CO_2-driven ocean acidification on the early developmental stages of invertebrates. *Marine Ecology Progress Series*, 373, 275-284.

Lamare, M. D., Mladenov, P.V. (2000) Modelling somatic growth in the sea urchin *Evechinus chloroticus* (Echinoidea: Echinometridae). *Journal of Experimental Marine Biology and Ecology*, vol. 243 (pg. 17-43)

Lang, C. and Mann, K.H., 1976. Changes in sea urchin populations after the destruction of kelp beds. *Marine Biology*, 36(4), pp.321-326.

Lauer, Christoph, Kilian Sillmann, Sebastian Haußmann, and Klaus G. Nickel. "..." *Bioinspiration & Biomimetics* 14, no. 1 (2018): 016018.

LaVigne, M., Hill, T. M., Sanford, E., Gaylord, B., Russell, A. D., Lenz, E. A., ... & Young, M. K. (2013). The elemental composition of purple sea urchin (Strongylocentrotus purpuratus) calcite and potential effects of p CO 2 during early life stages. *Biogeosciences*, 10(6).

Levitan, D. R. (1991). Skeletal changes in the test and jaws of the sea urchin *Diadema antillarum* in response to food limitation. *Marine Biology*, 111(3), 431-435.

Ling, S. D., & Johnson, C. R. (2009). Population dynamics of an ecologically important range-extender: kelp beds versus sea urchin barrens. *Marine Ecology Progress Series*, 374, 113-125.

Ling, S. D., Scheibling, R. E., Rassweiler, A., Johnson, C. R., Shears, N., Connell, S. D., ... & Clemente, S. (2015). Global regime shift dynamics of catastrophic sea urchin overgrazing. *Philosophical Transactions of the Royal Society B: Biological Sciences*, 370(1659), 20130269.

Linse, K., Barnes, D. K., & Enderlein, P. (2006). Body size and growth of benthic invertebrates along an Antarctic latitudinal gradient. Deep Sea Research Part II. *Topical Studies in Oceanography*, 53(8-10), 921-931.

Llodra, E. R. (2002). Fecundity and life-history strategies in marine invertebrates. *Advances in Marine Biology*, 43, 88-172.

Ma, Y., Aichmayer, B., Paris, O., Fratzl, P., Meibom, A., Metzler, R. A., ... & Weiner, S. (2009). The grinding tip of the sea urchin tooth exhibits exquisite control over calcite crystal orientation and Mg distribution. *Proceedings of the National Academy of Sciences*, 106(15), 6048-6053.

MacKenzie, L. (1991). Toxic and noxious phytoplankton in Big Glory Bay, Stewart Island, New Zealand. *Journal of Applied Phycology*, 3(1), 19-34.

Magdans, U., & Gies, H. (2004). Single crystal structure analysis of sea urchin spine calcites: Systematic investigations of the Ca/Mg distribution as a function of habitat of the sea urchin and the sample location in the spine. *European Journal of Mineralogy*, 16(2), 261-268.

Malone, P. G., & Dodd, J. R. (1967). Temperature and salinity effects on calcification rate in Mytilus edulis and its paleoecological implications 1. *Limnology and Oceanography*, 12(3), 432-436.

Martin, S., Richier, S., Pedrotti, M. L., Dupont, S., Castejon, C., Gerakis, Y., ... & Gattuso, J. P. (2011). Early development and molecular plasticity in the Mediterranean sea urchin Paracentrotus lividus exposed to CO_2-driven acidification. *Journal of Experimental Biology*, 214(8), 1357-1368.

McClintock, J. B., Amsler, M. O., Angus, R. A., Challener, R. C., Schram, J. B., Amsler, C. D., ... & Baker, B. J. (2011). The Mg-calcite composition of Antarctic echinoderms: Important implications for predicting the impacts of ocean acidification. *The Journal of Geology*, 119(5), 457-466.

Menon, S., Denman, K. L., Brasseur, G., Chidthaisong, A., Ciais, P., Cox, P. M., ... & Jacob, D. (2007). Couplings between changes in the climate system and biogeochemistry (No. LBNL-464E). Lawrence Berkeley National Lab.(LBNL), Berkeley, CA (United States).

Miles, H., Widdicombe, S., Spicer, J. I., & Hall-Spencer, J. (2007). Effects of anthropogenic seawater acidification on acid–base balance in the sea urchin *Psammechinus miliaris*. *Marine pollution bulletin*, 54(1), 89-96.

Moore, H. B. (1935). A comparison of the biology of *Echinus esculentus* in different habitats. Part II. *Journal of the Marine Biological Association of the United Kingdom*, 20(1), 109-128.

Morse, J. W., Arvidson, R. S., & Lüttge, A. (2007). Calcium carbonate formation and dissolution. *Chemical Reviews*, 107(2), 342-381.

Moulin, L., Grosjean, P., Leblud, J., Batigny, A., & Dubois, P. (2014). Impact of elevated pCO_2 on acid–base regulation of the sea urchin *Echinometra mathaei* and its relation to resistance to ocean acidification: a study in mesocosms. *Journal of experimental Marine Biology and Ecology*, 457, 97-104.

Moureaux, C., Perez-Huerta, A., Compère, P., Zhu, W., Leloup, T., Cusack, M., & Dubois, P. (2010). Structure, composition and mechanical relations to function in sea urchin spine. *Journal of Structural Biology,* 170(1), 41-49.

New Zealand, Auckland, Auckland, T and data (2019) Climate Auckland: Temperature, Climograph, Climate Table For Auckland - Climate-Data.Org. [online] En.climate-data.org. Available at: < *https://en.climate-data.org/oceania/new-zealand/auckland/auckland-3605/*> [Accessed 15 February 2019].

New Zealand, Wellington, Wellington, T and data (2019) Climate Wellington: Temperature, Climograph, Climate Table For Wellington - Climate-Data.Org. [online] En.climate-data.org. Available at: < *https://en.climate-data.org/oceania/new-zealand/wellington/wellington-2/*> [Accessed 15 February 2019].

Nickel, K. G., Klang, K., Lauer, C., & Buck, G. (2018). Sea urchin spines as role models for biologic design and integrative structures. *Highlights of Applied Mineralogy,* 1-14.

NRLMG (2008). Annual Report. National Rock Lobster Management Group.

O'Connor, M. I. (2009). Warming strengthens an herbivore–plant interaction. *Ecology*, 90(2), 388-398.

O'Connor, M. I., Bruno, J. F., Gaines, S. D., Halpern, B. S., Lester, S. E., Kinlan, B. P., & Weiss, J. M. (2007). Temperature control of larval dispersal and the implications for marine ecology, evolution, and conservation. *Proceedings of the National Academy of Sciences*, 104(4), 1266-1271.

Orr, J. C. (2011). Recent and future changes in ocean carbonate chemistry. *Ocean Acidification*, 2, 41-66.

Pomory, C. M., & Lares, M. T. (2011). Scaling in the Aristotle's Lantern of *Lytechinus variegatus* (Echinodermata: Echinoidea). *Gulf of Mexico Science*, 29(2), 5.

Pörtner, H. O. (2010). Oxygen-and capacity-limitation of thermal tolerance: a matrix for integrating climate-related stressor effects in marine ecosystems. *Journal of Experimental Biology*, 213(6), 881-893.

Pörtner, H. O., & Peck, M. A. (2010). Climate change effects on fishes and fisheries: towards a cause-and-effect understanding. *Journal of Fish Biology,* 77(8), 1745-1779.

Presser, V., Schultheiß, S., Berthold, C. and Nickel, K.G. (2009). Sea urchin spines as a model-system for permeable, light-weight ceramics with graceful failure behavior. Part I. Mechanical behavior of sea urchin spines under compression. *Journal of Bionic Engineering*, 6(3), pp.203-213.

Przeslawski, R., Ahyong, S., Byrne, M., Woerheide, G., & Hutchings, P. A. T. (2008). Beyond corals and fish: the effects of climate change on noncoral benthic invertebrates of tropical reefs. *Global Change Biology*, 14(12), 2773-2795.

Richter, D.K., and Bruckschen, P. (1998), Geochemistry of recent tests of Echinocyamus pusillus: Constraints for temperature and salinity. *Carbonates & Evaporites*, v. 13, p. 157–167.

Ridgway, K., & Hill, K. (2012). East Australian Current. *A Marine Climate Change Impacts and Adaptation Report card for Australia*, 2012.

Riebesell, U., & Gattuso, J. P. (2015). Lessons learned from ocean acidification research. *Nature Climate Change,* 5(1), 12-14.

Riebesell, U., Zondervan, I., Rost, B., Tortell, P. D., Zeebe, R. E., & Morel, F. M. (2000). Reduced calcification of marine plankton in response to increased atmospheric CO 2. *Nature,* 407(6802), 364-367.

Ries, J. B. (2004). Effect of ambient Mg/Ca ratio on Mg fractionation in calcareous marine invertebrates: A record of the oceanic Mg/Ca ratio over the Phanerozoic. *Geology*, 32(11), 981-984.

Sabine, C. L., Feely, R. A., Gruber, N., Key, R. M., Lee, K., Bullister, J. L., ... & Millero, F. J. (2004). The oceanic sink for anthropogenic CO_2. *Science*, 305(5682), 367-371.

San Chan, V. B., Li, C., Lane, A. C., Wang, Y., Lu, X., Shih, K., ... & Thiyagarajan, V. (2012). CO_2-driven ocean acidification alters and weakens integrity of the calcareous tubes produced by the serpulid tubeworm, Hydroides elegans. *PLoS one*, 7(8).

Sanford, E., & Kelly, M. W. (2011). Local adaptation in marine invertebrates. *Annual Review of Marine Science,* 3, 509-535.

Schlegel, P., Havenhand, J. N., Gillings, M. R., & Williamson, J. E. (2012). Individual variability in reproductive success determines winners and losers under ocean acidification: a case study with sea urchins. *PloS one*, 7(12).

Sheridan, J. A., & Bickford, D. (2011). Shrinking body size as an ecological response to climate change. *Nature Climate Change*, 1(8), 401.

Shirayama, Y., & Thornton, H. (2005). Effect of increased atmospheric CO_2 on shallow water marine benthos. Journal of Geophysical Research. *Oceans*, 110(C9).

Smith, A. M., Clark, D. E., Lamare, M. D., Winter, D. J., & Byrne, M. (2016). Risk and resilience: variations in magnesium in echinoid skeletal calcite. *Marine Ecology Progress Series*, 561, 1-16.

Stanley, S. M. (2006). Influence of seawater chemistry on biomineralization throughout Phanerozoic time: Paleontological and experimental evidence. *Palaeogeography, Palaeoclimatology, Palaeoecology*, 232(2-4), 214-236.

Stanton, B. R., & Pickard, G. L. (1980). Physical oceanography of the New Zealand fjords. *In Fjord oceanography* (pp. 329-332). Springer, Boston, MA.

Stephenson, A. E., Hunter, J. L., Han, N., DeYoreo, J. J., & Dove, P. M. (2011). Effect of ionic strength on the Mg content of calcite: Toward a physical basis for minor element uptake during step growth. *Geochimica et Cosmochimica Acta*, 75(15), 4340-4350.

Stevens, C., & Chiswell, C. (2019) 'Ocean currents and tides - Currents', Te Ara - the Encyclopedia of New Zealand, Available at: < *http://www.TeAra.govt.nz/en/ocean-currents-and-tides/page-1*> [accessed 20 February 2019].

Strathmann, R. R. (1981). The role of spines in preventing structural damage to echinoid tests. *Paleobiology*, 7(3), 400-406.

Stumpp, M., Wren, J., Melzner, F., Thorndyke, M. C., & Dupont, S. T. (2011). CO_2 induced seawater acidification impacts sea urchin larval development I: elevated metabolic rates decrease scope for growth and induce developmental delay. *Comparative Biochemistry and Physiology Part A: Molecular & Integrative Physiology*, 160(3), 331-340.

Su, X., Kamat, S., & Heuer, A. H. (2000). The structure of sea urchin spines, large biogenic single crystals of calcite. *Journal of Materials Science,* 35(22), 5545-5551.

Sumich, J. L., & McCauley, J. E. (1972). Calcium-magnesium ratios in the test plates of Allocentrotus fragilis. *Marine Chemistry*, 1(1), 55-59.

Sutton, P. J. (2003). The Southland Current: a subantarctic current. *New Zealand Journal of Marine and Freshwater Research*, 37(3), 645-652.

Tait, P., & Tait, J. (2001). White Island: New Zealand's Most Active Volcano. *Godwit*.

Tegner, M.J. and Levin, L.A., 1983. Spiny lobsters and sea urchins: analysis of a predator-prey interaction. *Journal of Experimental Marine Biology and Ecology*, 73(2), pp.125-150.

Terhaar, J., Kwiatkowski, L., & Bopp, L. (2020). Emergent constraint on Arctic Ocean acidification in the twenty-first century. Nature, 582(7812), 379-383.

Thomas, Luke. (2020). Population Genetics of the Red Rock Lobster, Jasus edwardsii. Thesis submitted for a Masters degree, Victoria, University of Wellington

Todgham, A. E., & Hofmann, G. E. (2009). Transcriptomic response of sea urchin larvae Strongylocentrotus purpuratus to CO_2-driven seawater acidification. *Journal of Experimental Biology*, 212(16), 2579-2594.

Trogu, P. (2015). Bioinspired Design: Aristotle's Lantern and Models of Rotational Geometry by Giorgio Scarpa. *In Abstracts, Design of Medical Devices Conference—Europe* (DMD EU 2015)(Wiener Neustadt, Austria, 8–9 September 2015).

Tsafnat, N., Gerald, J. D. F., Le, H. N., & Stachurski, Z. H. (2012). Micromechanics of sea urchin spines. *PloS one*, 7(9).

Uthicke, S., Soars, N., Foo, S., & Byrne, M. (2013). Effects of elevated pCO 2 and the effect of parent acclimation on development in the tropical Pacific sea urchin Echinometra mathaei. *Marine Biology*, 160(8), 1913-1926.

Vance, J. M., Currie, K. I., Law, C. S., Murdoch, J., & Zeldis, J. (2020). NZOA-ON: the New Zealand Ocean Acidification Observing Network. *Marine and Freshwater Research*, 71(3), 281-299.

Villouta, E., Chadderton, W. L., Pugsley, C. W., & Hay, C. H. (2001). Effects of sea urchin (*Evechinus chloroticus*) grazing in dusky sound, Fiordland, New Zealand. New Zealand *Journal of Marine and Freshwater Research,* 35(5), 1007-1024.

Vink, M. J., Boezeman, D., Dewulf, A., & Termeer, C. J. (2013). Changing climate, changing frames: Dutch water policy frame developments in the context of a rise and fall of attention to climate change. *Environmental Science & Policy*, 30, 90-101.

Weber, J. N. (1973). Temperature dependence of magnesium in echinoid and asteroid skeletal calcite: a reinterpretation of its significance. *The Journal of Geology*, 81(5), 543-556.

Weber, J. N. (1973). Temperature dependence of magnesium in echinoid and asteroid skeletal calcite: a reinterpretation of its significance. *The Journal of Geology*, 81(5), 543-556.

Wernberg, T., Russell, B. D., Moore, P. J., Ling, S. D., Smale, D. A., Campbell, A., ... & Connell, S. D. (2011). Impacts of climate change in a global hotspot for temperate marine biodiversity and ocean warming. *Journal of Experimental Marine Biology and Ecology*, 400(1-2), 7-16.

Willan, R. C. (1981). Soft-bottom assemblages of Paterson Inlet, Stewart Island. *New Zealand Journal of Zoology*, 8(2), 229-248.

Wing, S. R., & Jack, L. (2010). Biological monitoring of the Fiordland (Te Moana o Atawhenua) *Marine Area and Fiordland's Marine Reserves*. 2010. Department of Conservation, Te Anau.

Wood, H. L., Spicer, J. I., & Widdicombe, S. (2008). Ocean acidification may increase calcification rates, but at a cost. *Proceedings of the Royal Society B: Biological Sciences,* 275(1644), 1767-1773.

Zitoun, R., Connell, S.D., Cornwall, C.E., Currie, K.I., Fabricius, K., Hoffmann, L.J., ... & Sewell, M. A. (2020). A unique temperate rocky coastal hydrothermal vent system (Whakaari–White Island, Bay of Plenty, New Zealand): constraints for ocean acidification studies. *Marine and Freshwater Research*, 71(3), 321-344.

Appendix A Raw Data for Whole Measurements

Table 7.1 Raw data measurements for whole *Evechinus chloroticus* collected from six locations around New Zealand

ID	Location	Height (mm)	Diameter 1 (mm)	Diameter 2 (mm)	Average Diameter (mm)	Wet Weight (g)	Wet Volume (cm^3)
EvChl-Stl-1	Stewart Island	64.15	101.08	100.68	100.88	389.10	341.82
EvChl-Stl-2	Stewart Island	51.09	93.60	100.43	97.02	281.20	251.46
EvChl-Stl-3	Stewart Island	49.45	92.88	88.13	90.51	267.30	211.94
EvChl-Stl-4	Stewart Island	55.86	87.42	87.33	87.38	267.80	223.29
EvChl-Stl-5	Stewart Island	48.13	94.50	93.90	94.20	300.00	223.62
EvChl-Stl-6	Stewart Island	50.60	90.41	91.15	90.78	282.50	218.33
EvChl-Stl-7	Stewart Island	55.86	97.70	96.12	96.91	355.90	274.67
EvChl-Stl-8	Stewart Island	59.89	100.50	96.79	98.65	384.10	305.03
EvChl-Stl-9	Stewart Island	63.95	96.38	97.11	96.75	386.20	313.39
EvChl-Stl-10	Stewart Island	49.64	85.93	86.48	86.21	255.00	193.15
EvChl-Frld-1	Fiordland	46.02	97.45	96.15	96.80	341.70	225.78
EvChl-Frld-2	Fiordland	55.20	108.25	107.61	107.93	451.60	336.68
EvChl-Frld-3	Fiordland	51.62	114.70	111.44	113.07	446.50	345.48
EvChl-Frld-4	Fiordland	42.95	90.68	88.10	89.39	250.00	179.66
EvChl-Frld-5	Fiordland	46.03	97.65	96.66	97.16	318.40	227.49
EvChl-Frld-6	Fiordland	48.07	100.40	98.80	99.60	367.50	249.67
EvChl-Frld-7	Fiordland	49.80	108.33	102.94	105.64	387.00	290.78
EvChl-Frld-8	Fiordland	54.76	112.54	109.54	111.04	485.90	353.46
EvChl-Frld-9	Fiordland	56.20	101.90	99.30	100.60	372.60	297.75
EvChl-Frld-10	Fiordland	34.80	75.15	74.58	74.87	158.00	102.12
EvChl-Pic-1	Picton	46.65	85.99	83.42	84.71	206.80	175.21
EvChl-Pic-2	Picton	46.64	89.10	88.86	88.98	191.40	193.35
EvChl-Pic-3	Picton	49.99	89.24	87.20	88.22	255.80	203.68
EvChl-Pic-4	Picton	42.59	81.34	81.12	81.23	207.50	147.14
EvChl-Pic-5	Picton	39.29	77.14	71.28	74.21	166.00	113.12
EvChl-Pic-6	Picton	45.88	87.24	85.47	86.36	238.90	179.12
EvChl-Pic-7	Picton	44.72	86.38	83.97	85.18	226.40	169.84
EvChl-Pic-8	Picton	47.90	88.87	88.77	88.82	267.10	197.86
EvChl-Pic-9	Picton	47.11	90.82	87.30	89.06	263.90	195.57
EvChl-Pic-10	Picton	44.26	88.82	85.12	86.97	228.20	175.21
EvChl-Akl-1	Auckland	30.86	57.71	57.22	57.47	51.00	53.36
EvChl-Akl-2	Auckland	30.51	60.04	59.45	59.75	59.00	57.02
EvChl-Akl-3	Auckland	41.07	71.63	71.50	71.57	88.00	110.13
EvChl-Akl-4	Auckland	34.90	62.33	62.28	62.31	58.00	70.94
EvChl-Akl-5	Auckland	37.65	67.66	67.31	67.49	106.00	89.78
EvChl-Akl-6	Auckland	31.09	57.69	56.69	57.19	43.00	53.24
EvChl-Akl-7	Auckland	29.55	55.51	54.04	54.78	46.00	46.41
EvChl-Akl-8	Auckland	29.48	55.58	54.94	55.26	55.00	47.13
EvChl-Akl-9	Auckland	42.60	76.91	75.71	76.31	114.00	129.88
EvChl-Akl-10	Auckland	31.85	59.90	59.36	59.63	59.00	59.30
EvChl-Whl-1	White Island	41.65	76.18	71.68	73.93	148.30	119.08
EvChl-Whl-2	White Island	40.24	72.67	72.07	72.37	135.40	110.35
EvChl-Whl-3	White Island	38.47	73.79	72.39	73.09	138.20	107.60
EvChl-Whl-4	White Island	40.83	71.57	71.30	71.44	128.70	109.09
EvChl-Whl-5	White Island	41.62	74.02	72.83	73.43	159.40	117.48
EvChl-Whl-6	White Island	38.39	75.83	74.27	75.05	151.10	113.21
EvChl-Whl-7	White Island	44.55	74.61	74.23	74.42	168.00	129.19
EvChl-Whl-8	White Island	42.19	75.27	74.68	74.98	186.30	124.18
EvChl-Whl-9	White Island	42.12	74.60	73.08	73.84	151.80	120.23
EvChl-Whl-10	White Island	40.11	72.79	71.39	72.09	144.10	109.13
EvChl-Wlg-1	Wellington	36.24	67.64	66.31	66.98	106.47	85.11
EvChl-Wlg-2	Wellington	33.92	65.64	65.63	65.64	93.44	76.51
EvChl-Wlg-3	Wellington	27.76	54.65	52.70	53.68	56.77	41.86
EvChl-Wlg-4	Wellington	33.33	63.18	61.33	62.26	91.09	67.62
EvChl-Wlg-5	Wellington	29.05	51.35	50.71	51.03	53.32	39.61

ID	Location	Height (mm)	Diameter 1 (mm)	Diameter 2 (mm)	Average Diameter (mm)	Wet Weight (g)	Wet Volume (cm^3)
EvChl-Wlg-6	Wellington	36.37	67.74	67.30	67.52	111.59	86.82
EvChl-Wlg-7	Wellington	32.63	65.93	63.07	64.50	88.95	71.04
EvChl-Wlg-8	Wellington	31.19	64.05	64.04	64.05	93.38	66.99
EvChl-Wlg-9	Wellington	34.70	66.24	64.32	65.28	97.26	77.41
EvChl-Wlg-10	Wellington	27.66	56.34	53.33	54.84	63.41	43.52
EvChl-Wlg-11	Wellington	37.28	69.11	68.99	69.05	107.68	93.07
EvChl-Wlg-12	Wellington	33.44	59.72	58.14	58.93	74.67	60.79
EvChl-Wlg-13	Wellington	33.04	59.97	59.48	59.73	80.83	61.71
EvChl-Wlg-14	Wellington	40.64	67.72	67.00	67.36	121.04	96.55

Appendix B Raw Data for Skeletal Elements

Table 7.2 Raw data for skeletal elements of *Evechinus chloroticus* collected from Stewart Island, New Zealand

ID	Location	Test	Primary Spine						Demi-pyramid			Rotula			Epiphysis
		Thickness	Length	Proximal Diameter	Distal Diameter	Weight	Volume	Density	Length	Width	Weight	Length	Width	Weight	Weight
		(mm)	(mm)	(mm)	(mm)	(g)	(cm^3)	(g/cm^3)	(mm)	(mm)	(g)	(mm)	(mm)	(g)	(g)
EvChl-Stl-1-A	Stewart Island	0.45	23.65	1.76	0.63	0.048	0.029	1.684	18.37	9.24	0.290	9.88	3.54	0.104	0.065
EvChl-Stl-1-B	Stewart Island	0.45	25.26	1.93	0.64	0.057	0.036	1.608	18.93	9.11	0.301	9.46	3.71	0.099	0.063
EvChl-Stl-1-C	Stewart Island	0.47	24.02	1.84	0.67	0.051	0.032	1.591	18.81	9.23	0.299	9.84	3.47	0.104	0.061
EvChl-Stl-1-D	Stewart Island	0.48	24.49	1.85	0.54	0.051	0.030	1.694	18.86	9.22	0.291	9.50	3.56	0.101	0.063
EvChl-Stl-1-E	Stewart Island	0.46	23.54	1.63	0.74	0.048	0.027	1.773	18.44	9.40	0.292	9.52	3.42	0.099	0.065
EvChl-Stl-1-F	Stewart Island	0.47	23.78	1.76	0.61	0.048	0.028	1.693	18.65	9.36	0.301				0.066
EvChl-Stl-1-G	Stewart Island	0.46	25.95	1.94	0.67	0.053	0.037	1.413	18.50	9.43	0.297				0.062
EvChl-Stl-1-H	Stewart Island	0.47	23.94	1.84	0.85	0.059	0.036	1.646	18.69	9.42	0.299				0.065
EvChl-Stl-1-I	Stewart Island	0.46	23.29	1.68	0.66	0.038	0.027	1.408	18.89	9.41	0.300				0.064
EvChl-Stl-1-J	Stewart Island	0.46	23.10	1.71	0.85	0.053	0.031	1.702	18.18	9.16	0.291				0.061
EvChl-Stl-2-A	Stewart Island	0.45	24.07	1.84	0.95	0.057	0.038	1.509	17.41	8.46	0.221	9.09	3.33	0.088	0.049
EvChl-Stl-2-B	Stewart Island	0.47	27.22	1.82	0.74	0.055	0.037	1.482	17.46	8.64	0.216	8.96	3.34	0.086	0.050
EvChl-Stl-2-C	Stewart Island	0.44	25.03	1.72	0.69	0.050	0.030	1.635	17.49	8.43	0.217	8.92	3.27	0.086	0.051
EvChl-Stl-2-D	Stewart Island	0.45	24.18	1.78	0.65	0.046	0.030	1.544	17.38	8.69	0.219	9.21	3.46	0.089	0.050
EvChl-Stl-2-E	Stewart Island	0.45	24.08	1.81	0.84	0.051	0.035	1.470	17.33	8.45	0.211	8.87	3.31	0.083	0.049
EvChl-Stl-2-F	Stewart Island	0.43	24.76	1.97	0.53	0.060	0.034	1.775	17.35	8.70	0.221				0.050
EvChl-Stl-2-G	Stewart Island	0.46	24.34	1.76	0.80	0.056	0.033	1.714	17.49	8.64	0.221				0.050
EvChl-Stl-2-H	Stewart Island	0.46	23.69	1.65	0.54	0.038	0.024	1.548	17.58	8.51	0.215				0.050
EvChl-Stl-2-I	Stewart Island	0.43	25.30	1.96	0.70	0.053	0.038	1.403	17.27	8.67	0.219				0.050
EvChl-Stl-2-J	Stewart Island	0.47	25.12	1.75	0.71	0.052	0.032	1.654	17.39	8.76	0.218				0.049
EvChl-Stl-3-A	Stewart Island	0.45	27.97	1.56	0.63	0.045	0.028	1.612	16.91	8.32	0.227	8.47	2.99	0.086	0.045
EvChl-Stl-3-B	Stewart Island	0.45	24.93	1.66	0.70	0.044	0.029	1.516	16.90	8.41	0.228	8.07	2.98	0.080	0.045
EvChl-Stl-3-C	Stewart Island	0.46	25.99	1.54	0.79	0.044	0.029	1.546	16.96	8.24	0.227	8.05	2.98	0.081	0.045
EvChl-Stl-3-D	Stewart Island	0.47	22.86	1.58	0.68	0.039	0.024	1.616	16.87	8.36	0.230	8.08	3.00	0.080	0.047
EvChl-Stl-3-E	Stewart Island	0.43	24.68	1.58	0.47	0.038	0.022	1.709	16.94	8.29	0.229	8.03	3.01	0.081	0.046
EvChl-Stl-3-F	Stewart Island	0.44	27.17	1.66	0.84	0.052	0.035	1.503	16.69	8.34	0.223				0.045
EvChl-Stl-3-G	Stewart Island	0.47	26.22	1.67	0.63	0.043	0.029	1.464	16.85	8.67	0.231				0.047
EvChl-Stl-3-H	Stewart Island	0.42	26.44	1.78	0.78	0.051	0.036	1.415	16.88	8.34	0.229				0.045
EvChl-Stl-3-I	Stewart Island	0.43	26.02	1.89	0.70	0.051	0.037	1.396	17.22	8.44	0.229				0.044
EvChl-Stl-3-J	Stewart Island	0.44	24.65	1.84	0.76	0.046	0.035	1.324	16.94	8.35	0.230				0.045
EvChl-Stl-4-A	Stewart Island	0.41	26.35	1.75	0.65	0.047	0.032	1.477	18.28	8.73	0.256	8.91	3.40	0.094	0.055
EvChl-Stl-4-B	Stewart Island	0.42	27.32	1.80	0.58	0.053	0.033	1.598	18.33	8.87	0.267	8.95	3.51	0.095	0.054
EvChl-Stl-4-C	Stewart Island	0.43	26.54	1.75	0.59	0.049	0.031	1.587	18.34	8.76	0.258	8.80	3.43	0.090	0.054
EvChl-Stl-4-D	Stewart Island	0.42	27.20	1.63	0.70	0.046	0.031	1.520	18.21	8.72	0.262	8.85	3.47	0.091	0.058
EvChl-Stl-4-E	Stewart Island	0.43	24.46	1.84	0.83	0.039	0.036	1.084	18.45	8.84	0.273	9.06	3.36	0.093	0.058
EvChl-Stl-4-F	Stewart Island	0.42	26.16	1.73	0.71	0.056	0.032	1.737	18.37	8.52	0.264				0.056

ID	Location	Test	Primary Spine						Demi-pyramid			Rotula			Epiphysis
		Thickness	Length	Proximal Diameter	Distal Diameter	Weight	Volume	Density	Length	Width	Weight	Length	Width	Weight	Weight
		(mm)	(mm)	(mm)	(mm)	(g)	(cm^3)	(g/cm^3)	(mm)	(mm)	(g)	(mm)	(mm)	(g)	(g)
EvChl-Stl-4-G	Stewart Island	0.45	25.73	1.86	0.63	0.050	0.034	1.488	18.39	8.82	0.255				0.054
EvChl-Stl-4-H	Stewart Island	0.41	22.97	1.85	0.93	0.047	0.036	1.295	18.21	8.87	0.258				0.058
EvChl-Stl-4-I	Stewart Island	0.42	22.71	1.84	0.67	0.046	0.030	1.524	18.4	8.72	0.270				0.056
EvChl-Stl-4-J	Stewart Island	0.42	26.66	1.79	0.70	0.052	0.035	1.515	18.4	8.92	0.266				0.053
EvChl-Stl-5-A	Stewart Island	0.44	23.46	2.11	0.59	0.044	0.037	1.177	17.89	8.26	0.269	8.21	3.47	0.088	0.049
EvChl-Stl-5-B	Stewart Island	0.45	25.88	1.70	0.56	0.048	0.028	1.705	17.88	8.44	0.279	8.11	3.53	0.086	0.051
EvChl-Stl-5-C	Stewart Island	0.47	25.73	1.78	0.57	0.046	0.030	1.512	18.02	8.30	0.274	8.54	3.52	0.088	0.052
EvChl-Stl-5-D	Stewart Island	0.46	25.29	1.75	0.71	0.059	0.032	1.859				8.51	3.54	0.091	0.042
EvChl-Stl-5-E	Stewart Island	0.43	23.45	1.73	0.76	0.046	0.030	1.520	18.27	8.29	0.273	8.28	3.46	0.088	0.053
EvChl-Stl-5-F	Stewart Island	0.42	23.20	1.59	0.4	0.030	0.020	1.501	17.85	8.18	0.268				0.050
EvChl-Stl-5-G	Stewart Island	0.46	25.81	1.61	0.64	0.046	0.027	1.677	18.22	8.48	0.280				0.052
EvChl-Stl-5-H	Stewart Island	0.47	24.74	1.74	0.68	0.044	0.030	1.464	17.8	8.41	0.275				0.052
EvChl-Stl-5-I	Stewart Island	0.48	25.17	1.81	0.69	0.049	0.033	1.487	18.94	8.34	0.269				0.053
EvChl-Stl-5-J	Stewart Island	0.46	22.96	1.91	0.59	0.038	0.031	1.224	18.11	8.3	0.264				0.051
EvChl-Stl-6-A	Stewart Island	0.45	21.83	1.65	0.69	0.042	0.025	1.690	17.68	8.52	0.218	8.46	3.08	0.082	0.046
EvChl-Stl-6-B	Stewart Island	0.43	21.11	1.57	0.71	0.035	0.023	1.542	17.71	8.34	0.229	8.66	3.15	0.086	0.044
EvChl-Stl-6-C	Stewart Island	0.44	22.76	1.65	0.66	0.038	0.025	1.498				8.53	3.14	0.084	0.043
EvChl-Stl-6-D	Stewart Island	0.44	22.96	1.59	0.58	0.041	0.023	1.788				8.48	3.09	0.083	0.047
EvChl-Stl-6-E	Stewart Island	0.43	24.28	1.83	0.66	0.043	0.032	1.358				8.43	3.14	0.082	
EvChl-Stl-6-F	Stewart Island	0.43	23.68	1.88	0.72	0.040	0.034	1.187							0.043
EvChl-Stl-6-G	Stewart Island	0.45	19.89	1.78	0.62	0.035	0.024	1.431							0.049
EvChl-Stl-6-H	Stewart Island	0.41	25.44	1.76	0.55	0.048	0.029	1.657							0.046
EvChl-Stl-6-I	Stewart Island	0.42	21.57	1.69	0.66	0.037	0.025	1.475							0.045
EvChl-Stl-6-J	Stewart Island	0.41	21.22	1.74	0.82	0.044	0.028	1.531							
EvChl-Stl-7-A	Stewart Island	0.43	23.74	1.69	0.79	0.050	0.030	1.667	18.10	8.53	0.243	8.61	2.99	0.077	0.046
EvChl-Stl-7-B	Stewart Island	0.42	26.10	1.89	0.85	0.058	0.040	1.441	17.82	8.51	0.241	8.64	3.10	0.077	0.047
EvChl-Stl-7-C	Stewart Island	0.46	27.22	1.70	0.83	0.062	0.036	1.735	17.96	8.70	0.243	8.58	2.98	0.077	0.048
EvChl-Stl-7-D	Stewart Island	0.45	27.94	1.91	0.72	0.061	0.041	1.500	18.18	8.49	0.241	8.66	3.15	0.076	0.047
EvChl-Stl-7-E	Stewart Island	0.45	27.53	1.86	0.69	0.059	0.038	1.571	18.07	8.56	0.243	8.75	2.96	0.077	0.046
EvChl-Stl-7-F	Stewart Island	0.47	29.68	1.94	0.79	0.061	0.046	1.326	17.98	8.47	0.240				0.047
EvChl-Stl-7-G	Stewart Island	0.42	28.22	1.90	0.81	0.066	0.043	1.532	17.71	8.81	0.241				0.046
EvChl-Stl-7-H	Stewart Island	0.45	27.19	1.73	0.68	0.063	0.033	1.917	17.90	8.69	0.238				0.049
EvChl-Stl-7-I	Stewart Island	0.45	27.93	2.00	0.77	0.069	0.045	1.528	18.20	8.79	0.238				0.047
EvChl-Stl-7-J	Stewart Island	0.46	28.81	1.84	0.79	0.063	0.041	1.539	18.1	8.71	0.243				
EvChl-Stl-8-A	Stewart Island	0.45	24.80	2.03	0.80	0.055	0.041	1.327	18.79	8.87	0.301	8.57	3.47	0.102	0.060
EvChl-Stl-8-B	Stewart Island	0.45	23.90	1.90	0.77	0.053	0.035	1.506	18.52	8.6	0.303	8.51	3.49	0.104	0.064
EvChl-Stl-8-C	Stewart Island	0.43	23.12	1.67	0.60	0.036	0.025	1.441	18.8	8.79	0.314	8.68	3.45	0.103	0.064
EvChl-Stl-8-D	Stewart Island	0.47	25.14	1.95	0.72	0.055	0.038	1.452	18.72	8.78	0.307	8.90	3.44	0.106	0.061
EvChl-Stl-8-E	Stewart Island	0.48	25.51	1.80	0.70	0.058	0.033	1.752	18.61	8.89	0.311	8.65	3.43	0.106	0.064
EvChl-Stl-8-F	Stewart Island	0.46	25.16	1.76	0.88	0.057	0.036	1.582	18.38	8.54	0.305				0.063
EvChl-Stl-8-G	Stewart Island	0.48	24.29	1.81	0.90	0.048	0.036	1.312	18.61	8.53	0.305				0.061
EvChl-Stl-8-H	Stewart Island	0.46	24.54	2.01	0.82	0.057	0.041	1.402	18.60	8.61	0.308				0.059

ID	Location	Test	Primary Spine						Demi-pyramid			Rotula			Epiphysis
		Thickness	Length	Proximal Diameter	Distal Diameter	Weight	Volume	Density	Length	Width	Weight	Length	Width	Weight	Weight
		(mm)	(mm)	(mm)	(mm)	(g)	(cm^3)	(g/cm^3)	(mm)	(mm)	(g)	(mm)	(mm)	(g)	(g)
EvChl-Stl-8-I	Stewart Island	0.47	25.19	2.07	0.73	0.056	0.042	1.342	18.57	8.50	0.306				0.062
EvChl-Stl-8-J	Stewart Island	0.45	23.12	1.54	0.72	0.040	0.024	1.665	18.56	8.50	0.301				0.059
EvChl-Stl-9-A	Stewart Island	0.45	27.28	1.93	0.68	0.051	0.039	1.286	18.06	8.89	0.294	8.75	3.03	0.086	0.060
EvChl-Stl-9-B	Stewart Island	0.47	28.31	1.87	0.83	0.061	0.043	1.423	18.26	8.87	0.300	8.56	3.36	0.087	0.063
EvChl-Stl-9-C	Stewart Island	0.46	30.55	1.94	0.73	0.071	0.046	1.554	18.31	8.79	0.291	8.93	3.01	0.087	0.060
EvChl-Stl-9-D	Stewart Island	0.43	28.88	1.77	0.81	0.065	0.039	1.636	18.21	8.73	0.289	8.64	3.07	0.091	0.061
EvChl-Stl-9-E	Stewart Island	0.45	29.15	1.93	0.69	0.062	0.042	1.457	18.40	8.83	0.297	8.79	3.37	0.090	0.060
EvChl-Stl-9-F	Stewart Island	0.46	29.1	1.77	0.83	0.060	0.040	1.494	18.42	8.88	0.299				0.060
EvChl-Stl-9-G	Stewart Island	0.47	29.68	1.93	0.67	0.063	0.042	1.485	18.45	8.89	0.300				0.058
EvChl-Stl-9-H	Stewart Island	0.45	29.14	2.06	0.7	0.065	0.047	1.371	18.45	8.81	0.301				0.060
EvChl-Stl-9-I	Stewart Island	0.44	28.93	1.87	0.71	0.056	0.040	1.390	18.29	8.93	0.294				0.061
EvChl-Stl-9-J	Stewart Island	0.45	28.28	1.83	0.85	0.062	0.042	1.488	18.28	8.85	0.297				0.063
EvChl-Stl-10-A	Stewart Island	0.42	22.95	1.6	0.67	0.037	0.025	1.505	18.17	9.75	0.273	9.62	3.81	0.112	0.072
EvChl-Stl-10-B	Stewart Island	0.42	22.79	1.68	0.79	0.041	0.028	1.429				9.67	3.64	0.114	0.068
EvChl-Stl-10-C	Stewart Island	0.42	24.69	1.65	0.74	0.041	0.029	1.399	17.75	9.93	0.278	9.83	3.69	0.111	0.061
EvChl-Stl-10-D	Stewart Island	0.42	23.8	1.63	0.73	0.033	0.027	1.224	18.02	9.80	0.279	9.54	3.62	0.109	0.070
EvChl-Stl-10-E	Stewart Island	0.42	26.81	1.71	0.8	0.054	0.035	1.545	17.71	9.72	0.277	10.00	3.87	0.123	0.068
EvChl-Stl-10-F	Stewart Island	0.41	25.12	1.63	0.77	0.043	0.030	1.445	17.93	9.82	0.281				0.061
EvChl-Stl-10-G	Stewart Island	0.43	24.25	1.96	0.91	0.051	0.041	1.242	17.96	9.75	0.273				
EvChl-Stl-10-H	Stewart Island	0.44	24	1.70	0.68	0.037	0.028	1.313	18.01	7.47	0.268				
EvChl-Stl-10-I	Stewart Island	0.43	25.53	1.66	0.79	0.043	0.031	1.384							
EvChl-Stl-10-J	Stewart Island	0.43	23.3	1.88	0.74	0.044	0.033	1.330							

Table 7.3 Raw data for skeletal elements of *Evechinus chloroticus* collected from Fiordland, New Zealand

ID	Location	Test	Primary Spine						Demi-pyramid			Rotula			Epiphysis
		Thickness	Length	Proximal Diameter	Distal Diameter	Weight	Volume	Density	Length	Width	Weight	Length	Width	Weight	Weight
		(mm)	(mm)	(mm)	(mm)	(g)	(cm^3)	(g/cm^3)	(mm)	(mm)	(g)	(mm)	(mm)	(g)	(g)
EvChl-Frld-1-A	Fiordland	0.47	25.36	1.85	0.67	0.044	0.034	1.291	18.20	8.74	0.270	8.79	3.32	0.0807	0.0491
EvChl-Frld-1-B	Fiordland	0.48	29.47	1.98	0.73	0.055	0.046	1.204	18.07	8.82	0.270	8.63	3.36	0.0868	0.0471
EvChl-Frld-1-C	Fiordland	0.46	26.83	1.90	0.85	0.061	0.042	1.458	18.21	8.75	0.267	8.76	3.22	0.0820	0.0473
EvChl-Frld-1-D	Fiordland	0.47	24.25	1.89	0.76	0.043	0.035	1.212	18.02	8.74	0.271	8.91	3.21	0.0840	0.0472
EvChl-Frld-1-E	Fiordland	0.46	26.53	2.06	0.85	0.055	0.047	1.177	17.95	8.77	0.276				0.0465
EvChl-Frld-1-F	Fiordland	0.47	24.86	1.74	0.75	0.043	0.032	1.362	17.98	8.90	0.269				0.0472
EvChl-Frld-1-G	Fiordland	0.45	26.49	1.77	0.74	0.046	0.035	1.318	18.27	8.84	0.277				0.0476
EvChl-Frld-1-H	Fiordland	0.49	26.59	2.01	0.70	0.058	0.041	1.413	18.14	8.91	0.278				0.0471
EvChl-Frld-1-I	Fiordland	0.47	24.73	2.04	0.81	0.049	0.042	1.172	18.3	8.80	0.277				0.0468
EvChl-Frld-1-J	Fiordland	0.44	22.43	1.82	0.82	0.043	0.032	1.346	18.3	8.74	0.273				0.0478
EvChl-Frld-2-A	Fiordland	0.54	33.89	1.89	0.90	0.070	0.054	1.291	17.22	9.34	0.288	9.30	2.88	0.0950	0.0603

ID	Location	Test	Primary Spine						Demi-pyramid			Rotula			Epiphysis
		Thickness	Length	Proximal Diameter	Distal Diameter	Weight	Volume	Density	Length	Width	Weight	Length	Width	Weight	Weight
		(mm)	(mm)	(mm)	(mm)	(g)	(cm^3)	(g/cm^3)	(mm)	(mm)	(g)	(mm)	(mm)	(g)	(g)
EvChl-Frld-2-B	Fiordland	0.53	31.61	1.86	0.93	0.068	0.050	1.351	17.47	9.14	0.286	9.41	2.98	0.0957	0.0572
EvChl-Frld-2-C	Fiordland	0.55	33.05	1.87	0.64	0.065	0.044	1.472	17.62	9.11	0.289	9.30	2.94	0.0949	0.0652
EvChl-Frld-2-D	Fiordland	0.47	36.10	1.87	0.64	0.071	0.048	1.462	17.5	9.13	0.288	9.30	2.89	0.0928	0.0606
EvChl-Frld-2-E	Fiordland	0.54	34.39	1.82	0.78	0.063	0.048	1.302	17.43	9.13	0.285	9.40	2.89	0.0949	0.0582
EvChl-Frld-2-F	Fiordland	0.56	35.45	1.78	0.93	0.071	0.053	1.341	17.61	9.20	0.291				0.0610
EvChl-Frld-2-G	Fiordland	0.52	32.91	1.81	0.94	0.070	0.050	1.380	17.52	9.23	0.289				0.0634
EvChl-Frld-2-H	Fiordland	0.54	34.64	1.81	0.79	0.071	0.048	1.471	17.24	9.13	0.291				0.0595
EvChl-Frld-2-I	Fiordland	0.54	34.18	1.97	0.84	0.072	0.056	1.291	17.40	9.21	0.290				0.0657
EvChl-Frld-2-J	Fiordland	0.54	33.38	1.78	0.95	0.073	0.050	1.456	17.55	9.26	0.287				0.0627
EvChl-Frld-3-A	Fiordland	0.51	35.10	2.05	0.67	0.073	0.055	1.313	18.13	9.10	0.268	9.17	3.22	0.0974	0.0522
EvChl-Frld-3-B	Fiordland	0.51	33.49	1.99	0.79	0.076	0.054	1.399	17.9	8.89	0.263	9.42	3.51	0.1010	0.0524
EvChl-Frld-3-C	Fiordland	0.50	33.20	1.84	0.70	0.075	0.045	1.669	17.83	9.03	0.264	9.31	3.30	0.0976	0.0526
EvChl-Frld-3-D	Fiordland	0.52	35.02	2.04	0.78	0.076	0.058	1.296	18.34	8.95	0.280	9.38	3.22	0.0971	0.0530
EvChl-Frld-3-E	Fiordland	0.53	33.43	2.00	0.86	0.067	0.057	1.187	18.05	9.01	0.268	9.26	3.36	0.0968	0.0523
EvChl-Frld-3-F	Fiordland	0.49	33.69	2.09	0.67	0.074	0.055	1.351	18.07	9.12	0.281				0.0528
EvChl-Frld-3-G	Fiordland	0.48	36.36	1.89	0.77	0.074	0.053	1.374	18.02	9.03	0.273				0.0528
EvChl-Frld-3-H	Fiordland	0.50	32.18	1.84	0.56	0.077	0.040	1.920	18.12	9.17	0.282				0.0526
EvChl-Frld-3-I	Fiordland	0.51	34.20	1.91	0.81	0.056	0.052	1.065	17.96	9.14	0.273				0.0520
EvChl-Frld-3-J	Fiordland	0.51	31.98	1.58	0.53	0.065	0.030	2.141	17.99	8.90	0.265				0.0531
EvChl-Frld-4-A	Fiordland	0.46	27.20	1.74	0.71	0.049	0.034	1.429	15.9	7.61	0.197	7.53	2.72	0.0574	0.0360
EvChl-Frld-4-B	Fiordland	0.46	26.63	1.60	0.60	0.036	0.027	1.338	15.93	7.61	0.194	7.64	2.69	0.0588	0.0354
EvChl-Frld-4-C	Fiordland	0.46	27.79	1.92	0.72	0.050	0.041	1.223	15.92	7.77	0.198	7.71	2.90	0.0600	0.0369
EvChl-Frld-4-D	Fiordland	0.44	28.84	1.77	0.63	0.056	0.035	1.588	15.95	7.62	0.199	7.64	2.70	0.0589	0.0374
EvChl-Frld-4-E	Fiordland	0.46	28.60	1.83	0.84	0.052	0.042	1.240	16.02	7.55	0.196	7.77	2.86	0.0574	0.0367
EvChl-Frld-4-F	Fiordland	0.47	26.02	1.88	0.82	0.051	0.039	1.313	15.89	7.63	0.196				0.0357
EvChl-Frld-4-G	Fiordland	0.47	28.93	1.73	0.59	0.049	0.033	1.489	16.05	7.71	0.199				0.0362
EvChl-Frld-4-H	Fiordland	0.43	29.03	1.71	0.7	0.050	0.035	1.435	16.05	7.71	0.199				0.0363
EvChl-Frld-4-I	Fiordland	0.42	28.99	1.91	0.71	0.054	0.042	1.292	16.04	7.71	0.201				0.0368
EvChl-Frld-4-J	Fiordland	0.44	28.33	1.78	0.75	0.053	0.038	1.408	15.99	7.68	0.198				0.0349
EvChl-Frld-5-A	Fiordland	0.48	30.55	2.16	1.17	0.079	0.068	1.158	17.31	8.42	0.241	8.33	3.02	0.0735	0.0410
EvChl-Frld-5-B	Fiordland	0.48	34.74	2.14	1.12	0.077	0.075	1.025	17.54	8.75	0.249	8.12	3.03	0.0715	0.0414
EvChl-Frld-5-C	Fiordland	0.42	28.98	1.87	0.88	0.059	0.045	1.323	17.46	8.50	0.244	8.34	2.99	0.0730	0.0409
EvChl-Frld-5-D	Fiordland	0.47	30.59	1.95	0.65	0.067	0.044	1.516	17.42	8.41	0.243	8.27	3.07	0.0727	0.0395
EvChl-Frld-5-E	Fiordland	0.46	32.81	1.89	0.68	0.072	0.046	1.582	17.19	8.39	0.238	8.19	2.99	0.0722	0.0415
EvChl-Frld-5-F	Fiordland	0.43	28.08	1.66	0.63	0.052	0.031	1.678	17.40	8.52	0.240				0.0409
EvChl-Frld-5-G	Fiordland	0.44	27.91	1.83	0.65	0.050	0.036	1.368	17.24	8.34	0.237				0.0398
EvChl-Frld-5-H	Fiordland	0.47	33.04	1.91	0.69	0.077	0.047	1.625	17.34	8.47	0.240				0.0397
EvChl-Frld-5-I	Fiordland	0.48	31.69	2.01	1.05	0.078	0.060	1.300	17.49	8.51	0.245				0.0402
EvChl-Frld-5-J	Fiordland	0.49	32.01	2.10	0.88	0.078	0.059	1.315	17.28	8.53	0.244				0.0402
EvChl-Frld-6-A	Fiordland	0.48	28.18	2.05	0.84	0.069	0.049	1.407	16.89	8.89	0.258	8.91	3.12	0.0860	0.0547
EvChl-Frld-6-B	Fiordland	0.49	32.48	2.08	0.75	0.080	0.055	1.457	16.76	8.81	0.257	8.79	3.09	0.0850	0.0489
EvChl-Frld-6-C	Fiordland	0.48	30.58	2.00	0.52	0.062	0.043	1.463	17.19	9.00	0.267	9.13	3.35	0.0864	0.0489

ID	Location	Test	Primary Spine						Demi-pyramid			Rotula			Epiphysis
		Thickness	Length	Proximal Diameter	Distal Diameter	Weight	Volume	Density	Length	Width	Weight	Length	Width	Weight	Weight
		(mm)	(mm)	(mm)	(mm)	(g)	(cm^3)	(g/cm^3)	(mm)	(mm)	(g)	(mm)	(mm)	(g)	(g)
EvChl-Frld-6-D	Fiordland	0.49	31.70	1.99	0.89	0.078	0.054	1.444	17.35	8.92	0.257	8.83	3.14	0.0887	0.0524
EvChl-Frld-6-E	Fiordland	0.49	27.73	1.75	0.53	0.046	0.031	1.477	17.20	8.91	0.261	8.91	3.30	0.0873	0.0490
EvChl-Frld-6-F	Fiordland	0.50	34.10	2.22	0.83	0.088	0.067	1.318	17.17	8.95	0.266				0.0521
EvChl-Frld-6-G	Fiordland	0.51	32.29	1.96	0.83	0.085	0.052	1.625	16.96	8.98	0.261				0.0501
EvChl-Frld-6-H	Fiordland	0.47	30.84	2.09	0.76	0.077	0.053	1.454	17.00	8.89	0.256				0.0516
EvChl-Frld-6-I	Fiordland	0.48	29.66	1.99	0.77	0.070	0.047	1.484	17.38	8.85	0.263				0.0497
EvChl-Frld-6-J	Fiordland	0.49	29.00	2.20	0.82	0.075	0.056	1.356	17.01	9.13	0.267				0.0490
EvChl-Frld-7-A	Fiordland	0.49	33.30	2.16	0.82	0.079	0.062	1.268	18.05	8.47	0.303	9.09	3.27	0.0980	0.0654
EvChl-Frld-7-B	Fiordland	0.49	31.70	1.85	0.85	0.082	0.047	1.722	18.84	8.40	0.302	9.05	3.37	0.0886	0.0558
EvChl-Frld-7-C	Fiordland	0.50	34.07	1.99	0.96	0.078	0.061	1.283	18.2	8.80	0.293	9.20	3.42	0.1059	0.0710
EvChl-Frld-7-D	Fiordland	0.48	31.05	1.95	0.93	0.082	0.053	1.564	18.29	8.43	0.288	8.73	3.77	0.0828	0.0646
EvChl-Frld-7-E	Fiordland	0.52	31.83	1.75	0.78	0.058	0.042	1.385	18.71	8.33	0.327	8.81	3.23	0.0825	0.0560
EvChl-Frld-7-F	Fiordland	0.48	32.36	1.77	0.77	0.062	0.043	1.431	18.43	8.56	0.283				0.0573
EvChl-Frld-7-G	Fiordland	0.49	31.61	1.91	0.81	0.072	0.048	1.479	18.39	8.58	0.284				0.0566
EvChl-Frld-7-H	Fiordland	0.49	30.84	1.72	0.74	0.059	0.039	1.527	18.59	8.33	0.296				0.0577
EvChl-Frld-7-I	Fiordland	0.46	32.30	1.88	0.81	0.060	0.048	1.234	18.13	8.43	0.317				0.0607
EvChl-Frld-7-J	Fiordland	0.51	30.25	1.94	0.79	0.069	0.047	1.465	18.53	8.96	0.309				0.0565
EvChl-Frld-8-A	Fiordland	0.52	32.73	2.05	0.93	0.081	0.060	1.362	18.86	9.22	0.329	9.56	3.68	0.1043	0.0642
EvChl-Frld-8-B	Fiordland	0.50	32.14	1.79	0.75	0.068	0.043	1.579	18.90	9.42	0.323	9.43	3.57	0.1032	0.0606
EvChl-Frld-8-C	Fiordland	0.50	29.98	1.71	0.79	0.065	0.038	1.683	18.82	9.52	0.325	9.40	3.57	0.1027	0.0645
EvChl-Frld-8-D	Fiordland	0.47	28.80	1.70	0.82	0.060	0.037	1.611	18.68	9.49	0.333	9.40	3.55	0.1032	0.0646
EvChl-Frld-8-E	Fiordland	0.52	31.78	1.94	0.78	0.072	0.049	1.464	18.95	9.44	0.322	9.43	3.50	0.1037	0.0654
EvChl-Frld-8-F	Fiordland	0.51	31.72	1.75	0.61	0.060	0.037	1.594	18.92	9.53	0.330				0.0649
EvChl-Frld-8-G	Fiordland	0.52	31.56	2.00	0.77	0.067	0.051	1.324	18.81	9.54	0.322				0.0645
EvChl-Frld-8-H	Fiordland	0.47	31.70	2.02	0.74	0.072	0.051	1.423	19.04	9.61	0.335				0.0655
EvChl-Frld-8-I	Fiordland	0.52	32.94	1.71	0.63	0.064	0.038	1.679	18.93	9.64	0.321				0.0646
EvChl-Frld-8-J	Fiordland	0.55	31.07	1.68	0.70	0.060	0.037	1.632	19.03	9.63	0.329				0.0637
EvChl-Frld-9-A	Fiordland	0.46	30.09	1.99	0.68	0.072	0.045	1.580	17.76	9.15	0.274	9.10	3.25	0.1000	0.0548
EvChl-Frld-9-B	Fiordland	0.46	30.35	1.82	0.80	0.064	0.043	1.480	17.99	9.13	0.276	9.16	3.24	0.1007	0.0551
EvChl-Frld-9-C	Fiordland	0.48	33.61	2.08	0.68	0.071	0.055	1.299	17.80	8.87	0.266	9.19	3.21	0.0996	0.0538
EvChl-Frld-9-D	Fiordland	0.45	33.04	2.22	0.78	0.086	0.063	1.368	17.68	9.03	0.271	9.30	3.23	0.0983	0.0526
EvChl-Frld-9-E	Fiordland	0.46	29.26	1.64	0.79	0.055	0.035	1.552	17.88	9.12	0.277	9.01	3.29	0.0986	0.0554
EvChl-Frld-9-F	Fiordland	0.45	30.06	1.68	0.62	0.051	0.033	1.528	17.69	9.04	0.279				0.0542
EvChl-Frld-9-G	Fiordland	0.43	33.99	1.97	0.90	0.080	0.058	1.382	17.66	8.98	0.270				0.0524
EvChl-Frld-9-H	Fiordland	0.46	33.62	1.93	0.80	0.081	0.052	1.561	17.65	8.96	0.263				0.0541
EvChl-Frld-9-I	Fiordland	0.46	33.24	2.00	0.86	0.084	0.056	1.500	17.55	9.03	0.264				0.0533
EvChl-Frld-9-J	Fiordland	0.47	35.00	1.99	0.87	0.084	0.059	1.413							0.0539
EvChl-Frld-10-A	Fiordland	0.48	27.18	1.80	0.74	0.054	0.036	1.488	12.73	6.19	0.109	6.19	2.30	0.0324	0.0184
EvChl-Frld-10-B	Fiordland	0.44	29.37	1.82	0.59	0.057	0.036	1.560	12.89	6.30	0.113	6.24	2.41	0.0320	0.0187
EvChl-Frld-10-C	Fiordland	0.44	26.79	1.79	0.84	0.050	0.038	1.312	12.73	6.32	0.113	6.27	2.42	0.0327	0.0186
EvChl-Frld-10-D	Fiordland	0.46	25.98	1.72	0.58	0.042	0.029	1.442	12.90	6.20	0.111	6.20	2.35	0.0319	0.0188
EvChl-Frld-10-E	Fiordland	0.45	25.32	1.69	0.57	0.040	0.027	1.463	12.87	6.24	0.111	6.29	2.34	0.0328	0.0185

ID	Location	Test	Primary Spine						Demi-pyramid			Rotula			Epiphysis
		Thickness	Length	Proximal Diameter	Distal Diameter	Weight	Volume	Density	Length	Width	Weight	Length	Width	Weight	Weight
		(mm)	(mm)	(mm)	(mm)	(g)	(cm^3)	(g/cm^3)	(mm)	(mm)	(g)	(mm)	(mm)	(g)	(g)
EvChl-Frld-10-F	Fiordland	0.46	28.11	1.82	0.66	0.050	0.036	1.365	12.78	6.19	0.112				0.0193
EvChl-Frld-10-G	Fiordland	0.44	27.98	1.70	0.84	0.055	0.037	1.500	12.73	6.18	0.110				0.0191
EvChl-Frld-10-H	Fiordland	0.43	26.77	1.80	0.76	0.055	0.036	1.511	12.81	6.27	0.112				0.0189
EvChl-Frld-10-I	Fiordland	0.44	24.90	1.68	0.70	0.045	0.029	1.528	12.85	6.20	0.123				0.0187
EvChl-Frld-10-J	Fiordland	0.43	27.04	1.75	0.79	0.052	0.036	1.455	12.87	6.15	0.109				0.0192

Table 7.4 Raw data for skeletal elements of *Evechinus chloroticus* collected from Picton, New Zealand

ID	Location	Test	Primary Spine						Demi-pyramid			Rotula			Epiphysis
		Thickness	Length	Proximal Diameter	Distal Diameter	Weight	Volume	Density	Length	Width	Weight	Length	Width	Weight	Weight
		(mm)	(mm)	(mm)	(mm)	(g)	(cm^3)	(g/cm^3)	(mm)	(mm)	(g)	(mm)	(mm)	(g)	(g)
EvChl-Pic-1-A	Picton	0.37	22.51	1.54	0.83	0.045	0.026	1.765				6.98	2.60	0.0504	0.0255
EvChl-Pic-1-B	Picton	0.36	22.86	1.58	0.94	0.046	0.029	1.567	14.01	6.75	0.157	6.94	2.65	0.0500	0.0256
EvChl-Pic-1-C	Picton	0.35	23.59	1.65	0.88	0.047	0.031	1.551	13.39	6.75	0.153	6.89	2.62	0.0507	0.0258
EvChl-Pic-1-D	Picton	0.36	20.83	1.58	0.78	0.043	0.024	1.830	13.76	6.60	0.156	6.99	2.67	0.0507	0.0255
EvChl-Pic-1-E	Picton	0.37	20.71	1.54	0.71	0.037	0.022	1.732	13.85	6.74	0.154	6.93	2.81	0.0505	0.0255
EvChl-Pic-1-F	Picton	0.37	21.77	1.57	0.92	0.042	0.027	1.535	13.81	6.60	0.155				0.0261
EvChl-Pic-1-G	Picton	0.36	21.03	1.63	0.65	0.039	0.023	1.723	13.87	6.68	0.153				0.0255
EvChl-Pic-1-H	Picton	0.37	20.50	1.63	0.91	0.039	0.027	1.466	13.87	6.71	0.156				0.0259
EvChl-Pic-1-I	Picton	0.35	22.15	1.65	0.94	0.042	0.030	1.415							0.0259
EvChl-Pic-1-J	Picton	0.36	22.30	1.55	0.92	0.045	0.027	1.640							0.0256
EvChl-Pic-2-A	Picton	0.40	21.04	1.59	0.88	0.042	0.026	1.631	13.82	7.08	0.169	7.42	3.03	0.0552	0.0330
EvChl-Pic-2-B	Picton	0.42	20.19	1.65	0.81	0.041	0.025	1.647	14.21	7.43	0.171	7.47	2.96	0.0550	0.0332
EvChl-Pic-2-C	Picton	0.42	21.94	1.61	0.82	0.044	0.026	1.672	14.3	7.26	0.169	7.17	2.99	0.0543	0.0326
EvChl-Pic-2-D	Picton	0.43	22.03	1.59	0.83	0.045	0.026	1.737	14.14	7.09	0.172	7.29	3.01	0.0553	0.0333
EvChl-Pic-2-E	Picton	0.41	20.83	1.62	0.84	0.041	0.026	1.620	14.25	7.13	0.171	7.33	3.00	0.0545	0.0332
EvChl-Pic-2-F	Picton	0.42	22.31	1.58	0.72	0.043	0.024	1.759	14.22	7.31	0.172				0.0326
EvChl-Pic-2-G	Picton	0.44	20.63	1.62	0.93	0.043	0.027	1.577							0.0334
EvChl-Pic-2-H	Picton	0.41	21.07	1.53	0.78	0.039	0.023	1.689							0.0330
EvChl-Pic-2-I	Picton	0.40	20.94	1.64	0.90	0.044	0.027	1.622							0.0329
EvChl-Pic-2-J	Picton	0.41	21.68	1.60	0.85	0.045	0.026	1.719							
EvChl-Pic-3-A	Picton	0.42	22.92	1.71	0.84	0.047	0.030	1.558	16.00	8.37	0.238	8.84	3.21	0.0890	0.0484
EvChl-Pic-3-B	Picton	0.41	22.12	1.75	0.86	0.045	0.031	1.464	16.12	8.44	0.236	8.94	3.15	0.0910	0.0483
EvChl-Pic-3-C	Picton	0.40	20.01	1.67	0.94	0.046	0.027	1.687	15.91	8.36	0.230	8.88	3.10	0.0901	0.0479
EvChl-Pic-3-D	Picton	0.40	22.82	1.56	0.64	0.041	0.023	1.766	15.80	8.34	0.235	8.86	3.26	0.0902	0.0491
EvChl-Pic-3-E	Picton	0.41	20.36	1.57	0.79	0.036	0.023	1.576	15.93	8.44	0.233	8.88	3.17	0.0890	0.0497
EvChl-Pic-3-F	Picton	0.39	22.68	1.66	0.90	0.050	0.030	1.655	16.29	8.44	0.242				0.0488
EvChl-Pic-3-G	Picton	0.38	22.13	1.56	0.80	0.048	0.025	1.925	15.95	8.24	0.233				0.0483
EvChl-Pic-3-H	Picton	0.42	22.49	1.61	0.93	0.050	0.029	1.709	15.73	8.50	0.240				0.0490

ID	Location	Test	Primary Spine						Demi-pyramid			Rotula			Epiphysis
		Thickness	Length	Proximal Diameter	Distal Diameter	Weight	Volume	Density	Length	Width	Weight	Length	Width	Weight	Weight
		(mm)	(mm)	(mm)	(mm)	(g)	(cm^3)	(g/cm^3)	(mm)	(mm)	(g)	(mm)	(mm)	(g)	(g)
EvChl-Pic-3-I	Picton	0.40	19.34	1.42	0.64	0.029	0.017	1.722	15.81	8.40	0.237				0.0509
EvChl-Pic-3-J	Picton	0.41	21.90	1.75	0.67	0.039	0.027	1.436	15.22	8.43	0.234				0.0468
EvChl-Pic-4-A	Picton	0.36	21.93	1.67	0.98	0.037	0.031	1.204	14.33	7.15	0.172	7.48	2.93	0.0515	0.0247
EvChl-Pic-4-B	Picton	0.35	19.91	1.62	0.86	0.034	0.025	1.352	14.40	7.20	0.171	7.42	2.93	0.0518	0.0239
EvChl-Pic-4-C	Picton	0.34	18.53	1.55	0.99	0.032	0.024	1.338	14.49	7.14	0.170	7.46	2.87	0.0519	0.0256
EvChl-Pic-4-D	Picton	0.36	20.81	1.62	0.87	0.034	0.026	1.294	14.50	7.45	0.171	7.36	2.86	0.0509	0.0237
EvChl-Pic-4-E	Picton	0.35	20.79	1.57	0.94	0.034	0.026	1.291	14.33	7.06	0.171	7.48	2.84	0.0522	0.0248
EvChl-Pic-4-F	Picton	0.36	21.42	1.58	0.93	0.035	0.027	1.277	14.38	7.17	0.175				0.0252
EvChl-Pic-4-G	Picton	0.34	18.50	1.52	0.87	0.032	0.021	1.524	14.39	7.22	0.174				0.0241
EvChl-Pic-4-H	Picton	0.36	20.75	1.58	0.71	0.031	0.022	1.391	14.51	7.13	0.172				0.0249
EvChl-Pic-4-I	Picton	0.34	19.11	1.57	0.99	0.037	0.025	1.483							0.0243
EvChl-Pic-4-J	Picton	0.35	19.02	1.51	1.01	0.035	0.024	1.451							
EvChl-Pic-5-A	Picton	0.33	21.56	1.51	0.80	0.038	0.023	1.619	13.81	6.88	0.159	6.92	2.79	0.0463	0.0253
EvChl-Pic-5-B	Picton	0.32	21.75	1.53	0.73	0.038	0.023	1.666	13.96	6.84	0.156	7.06	2.76	0.0477	0.0264
EvChl-Pic-5-C	Picton	0.34	21.83	1.51	0.87	0.042	0.025	1.679	13.82	6.73	0.155	6.87	2.75	0.0468	0.0257
EvChl-Pic-5-D	Picton	0.35	22.08	1.50	0.82	0.042	0.024	1.755	13.84	6.75	0.157	6.84	2.71	0.0462	0.0257
EvChl-Pic-5-E	Picton	0.32	20.48	1.56	0.71	0.036	0.022	1.676	13.83	6.77	0.155	6.95	2.77	0.0467	0.0251
EvChl-Pic-5-F	Picton	0.34	19.93	1.56	0.68	0.032	0.021	1.534	13.94	6.88	0.159				0.0252
EvChl-Pic-5-G	Picton	0.35	22.68	1.54	0.72	0.041	0.024	1.719	13.87	6.74	0.156				0.0254
EvChl-Pic-5-H	Picton	0.36	18.17	1.55	1.02	0.037	0.024	1.560	13.85	6.89	0.157				0.0251
EvChl-Pic-5-I	Picton	0.34	19.09	1.49	0.86	0.033	0.021	1.567							0.0254
EvChl-Pic-5-J	Picton	0.35	17.78	1.42	0.93	0.031	0.020	1.589							0.0254
EvChl-Pic-6-A	Picton	0.41	22.41	1.54	0.76	0.034	0.024	1.399	15.97	7.62	0.190	8.03	3.02	0.0605	0.0287
EvChl-Pic-6-B	Picton	0.42	21.60	1.60	0.68	0.036	0.023	1.535	15.77	7.65	0.187	7.96	3.01	0.0595	0.0289
EvChl-Pic-6-C	Picton	0.40	20.52	1.57	0.76	0.036	0.023	1.586	15.99	7.69	0.195	7.87	2.91	0.0581	0.0292
EvChl-Pic-6-D	Picton	0.38	22.74	1.72	0.65	0.037	0.027	1.384	16.01	7.59	0.190	7.92	3.01	0.0596	0.0291
EvChl-Pic-6-E	Picton	0.39	22.54	1.52	0.83	0.044	0.025	1.732	15.98	7.80	0.200	7.84	2.85	0.0582	0.0291
EvChl-Pic-6-F	Picton	0.34	20.14	1.45	0.88	0.034	0.022	1.575	15.76	7.22	0.184				0.0284
EvChl-Pic-6-G	Picton	0.39	20.69	1.58	0.81	0.038	0.024	1.592	16.01	7.80	0.192				0.0290
EvChl-Pic-6-H	Picton	0.41	22.39	1.66	0.76	0.037	0.027	1.379	15.79	7.65	0.187				0.0293
EvChl-Pic-6-I	Picton	0.42	21.48	1.57	0.77	0.034	0.024	1.417	15.9	7.86	0.193				0.0284
EvChl-Pic-6-J	Picton	0.40	20.19	1.55	0.90	0.037	0.024	1.502							0.0286
EvChl-Pic-7-A	Picton	0.39	23.17	1.60	0.89	0.048	0.029	1.653	14.35	7.00	0.182	7.13	2.95	0.0556	0.0321
EvChl-Pic-7-B	Picton	0.39	22.12	1.50	0.89	0.043	0.025	1.707	14.35	7.04	0.179	7.15	2.89	0.0562	0.0307
EvChl-Pic-7-C	Picton	0.34	20.98	1.61	0.94	0.036	0.027	1.317	14.51	7.17	0.182	7.14	2.85	0.0563	0.0307
EvChl-Pic-7-D	Picton	0.36	19.30	1.30	0.78	0.029	0.017	1.744	14.46	7.01	0.182	7.23	2.87	0.0560	0.0318
EvChl-Pic-7-E	Picton	0.40	20.16	1.50	0.72	0.037	0.020	1.820	14.47	7.27	0.183	7.07			0.0310
EvChl-Pic-7-F	Picton	0.38	20.57	1.57	0.94	0.042	0.026	1.625	14.38	7.15	0.184				0.0311
EvChl-Pic-7-G	Picton	0.36	22.63	1.54	0.90	0.044	0.027	1.634	14.4	7.11	0.180				0.0318
EvChl-Pic-7-H	Picton	0.30	20.36	1.53	0.61	0.035	0.019	1.789	14.37	7.30	0.182				0.0315
EvChl-Pic-7-I	Picton	0.36	19.24	1.53	0.99	0.042	0.024	1.724	14.33	7.15	0.181				0.0310
EvChl-Pic-7-J	Picton	0.37	21.52	1.52	1.00	0.041	0.027	1.511	14.4	7.32	0.185				

ID	Location	Test	Primary Spine						Demi-pyramid			Rotula			Epiphysis
		Thickness	Length	Proximal Diameter	Distal Diameter	Weight	Volume	Density	Length	Width	Weight	Length	Width	Weight	Weight
		(mm)	(mm)	(mm)	(mm)	(g)	(cm^3)	(g/cm^3)	(mm)	(mm)	(g)	(mm)	(mm)	(g)	(g)
EvChl-Pic-8-A	Picton	0.38	23.52	1.57	0.80	0.042	0.027	1.575	16.02	7.43	0.205	7.77	3.02	0.0618	0.0326
EvChl-Pic-8-B	Picton	0.39	22.38	1.55	0.81	0.041	0.025	1.613	16.04	7.52	0.202	7.71	3.07	0.0619	0.0333
EvChl-Pic-8-C	Picton	0.37	22.36	1.52	0.94	0.049	0.027	1.799	15.54	7.23	0.201	7.71	2.98	0.0600	0.0330
EvChl-Pic-8-D	Picton	0.39	23.27	1.60	0.92	0.049	0.030	1.638	16.01	7.49	0.207	7.64	3.01	0.0615	0.0326
EvChl-Pic-8-E	Picton	0.39	22.47	1.63	0.76	0.043	0.026	1.639	15.56	7.46	0.205	7.67	2.99	0.0602	0.0330
EvChl-Pic-8-F	Picton	0.40	22.54	1.62	0.97	0.047	0.030	1.554	15.95	7.33	0.202				0.0331
EvChl-Pic-8-G	Picton	0.37	21.67	1.63	0.80	0.042	0.026	1.592	15.85	7.51	0.205				0.0331
EvChl-Pic-8-H	Picton	0.42	20.20	1.62	0.95	0.043	0.027	1.605	15.92	7.38	0.206				0.0340
EvChl-Pic-8-I	Picton	0.41	21.30	1.42	0.68	0.036	0.019	1.867	15.98	7.40	0.204				0.0329
EvChl-Pic-8-J	Picton	0.39	21.01	1.44	0.63	0.033	0.019	1.801	15.55	7.30	0.203				0.0340
EvChl-Pic-9-A	Picton	0.40	24.98	1.59	0.68	0.050	0.027	1.863	16.11	7.65	0.203	7.65	2.97	0.0579	0.0331
EvChl-Pic-9-B	Picton	0.40	23.62	1.68	0.73	0.039	0.028	1.392	16.08	7.64	0.198	7.70	2.88	0.0579	0.0339
EvChl-Pic-9-C	Picton	0.41	20.50	1.47	0.62	0.032	0.019	1.726	16.03	7.60	0.198	7.70	2.83	0.0573	0.0338
EvChl-Pic-9-D	Picton	0.42	21.00	1.73	0.90	0.042	0.029	1.418	16.16	7.66	0.201	7.66	2.89	0.0586	0.0334
EvChl-Pic-9-E	Picton	0.41	21.06	1.69	0.91	0.046	0.029	1.583	16.03	7.44	0.196	7.82	2.81	0.0585	0.0336
EvChl-Pic-9-F	Picton	0.40	22.71	1.76	0.82	0.045	0.031	1.465	16.11	7.32	0.202				0.0335
EvChl-Pic-9-G	Picton	0.43	21.18	1.61	0.80	0.045	0.025	1.781	15.81	7.41	0.199				0.0331
EvChl-Pic-9-H	Picton	0.41	19.92	1.47	0.64	0.029	0.018	1.606	16.06	7.64	0.199				0.0330
EvChl-Pic-9-I	Picton	0.41	23.76	1.60	0.81	0.044	0.028	1.554	16.02	7.58	0.205				0.0340
EvChl-Pic-9-J	Picton	0.42	21.01	1.63	0.70	0.043	0.024	1.831	16.18	7.53	0.200				0.0335
EvChl-Pic-10-A	Picton	0.39	20.88	1.62	0.86	0.038	0.026	1.478	14.91	7.37	0.176	7.70	3.05	0.0612	0.0322
EvChl-Pic-10-B	Picton	0.38	21.66	1.53	0.88	0.043	0.025	1.707	14.79	6.93	0.179	7.77	3.10	0.0617	0.0319
EvChl-Pic-10-C	Picton	0.37	22.21	1.61	0.97	0.046	0.030	1.566	14.86	7.37	0.175	7.69	3.08	0.0617	0.0311
EvChl-Pic-10-D	Picton	0.38	20.56	1.61	0.95	0.043	0.027	1.591	15.19	7.39	0.178	7.76	3.05	0.0613	0.0310
EvChl-Pic-10-E	Picton	0.39	20.55	1.59	0.96	0.044	0.027	1.632	15.09	7.49	0.179	7.86	3.15	0.0630	0.0314
EvChl-Pic-10-F	Picton	0.38	21.11	1.53	0.65	0.037	0.021	1.793	14.93	7.52	0.175				0.0311
EvChl-Pic-10-G	Picton	0.37	20.83	1.65	0.78	0.038	0.025	1.508	14.28	7.64	0.188				0.0320
EvChl-Pic-10-H	Picton	0.36	21.74	1.51	0.74	0.036	0.022	1.605	14.97	7.58	0.180				0.0314
EvChl-Pic-10-I	Picton	0.38	19.47	1.65	0.94	0.040	0.026	1.505	14.67	7.58	0.164				0.0306
EvChl-Pic-10-J	Picton	0.37	20.09	1.58	1.00	0.040	0.027	1.509							0.0321

Table 7.5 Raw data for skeletal elements of *Evechinus chloroticus* collected from Auckland, New Zealand

ID	Location	Test	Primary Spine						Demi-pyramid			Rotula			Epiphysis
		Thickness	Length	Proximal Diameter	Distal Diameter	Weight	Volume	Density	Length	Width	Weight	Length	Width	Weight	Weight
		(mm)	(mm)	(mm)	(mm)	(g)	(cm^3)	(g/cm^3)	(mm)	(mm)	(g)	(mm)	(mm)	(g)	(g)
EvChl-Akl-1-A	Auckland	0.29	17.66	1.51	0.63	0.029	0.017	1.740	11.84	5.55	0.092	5.91	2.32	0.0252	0.0152
EvChl-Akl-1-B	Auckland	0.28	19.41	1.47	0.59	0.030	0.017	1.765	11.95	5.59	0.093	5.72	2.31	0.0254	0.0154
EvChl-Akl-1-C	Auckland	0.29	19.69	1.41	0.56	0.028	0.016	1.746	12.08	5.56	0.091	5.76	2.30	0.0260	0.0158

ID	Location	Test	Primary Spine						Demi-pyramid			Rotula			Epiphysis
		Thickness	Length	Proximal Diameter	Distal Diameter	Weight	Volume	Density	Length	Width	Weight	Length	Width	Weight	Weight
		(mm)	(mm)	(mm)	(mm)	(g)	(cm^3)	(g/cm^3)	(mm)	(mm)	(g)	(mm)	(mm)	(g)	(g)
EvChl-Akl-1-D	Auckland	0.26	18.70	1.34	0.56	0.026	0.014	1.844	12.09	5.49	0.091	5.70	2.28	0.0256	0.0151
EvChl-Akl-1-E	Auckland	0.30	17.43	1.53	0.63	0.029	0.017	1.696	12.18	5.58	0.088	5.74	2.31	0.0249	0.0158
EvChl-Akl-1-F	Auckland	0.31	18.89	1.24	0.67	0.027	0.014	1.948	12.14	5.53	0.090				0.0154
EvChl-Akl-1-G	Auckland	0.39	17.02	1.39	0.69	0.026	0.015	1.753	12.22	5.49	0.090				0.0167
EvChl-Akl-1-H	Auckland	0.29	18.07	1.23	0.60	0.023	0.012	1.875	12.03	5.61	0.093				0.0154
EvChl-Akl-1-I	Auckland	0.28	17.43	1.50	0.57	0.025	0.016	1.595	12.11	5.45	0.090				0.0158
EvChl-Akl-1-J	Auckland	0.28	17.10	1.32	0.62	0.024	0.013	1.785							
EvChl-Akl-2-A	Auckland	0.31	19.41	1.33	0.60	0.028	0.015	1.891	12.99	6.10	0.114	6.28	2.64	0.0329	0.0197
EvChl-Akl-2-B	Auckland	0.31	18.24	1.47	0.59	0.029	0.016	1.781	12.91	5.99	0.111	6.38	2.67	0.0348	0.0195
EvChl-Akl-2-C	Auckland	0.30	16.55	1.36	0.73	0.026	0.015	1.796	12.97	6.03	0.111	6.41	2.48	0.0342	0.0199
EvChl-Akl-2-D	Auckland	0.29	18.95	1.48	0.59	0.032	0.017	1.879	13.07	6.20	0.114	6.35	2.43	0.0331	0.0199
EvChl-Akl-2-E	Auckland	0.31	16.62	1.42	0.52	0.027	0.013	2.042	13.07	5.90	0.115	6.32	2.44	0.0330	0.0203
EvChl-Akl-2-F	Auckland	0.29	18.31	1.58	0.58	0.029	0.018	1.613	12.95	6.02	0.114				0.0196
EvChl-Akl-2-G	Auckland	0.31	17.42	1.39	0.81	0.027	0.017	1.582	12.76	5.91	0.114				0.0191
EvChl-Akl-2-H	Auckland	0.30	16.51	1.49	0.71	0.025	0.016	1.544	12.97	6.02	0.111				0.0193
EvChl-Akl-2-I	Auckland	0.29	17.28	1.27	0.52	0.025	0.012	2.215	12.92	6.03	0.113				0.0197
EvChl-Akl-2-J	Auckland	0.29	16.58	1.43	0.86	0.030	0.017	1.744	12.91	6.14	0.112				0.0193
EvChl-Akl-3-A	Auckland	0.31	18.68	1.59	0.87	0.037	0.023	1.611	13.56	6.70	0.138	6.84	2.75	0.0434	0.0259
EvChl-Akl-3-B	Auckland	0.33	18.52	1.64	0.90	0.037	0.024	1.547	13.48	6.67	0.136	6.78	2.79	0.0443	0.0258
EvChl-Akl-3-C	Auckland	0.32	19.57	1.75	0.67	0.039	0.024	1.641	13.63	6.82	0.135	6.95	2.67	0.0437	0.0263
EvChl-Akl-3-D	Auckland	0.35	18.22	1.54	0.92	0.038	0.022	1.735	13.65	6.72	0.135	6.99	2.79	0.0444	0.0257
EvChl-Akl-3-E	Auckland	0.34	18.24	1.49	0.69	0.036	0.018	2.038	13.66	6.63	0.136	6.88	2.62	0.0451	0.0256
EvChl-Akl-3-F	Auckland	0.35	17.25	1.46	0.95	0.037	0.020	1.858	13.60	6.60	0.138				0.0259
EvChl-Akl-3-G	Auckland	0.34	18.03	1.57	0.97	0.040	0.023	1.730	13.47	6.81	0.138				0.0260
EvChl-Akl-3-H	Auckland	0.33	18.68	1.33	0.57	0.026	0.014	1.845	13.58	6.77	0.138				0.0251
EvChl-Akl-3-I	Auckland	0.33	18.23	1.45	0.61	0.036	0.016	2.259	13.39	6.74	0.135				0.0269
EvChl-Akl-3-J	Auckland	0.34	18.22	1.54	0.79	0.035	0.020	1.757							0.0258
EvChl-Akl-4-A	Auckland	0.34	17.41	1.23	0.63	0.032	0.012	2.621	12.55	6.08	0.103	6.51	2.34	0.0310	0.0181
EvChl-Akl-4-B	Auckland	0.33	18.87	1.39	0.76	0.030	0.018	1.718	12.55	6.12	0.107	6.59	2.18	0.0296	0.0182
EvChl-Akl-4-C	Auckland	0.31	21.00	1.53	0.78	0.036	0.023	1.572	12.68	6.11	0.106	6.27	2.22	0.0290	0.0189
EvChl-Akl-4-D	Auckland	0.34	19.14	1.51	0.73	0.032	0.020	1.646	12.58	5.99	0.105	6.39	2.18	0.0295	0.0188
EvChl-Akl-4-E	Auckland	0.34	18.39	1.47	0.77	0.032	0.019	1.732	12.70	6.10	0.107				0.0180
EvChl-Akl-4-F	Auckland	0.30	18.94	1.35	0.93	0.033	0.020	1.704	12.54	6.14	0.105				0.0183
EvChl-Akl-4-G	Auckland	0.31	17.74	1.26	0.80	0.029	0.015	1.902	12.57	5.97	0.106				0.0186
EvChl-Akl-4-H	Auckland	0.32	18.64	1.44	0.87	0.034	0.020	1.710	12.48	6.03	0.103				0.0182
EvChl-Akl-4-I	Auckland	0.34	17.90	1.37	0.60	0.029	0.014	2.024							0.0187
EvChl-Akl-4-J	Auckland	0.33	17.48	1.41	0.72	0.032	0.016	1.963							
EvChl-Akl-5-A	Auckland	0.31	18.61	1.48	0.57	0.029	0.016	1.751	12.97	6.28	0.111	6.51	2.33	0.0365	0.0202
EvChl-Akl-5-B	Auckland	0.31	17.95	1.38	0.73	0.027	0.016	1.697	12.99	6.25	0.111	6.72	2.32	0.0352	0.0200
EvChl-Akl-5-C	Auckland	0.32	17.17	1.38	0.74	0.026	0.016	1.637	12.98	6.15	0.112	6.53	2.31	0.0359	0.0193
EvChl-Akl-5-D	Auckland	0.33	18.07	1.54	0.72	0.030	0.019	1.565	13.02	6.18	0.111	6.56	2.38	0.0356	0.0193
EvChl-Akl-5-E	Auckland	0.34	16.80	1.55	0.65	0.026	0.017	1.519	12.93	6.27	0.111	6.66	2.41	0.0369	0.0204

ID	Location	Test	Primary Spine						Demi-pyramid			Rotula			Epiphysis
		Thickness	Length	Proximal Diameter	Distal Diameter	Weight	Volume	Density	Length	Width	Weight	Length	Width	Weight	Weight
		(mm)	(mm)	(mm)	(mm)	(g)	(cm^3)	(g/cm^3)	(mm)	(mm)	(g)	(mm)	(mm)	(g)	(g)
EvChl-Akl-5-F	Auckland	0.34	17.80	1.43	0.70	0.028	0.016	1.705	13.07	6.25	0.109				0.0195
EvChl-Akl-5-G	Auckland	0.35	15.75	1.23	0.65	0.022	0.011	1.938	13.00	6.35	0.111				0.0196
EvChl-Akl-5-H	Auckland	0.34	15.99	1.46	0.87	0.026	0.017	1.522	13.16	6.21	0.116				0.0213
EvChl-Akl-5-I	Auckland	0.35	16.68	1.31	0.63	0.024	0.013	1.885	13.00	6.24	0.112				0.0197
EvChl-Akl-5-J	Auckland	0.33	16.17	1.36	0.78	0.026	0.015	1.769	12.99	6.18	0.109				0.0195
EvChl-Akl-6-A	Auckland	0.31	19.34	1.25	0.48	0.025	0.012	2.071	10.98	5.56	0.078	6.02	2.30	0.0282	0.0161
EvChl-Akl-6-B	Auckland	0.30	18.16	1.43	0.56	0.025	0.015	1.632	11.03	5.57	0.079	5.90	2.34	0.0277	0.0159
EvChl-Akl-6-C	Auckland	0.29	17.66	1.28	0.52	0.022	0.012	1.808	11.05	5.83	0.081	5.97	2.30	0.0284	0.0159
EvChl-Akl-6-D	Auckland	0.28	18.67	1.43	0.62	0.026	0.016	1.594	11.07	5.47	0.078	5.99	2.27	0.0282	0.0161
EvChl-Akl-6-E	Auckland	0.30	18.52	1.31	0.61	0.023	0.014	1.669	11.09	5.58	0.080	5.89	2.29	0.0284	0.0161
EvChl-Akl-6-F	Auckland	0.30	18.58	1.39	0.65	0.024	0.016	1.499	11.09	5.64	0.078				0.0163
EvChl-Akl-6-G	Auckland	0.31	18.13	1.22	0.67	0.025	0.013	1.927	11.11	5.59	0.078				0.0159
EvChl-Akl-6-H	Auckland	0.29	20.27	1.39	0.68	0.028	0.018	1.581	10.97	5.60	0.078				0.0164
EvChl-Akl-6-I	Auckland	0.27	20.66	1.32	0.67	0.028	0.017	1.685	10.94	5.74	0.079				0.0162
EvChl-Akl-6-J	Auckland	0.31	17.44	1.37	0.51	0.021	0.013	1.643	10.99	5.42	0.080				0.0158
EvChl-Akl-7-A	Auckland	0.27	19.95	1.61	0.71	0.031	0.022	1.418	11.15	5.12	0.067	5.37	2.25	0.0225	0.0139
EvChl-Akl-7-B	Auckland	0.27	16.95	1.35	0.64	0.022	0.014	1.616	11.05	5.20	0.068	5.31	2.09	0.0221	0.0137
EvChl-Akl-7-C	Auckland	0.26	17.90	1.38	0.59	0.025	0.014	1.758	11.02	5.14	0.069	5.49	2.16	0.0224	0.0139
EvChl-Akl-7-D	Auckland	0.27	17.63	1.38	0.70	0.027	0.016	1.717	11.10	5.47	0.069	5.39	2.06	0.0222	0.0143
EvChl-Akl-7-E	Auckland	0.27	15.97	1.39	0.54	0.022	0.012	1.775	11.23	5.20	0.068	5.43	2.09	0.0227	0.0138
EvChl-Akl-7-F	Auckland	0.26	17.19	1.35	0.57	0.022	0.013	1.684	10.84	5.23	0.070				0.0139
EvChl-Akl-7-G	Auckland	0.28	17.20	1.43	0.69	0.026	0.016	1.640	10.97	5.49	0.068				0.0138
EvChl-Akl-7-H	Auckland	0.28	15.97	1.53	0.65	0.023	0.016	1.477	11.10	5.11	0.069				0.0140
EvChl-Akl-7-I	Auckland	0.24	16.60	1.48	0.69	0.024	0.016	1.482	11.37	5.53	0.068				0.0139
EvChl-Akl-7-J	Auckland	0.26	15.72	1.34	0.54	0.021	0.012	1.807	11.10	5.16	0.069				0.0138
EvChl-Akl-8-A	Auckland	0.26	19.11	1.51	0.69	0.030	0.019	1.567	11.19	5.36	0.085	5.81	2.26	0.0265	0.0168
EvChl-Akl-8-B	Auckland	0.27	18.11	1.37	0.55	0.029	0.014	2.054	11.41	5.40	0.085	5.84	2.29	0.0275	0.0182
EvChl-Akl-8-C	Auckland	0.28	18.68	1.39	0.64	0.029	0.016	1.841	11.22	5.49	0.084	5.78	2.28	0.0269	0.0185
EvChl-Akl-8-D	Auckland	0.29	17.88	1.38	0.75	0.031	0.016	1.900	11.31	5.15	0.085	5.84	2.28	0.0269	0.0172
EvChl-Akl-8-E	Auckland	0.31	17.86	1.28	0.54	0.027	0.012	2.214	11.47	5.37	0.086	5.91	2.23	0.0271	0.0184
EvChl-Akl-8-F	Auckland	0.31	16.91	1.24	0.73	0.026	0.013	1.983	11.32	5.32	0.082				0.0173
EvChl-Akl-8-G	Auckland	0.32	17.06	1.43	0.77	0.031	0.017	1.858	11.26	5.44	0.085				0.0173
EvChl-Akl-8-H	Auckland	0.29	17.03	1.30	0.72	0.029	0.014	2.084	11.42	5.34	0.084				0.0177
EvChl-Akl-8-I	Auckland	0.28	16.66	1.24	0.50	0.024	0.011	2.265	11.25	5.47	0.084				0.0172
EvChl-Akl-8-J	Auckland	0.31	16.12	1.37	0.84	0.027	0.016	1.707	11.37	5.50	0.086				0.0183
EvChl-Akl-9-A	Auckland	0.33	19.19	1.63	0.79	0.038	0.023	1.675	14.64	6.55	0.145	6.82	2.71	0.0455	0.0260
EvChl-Akl-9-B	Auckland	0.34	18.30	1.52	0.87	0.036	0.021	1.727	14.37	6.46	0.144	6.74	2.69	0.0443	0.0266
EvChl-Akl-9-C	Auckland	0.33	17.64	1.57	0.79	0.034	0.020	1.711	14.62	6.47	0.144	6.74	2.71	0.0443	0.0265
EvChl-Akl-9-D	Auckland	0.31	19.48	1.52	0.79	0.036	0.021	1.703	14.40	6.49	0.138	7.01	2.69	0.0447	0.0264
EvChl-Akl-9-E	Auckland	0.33	17.64	1.53	0.65	0.035	0.017	2.008	14.53	6.54	0.144	7.04	2.71	0.0451	0.0263
EvChl-Akl-9-F	Auckland	0.34	19.68	1.43	0.77	0.039	0.019	2.016	14.49	5.99	0.143				0.0267
EvChl-Akl-9-G	Auckland	0.33	17.62	1.59	0.88	0.042	0.022	1.919	14.41	6.45	0.144				0.0266

ID	Location	Test	Primary Spine						Demi-pyramid			Rotula			Epiphysis
		Thickness	Length	Proximal Diameter	Distal Diameter	Weight	Volume	Density	Length	Width	Weight	Length	Width	Weight	Weight
		(mm)	(mm)	(mm)	(mm)	(g)	(cm^3)	(g/cm^3)	(mm)	(mm)	(g)	(mm)	(mm)	(g)	(g)
EvChl-Akl-9-H	Auckland	0.34	18.32	1.47	0.85	0.036	0.020	1.824	14.28	6.52	0.144				0.0265
EvChl-Akl-9-I	Auckland	0.32	18.08	1.41	0.85	0.033	0.019	1.765	14.47	6.46	0.147				0.0271
EvChl-Akl-9-J	Auckland	0.33	17.12	1.72	0.70	0.033	0.021	1.592	14.60	6.56	0.145				0.0269
EvChl-Akl-10-A	Auckland	0.32	18.18	1.48	0.68	0.032	0.017	1.842	12.08	5.51	0.084	5.93	2.28	0.0255	0.0150
EvChl-Akl-10-B	Auckland	0.31	18.79	1.47	0.83	0.033	0.020	1.642	12.08	5.74	0.087	5.91	2.35	0.0257	0.0151
EvChl-Akl-10-C	Auckland	0.33	18.26	1.45	0.73	0.031	0.018	1.779	12.15	5.85	0.085	6.15	2.26	0.0255	0.0150
EvChl-Akl-10-D	Auckland	0.32	17.69	1.44	0.71	0.024	0.017	1.458	12.04	5.82	0.084	5.96	2.24	0.0258	0.0153
EvChl-Akl-10-E	Auckland	0.33	16.20	1.39	0.79	0.028	0.015	1.777	12.02	5.67	0.085	5.86	2.27	0.0255	0.0147
EvChl-Akl-10-F	Auckland	0.33	17.49	1.40	0.58	0.027	0.014	1.865	12.00	5.82	0.082				0.0145
EvChl-Akl-10-G	Auckland	0.32	17.91	1.49	0.62	0.026	0.017	1.584	11.87	5.67	0.085				0.0147
EvChl-Akl-10-H	Auckland	0.31	16.18	1.25	0.63	0.024	0.012	2.032	11.98	5.64	0.083				0.0146
EvChl-Akl-10-I	Auckland	0.30	16.24	1.47	0.76	0.029	0.016	1.742	11.92	5.65	0.083				0.0150
EvChl-Akl-10-J	Auckland	0.31	16.34	1.23	0.71	0.024	0.012	1.944	11.97	5.77	0.083				0.0149

Table 7.6 Raw data for skeletal elements of *Evechinus chloroticus* collected from White Island, New Zealand

ID	Location	Test	Primary Spine						Demi-pyramid			Rotula			Epiphysis
		Thickness	Length	Proximal Diameter	Distal Diameter	Weight	Volume	Density	Length	Width	Weight	Length	Width	Weight	Weight
		(mm)	(mm)	(mm)	(mm)	(g)	(cm^3)	(g/cm^3)	(mm)	(mm)	(g)	(mm)	(mm)	(g)	(g)
EvChl-Whl-1-A	White Island	0.35	18.63	1.57	1.00	0.041	0.025	1.681	12.82	6.32	0.127	6.78	2.37	0.0408	0.0238
EvChl-Whl-1-B	White Island	0.36	20.33	1.63	0.84	0.045	0.025	1.785	12.9	6.37	0.129	6.91	2.32	0.0430	0.0230
EvChl-Whl-1-C	White Island	0.34	20.14	1.71	0.92	0.047	0.028	1.659	12.81	6.47	0.129	6.81	2.36	0.0409	0.0225
EvChl-Whl-1-D	White Island	0.32	19.45	1.58	1.00	0.044	0.026	1.691	12.90	6.26	0.130	6.90	2.38	0.0430	0.0229
EvChl-Whl-1-E	White Island	0.34	18.72	1.47	0.80	0.037	0.019	1.889	12.68	6.40	0.129	6.78	2.35	0.0410	0.0244
EvChl-Whl-1-F	White Island	0.35	18.74	1.50	0.83	0.038	0.021	1.855	12.73	6.40	0.130				0.0233
EvChl-Whl-1-G	White Island	0.32	18.65	1.54	0.87	0.040	0.022	1.812	12.61	6.39	0.127				0.0238
EvChl-Whl-1-H	White Island	0.34	19.27	1.54	0.78	0.038	0.021	1.808	12.85	6.37	0.128				0.0234
EvChl-Whl-1-I	White Island	0.35	20.57	1.47	0.86	0.041	0.022	1.817	12.93	6.41	0.128				0.0231
EvChl-Whl-1-J	White Island	0.34	16.50	1.51	0.95	0.037	0.020	1.846	12.39	6.25	0.126				
EvChl-Whl-2-A	White Island	0.35	16.36	1.33	0.61	0.024	0.013	1.932	12.2	6.31	0.113	6.40	2.24	0.0308	0.0189
EvChl-Whl-2-B	White Island	0.34	17.23	1.38	0.83	0.028	0.017	1.656	12.29	6.31	0.115	6.41	2.23	0.0307	0.0190
EvChl-Whl-2-C	White Island	0.35	17.48	1.37	0.73	0.028	0.016	1.795	12.05	6.17	0.113	6.48	2.23	0.0309	0.0192
EvChl-Whl-2-D	White Island	0.35	17.98	1.34	0.77	0.029	0.016	1.775	11.95	5.97	0.114	6.35	2.19	0.0298	0.0187
EvChl-Whl-2-E	White Island	0.36	17.85	1.33	0.64	0.027	0.014	1.897	12.20	6.19	0.113	6.38	2.23	0.0304	0.0194
EvChl-Whl-2-F	White Island	0.35	17.65	1.35	0.72	0.028	0.015	1.838	12.24	6.27	0.111				0.0185
EvChl-Whl-2-G	White Island	0.36	15.51	1.26	0.96	0.026	0.015	1.743	12.15	6.21	0.114				0.0187
EvChl-Whl-2-H	White Island	0.34	16.02	1.29	0.74	0.026	0.013	1.943	12.31	5.88	0.112				0.0191
EvChl-Whl-2-I	White Island	0.33	15.79	1.29	0.75	0.024	0.013	1.837	12.20	6.07	0.113				0.0191
EvChl-Whl-2-J	White Island	0.34	14.92	1.18	0.63	0.019	0.010	1.922	12.38	6.51	0.113				0.0190

ID	Location	Test	Primary Spine						Demi-pyramid			Rotula			Epiphysis
		Thickness	Length	Proximal Diameter	Distal Diameter	Weight	Volume	Density	Length	Width	Weight	Length	Width	Weight	Weight
		(mm)	(mm)	(mm)	(mm)	(g)	(cm^3)	(g/cm^3)	(mm)	(mm)	(g)	(mm)	(mm)	(g)	(g)
EvChl-Whl-3-A	White Island	0.35	16.85	1.33	0.65	0.030	0.013	2.240	13.01	6.42	0.127	6.93	2.43	0.0391	0.0226
EvChl-Whl-3-B	White Island	0.34	16.95	1.30	0.55	0.026	0.012	2.194	12.99	6.60	0.129	7.08	2.42	0.0392	0.0237
EvChl-Whl-3-C	White Island	0.35	16.17	1.34	0.72	0.026	0.014	1.897	12.82	6.52	0.127	6.97	2.39	0.0375	0.0226
EvChl-Whl-3-D	White Island	0.34	17.30	1.40	0.77	0.032	0.016	1.923	13.05	6.43	0.128	6.85	2.42	0.0386	0.0242
EvChl-Whl-3-E	White Island	0.32	17.78	1.29	0.73	0.032	0.015	2.194	13.08	6.66	0.127	6.90	2.45	0.0387	0.0237
EvChl-Whl-3-F	White Island	0.36	17.03	1.33	0.72	0.028	0.014	1.928	12.94	6.52	0.128				0.0230
EvChl-Whl-3-G	White Island	0.35	16.83	1.12	0.52	0.023	0.009	2.461	13.15	6.49	0.129				0.0237
EvChl-Whl-3-H	White Island	0.34	18.67	1.28	0.63	0.033	0.014	2.349	12.90	6.53	0.131				0.0231
EvChl-Whl-3-I	White Island	0.33	17.78	1.51	0.63	0.032	0.017	1.895	13.07	6.44	0.128				0.0238
EvChl-Whl-3-J	White Island	0.34	16.00	1.31	0.59	0.025	0.012	2.078	12.93	6.54	0.128				0.0230
EvChl-Whl-4-A	White Island	0.34	16.87	1.15	0.76	0.028	0.012	2.325	13.18	6.45	0.139	6.89	2.55	0.0393	0.0222
EvChl-Whl-4-B	White Island	0.33	17.75	1.42	0.83	0.032	0.018	1.758	13.18	6.69	0.138	6.92	2.57	0.0403	0.0233
EvChl-Whl-4-C	White Island	0.34	18.24	1.59	0.84	0.033	0.022	1.498	13.15	6.82	0.142	6.94	2.61	0.0404	0.0230
EvChl-Whl-4-D	White Island	0.35	16.51	1.41	0.77	0.028	0.016	1.776	13.14	6.79	0.139	6.93	2.50	0.0406	0.0230
EvChl-Whl-4-E	White Island	0.34	16.60	1.52	0.83	0.032	0.019	1.711	13.13	6.61	0.137	6.71	2.61	0.0392	0.0240
EvChl-Whl-4-F	White Island	0.32	17.10	1.47	0.84	0.032	0.018	1.731	13.19	6.68	0.137				0.0225
EvChl-Whl-4-G	White Island	0.34	14.80	1.44	0.89	0.029	0.016	1.781	13.06	6.77	0.140				0.0227
EvChl-Whl-4-H	White Island	0.33	15.83	1.40	0.85	0.027	0.016	1.695	13.42	6.72	0.138				0.0223
EvChl-Whl-4-I	White Island	0.32	15.27	1.36	0.90	0.027	0.016	1.709	13.20	6.57	0.138				0.0219
EvChl-Whl-4-J	White Island	0.34	14.52	1.23	0.78	0.022	0.012	1.916	13.27	6.79	0.140				0.0222
EvChl-Whl-5-A	White Island	0.38	17.02	1.30	0.78	0.031	0.015	2.077	13.00	6.40	0.116	6.79	2.29	0.0344	0.0202
EvChl-Whl-5-B	White Island	0.37	17.76	1.38	0.71	0.031	0.016	1.959	12.67	6.37	0.115	6.72	2.25	0.0343	0.0199
EvChl-Whl-5-C	White Island	0.36	18.29	1.41	0.75	0.035	0.017	2.044	12.97	6.39	0.115	6.83	2.34	0.0353	0.0197
EvChl-Whl-5-D	White Island	0.34	16.73	1.27	0.81	0.032	0.014	2.204	12.81	6.33	0.117	6.86	2.24	0.0349	0.0198
EvChl-Whl-5-E	White Island	0.36	16.68	1.57	0.85	0.034	0.020	1.720	12.77	6.41	0.116	6.62	2.22	0.0340	0.0199
EvChl-Whl-5-F	White Island	0.38	18.15	1.35	0.72	0.029	0.016	1.867	12.69	6.42	0.115				0.0196
EvChl-Whl-5-G	White Island	0.37	16.03	1.26	0.68	0.026	0.012	2.123	12.99	6.41	0.118				0.0199
EvChl-Whl-5-H	White Island	0.36	16.31	1.41	0.75	0.029	0.015	1.876	12.9	6.42	0.116				0.0198
EvChl-Whl-5-I	White Island	0.37	17.55	1.27	0.72	0.031	0.014	2.195	12.83	6.39	0.113				0.0195
EvChl-Whl-5-J	White Island	0.36	16.12	1.39	0.81	0.028	0.016	1.770	12.68	6.41	0.115				0.0198
EvChl-Whl-6-A	White Island	0.37	18.09	1.47	0.75	0.037	0.018	2.068	12.71	6.27	0.188	6.74	2.36	0.0329	0.0202
EvChl-Whl-6-B	White Island	0.38	19.01	1.54	0.79	0.038	0.021	1.795	12.56		0.099	6.64	2.35	0.0324	0.0206
EvChl-Whl-6-C	White Island	0.37	19.69	1.30	0.72	0.037	0.016	2.291	12.76	6.23	0.118	6.61	2.36	0.0327	0.0205
EvChl-Whl-6-D	White Island	0.36	17.19	1.26	0.75	0.028	0.014	2.032	12.63	6.28	0.117	6.56	2.37	0.0326	0.0207
EvChl-Whl-6-E	White Island	0.37	18.50	1.41	0.75	0.036	0.017	2.056	12.80	6.35	0.118	6.67	2.32	0.0329	0.0217
EvChl-Whl-6-F	White Island	0.37	18.13	1.59	0.83	0.037	0.022	1.704	12.62	6.40	0.120				0.0203
EvChl-Whl-6-G	White Island	0.36	17.32	1.35	0.70	0.029	0.015	1.996	12.62	6.37	0.116				0.0200
EvChl-Whl-6-H	White Island	0.37	18.71	1.54	0.94	0.042	0.023	1.803	12.60	6.28	0.117				0.0197
EvChl-Whl-6-I	White Island	0.36	16.81	1.40	0.73	0.030	0.015	1.907	12.65	6.29	0.118				0.0202
EvChl-Whl-6-J	White Island	0.36	16.64	1.43	0.72	0.029	0.016	1.824	12.66		0.103				0.0197
EvChl-Whl-7-A	White Island	0.36	15.62	1.30	0.64	0.024	0.012	2.005	13.09	6.22	0.112	6.39	2.12	0.0296	0.0175
EvChl-Whl-7-B	White Island	0.37	15.67	1.30	0.7	0.027	0.013	2.154	12.84	6.52	0.113	6.52	2.25	0.0297	0.0179

ID	Location	Test	Primary Spine						Demi-pyramid			Rotula			Epiphysis
		Thickness	Length	Proximal Diameter	Distal Diameter	Weight	Volume	Density	Length	Width	Weight	Length	Width	Weight	Weight
		(mm)	(mm)	(mm)	(mm)	(g)	(cm^3)	(g/cm^3)	(mm)	(mm)	(g)	(mm)	(mm)	(g)	(g)
EvChl-Whl-7-C	White Island	0.38	14.67	1.37	0.74	0.027	0.013	2.041	12.83	6.51	0.113	6.45	2.21	0.0298	0.0177
EvChl-Whl-7-D	White Island	0.38	14.56	1.22	0.75	0.021	0.011	1.842	13.00	6.25	0.114	6.42	2.24	0.0297	0.0171
EvChl-Whl-7-E	White Island	0.37	15.31	1.39	0.71	0.028	0.014	2.013	12.76	6.28	0.113	6.48	2.27	0.0310	0.0210
EvChl-Whl-7-F	White Island	0.36	16.30	1.39	0.81	0.029	0.016	1.858	12.89	6.48	0.115				0.0192
EvChl-Whl-7-G	White Island	0.38	15.32	1.39	0.78	0.029	0.015	1.990	13.13	6.48	0.114				0.0181
EvChl-Whl-7-H	White Island	0.39	16.12	1.39	0.81	0.026	0.016	1.677	12.89	6.22	0.121				0.0181
EvChl-Whl-7-I	White Island	0.40	15.08	1.23	0.69	0.023	0.011	2.075	13.04	6.17	0.114				0.0175
EvChl-Whl-7-J	White Island	0.37	14.72	1.43	0.74	0.025	0.014	1.782	12.86	6.19	0.116				0.0152
EvChl-Whl-8-A	White Island	0.36	19.05	1.59	0.94	0.042	0.024	1.702	14.22	6.86	0.139	7.04	2.51	0.0424	0.0254
EvChl-Whl-8-B	White Island	0.36	18.05	1.51	0.83	0.036	0.020	1.793	14.25	6.45	0.141	7.13	2.53	0.0425	0.0264
EvChl-Whl-8-C	White Island	0.33	17.95	1.58	0.55	0.033	0.017	1.901	14.20	6.96	0.141	7.07	2.46	0.0421	0.0260
EvChl-Whl-8-D	White Island	0.34	19.03	1.47	0.52	0.033	0.016	2.068	13.98	6.89	0.143	7.17	2.43	0.0425	0.0256
EvChl-Whl-8-E	White Island	0.36	18.35	1.59	0.62	0.029	0.019	1.574	14.27	6.61	0.140				0.0256
EvChl-Whl-8-F	White Island	0.34	17.46	1.51	0.63	0.030	0.017	1.823	14.20	6.73	0.141				0.0258
EvChl-Whl-8-G	White Island	0.36	17.20	1.53	0.81	0.031	0.019	1.632	14.07	6.82	0.141				0.0266
EvChl-Whl-8-H	White Island	0.37	18.20	1.45	0.63	0.031	0.016	1.898	14.42	6.75	0.142				0.0260
EvChl-Whl-8-I	White Island	0.35	20.41	1.46	0.73	0.040	0.020	1.991	14.19	6.79	0.142				0.0293
EvChl-Whl-8-J	White Island	0.36	17.25	1.47	0.78	0.030	0.018	1.702	14.24	6.78	0.142				
EvChl-Whl-9-A	White Island	0.37	16.22	1.49	0.81	0.029	0.017	1.664	12.79	6.37	0.135	6.87	2.42	0.0384	0.0231
EvChl-Whl-9-B	White Island	0.38	18.33	1.44	0.81	0.038	0.019	2.014	12.80	6.19	0.136	6.95	2.29	0.0378	0.0227
EvChl-Whl-9-C	White Island	0.37	18.52	1.41	0.83	0.036	0.019	1.938	12.64	6.47	0.134	6.85	2.30	0.0387	0.0231
EvChl-Whl-9-D	White Island	0.35	17.63	1.52	0.86	0.033	0.020	1.652	12.60	6.44	0.136	6.99	2.37	0.0383	0.0234
EvChl-Whl-9-E	White Island	0.38	17.28	1.57	0.70	0.032	0.018	1.736	12.73	6.42	0.132	7.13	2.32	0.0379	0.0230
EvChl-Whl-9-F	White Island	0.39	16.21	1.79	0.81	0.029	0.023	1.290	12.71	6.51	0.134				0.0224
EvChl-Whl-9-G	White Island	0.34	16.81	1.42	0.85	0.031	0.017	1.764	12.86	6.49	0.135				0.0234
EvChl-Whl-9-H	White Island	0.37	18.44	1.53	0.72	0.037	0.019	1.927	12.85	6.50	0.135				0.0232
EvChl-Whl-9-I	White Island	0.36	16.96	1.45	0.81	0.031	0.017	1.769	12.64	6.54	0.134				0.0230
EvChl-Whl-9-J	White Island	0.37	16.93	1.54	0.79	0.032	0.019	1.701	12.62	6.42	0.135				0.0232
EvChl-Whl-10-A	White Island	0.34	15.16	1.35	0.81	0.025	0.014	1.761	12.84	6.37	0.126	6.57	2.22	0.0343	0.0202
EvChl-Whl-10-B	White Island	0.35	15.28	1.50	0.76	0.030	0.016	1.901	12.97	6.20	0.126	6.60	2.46	0.0343	0.0198
EvChl-Whl-10-C	White Island	0.35	15.64	1.55	0.78	0.030	0.017	1.739	12.9	6.40	0.126	6.64	2.19	0.0337	0.0199
EvChl-Whl-10-D	White Island	0.35	16.71	1.63	0.81	0.032	0.020	1.602	12.97	6.46	0.126	6.62	2.41	0.0340	0.0202
EvChl-Whl-10-E	White Island	0.34	15.21	1.64	0.77	0.032	0.018	1.758	13.02	6.42	0.127	6.62	2.15	0.0342	0.0199
EvChl-Whl-10-F	White Island	0.36	15.19	1.49	0.87	0.030	0.017	1.749	12.90	6.38	0.127				0.0200
EvChl-Whl-10-G	White Island	0.34	14.61	1.53	0.67	0.027	0.015	1.843	12.90	6.61	0.126				0.0197
EvChl-Whl-10-H	White Island	0.35	14.77	1.38	0.69	0.025	0.013	1.921	12.62	6.14	0.123				0.0170
EvChl-Whl-10-I	White Island	0.36	15.29	1.61	0.95	0.033	0.020	1.648							
EvChl-Whl-10-J	White Island	0.35	14.94	1.50	0.78	0.024	0.016	1.552							

Table 7.7 Raw data for skeletal elements of *Evechinus chloroticus* collected from Wellington, New Zealand

ID	Location	Test	Primary Spine						Demi-pyramid			Rotula			Epiphysis
		Thickness	Length	Proximal Diameter	Distal Diameter	Weight	Volume	Density	Length	Width	Weight	Length	Width	Weight	Weight
		(mm)	(mm)	(mm)	(mm)	(g)	(cm^3)	(g/cm^3)	(mm)	(mm)	(g)	(mm)	(mm)	(g)	(g)
EvChl-Wlg-1-A	Wellington	0.32	22.77	1.50	0.58	0.032	0.021	1.550	13.67	6.71	0.144	6.91	2.75	0.0444	0.0254
EvChl-Wlg-1-B	Wellington	0.32	20.88	1.63	0.61	0.036	0.022	1.630	13.98	6.64	0.141	6.78	2.77	0.0437	0.0261
EvChl-Wlg-1-C	Wellington	0.32	22.04	1.45	0.63	0.027	0.020	1.360	13.88	6.71	0.141	6.84	2.71	0.0441	0.0257
EvChl-Wlg-1-D	Wellington	0.33	20.14	1.59	0.60	0.031	0.020	1.535	13.92	6.64	0.146	6.66	2.72	0.0440	0.0259
EvChl-Wlg-1-E	Wellington	0.31	21.16	1.49	0.50	0.033	0.018	1.826	14.02	6.67	0.142	6.79	2.83	0.0457	0.0254
EvChl-Wlg-1-F	Wellington	0.32	20.11	1.43	0.59	0.032	0.017	1.907	13.88	6.79	0.141				
EvChl-Wlg-1-G	Wellington	0.34	20.73	1.50	0.59	0.032	0.019	1.671	14.05	6.73	0.146				0.0260
EvChl-Wlg-1-H	Wellington	0.35	20.04	1.61	0.43	0.025	0.018	1.361	13.99	6.62	0.144				0.0261
EvChl-Wlg-1-I	Wellington	0.33	20.03	1.49	0.57	0.028	0.018	1.547	14.05	6.75	0.148				0.0255
EvChl-Wlg-1-J	Wellington	0.31	20.23	1.51	0.49	0.029	0.017	1.656	13.87	6.70	0.146				0.0257
EvChl-Wlg-2-A	Wellington	0.30	20.13	1.41	0.51	0.028	0.016	1.821	13.48	6.68	0.145	7.05	2.42	0.0402	0.0272
EvChl-Wlg-2-B	Wellington	0.31	21.03	1.38	0.52	0.028	0.016	1.787	13.69	6.81	0.147	6.91	2.44	0.0392	0.0261
EvChl-Wlg-2-C	Wellington	0.29	18.86	1.29	0.55	0.024	0.013	1.785	13.75	6.86	0.149	6.95	2.43	0.0390	0.0260
EvChl-Wlg-2-D	Wellington	0.30	22.05	1.49	0.77	0.035	0.023	1.538	13.81	6.90	0.146	6.91	2.44	0.0400	0.0261
EvChl-Wlg-2-E	Wellington	0.30	21.53	1.45	0.55	0.033	0.018	1.817	13.69	6.77	0.146	6.85	2.43	0.0383	0.0271
EvChl-Wlg-2-F	Wellington	0.29	21.95	1.39	0.58	0.031	0.018	1.747	13.67	6.94	0.148				0.0265
EvChl-Wlg-2-G	Wellington	0.28	18.77	1.43	0.58	0.028	0.016	1.747	13.77	6.87	0.146				0.0264
EvChl-Wlg-2-H	Wellington	0.32	17.71	1.42	0.71	0.030	0.016	1.826	13.93	6.89	0.150				0.0271
EvChl-Wlg-2-I	Wellington	0.30	19.07	1.17	0.46	0.023	0.011	2.152	13.75	6.95	0.151				0.0271
EvChl-Wlg-2-J	Wellington	0.31	16.78	1.23	0.64	0.021	0.012	1.745	13.58	6.89	0.148				
EvChl-Wlg-3-A	Wellington	0.30	18.96	1.43	0.59	0.022	0.016	1.391	11.71	5.52	0.085	5.69	2.17	0.0247	0.0148
EvChl-Wlg-3-B	Wellington	0.34	18.60	1.36	0.74	0.031	0.017	1.846	11.61	5.57	0.084	5.74	2.26	0.0260	0.0143
EvChl-Wlg-3-C	Wellington	0.34	21.39	1.37	0.50	0.027	0.016	1.738	11.65	5.51	0.085	5.66	2.32	0.0251	0.0141
EvChl-Wlg-3-D	Wellington	0.33	20.10	1.42	0.45	0.027	0.015	1.817	11.62	5.47	0.084	5.67	2.20	0.0254	0.0146
EvChl-Wlg-3-E	Wellington	0.31	19.22	1.16	0.53	0.022	0.011	1.981	11.72	5.51	0.086	5.68	2.29	0.0254	
EvChl-Wlg-3-F	Wellington	0.30	18.10	1.43	0.60	0.028	0.015	1.815							
EvChl-Wlg-3-G	Wellington	0.31	19.01	1.33	0.75	0.028	0.017	1.708							
EvChl-Wlg-3-H	Wellington	0.31	19.37	1.37	0.61	0.029	0.016	1.845							
EvChl-Wlg-3-I	Wellington	0.32	18.38	1.42	0.60	0.027	0.016	1.730							
EvChl-Wlg-3-J	Wellington	0.33	17.85	1.35	0.44	0.021	0.012	1.704							
EvChl-Wlg-4-A	Wellington	0.30	21.27	1.36	0.58	0.030	0.017	1.839	12.91	6.68	0.119	6.87	2.52	0.0400	0.0216
EvChl-Wlg-4-B	Wellington	0.31	21.67	1.32	0.74	0.029	0.019	1.589	12.88	6.56	0.117	6.91	2.51	0.0393	0.0223
EvChl-Wlg-4-C	Wellington	0.29	21.13	1.44	0.60	0.032	0.018	1.748	12.76	6.60	0.117	6.86	2.52	0.0394	0.0216
EvChl-Wlg-4-D	Wellington	0.30	21.66	1.40	0.57	0.027	0.017	1.566	12.96	6.55	0.117	6.84	2.53	0.0393	0.0228
EvChl-Wlg-4-E	Wellington	0.31	21.57	1.37	0.47	0.027	0.015	1.712	12.72	6.50	0.115	6.98	2.52	0.0417	0.0219
EvChl-Wlg-4-F	Wellington	0.31	20.86	1.32	0.49	0.027	0.014	1.898	12.88	6.64	0.118				0.0221
EvChl-Wlg-4-G	Wellington	0.29	21.33	1.35	0.55	0.025	0.016	1.554	12.78	6.60	0.118				0.0227
EvChl-Wlg-4-H	Wellington	0.28	19.88	1.45	0.67	0.029	0.018	1.601	12.74	6.60	0.121				
EvChl-Wlg-4-I	Wellington	0.29	20.32	1.43	0.67	0.030	0.018	1.648	12.93	6.58	0.118				0.0218

ID	Location	Test	Primary Spine						Demi-pyramid			Rotula			Epiphysis
		Thickness	Length	Proximal Diameter	Distal Diameter	Weight	Volume	Density	Length	Width	Weight	Length	Width	Weight	Weight
		(mm)	(mm)	(mm)	(mm)	(g)	(cm^3)	(g/cm^3)	(mm)	(mm)	(g)	(mm)	(mm)	(g)	(g)
EvChl-Wlg-4-J	Wellington	0.30	19.91	1.37	0.71	0.029	0.017	1.633	12.74	6.67	0.119				
EvChl-Wlg-5-A	Wellington	0.26	16.20	1.33	0.51	0.019	0.011	1.615	12.2	5.91	0.098	6.08	2.21	0.0294	0.0182
EvChl-Wlg-5-B	Wellington	0.26	16.76	1.21	0.56	0.018	0.011	1.645	12.19	5.93	0.095	6.20	2.41	0.0297	0.0187
EvChl-Wlg-5-C	Wellington	0.27	17.64	1.35	0.55	0.022	0.013	1.649	12.1	6.00	0.096	6.29	2.32	0.0298	0.0192
EvChl-Wlg-5-D	Wellington	0.28	17.49	1.27	0.54	0.017	0.012	1.460	12.27	6.05	0.098	6.32	2.37	0.0299	0.0185
EvChl-Wlg-5-E	Wellington	0.25	16.80	1.41	0.60	0.020	0.014	1.429	12.24	5.92	0.098	6.31	2.32	0.0302	0.0186
EvChl-Wlg-5-F	Wellington	0.26	17.06	1.31	0.57	0.019	0.012	1.486	12.31	6.05	0.096				0.0182
EvChl-Wlg-5-G	Wellington	0.27	18.54	1.36	0.53	0.021	0.014	1.520	12.12	5.89	0.098				0.0182
EvChl-Wlg-5-H	Wellington	0.26	15.47	1.26	0.58	0.017	0.016	1.082	12.30	5.91	0.096				0.0189
EvChl-Wlg-5-I	Wellington	0.25	16.48	1.26	0.56	0.019	0.011	1.688	12.14	6.01	0.098				0.0183
EvChl-Wlg-5-J	Wellington	0.27	15.99	1.25	0.53	0.019	0.010	1.790	12.18	6.03	0.096				
EvChl-Wlg-6-A	Wellington	0.34	18.62	1.41	0.72	0.036	0.017	2.103	13.88	6.63	0.135	6.89	2.68	0.0439	0.0260
EvChl-Wlg-6-B	Wellington	0.40	19.50	1.34	0.56	0.035	0.015	2.396	13.86	6.79	0.137	7.30	2.73	0.0480	0.0268
EvChl-Wlg-6-C	Wellington	0.34	20.10	1.40	0.66	0.038	0.017	2.151	13.61	6.61	0.138	6.87	2.74	0.0445	0.0266
EvChl-Wlg-6-D	Wellington	0.32	17.87	1.44	0.68	0.035	0.016	2.109	14.09	6.60	0.139	7.05	2.75	0.0446	0.0264
EvChl-Wlg-6-E	Wellington	0.31	19.90	1.40	0.49	0.036	0.015	2.392	14.03	6.64	0.142	6.88	2.68	0.0440	0.0262
EvChl-Wlg-6-F	Wellington	0.33	19.22	1.37	0.55	0.036	0.015	2.449	13.95	6.55	0.134				0.0276
EvChl-Wlg-6-G	Wellington	0.30	19.42	1.40	0.63	0.034	0.016	2.094	13.81	6.84	0.142				0.0286
EvChl-Wlg-6-H	Wellington	0.31	18.70	1.44	0.57	0.034	0.016	2.166	13.80	6.70	0.140				0.0274
EvChl-Wlg-6-I	Wellington	0.31	16.49	1.35	0.61	0.035	0.013	2.648	13.96	6.65	0.136				0.0273
EvChl-Wlg-6-J	Wellington	0.30	18.30	1.28	0.54	0.034	0.013	2.736	13.82	6.66	0.138				0.0261
EvChl-Wlg-7-A	Wellington	0.30	18.93	1.51	0.52	0.032	0.017	1.938	12.90	6.61	0.130	6.86	2.71	0.0408	0.0257
EvChl-Wlg-7-B	Wellington	0.31	19.44	1.42	0.44	0.027	0.014	1.889	13.00	6.59	0.127	6.74	2.73	0.0402	0.0248
EvChl-Wlg-7-C	Wellington	0.30	20.09	1.53	0.58	0.033	0.019	1.761	12.94	6.71	0.127	6.77	2.69	0.0405	0.0252
EvChl-Wlg-7-D	Wellington	0.29	20.21	1.46	0.60	0.032	0.018	1.812	12.92	6.50	0.127	6.73	2.68	0.0395	0.0252
EvChl-Wlg-7-E	Wellington	0.26	18.46	1.44	0.74	0.032	0.018	1.804	12.89	6.50	0.130	6.85	2.66	0.0414	0.0301
EvChl-Wlg-7-F	Wellington	0.31	18.97	1.42	0.61	0.028	0.016	1.701	12.78	6.51	0.128				0.0245
EvChl-Wlg-7-G	Wellington	0.31	18.44	1.42	0.58	0.031	0.015	2.011	12.90	6.47	0.129				0.0252
EvChl-Wlg-7-H	Wellington	0.30	18.59	1.44	0.62	0.028	0.016	1.707	12.96	6.53	0.127				0.0261
EvChl-Wlg-7-I	Wellington	0.28	17.63	1.36	0.43	0.026	0.012	2.122	12.89	6.65	0.127				0.0246
EvChl-Wlg-7-J	Wellington	0.29	16.88	1.44	0.63	0.026	0.015	1.754	12.94	6.45	0.127				0.0244
EvChl-Wlg-8-A	Wellington	0.31	19.04	1.47	0.62	0.028	0.017	1.628	13.87	6.71	0.133	6.72	2.76	0.0412	0.0255
EvChl-Wlg-8-B	Wellington	0.31	18.84	1.24	0.59	0.024	0.013	1.841	13.87	6.77	0.136	6.79	2.62	0.0413	0.0304
EvChl-Wlg-8-C	Wellington	0.29	19.67	1.25	0.41	0.020	0.012	1.745	13.72	6.58	0.136	6.91	2.72	0.0435	0.0257
EvChl-Wlg-8-D	Wellington	0.34	19.91	1.34	0.66	0.027	0.016	1.668	13.68	6.56	0.130	6.95	2.87	0.0464	0.0259
EvChl-Wlg-8-E	Wellington	0.29	21.08	1.46	0.52	0.027	0.017	1.540	13.66	6.63	0.131	6.85	2.72	0.0430	0.0285
EvChl-Wlg-8-F	Wellington	0.34	21.75	1.41	0.56	0.029	0.018	1.647	13.73	6.77	0.134				0.0256
EvChl-Wlg-8-G	Wellington	0.31	20.96	1.37	0.53	0.027	0.016	1.711	13.74	6.83	0.136				0.0250
EvChl-Wlg-8-H	Wellington	0.32	21.61	1.35	0.52	0.028	0.016	1.781	13.66	6.74	0.136				0.0240
EvChl-Wlg-8-I	Wellington	0.33	20.38	1.35	0.61	0.026	0.016	1.641	13.57	6.72	0.135				0.0248
EvChl-Wlg-8-J	Wellington	0.31	22.18	1.45	0.59	0.027	0.019	1.395	13.92	6.63	0.135				0.0254
EvChl-Wlg-9-A	Wellington	0.33	19.55	1.53	0.67	0.030	0.020	1.526	12.85	6.19	0.124	6.30	2.53	0.0367	0.0242

ID	Location	Test	Primary Spine						Demi-pyramid			Rotula			Epiphysis
		Thickness	Length	Proximal Diameter	Distal Diameter	Weight	Volume	Density	Length	Width	Weight	Length	Width	Weight	Weight
		(mm)	(mm)	(mm)	(mm)	(g)	(cm^3)	(g/cm^3)	(mm)	(mm)	(g)	(mm)	(mm)	(g)	(g)
EvChl-Wlg-9-B	Wellington	0.34	21.47	1.49	0.49	0.031	0.018	1.738	13.07	6.07	0.125	6.27	2.53	0.0651	0.0224
EvChl-Wlg-9-C	Wellington	0.34	21.63	1.55	0.57	0.035	0.020	1.728	12.79	6.06	0.119	6.26	2.50	0.0358	0.0224
EvChl-Wlg-9-D	Wellington	0.35	22.39	1.51	0.56	0.030	0.020	1.482	12.81	6.04	0.123	6.51	2.53	0.0369	0.0248
EvChl-Wlg-9-E	Wellington	0.32	21.03	1.59	0.57	0.032	0.021	1.558	12.92	6.19	0.127	6.25	2.52	0.0352	0.0228
EvChl-Wlg-9-F	Wellington	0.33	20.44	1.51	0.69	0.031	0.020	1.532	13.01	6.22	0.126				0.0230
EvChl-Wlg-9-G	Wellington	0.32	19.77	1.55	0.66	0.031	0.020	1.551	13.08	6.06	0.126				0.0227
EvChl-Wlg-9-H	Wellington	0.34	20.10	1.52	0.53	0.029	0.018	1.623	13.00	6.20	0.127				0.0231
EvChl-Wlg-9-I	Wellington	0.36	20.79	1.58	0.66	0.032	0.022	1.469	12.84	6.09	0.122				0.0245
EvChl-Wlg-9-J	Wellington	0.34	19.47	1.49	0.65	0.030	0.018	1.634	12.88	6.09	0.122				0.0227
EvChl-Wlg-10-A	Wellington	0.29	17.60	1.31	0.63	0.023	0.014	1.665	11.37	5.69	0.084	5.89	2.46	0.0283	0.0161
EvChl-Wlg-10-B	Wellington	0.30	19.87	1.33	0.43	0.025	0.013	1.878	11.38	5.66	0.083	5.81	2.46	0.0284	0.0166
EvChl-Wlg-10-C	Wellington	0.31	18.28	1.21	0.55	0.023	0.012	1.994	11.33	5.60	0.083	5.85	2.42	0.0284	0.0160
EvChl-Wlg-10-D	Wellington	0.28	18.09	1.23	0.53	0.022	0.012	1.892	11.06	5.59	0.085	5.85	2.47	0.0280	0.0163
EvChl-Wlg-10-E	Wellington	0.28	18.91	1.31	0.51	0.023	0.013	1.791	11.25	5.70	0.086	6.13	2.34	0.0282	0.0157
EvChl-Wlg-10-F	Wellington	0.27	18.58	1.24	0.50	0.022	0.012	1.840	11.26	5.70	0.088				0.0159
EvChl-Wlg-10-G	Wellington	0.28	18.38	1.32	0.53	0.024	0.013	1.829	11.34	5.63	0.084				0.0161
EvChl-Wlg-10-H	Wellington	0.29	16.66	1.28	0.56	0.019	0.012	1.589	11.18	5.66	0.085				0.0160
EvChl-Wlg-10-I	Wellington	0.28	18.74	1.31	0.48	0.024	0.013	1.901	11.48	5.65	0.084				0.0156
EvChl-Wlg-10-J	Wellington	0.27	18.15	1.30	0.62	0.024	0.014	1.732	11.43	5.56	0.083				
EvChl-Wlg-11-A	Wellington	0.35	22.20	1.67	0.70	0.042	0.026	1.612	12.94	6.33	0.121	6.31	2.69	0.0349	0.0225
EvChl-Wlg-11-B	Wellington	0.34	21.21	1.61	0.57	0.039	0.021	1.809	12.92	6.37	0.122	6.77	2.62	0.0367	0.0218
EvChl-Wlg-11-C	Wellington	0.34	22.52	1.53	0.89	0.043	0.026	1.629	13.18	6.39	0.117	6.40	2.72	0.0360	0.0229
EvChl-Wlg-11-D	Wellington	0.33	22.31	1.68	0.55	0.039	0.024	1.647	12.94	6.21	0.116	6.44	2.66	0.0354	0.0234
EvChl-Wlg-11-E	Wellington	0.34	22.67	1.70	0.63	0.042	0.026	1.618	13.08	6.34	0.119	6.39	2.55	0.0363	0.0223
EvChl-Wlg-11-F	Wellington	0.34	21.47	1.56	0.69	0.039	0.022	1.736	13.36	6.20	0.117				0.0223
EvChl-Wlg-11-G	Wellington	0.31	22.36	1.63	0.78	0.042	0.027	1.571	13.01	6.29	0.118				0.0219
EvChl-Wlg-11-H	Wellington	0.34	23.22	1.53	0.63	0.038	0.023	1.694	13.01	6.44	0.119				0.0230
EvChl-Wlg-11-I	Wellington	0.34	22.47	1.69	0.53	0.035	0.031	1.134	12.92	6.29	0.116				0.0229
EvChl-Wlg-11-J	Wellington	0.40	21.30	1.55	0.77	0.037	0.023	1.597	12.92	6.33	0.121				0.0226
EvChl-Wlg-12-A	Wellington	0.29	23.50	1.61	0.71	0.031	0.026	1.177	12.57	5.98	0.116	6.28	2.47	0.0338	0.0194
EvChl-Wlg-12-B	Wellington	0.29	23.03	1.56	0.60	0.027	0.022	1.214	12.74	5.97	0.117	6.31	2.48	0.0338	0.0194
EvChl-Wlg-12-C	Wellington	0.29	21.70	1.68	0.86	0.032	0.028	1.117	12.23	6.08	0.117	6.34	2.60	0.0329	0.0192
EvChl-Wlg-12-D	Wellington	0.29	22.19	1.54	0.68	0.028	0.023	1.239	12.54	5.99	0.119	6.42	2.43	0.0335	0.0192
EvChl-Wlg-12-E	Wellington	0.29	23.42	1.51	0.68	0.029	0.023	1.260	12.63	6.02	0.118	6.32	2.53	0.0345	0.0188
EvChl-Wlg-12-F	Wellington	0.28	22.91	1.63	0.65	0.025	0.025	0.999	12.65	6.10	0.120				0.0189
EvChl-Wlg-12-G	Wellington	0.27	22.15	1.61	0.65	0.028	0.024	1.197	12.66	6.01	0.117				0.0191
EvChl-Wlg-12-H	Wellington	0.30	20.95	1.49	0.86	0.025	0.023	1.088	12.7	6.00	0.115				0.0202
EvChl-Wlg-12-I	Wellington	0.29	21.37	1.53	0.63	0.023	0.021	1.102	12.82	6.03	0.121				0.0193
EvChl-Wlg-12-J	Wellington	0.31	23.34	1.52	0.54	0.026	0.021	1.240	12.63	6.05	0.117				0.0194
EvChl-Wlg-13-A	Wellington	0.34	23.00	1.57	0.61	0.035	0.023	1.524	13.31	6.98	0.143	7.05	2.55	0.0453	0.0262
EvChl-Wlg-13-B	Wellington	0.33	22.76	1.53	0.62	0.035	0.022	1.606	13.57	6.88	0.147	7.21	2.56	0.0461	0.0270
EvChl-Wlg-13-C	Wellington	0.31	22.46	1.55	0.71	0.035	0.024	1.496	13.37	6.96	0.140	7.13	2.58	0.0459	0.0266

ID	Location	Test	Primary Spine						Demi-pyramid			Rotula			Epiphysis
		Thickness	Length	Proximal Diameter	Distal Diameter	Weight	Volume	Density	Length	Width	Weight	Length	Width	Weight	Weight
		(mm)	(mm)	(mm)	(mm)	(g)	(cm^3)	(g/cm^3)	(mm)	(mm)	(g)	(mm)	(mm)	(g)	(g)
EvChl-Wlg-13-D	Wellington	0.34	20.92	1.53	0.76	0.033	0.022	1.484	13.3	6.76	0.142	7.17	2.57	0.0451	0.0268
EvChl-Wlg-13-E	Wellington	0.31	21.28	1.56	0.78	0.037	0.024	1.556	13.34	6.95	0.141	7.06	2.53	0.0459	0.0276
EvChl-Wlg-13-F	Wellington	0.32	21.83	1.41	0.6	0.031	0.018	1.716	13.30	6.77	0.140				0.0260
EvChl-Wlg-13-G	Wellington	0.34	21.92	1.47	0.70	0.034	0.021	1.591	13.49	7.04	0.142				0.0254
EvChl-Wlg-13-H	Wellington	0.30	20.89	1.48	0.67	0.034	0.020	1.688	13.31	6.92	0.141				0.0267
EvChl-Wlg-13-I	Wellington	0.35	20.46	1.42	0.85	0.036	0.021	1.706	13.48	6.92	0.145				0.0254
EvChl-Wlg-13-J	Wellington	0.31	20.42	1.42	0.57	0.030	0.017	1.758	13.31	6.85	0.145				0.0258
EvChl-Wlg-14-A	Wellington	0.29	21.83	1.66	0.79	0.046	0.027	1.728	13.74	6.36	0.135	6.50	2.71	0.0422	0.0253
EvChl-Wlg-14-B	Wellington	0.28	22.57	1.76	0.74	0.050	0.029	1.723	13.57	6.24	0.136	6.60	2.74	0.0419	0.0261
EvChl-Wlg-14-C	Wellington	0.29	22.95	1.74	0.64	0.047	0.027	1.734	13.54	6.32	0.140	6.48	2.62	0.0414	0.0246
EvChl-Wlg-14-D	Wellington	0.28	21.05	1.60	0.77	0.047	0.024	1.938	12.86	6.49	0.137	6.52	2.73	0.0420	0.0256
EvChl-Wlg-14-E	Wellington	0.27	21.61	1.57	0.83	0.046	0.025	1.837	13.73	6.35	0.138	6.56	2.74	0.0428	0.0259
EvChl-Wlg-14-F	Wellington	0.29	23.00	2.09	0.69	0.050	0.038	1.318	13.65	6.27	0.137				0.0256
EvChl-Wlg-14-G	Wellington	0.27	23.18	1.73	0.61	0.050	0.027	1.846	13.85	6.32	0.136				0.0257
EvChl-Wlg-14-H	Wellington	0.26	20.89	1.72	0.92	0.047	0.029	1.608	13.65	6.37	0.137				
EvChl-Wlg-14-I	Wellington	0.26	21.12	1.55	0.63	0.044	0.021	2.108	13.86	6.29	0.138				
EvChl-Wlg-14-J	Wellington	0.25	23.06	1.70	0.62	0.049	0.026	1.863	13.65	6.25	0.138				

Appendix C Raw Biomineralogy Data

Table 7.8 Raw data for biomineralogy of skeletal elements from *Evechinus chloroticus* collected around New Zealand

Sample ID	Location	Body Part	Replicate #	Wt% $MgCO_3$ in calcite
Stl-6-spn-a	Stewart Island	spine	a	4.64
Stl-6-spn-b	Stewart Island	spine	b	4.51
Stl-6-spn-c	Stewart Island	spine	c	4.03
Stl-6-rot-a	Stewart Island	rotula	a	8.69
Stl-6-rot-b	Stewart Island	rotula	b	9.18
Stl-6-rot-c	Stewart Island	rotula	c	8.92
Stl-6-epi-a	Stewart Island	epiphysis	a	8.84
Stl-6-epi-b	Stewart Island	epiphysis	b	10.45
Stl-6-epi-c	Stewart Island	epiphysis	c	8.65
Stl-6-demi-a	Stewart Island	demi-pyramid	a	9.88
Stl-6-demi-b	Stewart Island	demi-pyramid	b	10.64
Stl-6-demi-c	Stewart Island	demi-pyramid	c	9.55
Stl-6-plate-a	Stewart Island	test plate	a	8.01
Stl-6-plate-b	Stewart Island	test plate	b	9.37
Stl-6-plate-c	Stewart Island	test plate	c	8.72
Stl-2-spn-a	Stewart Island	spine	a	4.46
Stl-2-spn-b	Stewart Island	spine	b	5.23
Stl-2-spn-c	Stewart Island	spine	c	4.19
Stl-2-rot-a	Stewart Island	rotula	a	9.72
Stl-2-rot-b	Stewart Island	rotula	b	9.60
Stl-2-rot-c	Stewart Island	rotula	c	9.12
Stl-2-epi-a	Stewart Island	epiphysis	a	9.15
Stl-2-epi-b	Stewart Island	epiphysis	b	10.22
Stl-2-epi-c	Stewart Island	epiphysis	c	9.41
Stl-2-demi-a	Stewart Island	demi-pyramid	a	9.06
Stl-2-demi-b	Stewart Island	demi-pyramid	b	9.56
Stl-2-demi-c	Stewart Island	demi-pyramid	c	9.79
Stl-2-plate-a	Stewart Island	test plate	a	8.70
Stl-2-plate-b	Stewart Island	test plate	b	9.36
Stl-2-plate-c	Stewart Island	test plate	c	8.93
Stl-5-spn-a	Stewart Island	spine	a	4.47
Stl-5-spn-b	Stewart Island	spine	b	6.21
Stl-5-spn-c	Stewart Island	spine	c	5.19
Stl-5-rot-a	Stewart Island	rotula	a	9.93
Stl-5-rot-b	Stewart Island	rotula	b	9.20
Stl-5-rot-c	Stewart Island	rotula	c	9.17
Stl-5-epi-a	Stewart Island	epiphysis	a	10.12
Stl-5-epi-b	Stewart Island	epiphysis	b	10.04
Stl-5-epi-c	Stewart Island	epiphysis	c	11.12
Stl-5-demi-a	Stewart Island	demi-pyramid	a	10.16
Stl-5-demi-b	Stewart Island	demi-pyramid	b	10.63
Stl-5-demi-c	Stewart Island	demi-pyramid	c	11.20
Stl-5-plate-a	Stewart Island	test plate	a	8.54
Stl-5-plate-b	Stewart Island	test plate	b	8.51
Stl-5-plate-c	Stewart Island	test plate	c	9.06
Frld-7-spn-a	Fiordland	spine	a	4.22
Frld-7-spn-b	Fiordland	spine	b	3.82
Frld-7-spn-c	Fiordland	spine	c	4.47
Frld-7-rot-a	Fiordland	rotula	a	8.58
Frld-7-rot-b	Fiordland	rotula	b	8.54
Frld-7-rot-c	Fiordland	rotula	c	8.25
Frld-7-epi-a	Fiordland	epiphysis	a	8.43

Sample ID	Location	Body Part	Replicate #	Wt% $MgCO_3$ in calcite
Frld-7-epi-b	Fiordland	epiphysis	b	9.89
Frld-7-epi-c	Fiordland	epiphysis	c	9.73
Frld-7-demi-a	Fiordland	demi-pyramid	a	10.40
Frld-7-demi-b	Fiordland	demi-pyramid	b	9.75
Frld-7-demi-c	Fiordland	demi-pyramid	c	9.21
Frld-7-plate-a	Fiordland	test plate	a	8.57
Frld-7-plate-b	Fiordland	test plate	b	10.52
Frld-7-plate-c	Fiordland	test plate	c	8.48
Frld-3-spn-a	Fiordland	spine	a	4.95
Frld-3-spn-b	Fiordland	spine	b	6.20
Frld-3-spn-c	Fiordland	spine	c	5.77
Frld-3-rot-a	Fiordland	rotula	a	8.78
Frld-3-rot-b	Fiordland	rotula	b	8.63
Frld-3-rot-c	Fiordland	rotula	c	8.84
Frld-3-epi-a	Fiordland	epiphysis	a	9.48
Frld-3-epi-b	Fiordland	epiphysis	b	9.01
Frld-3-epi-c	Fiordland	epiphysis	c	9.81
Frld-3-demi-a	Fiordland	demi-pyramid	a	10.24
Frld-3-demi-b	Fiordland	demi-pyramid	b	10.05
Frld-3-demi-c	Fiordland	demi-pyramid	c	9.53
Frld-3-plate-a	Fiordland	test plate	a	9.69
Frld-3-plate-b	Fiordland	test plate	b	10.16
Frld-3-plate-c	Fiordland	test plate	c	9.53
Frld-5-spn-a	Fiordland	spine	a	3.73
Frld-5-spn-b	Fiordland	spine	b	5.36
Frld-5-spn-c	Fiordland	spine	c	5.88
Frld-5-rot-a	Fiordland	rotula	a	10.84
Frld-5-rot-b	Fiordland	rotula	b	9.28
Frld-5-rot-c	Fiordland	rotula	c	9.61
Frld-5-epi-a	Fiordland	epiphysis	a	9.84
Frld-5-epi-b	Fiordland	epiphysis	b	9.64
Frld-5-epi-c	Fiordland	epiphysis	c	9.30
Frld-5-demi-a	Fiordland	demi-pyramid	a	10.01
Frld-5-demi-b	Fiordland	demi-pyramid	b	10.79
Frld-5-demi-c	Fiordland	demi-pyramid	c	11.25
Frld-5-plate-a	Fiordland	test plate	a	9.20
Frld-5-plate-b	Fiordland	test plate	b	10.32
Frld-5-plate-c	Fiordland	test plate	c	9.12
Pic-2-spn-a	Picton	spine	a	5.38
Pic-2-spn-b	Picton	spine	b	4.99
Pic-2-spn-c	Picton	spine	c	4.92
Pic-2-rot-a	Picton	rotula	a	8.65
Pic-2-rot-b	Picton	rotula	b	8.80
Pic-2-rot-c	Picton	rotula	c	9.33
Pic-2-epi-a	Picton	epiphysis	a	10.11
Pic-2-epi-b	Picton	epiphysis	b	10.31
Pic-2-epi-c	Picton	epiphysis	c	10.58
Pic-2-demi-a	Picton	demi-pyramid	a	8.55
Pic-2-demi-b	Picton	demi-pyramid	b	9.46
Pic-2-demi-c	Picton	demi-pyramid	c	9.69
Pic-2-plate-a	Picton	test plate	a	9.64
Pic-2-plate-b	Picton	test plate	b	8.90
Pic-2-plate-c	Picton	test plate	c	8.42
Pic-9-spn-a	Picton	spine	a	5.76
Pic-9-spn-b	Picton	spine	b	5.47
Pic-9-spn-c	Picton	spine	c	4.31
Pic-9-rot-a	Picton	rotula	a	8.69
Pic-9-rot-b	Picton	rotula	b	7.97
Pic-9-rot-c	Picton	rotula	c	9.13

Sample ID	Location	Body Part	Replicate #	Wt% $MgCO_3$ in calcite
Pic-9-epi-a	Picton	epiphysis	a	9.40
Pic-9-epi-b	Picton	epiphysis	b	9.85
Pic-9-epi-c	Picton	epiphysis	c	9.52
Pic-9-demi-a	Picton	demi-pyramid	a	9.10
Pic-9-demi-b	Picton	demi-pyramid	b	9.95
Pic-9-demi-c	Picton	demi-pyramid	c	9.00
Pic-9-plate-a	Picton	test plate	a	10.08
Pic-9-plate-b	Picton	test plate	b	9.88
Pic-9-plate-c	Picton	test plate	c	8.44
Pic-8-spn-a	Picton	spine	a	5.01
Pic-8-spn-b	Picton	spine	b	5.36
Pic-8-spn-c	Picton	spine	c	5.09
Pic-8-rot-a	Picton	rotula	a	9.54
Pic-8-rot-b	Picton	rotula	b	8.81
Pic-8-rot-c	Picton	rotula	c	8.59
Pic-8-epi-a	Picton	epiphysis	a	10.63
Pic-8-epi-b	Picton	epiphysis	b	10.42
Pic-8-epi-c	Picton	epiphysis	c	9.94
Pic-8-demi-a	Picton	demi-pyramid	a	9.76
Pic-8-demi-b	Picton	demi-pyramid	b	9.51
Pic-8-demi-c	Picton	demi-pyramid	c	10.07
Pic-8-plate-a	Picton	test plate	a	8.75
Pic-8-plate-b	Picton	test plate	b	9.79
Pic-8-plate-c	Picton	test plate	c	9.99
Akl-3-spn-a	Auckland	spine	a	3.81
Akl-3-spn-b	Auckland	spine	b	5.79
Akl-3-spn-c	Auckland	spine	c	4.87
Akl-3-rot-a	Auckland	rotula	a	9.51
Akl-3-rot-b	Auckland	rotula	b	8.12
Akl-3-rot-c	Auckland	rotula	c	8.61
Akl-3-epi-a	Auckland	epiphysis	a	9.52
Akl-3-epi-b	Auckland	epiphysis	b	10.34
Akl-3-epi-c	Auckland	epiphysis	c	9.92
Akl-3-demi-a	Auckland	demi-pyramid	a	9.53
Akl-3-demi-b	Auckland	demi-pyramid	b	9.40
Akl-3-demi-c	Auckland	demi-pyramid	c	10.01
Akl-3-plate-a	Auckland	test plate	a	11.05
Akl-3-plate-b	Auckland	test plate	b	9.04
Akl-3-plate-c	Auckland	test plate	c	9.23
Akl-4-spn-a	Auckland	spine	a	3.17
Akl-4-spn-b	Auckland	spine	b	6.08
Akl-4-spn-c	Auckland	spine	c	5.28
Akl-4-rot-a	Auckland	rotula	a	10.18
Akl-4-rot-b	Auckland	rotula	b	8.65
Akl-4-rot-c	Auckland	rotula	c	8.04
Akl-4-epi-a	Auckland	epiphysis	a	10.64
Akl-4-epi-b	Auckland	epiphysis	b	9.50
Akl-4-epi-c	Auckland	epiphysis	c	9.42
Akl-4-demi-a	Auckland	demi-pyramid	a	9.24
Akl-4-demi-b	Auckland	demi-pyramid	b	9.69
Akl-4-demi-c	Auckland	demi-pyramid	c	9.64
Akl-4-plate-a	Auckland	test plate	a	9.28
Akl-4-plate-b	Auckland	test plate	b	10.31
Akl-4-plate-c	Auckland	test plate	c	9.54
Akl-1-spn-a	Auckland	spine	a	3.27
Akl-1-spn-b	Auckland	spine	b	4.76
Akl-1-spn-c	Auckland	spine	c	3.50
Akl-1-rot-a	Auckland	rotula	a	7.99
Akl-1-rot-b	Auckland	rotula	b	10.03

Sample ID	Location	Body Part	Replicate #	Wt% $MgCO_3$ in calcite
Akl-1-rot-c	Auckland	rotula	c	8.87
Akl-1-epi-a	Auckland	epiphysis	a	8.90
Akl-1-epi-b	Auckland	epiphysis	b	9.15
Akl-1-epi-c	Auckland	epiphysis	c	9.53
Akl-1-demi-a	Auckland	demi-pyramid	a	9.26
Akl-1-demi-b	Auckland	demi-pyramid	b	9.10
Akl-1-demi-c	Auckland	demi-pyramid	c	11.24
Akl-1-plate-a	Auckland	test plate	a	10.93
Akl-1-plate-b	Auckland	test plate	b	10.45
Akl-1-plate-c	Auckland	test plate	c	9.06
Whl-8-spn-a	White Island	spine	a	31.68
Whl-8-spn-b	White Island	spine	b	31.68
Whl-8-spn-c	White Island	spine	c	31.69
Whl-8-rot-a	White Island	rotula	a	31.66
Whl-8-rot-b	White Island	rotula	b	31.59
Whl-8-rot-c	White Island	rotula	c	31.73
Whl-8-epi-a	White Island	epiphysis	a	31.70
Whl-8-epi-b	White Island	epiphysis	b	31.77
Whl-8-epi-c	White Island	epiphysis	c	31.72
Whl-8-demi-a	White Island	demi-pyramid	a	31.72
Whl-8-demi-b	White Island	demi-pyramid	b	31.73
Whl-8-demi-c	White Island	demi-pyramid	c	31.72
Whl-8-plate-a	White Island	test plate	a	31.77
Whl-8-plate-b	White Island	test plate	b	31.74
Whl-8-plate-c	White Island	test plate	c	31.64
Whl-4-spn-a	White Island	spine	a	31.60
Whl-4-spn-b	White Island	spine	b	31.67
Whl-4-spn-c	White Island	spine	c	31.72
Whl-4-rot-a	White Island	rotula	a	31.68
Whl-4-rot-b	White Island	rotula	b	31.53
Whl-4-rot-c	White Island	rotula	c	31.67
Whl-4-epi-a	White Island	epiphysis	a	31.76
Whl-4-epi-b	White Island	epiphysis	b	31.72
Whl-4-epi-c	White Island	epiphysis	c	31.74
Whl-4-demi-a	White Island	demi-pyramid	a	31.77
Whl-4-demi-b	White Island	demi-pyramid	b	31.70
Whl-4-demi-c	White Island	demi-pyramid	c	31.80
Whl-4-plate-a	White Island	test plate	a	31.54
Whl-4-plate-b	White Island	test plate	b	31.73
Whl-4-plate-c	White Island	test plate	c	31.66
Whl-5-spn-a	White Island	spine	a	31.67
Whl-5-spn-b	White Island	spine	b	31.72
Whl-5-spn-c	White Island	spine	c	31.70
Whl-5-rot-a	White Island	rotula	a	31.70
Whl-5-rot-b	White Island	rotula	b	31.71
Whl-5-rot-c	White Island	rotula	c	31.72
Whl-5-epi-a	White Island	epiphysis	a	31.62
Whl-5-epi-b	White Island	epiphysis	b	31.68
Whl-5-epi-c	White Island	epiphysis	c	31.67
Whl-5-demi-a	White Island	demi-pyramid	a	31.78
Whl-5-demi-b	White Island	demi-pyramid	b	31.77
Whl-5-demi-c	White Island	demi-pyramid	c	31.70
Whl-5-plate-a	White Island	test plate	a	31.67
Whl-5-plate-b	White Island	test plate	b	31.71
Whl-5-plate-c	White Island	test plate	c	31.73
Wlg-1-spn-a	Wellington	spine	a	5.45
Wlg-1-spn-b	Wellington	spine	b	6.86
Wlg-1-spn-c	Wellington	spine	c	3.63
Wlg-1-rot-a	Wellington	rotula	a	8.77

Sample ID	Location	Body Part	Replicate #	Wt% $MgCO_3$ in calcite
Wlg-1-rot-b	Wellington	rotula	b	9.93
Wlg-1-rot-c	Wellington	rotula	c	8.94
Wlg-1-epi-a	Wellington	epiphysis	a	9.93
Wlg-1-epi-b	Wellington	epiphysis	b	9.59
Wlg-1-epi-c	Wellington	epiphysis	c	9.62
Wlg-1-demi-a	Wellington	demi-pyramid	a	10.49
Wlg-1-demi-b	Wellington	demi-pyramid	b	10.64
Wlg-1-demi-c	Wellington	demi-pyramid	c	9.85
Wlg-1-plate-a	Wellington	test plate	a	9.37
Wlg-1-plate-b	Wellington	test plate	b	8.80
Wlg-1-plate-c	Wellington	test plate	c	9.71
Wlg-9-spn-a	Wellington	spine	a	4.85
Wlg-9-spn-b	Wellington	spine	b	4.60
Wlg-9-spn-c	Wellington	spine	c	3.93
Wlg-9-rot-a	Wellington	rotula	a	8.73
Wlg-9-rot-b	Wellington	rotula	b	8.46
Wlg-9-rot-c	Wellington	rotula	c	9.53
Wlg-9-epi-a	Wellington	epiphysis	a	9.86
Wlg-9-epi-b	Wellington	epiphysis	b	10.13
Wlg-9-epi-c	Wellington	epiphysis	c	9.75
Wlg-9-demi-a	Wellington	demi-pyramid	a	9.12
Wlg-9-demi-b	Wellington	demi-pyramid	b	10.36
Wlg-9-demi-c	Wellington	demi-pyramid	c	9.81
Wlg-9-plate-a	Wellington	test plate	a	8.53
Wlg-9-plate-b	Wellington	test plate	b	9.50
Wlg-9-plate-c	Wellington	test plate	c	9.26
Wlg-3-spn-a	Wellington	spine	a	4.56
Wlg-3-spn-b	Wellington	spine	b	5.70
Wlg-3-spn-c	Wellington	spine	c	4.34
Wlg-3-rot-a	Wellington	rotula	a	9.07
Wlg-3-rot-b	Wellington	rotula	b	9.02
Wlg-3-rot-c	Wellington	rotula	c	9.43
Wlg-3-epi-a	Wellington	epiphysis	a	10.29
Wlg-3-epi-b	Wellington	epiphysis	b	10.57
Wlg-3-epi-c	Wellington	epiphysis	c	8.94
Wlg-3-demi-a	Wellington	demi-pyramid	a	7.73
Wlg-3-demi-b	Wellington	demi-pyramid	b	10.46
Wlg-3-demi-c	Wellington	demi-pyramid	c	9.17
Wlg-3-plate-a	Wellington	test plate	a	9.43
Wlg-3-plate-b	Wellington	test plate	b	9.03
Wlg-3-plate-c	Wellington	test plate	c	8.90

Appendix D Raw Data for Spine Strength

Table 7.9 Raw data for spine strength of *Evechinus chloroticus* collected around New Zealand

Sample	Location	Spine length (mm)	Flexural strength (Mpa)	Strength:Length (Mpa:mm)
EvChl-StI-1	Stewart Island	23.65	79.43	3.36
EvChl-StI-1	Stewart Island	25.26	77.81	3.08
EvChl-StI-1	Stewart Island	24.02	87.72	3.65
EvChl-StI-1	Stewart Island	24.49	75.33	3.08
EvChl-StI-1	Stewart Island	23.54	123.44	5.24
EvChl-StI-1	Stewart Island	23.78	93.77	3.94
EvChl-StI-1	Stewart Island	25.95	63.72	2.46
EvChl-StI-1	Stewart Island	23.94	88.47	3.70
EvChl-StI-1	Stewart Island	23.29	110.72	4.75
EvChl-StI-1	Stewart Island	23.10	86.94	3.76
EvChl-StI-2	Stewart Island	24.07	108.21	4.50
EvChl-StI-2	Stewart Island	27.22	103.23	3.79
EvChl-StI-2	Stewart Island	25.03	87.38	3.49
EvChl-StI-2	Stewart Island	24.18	90.71	3.75
EvChl-StI-2	Stewart Island	24.08	88.29	3.67
EvChl-StI-2	Stewart Island	24.76	100.51	4.06
EvChl-StI-2	Stewart Island	24.34	102.66	4.22
EvChl-StI-2	Stewart Island	23.69	108.11	4.56
EvChl-StI-2	Stewart Island	25.30	89.93	3.55
EvChl-StI-2	Stewart Island	25.12	98.31	3.91
EvChl-StI-3	Stewart Island	27.97	84.12	3.01
EvChl-StI-3	Stewart Island	24.93	103.73	4.16
EvChl-StI-3	Stewart Island	25.99	80.10	3.08
EvChl-StI-3	Stewart Island	22.86	79.14	3.46
EvChl-StI-3	Stewart Island	24.68	72.43	2.93
EvChl-StI-3	Stewart Island	27.17	84.55	3.11
EvChl-StI-3	Stewart Island	26.22	77.73	2.96
EvChl-StI-3	Stewart Island	26.44	80.34	3.04
EvChl-StI-3	Stewart Island	26.02	98.61	3.79
EvChl-StI-3	Stewart Island	24.65	87.72	3.56
EvChl-StI-4	Stewart Island	26.35	102.71	3.90
EvChl-StI-4	Stewart Island	27.32	91.66	3.36
EvChl-StI-4	Stewart Island	26.54	100.33	3.78
EvChl-StI-4	Stewart Island	27.20	84.70	3.11
EvChl-StI-4	Stewart Island	24.46	97.59	3.99
EvChl-StI-4	Stewart Island	26.16	100.02	3.82
EvChl-StI-4	Stewart Island	25.73	81.19	3.16
EvChl-StI-4	Stewart Island	22.97	96.76	4.21
EvChl-StI-4	Stewart Island	22.71	92.83	4.09
EvChl-StI-4	Stewart Island	26.66	96.31	3.61
EvChl-StI-5	Stewart Island	23.46	66.33	2.83
EvChl-StI-5	Stewart Island	25.88	92.29	3.57
EvChl-StI-5	Stewart Island	25.73	88.09	3.42
EvChl-StI-5	Stewart Island	25.29	95.15	3.76
EvChl-StI-5	Stewart Island	23.45	71.64	3.06
EvChl-StI-5	Stewart Island	23.20	78.45	3.38
EvChl-StI-5	Stewart Island	25.81	68.38	2.65
EvChl-StI-5	Stewart Island	24.74	78.31	3.17
EvChl-StI-5	Stewart Island	25.17	78.26	3.11
EvChl-StI-5	Stewart Island	22.96	82.18	3.58

Sample	Location	Spine length (mm)	Flexural strength (Mpa)	Strength:Length (Mpa:mm)
EvChl-StI-6	Stewart Island	21.83	103.23	4.73
EvChl-StI-6	Stewart Island	21.11	85.68	4.06
EvChl-StI-6	Stewart Island	22.76	88.61	3.89
EvChl-StI-6	Stewart Island	22.96	82.44	3.59
EvChl-StI-6	Stewart Island	24.28	100.54	4.14
EvChl-StI-6	Stewart Island	23.68	86.52	3.65
EvChl-StI-6	Stewart Island	19.89	83.43	4.19
EvChl-StI-6	Stewart Island	25.44	100.15	3.94
EvChl-StI-6	Stewart Island	21.57	102.08	4.73
EvChl-StI-6	Stewart Island	21.22	83.11	3.92
EvChl-StI-7	Stewart Island	23.74	98.82	4.16
EvChl-StI-7	Stewart Island	26.10	90.45	3.47
EvChl-StI-7	Stewart Island	27.22	86.54	3.18
EvChl-StI-7	Stewart Island	27.94	88.10	3.15
EvChl-StI-7	Stewart Island	27.53	98.12	3.56
EvChl-StI-7	Stewart Island	29.68	102.50	3.45
EvChl-StI-7	Stewart Island	28.22	95.61	3.39
EvChl-StI-7	Stewart Island	27.19	69.14	2.54
EvChl-StI-7	Stewart Island	27.93	80.01	2.86
EvChl-StI-7	Stewart Island	28.81	93.44	3.24
EvChl-StI-8	Stewart Island	24.80	79.37	3.20
EvChl-StI-8	Stewart Island	23.90	81.40	3.41
EvChl-StI-8	Stewart Island	23.12	111.11	4.81
EvChl-StI-8	Stewart Island	25.14	75.18	2.99
EvChl-StI-8	Stewart Island	25.51	106.57	4.18
EvChl-StI-8	Stewart Island	25.16	114.84	4.56
EvChl-StI-8	Stewart Island	24.29	97.74	4.02
EvChl-StI-8	Stewart Island	24.54	83.93	3.42
EvChl-StI-8	Stewart Island	25.19	81.36	3.23
EvChl-StI-8	Stewart Island	23.12	160.23	6.93
EvChl-StI-9	Stewart Island	27.28	91.37	3.35
EvChl-StI-9	Stewart Island	28.31	97.68	3.45
EvChl-StI-9	Stewart Island	30.55	99.32	3.25
EvChl-StI-9	Stewart Island	28.88	88.19	3.05
EvChl-StI-9	Stewart Island	29.15	91.92	3.15
EvChl-StI-9	Stewart Island	29.10	107.28	3.69
EvChl-StI-9	Stewart Island	29.68	93.82	3.16
EvChl-StI-9	Stewart Island	29.14	93.24	3.20
EvChl-StI-9	Stewart Island	28.93	102.29	3.54
EvChl-StI-9	Stewart Island	28.28	81.36	2.88
EvChl-StI-10	Stewart Island	22.95	116.28	5.07
EvChl-StI-10	Stewart Island	22.79	105.75	4.64
EvChl-StI-10	Stewart Island	24.69	104.02	4.21
EvChl-StI-10	Stewart Island	23.80	101.52	4.27
EvChl-StI-10	Stewart Island	26.81	86.29	3.22
EvChl-StI-10	Stewart Island	25.12	85.76	3.41
EvChl-StI-10	Stewart Island	24.25	81.39	3.36
EvChl-StI-10	Stewart Island	24.00	105.36	4.39
EvChl-StI-10	Stewart Island	25.53	77.06	3.02
EvChl-StI-10	Stewart Island	23.30	76.06	3.26
EvChl-Frld-1	Fiordland	25.36	66.77	2.63
EvChl-Frld-1	Fiordland	29.47	61.02	2.07
EvChl-Frld-1	Fiordland	26.83	61.40	2.29
EvChl-Frld-1	Fiordland	24.25	66.44	2.74
EvChl-Frld-1	Fiordland	26.53	58.97	2.22

Sample	Location	Spine length (mm)	Flexural strength (Mpa)	Strength:Length (Mpa:mm)
EvChl-Frld-1	Fiordland	24.86	43.91	1.77
EvChl-Frld-1	Fiordland	26.49	50.31	1.90
EvChl-Frld-1	Fiordland	26.59	63.60	2.39
EvChl-Frld-1	Fiordland	24.73	52.34	2.12
EvChl-Frld-1	Fiordland	22.43	53.13	2.37
EvChl-Frld-2	Fiordland	33.89	85.31	2.52
EvChl-Frld-2	Fiordland	31.61	85.91	2.72
EvChl-Frld-2	Fiordland	33.05	81.75	2.47
EvChl-Frld-2	Fiordland	36.10	53.67	1.49
EvChl-Frld-2	Fiordland	34.39	63.25	1.84
EvChl-Frld-2	Fiordland	35.45	47.54	1.34
EvChl-Frld-2	Fiordland	32.91	70.72	2.15
EvChl-Frld-2	Fiordland	34.64	46.92	1.35
EvChl-Frld-2	Fiordland	34.18	68.22	2.00
EvChl-Frld-2	Fiordland	33.38	65.47	1.96
EvChl-Frld-3	Fiordland	35.10	81.65	2.33
EvChl-Frld-3	Fiordland	33.49	74.02	2.21
EvChl-Frld-3	Fiordland	33.20	49.49	1.49
EvChl-Frld-3	Fiordland	35.02	44.15	1.26
EvChl-Frld-3	Fiordland	33.43	68.49	2.05
EvChl-Frld-3	Fiordland	33.69	27.03	0.80
EvChl-Frld-3	Fiordland	36.36	27.43	0.75
EvChl-Frld-3	Fiordland	32.18	42.65	1.33
EvChl-Frld-3	Fiordland	34.20	64.57	1.89
EvChl-Frld-3	Fiordland	31.98	79.80	2.50
EvChl-Frld-4	Fiordland	27.20	59.27	2.18
EvChl-Frld-4	Fiordland	26.63	47.61	1.79
EvChl-Frld-4	Fiordland	27.79	71.23	2.56
EvChl-Frld-4	Fiordland	28.84	67.68	2.35
EvChl-Frld-4	Fiordland	28.60	89.15	3.12
EvChl-Frld-4	Fiordland	26.02	60.91	2.34
EvChl-Frld-4	Fiordland	28.93	44.99	1.56
EvChl-Frld-4	Fiordland	29.03	63.01	2.17
EvChl-Frld-4	Fiordland	28.99	71.41	2.46
EvChl-Frld-4	Fiordland	28.33	77.21	2.73
EvChl-Frld-5	Fiordland	30.55	65.94	2.16
EvChl-Frld-5	Fiordland	34.74	69.70	2.01
EvChl-Frld-5	Fiordland	28.98	64.24	2.22
EvChl-Frld-5	Fiordland	30.59	50.20	1.64
EvChl-Frld-5	Fiordland	32.81	51.68	1.58
EvChl-Frld-5	Fiordland	28.08	55.99	1.99
EvChl-Frld-5	Fiordland	27.91	57.06	2.04
EvChl-Frld-5	Fiordland	33.04	63.39	1.92
EvChl-Frld-5	Fiordland	31.69	66.32	2.09
EvChl-Frld-5	Fiordland	32.01	53.78	1.68
EvChl-Frld-6	Fiordland	28.18	56.12	1.99
EvChl-Frld-6	Fiordland	32.48	52.52	1.62
EvChl-Frld-6	Fiordland	30.58	62.04	2.03
EvChl-Frld-6	Fiordland	31.70	77.64	2.45
EvChl-Frld-6	Fiordland	27.73	44.59	1.61
EvChl-Frld-6	Fiordland	34.10	62.22	1.82
EvChl-Frld-6	Fiordland	32.29	64.39	1.99
EvChl-Frld-6	Fiordland	30.84	48.09	1.56
EvChl-Frld-6	Fiordland	29.66	69.66	2.35
EvChl-Frld-6	Fiordland	29.00	47.54	1.64

Sample	Location	Spine length (mm)	Flexural strength (Mpa)	Strength:Length (Mpa:mm)
EvChl-Frld-7	Fiordland	33.30	47.54	1.43
EvChl-Frld-7	Fiordland	31.70	82.78	2.61
EvChl-Frld-7	Fiordland	34.07	50.62	1.49
EvChl-Frld-7	Fiordland	31.05	76.03	2.45
EvChl-Frld-7	Fiordland	31.83	59.47	1.87
EvChl-Frld-7	Fiordland	32.36	67.97	2.10
EvChl-Frld-7	Fiordland	31.61	49.93	1.58
EvChl-Frld-7	Fiordland	30.84	77.72	2.52
EvChl-Frld-7	Fiordland	32.30	56.94	1.76
EvChl-Frld-7	Fiordland	30.25	54.25	1.79
EvChl-Frld-8	Fiordland	32.73	63.27	1.93
EvChl-Frld-8	Fiordland	32.14	63.73	1.98
EvChl-Frld-8	Fiordland	29.98	59.27	1.98
EvChl-Frld-8	Fiordland	28.80	40.15	1.39
EvChl-Frld-8	Fiordland	31.78	59.28	1.87
EvChl-Frld-8	Fiordland	31.72	69.93	2.20
EvChl-Frld-8	Fiordland	31.56	74.68	2.37
EvChl-Frld-8	Fiordland	31.70	48.03	1.52
EvChl-Frld-8	Fiordland	32.94	66.57	2.02
EvChl-Frld-8	Fiordland	31.07	54.20	1.74
EvChl-Frld-9	Fiordland	30.09	55.99	1.86
EvChl-Frld-9	Fiordland	30.35	47.84	1.58
EvChl-Frld-9	Fiordland	33.61	46.09	1.37
EvChl-Frld-9	Fiordland	33.04	57.31	1.73
EvChl-Frld-9	Fiordland	29.26	70.85	2.42
EvChl-Frld-9	Fiordland	30.06	58.47	1.95
EvChl-Frld-9	Fiordland	33.99	52.10	1.53
EvChl-Frld-9	Fiordland	33.62	56.69	1.69
EvChl-Frld-9	Fiordland	33.24	63.36	1.91
EvChl-Frld-9	Fiordland	35.00	66.25	1.89
EvChl-Frld-10	Fiordland	27.18	56.61	2.08
EvChl-Frld-10	Fiordland	29.37	50.44	1.72
EvChl-Frld-10	Fiordland	26.79	75.94	2.83
EvChl-Frld-10	Fiordland	25.98	61.00	2.35
EvChl-Frld-10	Fiordland	25.32	62.57	2.47
EvChl-Frld-10	Fiordland	28.11	72.22	2.57
EvChl-Frld-10	Fiordland	27.98	63.26	2.26
EvChl-Frld-10	Fiordland	26.77	53.56	2.00
EvChl-Frld-10	Fiordland	24.90	49.18	1.98
EvChl-Frld-10	Fiordland	27.04	53.55	1.98
EvChl-Pic-1	Picton	22.51	113.19	5.03
EvChl-Pic-1	Picton	22.86	103.90	4.55
EvChl-Pic-1	Picton	23.59	99.52	4.22
EvChl-Pic-1	Picton	20.83	115.57	5.55
EvChl-Pic-1	Picton	20.71	139.43	6.73
EvChl-Pic-1	Picton	21.77	117.92	5.42
EvChl-Pic-1	Picton	21.03	119.25	5.67
EvChl-Pic-1	Picton	20.50	105.47	5.14
EvChl-Pic-1	Picton	22.15	118.18	5.34
EvChl-Pic-1	Picton	22.30	91.31	4.09
EvChl-Pic-2	Picton	21.04	122.57	5.83
EvChl-Pic-2	Picton	20.19	102.47	5.08
EvChl-Pic-2	Picton	21.94	120.34	5.49
EvChl-Pic-2	Picton	22.03	113.71	5.16
EvChl-Pic-2	Picton	20.83	92.22	4.43

Sample	Location	Spine length (mm)	Flexural strength (Mpa)	Strength:Length (Mpa:mm)
EvChl-Pic-2	Picton	22.31	141.83	6.36
EvChl-Pic-2	Picton	20.63	137.45	6.66
EvChl-Pic-2	Picton	21.07	73.60	3.49
EvChl-Pic-2	Picton	20.94	142.53	6.81
EvChl-Pic-2	Picton	21.68	88.71	4.09
EvChl-Pic-3	Picton	22.92	92.89	4.05
EvChl-Pic-3	Picton	22.12	97.39	4.40
EvChl-Pic-3	Picton	20.01	91.62	4.58
EvChl-Pic-3	Picton	22.82	109.17	4.78
EvChl-Pic-3	Picton	20.36	107.23	5.27
EvChl-Pic-3	Picton	22.68	110.98	4.89
EvChl-Pic-3	Picton	22.13	101.98	4.61
EvChl-Pic-3	Picton	22.49	125.04	5.56
EvChl-Pic-3	Picton	19.34	167.56	8.66
EvChl-Pic-3	Picton	21.90	103.33	4.72
EvChl-Pic-4	Picton	21.93	94.29	4.30
EvChl-Pic-4	Picton	19.91	108.50	5.45
EvChl-Pic-4	Picton	18.53	117.87	6.36
EvChl-Pic-4	Picton	20.81	121.40	5.83
EvChl-Pic-4	Picton	20.79	106.90	5.14
EvChl-Pic-4	Picton	21.42	119.12	5.56
EvChl-Pic-4	Picton	18.50	103.48	5.59
EvChl-Pic-4	Picton	20.75	128.12	6.17
EvChl-Pic-4	Picton	19.11	101.78	5.33
EvChl-Pic-4	Picton	19.02	129.59	6.81
EvChl-Pic-5	Picton	21.56	115.13	5.34
EvChl-Pic-5	Picton	21.75	110.26	5.07
EvChl-Pic-5	Picton	21.83	91.77	4.20
EvChl-Pic-5	Picton	22.08	125.55	5.69
EvChl-Pic-5	Picton	20.48	118.08	5.77
EvChl-Pic-5	Picton	19.93	102.00	5.12
EvChl-Pic-5	Picton	22.68	92.57	4.08
EvChl-Pic-5	Picton	18.17	112.57	6.20
EvChl-Pic-5	Picton	19.09	104.75	5.49
EvChl-Pic-5	Picton	17.78	90.54	5.09
EvChl-Pic-6	Picton	22.41	98.91	4.41
EvChl-Pic-6	Picton	21.60	106.46	4.93
EvChl-Pic-6	Picton	20.52	110.69	5.39
EvChl-Pic-6	Picton	22.74	96.34	4.24
EvChl-Pic-6	Picton	22.54	94.37	4.19
EvChl-Pic-6	Picton	20.14	111.20	5.52
EvChl-Pic-6	Picton	20.69	114.10	5.51
EvChl-Pic-6	Picton	22.39	107.22	4.79
EvChl-Pic-6	Picton	21.48	112.74	5.25
EvChl-Pic-6	Picton	20.19	119.81	5.93
EvChl-Pic-7	Picton	23.17	87.29	3.77
EvChl-Pic-7	Picton	22.12	114.66	5.18
EvChl-Pic-7	Picton	20.98	88.15	4.20
EvChl-Pic-7	Picton	19.30	132.79	6.88
EvChl-Pic-7	Picton	20.16	112.68	5.59
EvChl-Pic-7	Picton	20.57	112.99	5.49
EvChl-Pic-7	Picton	22.63	124.84	5.52
EvChl-Pic-7	Picton	20.36	125.33	6.16
EvChl-Pic-7	Picton	19.24	94.28	4.90
EvChl-Pic-7	Picton	21.52	126.96	5.90

Sample	Location	Spine length (mm)	Flexural strength (Mpa)	Strength:Length (Mpa:mm)
EvChl-Pic-8	Picton	23.52	87.87	3.74
EvChl-Pic-8	Picton	22.38	110.72	4.95
EvChl-Pic-8	Picton	22.36	160.51	7.18
EvChl-Pic-8	Picton	23.27	106.00	4.56
EvChl-Pic-8	Picton	22.47	101.97	4.54
EvChl-Pic-8	Picton	22.54	106.99	4.75
EvChl-Pic-8	Picton	21.67	92.33	4.26
EvChl-Pic-8	Picton	20.20	93.40	4.62
EvChl-Pic-8	Picton	21.30	126.10	5.92
EvChl-Pic-8	Picton	21.01	132.71	6.32
EvChl-Pic-9	Picton	24.98	136.25	5.45
EvChl-Pic-9	Picton	23.62	115.18	4.88
EvChl-Pic-9	Picton	20.50	154.84	7.55
EvChl-Pic-9	Picton	21.00	86.10	4.10
EvChl-Pic-9	Picton	21.06	75.86	3.60
EvChl-Pic-9	Picton	22.71	81.41	3.58
EvChl-Pic-9	Picton	21.18	114.61	5.41
EvChl-Pic-9	Picton	19.92	97.77	4.91
EvChl-Pic-9	Picton	23.76	89.12	3.75
EvChl-Pic-9	Picton	21.01	101.01	4.81
EvChl-Pic-10	Picton	20.88	107.30	5.14
EvChl-Pic-10	Picton	21.66	100.25	4.63
EvChl-Pic-10	Picton	22.21	96.98	4.37
EvChl-Pic-10	Picton	20.56	98.38	4.79
EvChl-Pic-10	Picton	20.55	118.49	5.77
EvChl-Pic-10	Picton	21.11	116.23	5.51
EvChl-Pic-10	Picton	20.83	115.29	5.53
EvChl-Pic-10	Picton	21.74	105.87	4.87
EvChl-Pic-10	Picton	19.47	96.13	4.94
EvChl-Pic-10	Picton	20.09	109.81	5.47
EvChl-Akl-1	Auckland	17.66	170.41	9.65
EvChl-Akl-1	Auckland	19.41	144.23	7.43
EvChl-Akl-1	Auckland	19.69	152.21	7.73
EvChl-Akl-1	Auckland	18.70	134.36	7.18
EvChl-Akl-1	Auckland	17.43	114.94	6.59
EvChl-Akl-1	Auckland	18.89	87.35	4.62
EvChl-Akl-1	Auckland	17.02	180.49	10.60
EvChl-Akl-1	Auckland	18.07	192.29	10.64
EvChl-Akl-1	Auckland	17.43	138.74	7.96
EvChl-Akl-1	Auckland	17.10	183.84	10.75
EvChl-Akl-2	Auckland	19.41	159.38	8.21
EvChl-Akl-2	Auckland	18.24	122.50	6.72
EvChl-Akl-2	Auckland	16.55	137.92	8.33
EvChl-Akl-2	Auckland	18.95	126.50	6.68
EvChl-Akl-2	Auckland	16.62	127.24	7.66
EvChl-Akl-2	Auckland	18.31	108.80	5.94
EvChl-Akl-2	Auckland	17.42	151.27	8.68
EvChl-Akl-2	Auckland	16.51	119.67	7.25
EvChl-Akl-2	Auckland	17.28	186.68	10.80
EvChl-Akl-2	Auckland	16.58	121.43	7.32
EvChl-Akl-3	Auckland	18.68	116.81	6.25
EvChl-Akl-3	Auckland	18.52	109.77	5.93
EvChl-Akl-3	Auckland	19.57	81.00	4.14
EvChl-Akl-3	Auckland	18.22	132.16	7.25
EvChl-Akl-3	Auckland	18.24	118.62	6.50

Sample	Location	Spine length (mm)	Flexural strength (Mpa)	Strength:Length (Mpa:mm)
EvChl-Akl-3	Auckland	17.25	137.93	8.00
EvChl-Akl-3	Auckland	18.03	103.10	5.72
EvChl-Akl-3	Auckland	18.68	199.85	10.70
EvChl-Akl-3	Auckland	18.23	139.97	7.68
EvChl-Akl-3	Auckland	18.22	108.59	5.96
EvChl-Akl-4	Auckland	17.41	122.41	7.03
EvChl-Akl-4	Auckland	18.87	153.12	8.11
EvChl-Akl-4	Auckland	21.00	132.11	6.29
EvChl-Akl-4	Auckland	19.14	118.26	6.18
EvChl-Akl-4	Auckland	18.39	124.90	6.79
EvChl-Akl-4	Auckland	18.94	141.73	7.48
EvChl-Akl-4	Auckland	17.74	159.89	9.01
EvChl-Akl-4	Auckland	18.64	140.30	7.53
EvChl-Akl-4	Auckland	17.90	147.45	8.24
EvChl-Akl-4	Auckland	17.48	148.09	8.47
EvChl-Akl-5	Auckland	18.61	127.44	6.85
EvChl-Akl-5	Auckland	17.95	119.14	6.64
EvChl-Akl-5	Auckland	17.17	142.28	8.29
EvChl-Akl-5	Auckland	18.07	102.46	5.67
EvChl-Akl-5	Auckland	16.80	100.59	5.99
EvChl-Akl-5	Auckland	17.80	124.04	6.97
EvChl-Akl-5	Auckland	15.75	148.20	9.41
EvChl-Akl-5	Auckland	15.99	120.50	7.54
EvChl-Akl-5	Auckland	16.68	178.32	10.69
EvChl-Akl-5	Auckland	16.17	157.28	9.73
EvChl-Akl-6	Auckland	19.34	148.83	7.70
EvChl-Akl-6	Auckland	18.16	148.24	8.16
EvChl-Akl-6	Auckland	17.66	127.50	7.22
EvChl-Akl-6	Auckland	18.67	136.11	7.29
EvChl-Akl-6	Auckland	18.52	118.69	6.41
EvChl-Akl-6	Auckland	18.58	117.75	6.34
EvChl-Akl-6	Auckland	18.13	154.07	8.50
EvChl-Akl-6	Auckland	20.27	124.78	6.16
EvChl-Akl-6	Auckland	20.66	140.95	6.82
EvChl-Akl-6	Auckland	17.44	163.01	9.35
EvChl-Akl-7	Auckland	19.95	102.91	5.16
EvChl-Akl-7	Auckland	16.95	161.50	9.53
EvChl-Akl-7	Auckland	17.90	158.25	8.84
EvChl-Akl-7	Auckland	17.63	157.43	8.93
EvChl-Akl-7	Auckland	15.97	128.56	8.05
EvChl-Akl-7	Auckland	17.19	176.53	10.27
EvChl-Akl-7	Auckland	17.20	140.26	8.15
EvChl-Akl-7	Auckland	15.97	113.18	7.09
EvChl-Akl-7	Auckland	16.60	108.85	6.56
EvChl-Akl-7	Auckland	15.72	135.03	8.59
EvChl-Akl-8	Auckland	19.11	124.15	6.50
EvChl-Akl-8	Auckland	18.11	127.88	7.06
EvChl-Akl-8	Auckland	18.68	150.87	8.08
EvChl-Akl-8	Auckland	17.88	155.09	8.67
EvChl-Akl-8	Auckland	17.86	110.99	6.21
EvChl-Akl-8	Auckland	16.91	119.29	7.05
EvChl-Akl-8	Auckland	17.06	133.97	7.85
EvChl-Akl-8	Auckland	17.03	133.28	7.83
EvChl-Akl-8	Auckland	16.66	146.28	8.78
EvChl-Akl-8	Auckland	16.12	130.36	8.09

Sample	Location	Spine length (mm)	Flexural strength (Mpa)	Strength:Length (Mpa:mm)
EvChl-Akl-9	Auckland	19.19	136.65	7.12
EvChl-Akl-9	Auckland	18.30	130.84	7.15
EvChl-Akl-9	Auckland	17.64	119.98	6.80
EvChl-Akl-9	Auckland	19.48	124.16	6.37
EvChl-Akl-9	Auckland	17.64	118.22	6.70
EvChl-Akl-9	Auckland	19.68	146.22	7.43
EvChl-Akl-9	Auckland	17.62	108.59	6.16
EvChl-Akl-9	Auckland	18.32	130.65	7.13
EvChl-Akl-9	Auckland	18.08	162.14	8.97
EvChl-Akl-9	Auckland	17.12	126.06	7.36
EvChl-Akl-10	Auckland	18.18	116.79	6.42
EvChl-Akl-10	Auckland	18.79	147.32	7.84
EvChl-Akl-10	Auckland	18.26	146.94	8.05
EvChl-Akl-10	Auckland	17.69	134.72	7.62
EvChl-Akl-10	Auckland	16.20	146.66	9.05
EvChl-Akl-10	Auckland	17.49	130.24	7.45
EvChl-Akl-10	Auckland	17.91	126.51	7.06
EvChl-Akl-10	Auckland	16.18	157.63	9.74
EvChl-Akl-10	Auckland	16.24	119.49	7.36
EvChl-Akl-10	Auckland	16.34	164.57	10.07
EvChl-Whl-1	White Island	18.63	154.24	8.28
EvChl-Whl-1	White Island	20.33	150.53	7.40
EvChl-Whl-1	White Island	20.14	158.86	7.89
EvChl-Whl-1	White Island	19.45	140.87	7.24
EvChl-Whl-1	White Island	18.72	167.78	8.96
EvChl-Whl-1	White Island	18.74	152.82	8.15
EvChl-Whl-1	White Island	18.65	144.73	7.76
EvChl-Whl-1	White Island	19.27	149.81	7.77
EvChl-Whl-1	White Island	20.57	173.34	8.43
EvChl-Whl-1	White Island	16.50	157.62	9.55
EvChl-Whl-2	White Island	16.36	153.71	9.40
EvChl-Whl-2	White Island	17.23	144.21	8.37
EvChl-Whl-2	White Island	17.48	167.88	9.60
EvChl-Whl-2	White Island	17.98	180.17	10.02
EvChl-Whl-2	White Island	17.85	168.09	9.42
EvChl-Whl-2	White Island	17.65	162.22	9.19
EvChl-Whl-2	White Island	15.51	166.40	10.73
EvChl-Whl-2	White Island	16.02	188.63	11.77
EvChl-Whl-2	White Island	15.79	166.40	10.54
EvChl-Whl-2	White Island	14.92	199.38	13.36
EvChl-Whl-3	White Island	16.85	160.79	9.54
EvChl-Whl-3	White Island	16.95	194.18	11.46
EvChl-Whl-3	White Island	16.17	161.96	10.02
EvChl-Whl-3	White Island	17.30	152.97	8.84
EvChl-Whl-3	White Island	17.78	193.20	10.87
EvChl-Whl-3	White Island	17.03	167.08	9.81
EvChl-Whl-3	White Island	16.83	245.20	14.57
EvChl-Whl-3	White Island	18.67	192.20	10.29
EvChl-Whl-3	White Island	17.78	121.01	6.81
EvChl-Whl-3	White Island	16.00	177.79	11.11
EvChl-Whl-4	White Island	16.87	168.17	9.97
EvChl-Whl-4	White Island	17.75	172.86	9.74
EvChl-Whl-4	White Island	18.24	152.94	8.39
EvChl-Whl-4	White Island	16.51	184.89	11.20
EvChl-Whl-4	White Island	16.60	154.43	9.30

Sample	Location	Spine length (mm)	Flexural strength (Mpa)	Strength:Length (Mpa:mm)
EvChl-Whl-4	White Island	17.10	167.73	9.81
EvChl-Whl-4	White Island	14.80	161.58	10.92
EvChl-Whl-4	White Island	15.83	170.79	10.79
EvChl-Whl-4	White Island	15.27	178.39	11.68
EvChl-Whl-4	White Island	14.52	177.00	12.19
EvChl-Whl-5	White Island	17.02	171.12	10.05
EvChl-Whl-5	White Island	17.76	154.29	8.69
EvChl-Whl-5	White Island	18.29	180.94	9.89
EvChl-Whl-5	White Island	16.73	175.62	10.50
EvChl-Whl-5	White Island	16.68	165.47	9.92
EvChl-Whl-5	White Island	18.15	157.27	8.66
EvChl-Whl-5	White Island	16.03	188.06	11.73
EvChl-Whl-5	White Island	16.31	175.84	10.78
EvChl-Whl-5	White Island	17.55	198.32	11.30
EvChl-Whl-5	White Island	16.12	173.79	10.78
EvChl-Whl-6	White Island	18.09	157.58	8.71
EvChl-Whl-6	White Island	19.01	166.05	8.73
EvChl-Whl-6	White Island	19.69	176.05	8.94
EvChl-Whl-6	White Island	17.19	216.51	12.60
EvChl-Whl-6	White Island	18.50	163.65	8.85
EvChl-Whl-6	White Island	18.13	186.82	10.30
EvChl-Whl-6	White Island	17.32	173.56	10.02
EvChl-Whl-6	White Island	18.71	184.12	9.84
EvChl-Whl-6	White Island	16.81	191.88	11.41
EvChl-Whl-6	White Island	16.64	169.25	10.17
EvChl-Whl-7	White Island	15.62	169.60	10.86
EvChl-Whl-7	White Island	15.67	161.36	10.30
EvChl-Whl-7	White Island	14.67	167.89	11.44
EvChl-Whl-7	White Island	14.56	192.38	13.21
EvChl-Whl-7	White Island	15.31	178.99	11.69
EvChl-Whl-7	White Island	16.30	143.55	8.81
EvChl-Whl-7	White Island	15.32	141.92	9.26
EvChl-Whl-7	White Island	16.12	190.54	11.82
EvChl-Whl-7	White Island	15.08	160.42	10.64
EvChl-Whl-7	White Island	14.72	162.59	11.05
EvChl-Whl-8	White Island	19.05	166.32	8.73
EvChl-Whl-8	White Island	18.05	170.48	9.44
EvChl-Whl-8	White Island	17.95	168.64	9.39
EvChl-Whl-8	White Island	19.03	160.40	8.43
EvChl-Whl-8	White Island	18.35	164.21	8.95
EvChl-Whl-8	White Island	17.46	183.81	10.53
EvChl-Whl-8	White Island	17.20	154.62	8.99
EvChl-Whl-8	White Island	18.20	155.64	8.55
EvChl-Whl-8	White Island	20.41	141.92	6.95
EvChl-Whl-8	White Island	17.25	141.52	8.20
EvChl-Whl-9	White Island	16.22	151.63	9.35
EvChl-Whl-9	White Island	18.33	135.94	7.42
EvChl-Whl-9	White Island	18.52	184.66	9.97
EvChl-Whl-9	White Island	17.63	190.33	10.80
EvChl-Whl-9	White Island	17.28	156.41	9.05
EvChl-Whl-9	White Island	16.21	148.58	9.17
EvChl-Whl-9	White Island	16.81	169.45	10.08
EvChl-Whl-9	White Island	18.44	152.66	8.28
EvChl-Whl-9	White Island	16.96	182.52	10.76
EvChl-Whl-9	White Island	16.93	160.04	9.45

Sample	Location	Spine length (mm)	Flexural strength (Mpa)	Strength:Length (Mpa:mm)
EvChl-WhI-10	White Island	15.16	160.73	10.60
EvChl-WhI-10	White Island	15.28	160.44	10.50
EvChl-WhI-10	White Island	15.64	150.44	9.62
EvChl-WhI-10	White Island	16.71	165.74	9.92
EvChl-WhI-10	White Island	15.21	157.55	10.36
EvChl-WhI-10	White Island	15.19	160.81	10.59
EvChl-WhI-10	White Island	14.61	182.16	12.47
EvChl-WhI-10	White Island	14.77	205.57	13.92
EvChl-WhI-10	White Island	15.29	162.45	10.62
EvChl-WhI-10	White Island	14.94	168.14	11.25
EvChl-Wlg-1	Wellington	22.77	95.71	4.20
EvChl-Wlg-1	Wellington	20.88	104.92	5.02
EvChl-Wlg-1	Wellington	22.04	100.15	4.54
EvChl-Wlg-1	Wellington	20.14	119.24	5.92
EvChl-Wlg-1	Wellington	21.16	107.20	5.07
EvChl-Wlg-1	Wellington	20.11	165.14	8.21
EvChl-Wlg-1	Wellington	20.73	112.20	5.41
EvChl-Wlg-1	Wellington	20.04	67.07	3.35
EvChl-Wlg-1	Wellington	20.03	113.68	5.68
EvChl-Wlg-1	Wellington	20.23	81.96	4.05
EvChl-Wlg-2	Wellington	20.13	101.23	5.03
EvChl-Wlg-2	Wellington	21.03	90.96	4.33
EvChl-Wlg-2	Wellington	18.86	114.50	6.07
EvChl-Wlg-2	Wellington	22.05	83.38	3.78
EvChl-Wlg-2	Wellington	21.53	142.58	6.62
EvChl-Wlg-2	Wellington	21.95	115.47	5.26
EvChl-Wlg-2	Wellington	18.77	116.64	6.21
EvChl-Wlg-2	Wellington	17.71	109.53	6.18
EvChl-Wlg-2	Wellington	19.07	97.93	5.14
EvChl-Wlg-2	Wellington	16.78	107.28	6.39
EvChl-Wlg-3	Wellington	18.96	112.93	5.96
EvChl-Wlg-3	Wellington	18.60	112.94	6.07
EvChl-Wlg-3	Wellington	21.39	140.32	6.56
EvChl-Wlg-3	Wellington	20.10	154.85	7.70
EvChl-Wlg-3	Wellington	19.22	162.07	8.43
EvChl-Wlg-3	Wellington	18.10	73.91	4.08
EvChl-Wlg-3	Wellington	19.01	158.02	8.31
EvChl-Wlg-3	Wellington	19.37	102.74	5.30
EvChl-Wlg-3	Wellington	18.38	102.21	5.56
EvChl-Wlg-3	Wellington	17.85	112.39	6.30
EvChl-Wlg-4	Wellington	21.27	126.17	5.93
EvChl-Wlg-4	Wellington	21.67	108.35	5.00
EvChl-Wlg-4	Wellington	21.13	120.70	5.71
EvChl-Wlg-4	Wellington	21.66	120.16	5.55
EvChl-Wlg-4	Wellington	21.57	133.55	6.19
EvChl-Wlg-4	Wellington	20.86	107.26	5.14
EvChl-Wlg-4	Wellington	21.33	124.15	5.82
EvChl-Wlg-4	Wellington	19.88	107.14	5.39
EvChl-Wlg-4	Wellington	20.32	127.90	6.29
EvChl-Wlg-4	Wellington	19.91	119.72	6.01
EvChl-Wlg-5	Wellington	16.20	124.71	7.70
EvChl-Wlg-5	Wellington	16.76	106.00	6.32
EvChl-Wlg-5	Wellington	17.64	106.37	6.03
EvChl-Wlg-5	Wellington	17.49	97.76	5.59
EvChl-Wlg-5	Wellington	16.80	121.27	7.22

Sample	Location	Spine length (mm)	Flexural strength (Mpa)	Strength:Length (Mpa:mm)
EvChl-Wlg-5	Wellington	17.06	124.95	7.32
EvChl-Wlg-5	Wellington	18.54	117.60	6.34
EvChl-Wlg-5	Wellington	15.47	107.71	6.96
EvChl-Wlg-5	Wellington	16.48	117.44	7.13
EvChl-Wlg-5	Wellington	15.99	118.79	7.43
EvChl-Wlg-6	Wellington	18.62	129.74	6.97
EvChl-Wlg-6	Wellington	19.50	149.46	7.66
EvChl-Wlg-6	Wellington	20.10	122.70	6.10
EvChl-Wlg-6	Wellington	17.87	115.03	6.44
EvChl-Wlg-6	Wellington	19.90	166.47	8.37
EvChl-Wlg-6	Wellington	19.22	95.70	4.98
EvChl-Wlg-6	Wellington	19.42	116.68	6.01
EvChl-Wlg-6	Wellington	18.70	109.56	5.86
EvChl-Wlg-6	Wellington	16.49	116.91	7.09
EvChl-Wlg-6	Wellington	18.30	106.44	5.82
EvChl-Wlg-7	Wellington	18.93	120.63	6.37
EvChl-Wlg-7	Wellington	19.44	140.56	7.23
EvChl-Wlg-7	Wellington	20.09	133.95	6.67
EvChl-Wlg-7	Wellington	20.21	133.65	6.61
EvChl-Wlg-7	Wellington	18.46	94.21	5.10
EvChl-Wlg-7	Wellington	18.97	133.75	7.05
EvChl-Wlg-7	Wellington	18.44	95.68	5.19
EvChl-Wlg-7	Wellington	18.59	111.00	5.97
EvChl-Wlg-7	Wellington	17.63	109.90	6.23
EvChl-Wlg-7	Wellington	16.88	104.74	6.20
EvChl-Wlg-8	Wellington	19.04	101.84	5.35
EvChl-Wlg-8	Wellington	18.84	116.40	6.18
EvChl-Wlg-8	Wellington	19.67	88.03	4.48
EvChl-Wlg-8	Wellington	19.91	104.77	5.26
EvChl-Wlg-8	Wellington	21.08	85.81	4.07
EvChl-Wlg-8	Wellington	21.75	100.45	4.62
EvChl-Wlg-8	Wellington	20.96	105.75	5.05
EvChl-Wlg-8	Wellington	21.61	94.52	4.37
EvChl-Wlg-8	Wellington	20.38	107.83	5.29
EvChl-Wlg-8	Wellington	22.18	117.20	5.28
EvChl-Wlg-9	Wellington	19.55	87.83	4.49
EvChl-Wlg-9	Wellington	21.47	101.86	4.74
EvChl-Wlg-9	Wellington	21.63	101.60	4.70
EvChl-Wlg-9	Wellington	22.39	71.96	3.21
EvChl-Wlg-9	Wellington	21.03	78.04	3.71
EvChl-Wlg-9	Wellington	20.44	92.66	4.53
EvChl-Wlg-9	Wellington	19.77	91.02	4.60
EvChl-Wlg-9	Wellington	20.10	74.33	3.70
EvChl-Wlg-9	Wellington	20.79	107.44	5.17
EvChl-Wlg-9	Wellington	19.47	78.64	4.04
EvChl-Wlg-10	Wellington	17.60	78.85	4.48
EvChl-Wlg-10	Wellington	19.87	109.64	5.52
EvChl-Wlg-10	Wellington	18.28	95.24	5.21
EvChl-Wlg-10	Wellington	18.09	107.02	5.92
EvChl-Wlg-10	Wellington	18.91	84.75	4.48
EvChl-Wlg-10	Wellington	18.58	105.37	5.67
EvChl-Wlg-10	Wellington	18.38	88.94	4.84
EvChl-Wlg-10	Wellington	16.66	100.80	6.05
EvChl-Wlg-10	Wellington	18.74	104.89	5.60
EvChl-Wlg-10	Wellington	18.15	113.05	6.23

Sample	Location	Spine length (mm)	Flexural strength (Mpa)	Strength:Length (Mpa:mm)
EvChl-Wlg-11	Wellington	22.20	107.52	4.84
EvChl-Wlg-11	Wellington	21.21	110.50	5.21
EvChl-Wlg-11	Wellington	22.52	116.34	5.17
EvChl-Wlg-11	Wellington	22.31	118.11	5.29
EvChl-Wlg-11	Wellington	22.67	88.97	3.92
EvChl-Wlg-11	Wellington	21.47	99.45	4.63
EvChl-Wlg-11	Wellington	22.36	109.41	4.89
EvChl-Wlg-11	Wellington	23.22	115.47	4.97
EvChl-Wlg-11	Wellington	22.47	93.03	4.14
EvChl-Wlg-11	Wellington	21.30	94.33	4.43
EvChl-Wlg-12	Wellington	23.50	93.66	3.99
EvChl-Wlg-12	Wellington	23.03	73.56	3.19
EvChl-Wlg-12	Wellington	21.70	99.59	4.59
EvChl-Wlg-12	Wellington	22.19	82.56	3.72
EvChl-Wlg-12	Wellington	23.42	96.52	4.12
EvChl-Wlg-12	Wellington	22.91	108.68	4.74
EvChl-Wlg-12	Wellington	22.15	113.26	5.11
EvChl-Wlg-12	Wellington	20.95	113.31	5.41
EvChl-Wlg-12	Wellington	21.37	84.72	3.96
EvChl-Wlg-12	Wellington	23.34	114.68	4.91
EvChl-Wlg-13	Wellington	23.00	101.83	4.43
EvChl-Wlg-13	Wellington	22.76	119.10	5.23
EvChl-Wlg-13	Wellington	22.46	115.90	5.16
EvChl-Wlg-13	Wellington	20.92	94.42	4.51
EvChl-Wlg-13	Wellington	21.28	88.98	4.18
EvChl-Wlg-13	Wellington	21.83	103.32	4.73
EvChl-Wlg-13	Wellington	21.92	122.69	5.60
EvChl-Wlg-13	Wellington	20.89	117.75	5.64
EvChl-Wlg-13	Wellington	20.46	105.28	5.15
EvChl-Wlg-13	Wellington	20.42	118.66	5.81
EvChl-Wlg-14	Wellington	21.83	96.61	4.43
EvChl-Wlg-14	Wellington	22.57	100.81	4.47
EvChl-Wlg-14	Wellington	22.95	107.50	4.68
EvChl-Wlg-14	Wellington	21.05	84.30	4.00
EvChl-Wlg-14	Wellington	21.61	104.03	4.81
EvChl-Wlg-14	Wellington	23.00	90.01	3.91
EvChl-Wlg-14	Wellington	23.18	91.52	3.95
EvChl-Wlg-14	Wellington	20.89	87.04	4.17
EvChl-Wlg-14	Wellington	21.12	90.03	4.26
EvChl-Wlg-14	Wellington	23.06	78.77	3.42